AMINO ACID, PEPTIDE AND DRUG TRANSPORT ACROSS MONOLAYERS OF HUMAN INTESTINAL (CACO-2) CELLS IN VITRO

PAUL LESLIE NICKLIN

Doctor of Philosophy

UNIVERSITY OF ASTON IN BIRMINGHAM

May 1993

UNIVERSITY OF ASTON IN BIRMINGHAM

AMINO ACID, PEPTIDE AND DRUG TRANSPORT ACROSS MONOLAYERS OF HUMAN INTESTINAL (CACO-2) CELLS IN VITRO

PAUL LESLIE NICKLIN
Doctor of Philosophy
1993

The properties of Caco-2 monolayers were compared on aluminium oxide and nitrocellulose permeable-supports. On nitrocellulose, Caco-2 cells displayed a higher rate of taurocholic acid transport than those cultured on aluminium oxide inserts. In addition, Caco-2 cells grown on these two inserts were not comparable with respect to cell morphology, cell numbers and transepithelial electrical resistance. The low adsorption potential of the aluminium oxide inserts, particularly for high molecular weight or lipophilic ligands, offers a distinct advantage over nitrocellulose inserts for drug transport studies.

The carrier-mediated uptake and transport of the imino acid (L-proline) and the acidic amino acids (L-aspartate and L-glutamate) have been studied. At pH7.4, L-proline uptake is mediated *via* an A-system carrier. Elevated uptake and transport under acidic conditions occurs by activation of a distinct carrier population. Acidic amino acid transport is mediated *via* a X^-_{AG} system. The flux of baclofen, CGP40116 and CGP40117 across Caco-2 monolayers was described by passive transport.

The transport of three peptides, thyrotrophin-releasing hormone, SQ29852 and cyclosporin were investigated. Thyrotrophin-releasing hormone transport across Caco-2 monolayers was characterised by a minor saturable (carrier-mediated, approximately 25%) pathway, superimposed onto a major non-saturable (diffusional) pathway. SQ29852 uptake into Caco-2 monolayers is described by a major saturable-mechanism (K_m = 0.91 mM) superimposed onto a minor passive component. However, the initial-rate of SQ29852 transport is consistent with a passive transepithelial transport mechanism. These data highlight the possibility that its basolateral efflux is severely retarded such that the passive paracellular transport dictates the overall transepithelial transport characteristics. In addition, model suitable for investigating the transepithelial transport of cyclosporin A has been developed.

A modification of the conventional Caco-2 model has been developed which has a calcium-free Ap donor-solution and a Bl receiver-solution containing the minimum calcium concentration required to maintain monolayer integrity (100 μM). The influence of calcium and magnesium on the absorption of [^{14}C]pamidronate was evaluated by comparing its transport across the conventional and minimum calcium Caco-2 models. Ap calcium and magnesium ions retard the Ap-to-Bl flux of pamidronate across Caco-2 monolayers.

The effect of self-emulsifying oleic acid-Tween 80 formulations on Caco-2 monolayer integrity has been investigated. Oleic acid-Tween 80 (10:1) formulations produced a dose-dependent disruption of Caco-2 monolayer integrity. This disruption was related to the oleic acid content of the formulation.

L-Aspartate, Formulation, Pamidronate, L-Proline, SQ29852.

ACKNOWLEDGEMENTS

This thesis has one author, but is a product of the many individuals that have made it possible. For their efforts I am sincerely grateful.

I thank my parents, **Roy** and **Kathleen Nicklin**, for their love and support which has been a source of strength throughout.

Secondly, I thank my supervisor, **Bill Irwin**, whose knowledge and wisdom have been an inspiration.

I thank **Ian Hassan**, **John Hastewell**, **Martin Mackay** and **Ian Williamson** (Ciba Pharmaceuticals) for the opportunities they have created and their enthusiastic encouragement.

I thank **Peter Timmins** (Bristol-Myers Squibb) whose efforts made the work with SQ29852 possible.

The work presented in this thesis was supported by the Science and Engineering Research Council and generous contributions from Aston University, Bristol-Myers Squibb and Ciba Pharmaceuticals.

TABLE OF CONTENTS

CHAPTER ONE General Introduction

1.1 Background 16
1.2 Architecture of the gastrointestinal tract 16
1.3 The gastrointestinal epithelium 18
1.3.1 Absorptive cells 22
1.3.2 Goblet cells 23
1.3.3 M-cells 23
1.3.4 Paneth cells 23
1.3.5 Tuft (caveolated) cells 23
1.4 Absorption models 24
1.4.1 In vivo models 24
1.4.1.1 Thiry-Vella fistula 24
1.4.1.2 Plasma appearance after intestinal administration 25
1.4.2 In situ models 25
1.4.3 In vitro models 26
1.4.3.1 Everted sacs 26
1.4.3.2 Intestinal rings 26
1.4.3.3 Intestinal sheets 27
1.4.3.4 Membrane vesicles 27
1.4.3.5 Isolated enterocytes 28
1.4.3.6 Cell culture models 29
1.5 Caco-2 cells 29
1.5.1 Amino acid transport 31
1.5.2 Cobalamin transport 33
1.5.3 Hexose transport 34
1.5.4 Peptide transport 35
1.5.5 Passive transport across Caco-2 monolayers 38
1.5.6 Unstirred water layer effects 40
1.5.7 Metabolism 41
1.5.8 Lectin binding 42
1.5.9 Bacterial adhesion 43
1.6 Heterogeneity 45
1.7 Are Caco-2 cells absorptive cells? 45
1.8 Caco-2 and HT29GlucH co-cultures 46
1.9 Objective of this thesis 47

CHAPTER TWO General materials and methods

2.1 Chemicals 49

2.2 Cell culture 49

2.2.1 Culture-media 49

2.2.2 Stock cultures 49

2.2.3 Cultures for uptake studies 52

2.2.4 Cultures for transport studies 52

2.3 Uptake and transport experiments 52

2.3.1 Transport-media 53

2.3.2 Uptake experiments 54

2.3.3 Transport experiments 54

2.4 Analytical methods 57

2.4.1 Liquid scintillation counting 57

2.4.2 Gamma counting 57

2.5 Transepithelial electrical resistance 57

2.6 Electron microscopy 58

2.6.1 Transmission electron microscopy 58

2.6.2 Scanning electron microscopy 58

2.7 Octanol-aqueous buffer distribution coefficients 58

2.8 Data presentation 59

CHAPTER THREE Permeable-support type influences the morphological and functional properties of Caco-2 cells

3.1 Background 61

3.2 Materials 62

3.3 Methods 62

3.3.1 Ligand adsorption to permeable-supports 62

3.3.2 D-Mannitol and testosterone transport 63

3.3.3 Light microscopy and cell counting 63

3.3.4 Horseradish peroxidase cytochemistry 63

3.3.5 Transepithelial electrical resistance 64

3.3.6 Taurocholic acid transport 64

3.3.7 Proline transport 64

3.4 Results 65

3.5 Discussion 80

3.6 Conclusion 82

CHAPTER FOUR Proline uptake into and transport across Caco-2 monolayers

4.1 Background 84
4.1.1 L-Proline 84
4.1.2 Baclofen 85
4.2 Materials 86
4.2.1 Chemicals 86
4.2.2 Transport-media 86
4.3 Methods 86
4.3.1 Cell culture 86
4.3.2 L-Proline uptake experiments 87
4.3.3 L-Proline transport experiments 87
4.3.4 Baclofen transport experiments 87
4.3.5 L-Proline identification by thin-layer chromatography 88
4.4 Results 88
4.4.1 L-Proline uptake 88
4.4.2 L-Proline transport 91
4.4.3 Baclofen 93
4.5 Discussion 113
4.5.1 L-Proline uptake 113
4.5.2 L-Proline transport 117
4.5.3 Baclofen transport 118
4.6 Conclusion 119

CHAPTER FIVE Transport of acidic amino acids and their analogues across Caco-2 monolayers

5.1 Background 121
5.1.1 Amino acid transport 121
5.1.2 Acidic amino acids in the central nervous system 121
5.2 Materials 124
5.2.1 Chemicals 124
5.3 Methods 124
5.3.1 Cell culture 124
5.3.2 Transport-media 124
5.3.3 Transport experiments 125
5.3.4 Experimental conditions 125
5.3.4.1 Acidic amino acids 126

5.3.4.1 CGP40116, CGP40117 and CGP37849 126
5.3.5 Identification of post-transport L-[^{3}H]aspartate 126
5.3.6 Inhibition constant (K_i) calculation 126
5.4 Results 127
5.4.1 Acidic amino acid transport 127
5.4.2 Transport of CGP37849, CGP40116 and CGP40117 130
5.5 Discussion 151
5.5.1 Acidic amino acids 151
5.5.2 CGP37849, CGP40116 and CGP40117 160
5.6 Conclusion 161

CHAPTER SIX Peptide transport across Caco-2 monolayers
6.1 Background 163
6.1.1 Thyrotrophin-releasing Hormone 163
6.1.2 Angiotensin-converting enzyme inhibitors 164
6.1.3 Cyclosporin 165
6.2 Materials 168
6.3 Methods 168
6.3.1 Thyrotrophin-releasing Hormone 168
6.3.1.1 Uptake experiments 168
6.3.1.2 Transport experiments 168
6.3.1.3 HPLC analysis 169
6.3.2 SQ29852 169
6.3.2.1 Uptake experiments 169
6.3.2.2 Transport experiments 170
6.3.2.3 SQ29852 radioimmunoassay 170
6.3.3 Cyclosporin 173
6.4 Results 174
6.4.1 Thyrotrophin-releasing Hormone 174
6.4.2 SQ29852 175
6.4.3 Cyclosporin 176
6.5 Discussion 190
6.5.1 Thyrotrophin-releasing Hormone 190
6.5.2 SQ29852 191
6.5.3 Cyclosporin 193
6.6 Conclusion 194

CHAPTER SEVEN Calcium and magnesium ions retard the transepithelial transport of pamidronate

7.1 Background 196
7.1.1 Pamidronate (CGP23339a) 196
7.1.2 Minimum calcium model 197
7.2 Materials 197
7.3 Methods 197
7.3.1 Cell culture 197
7.3.2 Titration of minimum calcium concentration 198
7.3.3 Transepithelial electrical resistance 198
7.3.4 Laser-scanning confocal microscopy 198
7.4 Results 199
7.5 Discussion 211
7.6 Conclusion 216

CHAPTER EIGHT Effect of self-emulsifying oleic acid-Tween 80 formulations on Caco-2 monolayers

8.1 Background 218
8.2 Materials 218
8.3 Methods 219
8.3.1 Emulsion preparation 219
8.3.2 Determination of oleic acid concentration 219
8.3.3 Assessment of monolayer integrity 219
8.3.3.1 D-Mannitol transport 219
8.3.3.2 Transepithelial electrical resistance 220
8.3.3.3 Microscopy 220
8.4 Results 220
8.5 Discussion 238
8.6 Conclusion 241

CHAPTER NINE Summary 243

REFERENCES 262
APENDIX ONE Abbreviations 265

TABLE OF TABLES

TABLE 3.1	Ligand adsorption to aluminium oxide and nitrocellulose permeable-supports	79
TABLE 3.2	Taurocholic acid transport across Caco-2 monolayers cultured on aluminium oxide inserts, normal pore-size (0.2 μm upper surface to 0.02 μm lower surface) and special pore-size (0.2 μm throughout)	79
TABLE 4.1	Inhibition of L-proline uptake by amino acids and their analogues	108
TABLE 4.2	Influence of feeding-regimen on L-proline uptake	109
TABLE 4.3	Effect of cycloheximide, glucose depletion and sodium azide on specific L-proline uptake	109
TABLE 4.4	Sodium- and energy-dependence of L-proline uptake and transport at pH7.4 and pH5.5	110
TABLE 4.5	Inhibition of L-proline transport (Ap pH5.5) by natural amino acids, stereoisomers and synthetic analogues	111
TABLE 4.6	Influence of beta-alanine on [^{14}C]baclofen transport	112
TABLE 5.1	L-Aspartate transport against a 10-fold concentration-gradient	146
TABLE 5.2	Cation- and anion-dependence of L-aspartate transport	146
TABLE 5.3	Kinetic parameters for acidic amino acid transport across Caco-2 monolayers	146
TABLE 5.4	Inhibition of acidic amino acid transport by natural amino acids	147
TABLE 5.5	Inhibition of acidic amino acid transport by synthetic analogues	148
TABLE 5.6	Estimated Ki values for a range of competitors of L-aspartate transport	149
TABLE 5.7	The influence of the permeable-support on P_{app} of acidic amino acids	150
TABLE 5.8	The radiochemical purities of ^{14}C]CGP37849, [^{14}C]CGP40116 and [^{14}C]CGP40117	150

TABLE 6.1	SQ29852 radioimmunoassay protocol	171
TABLE 6.2	Cross-inhibition of TRH uptake	187
TABLE 6.2	Cross-inhibition of TRH transport	188
TABLE 6.4	Cross-inhibition of SQ29852 uptake and transport	188
TABLE 6.5	Inhibition of [^{3}H]CsA surface adsorption by receiver-media	189

TABLE 7.1	Comparative effect of calcium concentration and distribution of CGP23339a and D-mannitol transport across Caco-2 monolayers	210
TABLE 7.2	Effect of Ap CGP23339a on the permeability of Caco-2 monolayers	210

TABLE 8.1	Oleic acid and Tween 80 concentrations at 0.1% v/v and 0.25% v/v as a function of formulation ratio	237

TABLE OF FIGURES

FIGURE 1.1	The obstacles for drug absorption to the systemic circulation	17
FIGURE 1.2	Schematic diagram of an epithelium	20
FIGURE 1.3	Opportunities for transepithelial transport	21
FIGURE 1.4	Schematic diagram of a small intestinal absorptive cell	22
FIGURE 1.5	Correlation between the passive transport of drug compounds across Caco-2 monolayers and their oral absorption in humans	39

FIGURE 2.1	Mycoplasma detection by fluorescence microscopy	50
FIGURE 2.2	Cell culture-inserts used for transport studies	51
FIGURE 2.3	The Caco-2 monolayer uptake model	56
FIGURE 2.4	The Caco-2 transport model	56

FIGURE 3.1	Phase-contrast light micrograph of 19 d Caco-2 cells cultured on aluminium oxide permeable-support	69
FIGURE 3.2	The influence of permeable-support type on D-mannitol and testosterone transport	69
FIGURE 3.3	Temporal-dependence of Caco-2 monolayer appearance on aluminium oxide and nitrocellulose permeable-supports	70
FIGURE 3.4	Temporal-dependence of Caco-2 cell numbers during culture on aluminium oxide and nitrocellulose permeable-supports	71
FIGURE 3.5	Caco-2 monolayer cultured on an aluminium oxide permeable-support for 14 d showing a blister-like dome	72
FIGURE 3.6	Transmission electron micrographs of Caco-2 cells cultured on aluminium oxide and nitrocellulose permeable-supports	73
FIGURE 3.7	Scanning electron micrographs of Caco-2 cells cultured on aluminium oxide and nitrocellulose permeable-supports	74
FIGURE 3.8	Cytochemical localisation of horseradish peroxidase following a 60 min basolateral incubation	75
FIGURE 3.9	Morphometric analysis of Caco-2 cells cultured on aluminium oxide and nitrocellulose permeable-supports	75
FIGURE 3.10	Temporal-dependence of transepithelial electrical resistance of Caco-2 monolayers cultured on aluminium oxide and nitrocellulose permeable-supports	76
FIGURE 3.11	Taurocholic acid transport	77
FIGURE 3.12	Temporal-dependence of apical and basolateral taurocholic acid uptake into Caco-2 monolayers cultured on aluminium oxide and nitrocellulose permeable-supports	78
FIGURE 3.13	Proline transport across Caco-2 monolayers cultured on aluminium oxide	78

FIGURE 4.1	Structures of L-proline (A) and baclofen (B)	85
FIGURE 4.2	Identification of L-[^{3}H]proline post-uptake	94
FIGURE 4.3	Kinetics of L-proline uptake into Caco-2 monolayers	94
FIGURE 4.4	Sodium-dependence of L-phenylalanine and L-proline uptake into Caco-2 monolayers	95
FIGURE 4.5	Influence of extracellular sodium concentration on L-proline uptake	96
FIGURE 4.6	Anion-dependence of L-proline uptake	96
FIGURE 4.7	Concentration-dependence of L-proline uptake	97

FIGURE 4.8	Temperature-dependence of L-proline uptake	98
FIGURE 4.9	The effect of pH on L-proline uptake	99
FIGURE 4.10	pH-dependence of L-proline transport	100
FIGURE 4.11	Ap-to-Bl L-proline transport kinetics at pH7.5 and pH5.5	101
FIGURE 4.12	Effect of ouabain and metabolic inhibitors on D-mannitol transport	101
FIGURE 4.13	Temporal-dependence of L-proline transport (Ap pH7.4 and 5.5)	102
FIGURE 4.14	Polarity of L-proline transport (Ap pH7.4 and 5.5)	103
FIGURE 4.15	Concentration-dependence of L-proline transport (Ap pH5.5)	104
FIGURE 4.16	pH-dependence of saturable L-[^{14}C]arginine transport	105
FIGURE 4.17	Baclofen transport kinetics	106
FIGURE 4.18	Concentration-dependence of baclofen transport	106
FIGURE 4.19	Polarity of baclofen transport kinetics	107
FIGURE 4.20	pH-dependence of baclofen transport	107

FIGURE 5.1	Structures of acidic amino acids and their analogues	123
FIGURE 5.2	Identification of post-transport L-[^{3}H]aspartate	132
FIGURE 5.3	Ap-to-Bl transport kinetics of L-aspartate	133
FIGURE 5.4	Polarity of L-aspartate transport at 21d of culture	134
FIGURE 5.5	The temporal-dependence of L-aspartate transport	135
FIGURE 5.6	Sodium-dependence of Ap-to-Bl L-aspartate transport	136
FIGURE 5.7	Ouabain-sensitivity and energy dependence of L-aspartate uptake and transport	137
FIGURE 5.8	Concentration-dependence of L-aspartate and L-glutamate transport	138
FIGURE 5.9	Effect of cycloheximide on L-aspartate transport	139
FIGURE 5.10	pH-dependence of L-aspartate transport	140
FIGURE 5.11	Temperature-dependence of Ap-to-Bl L-aspartate transport	141
FIGURE 5.12	Ap-to-Bl transport kinetics for [^{14}C]CGP37849, [^{14}C]CGP40116 and [^{14}C]CGP40117	142
FIGURE 5.13	Concentration-dependence of [^{14}C]CGP40116 and [^{14}C]CGP40117 transport	143

FIGURE 5.14	Temperature-dependence of CGP40116 and CGP40117 transport	144
FIGURE 5.15	Ap-to-Bl and Bl-to-Ap CGP40116 and CGP40117 transport	145
FIGURE 5.16	Proposed recognition of acidic amino acids by the X^-_{AG} carrier	157

FIGURE 6.1	Structures of thyrotrophin-releasing hormone (A), SQ29852 (B) and cyclosporin (C)	167
FIGURE 6.2	SQ29852 radioimmunoassay	170
FIGURE 6.3	Identification of post-incubation [^{3}H]TRH	178
FIGURE 6.4	Ap(pH6.0)-to-Bl(pH7.4) transport kinetics of [^{3}H]TRH	178
FIGURE 6.5	Concentration-dependence of TRH transport	179
FIGURE 6.6	Temperature-dependent polarity of TRH transport	180
FIGURE 6.7	pH-dependence of TRH transport and Log D	181
FIGURE 6.8	SQ29852 radioimmunoassay standard curve	182
FIGURE 6.9	SQ29852 transport kinetics	183
FIGURE 6.10	Concentration-dependence of SQ29852 uptake and transport	184
FIGURE 6.11	Influence of alternative receiver-media on D-mannitol and testosterone transport	185
FIGURE 6.12	[^{3}H]CsA transport	186

FIGURE 7.1	Pamidronate (CGP23339a)	196
FIGURE 7.2	Sample mounting for confocal microscopy	199
FIGURE 7.3	Influence of the distribution of calcium and magnesium ions on TER	203
FIGURE 7.4	The influence of Bl calcium and magnesium concentrations on Caco-2 monolayer integrity	204
FIGURE 7.5	Dose-response curves for permeability indices as a function of Bl calcium concentration	205
FIGURE 7.6	Effect of calcium on Caco-2 monolayer appearance	206
FIGURE 7.7	Effect of calcium removal on CGP23339a and D-mannitol transport	207
FIGURE 7.8	Effect of Ap CGP23339a on the permeability of the minimum calcium model	208

FIGURE 7.9	Oral bioavailability predictions from the apparent permeability coefficients of CGP23339a transport across the conventional and minimum calcium Caco-2 monolayer models	209
FIGURE 8.1	Effect of oleic acid-Tween 80 (10:1) formulation on D-mannitol transport	225
FIGURE 8.2	Effect of oleic acid-Tween 80 (10:1) formulation on post-transport TER values	226
FIGURE 8.3	A dose-response for the initial effect of oleic acid-Tween 80 (10:1)formulation on D-mannitol transport	226
FIGURE 8.4	The influence of emulsion composition on D-mannitol transport	227
FIGURE 8.5	The influence of emulsion composition on post-transport TER	228
FIGURE 8.6	The influence of oleic acid on Caco-2 monolayer integrity	229
FIGURE 8.7	The influence of Tween 80 on Caco-2 monolayer integrity	230
FIGURE 8.8	Confocal laser-scanning micrographs of control Caco-2 monolayers	231
FIGURE 8.9	Transmission electron micrographs of control Caco-2 monolayers	232
FIGURE 8.10	Confocal laser-scanning micrographs of Caco-2 monolayers after exposure to 0.1% v/v oleic acid-Tween 80 (10:1) formulation	233
FIGURE 8.11	Transmission electron micrographs of Caco-2 monolayers after exposure to 0.1% v/v oleic acid-Tween 80 (10:1) formulation	234
FIGURE 8.12	Confocal laser-scanning micrographs of Caco-2 monolayers after exposure to 0.25% v/v oleic acid-Tween 80 (10:1) formulation	235
FIGURE 8.13	Transmission electron micrographs of Caco-2 monolayers after exposure to 0.25% v/v oleic acid-Tween 80 (10:1) formulation	236

CHAPTER ONE

GENERAL INTRODUCTION

ABSTRACT

The specialisations of the gastrointestinal epithelium which permit efficient and selective absorption of electrolytes and nutrients from the gastrointestinal tract are considered. The possibilities and limitations for a range of *in vivo*, *in situ* and *in vitro* absorption models are discussed. Finally, the morphological and functional properties of Caco-2 cells, pertinent to their use as a putative *in vitro* model of the human gastrointestinal epithelium, are presented.

This general introduction is supplemented by a short background to each series of experiments at the beginning of each experimental chapter.

1.1 BACKGROUND

Increased molecular definition of (patho)physiological states has prompted the development of many novel drug candidates, notably natural peptides and their analogues. However, the initial enthusiasm for these *next-generation* drugs has been tempered by their poor enzymatic stabilities and/or inappropriate physico-chemical properties which result in low oral bioavailabilities. The limited success with oral peptide delivery has prompted research into alternative non-parenteral routes of administration. Delivery *via* the buccal, nasal, ocular, percutaneous, pulmonary, rectal and vaginal routes has been investigated and a moderate degree of success reported [Wearley, 1991]. However, whilst these alternative mucosae present less formidable biological barriers to peptide absorption, they are associated with a lower patient acceptability and familiarity. For this reason there is considerable interest in designing orally active peptide analogues and delivery systems that safely promote the oral absorption of peptides.

The challenge offered by the poor oral bioavailabilities of these molecules has stimulated considerable interest into the biological barriers which control absorption from the gastrointestinal (GI) tract.

1.2 ARCHITECTURE OF THE GASTROINTESTINAL TRACT

Longitudinally, the GI tract can be divided into anatomically distinct regions. In the proximal (mouth) to distal (anus) direction these are, sequentially; the oesophagus, stomach, small intestine (duodenum, jejunum, ileum), large intestine (caecum and ascending, transverse and descending colon) and the rectum. Although there is considerable interest in the absorption across the large intestinal mucosa, particularly for peptide pharmaceuticals (*eg:* calcitonin [Antonin *et al.*, 1992; Hastewell *et al.*, 1992]), the small intestine is the principle site of drug and nutrient absorption.

The main thickness of the intestinal wall, the lamina muscularis externa, has an outer longitudinal layer and an inner circular layer of smooth muscle. Coordinated contractions of these muscle layers generates a peristaltic wave which propel the luminal contents across the absorptive surface in a proximal to distal direction. Internal to the muscularis external there is a layer of dense and elastic connective tissue called the lamina submucosa. The innermost layer of the intestinal wall is the mucosa. In turn, the mucosa is composed of three distinct layers, the muscularis mucosa, the lamina propria and the epithelium.

The small intestine is organised to amplify the luminal surface area and maximise its absorption-potential. Luminal surface area is primarily increased by macroscopic circular folds (plicae circulares) of the submucosa and secondarily by numerous extensions (villi) and invaginations (crypts of Lieberkühn) of the mucosa. Finally, the absorptive cells of the GI epithelium bear a dense brush-border of microvilli. These structural features help to increase the luminal surface area of the small intestine over 200 m^2.

The biological obstacles to absorption from the GI tract are summarised in Fig. 1.1. A permeant does not have to traverse the entire gut wall during absorption. However, it must penetrate the unstirred water and mucus layers, the epithelium and basement membrane into the lamina propria which contains an extensive blood capillary and lymphatic network. Distribution to the systemic circulation occurs through the hepatic portal system *via* the liver, or by lymphatic drainage *via* the thoracic duct.

FIGURE 1.1 *The obstacles for drug absorption to the systemic circulation (modified from Humphery 1986)*

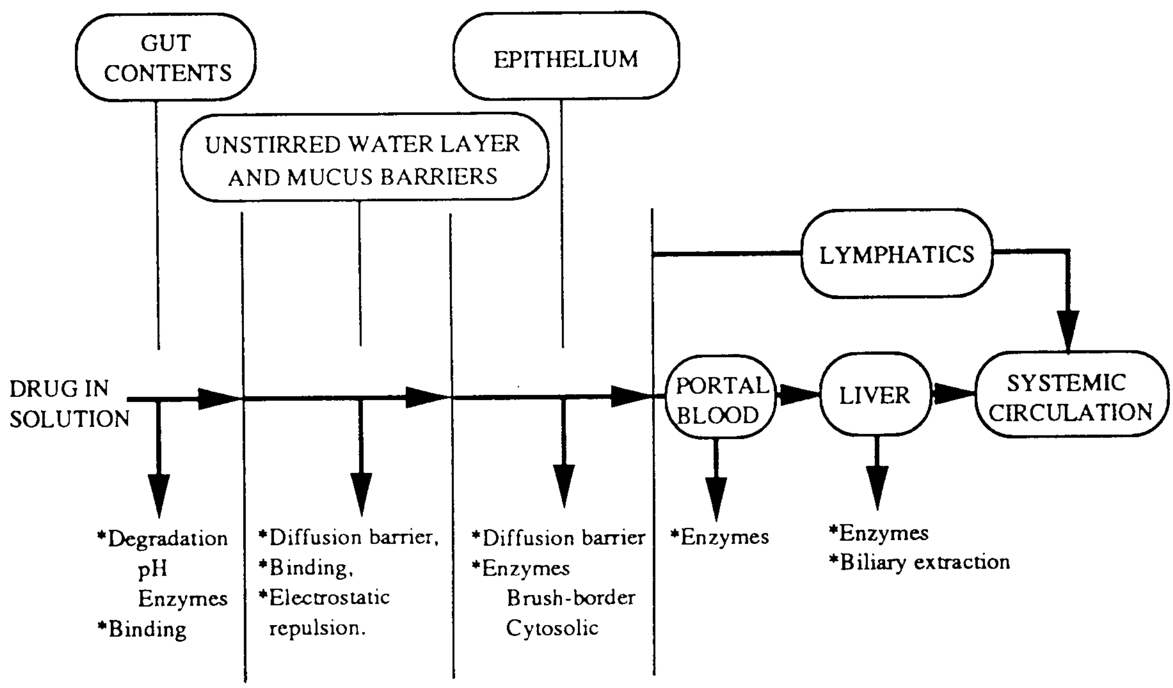

1.3 THE GASTROINTESTINAL EPITHELIUM

The GI tract has conflicting functional requirements. It must efficiently absorb electrolytes and a diverse range of nutrients, yet simultaneously provide an absolute barrier to micro-organisms and toxins. This selective absorption is controlled, at least in part, by the GI epithelium which is located at the strategic interface between the environment (gut lumen) and body interior.

The GI epithelium is composed of a single sheet of closely-opposed cells joined at their lateral surfaces by junctional complexes (Fig. 1.2). Junctional-complexes are composed of three principle components; the tight-junction, the intermediate-junction and desmosomes. The tight-junction is the most apical component of the junctional complex and appears as a region of exceptionally close contact between adjacent cells. Penetration studies using horse-radish peroxidase, lanthanum hydroxide and ruthenium red have shown that the tight junction is the structure that restricts transport through the tight junctional complex, hence through the intercellular space [Farquhar and Palade, 1963; Mazariegos *et al.*, 1984; Pinto da Silva and Katchar, 1982].

There are two distinct pathways by which a permeant may traverse an epithelium. Paracellular transport involves diffusion between cells across the junctional-complexes or through the transient gaps between cells at the extrusion-zones on the villus tips. Transcellular transport involves transport across the epithelial cells. It is a multi-stage process embracing uptake at the luminal (apical, Ap) surface, movement across the cytosol and export from the basolateral (Bl) surfaces. Both import and export can occur by passive or carrier-mediated mechanisms. Passive mechanisms include lipid-partitioning, diffusion through aqueous pores or fluid-phase pinocytotic vesicular transport. Carrier-mediated mechanisms include facilitated transport, active transport and receptor-mediated transcytosis (Fig. 1.3).

The tight-junction is an important determinant of transepithelial transport processes. Firstly, it regulates the diffusion of permeants through the paracellular pathway. Secondly, it is involved in the organisation of the epithelial cell plasma membrane into distinct apical and basolateral domains. In turn, the polarised distribution of ion-channels, nutrient-transporters and receptors is responsible for vectorial transcellular transport [Gumbiner, 1987].

To serve its function as a selective permeability barrier, the GI epithelium is a highly organised and dynamic structure composed of numerous cell-types with morphological and biochemical specialisations. These multiple cell-types originate from a single population of undifferentiated and proliferating precursor cells at the base of the crypts of Lieberkühn. Daughter cells differentiate as they migrate along the crypt-villus axis, with the specialisations being established by the time they leave the crypt mouth at the base of the villus. Enterocyte migration is a continuous process and the cells are finally shed into the GI lumen from extrusion-zones at the tips of the villi. In man, as many as 1.0×10^{11} cells are sloughed per day from the small intestine, which represents 40% of the cells on the villi [Potten and Morris, 1988]. One can hypothesise that the rapid epithelial turnover probably serve as a continuous repair mechanism for the abrasion and insult which the GI epithelium endures. This would ensure that an integral cellular barrier between the environment and the body interior is maintained.

FIGURE 1.2 *Schematic diagram of an epithelium.*

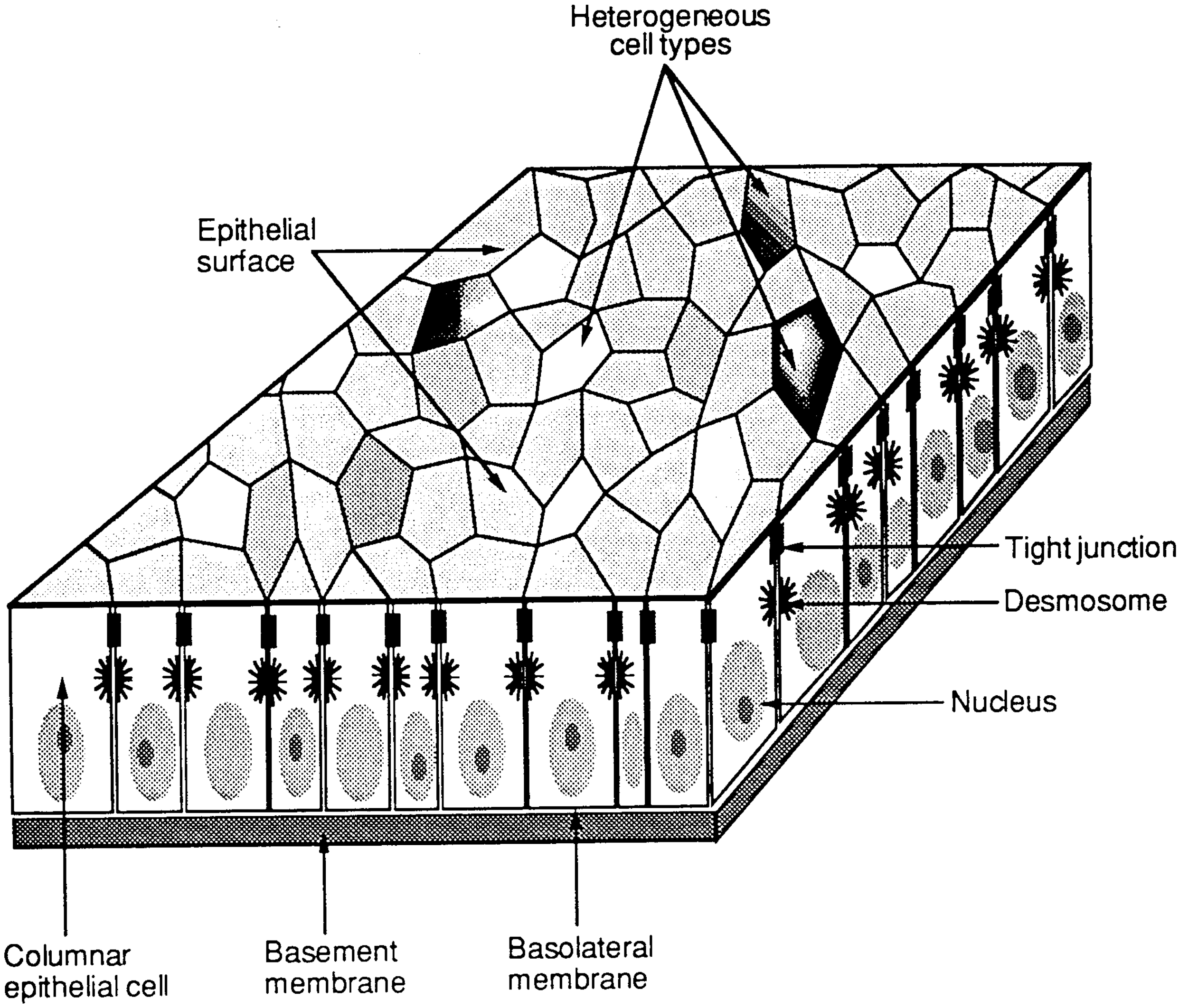

FIGURE 1.3 *The opportunities for transepithelial transport.*

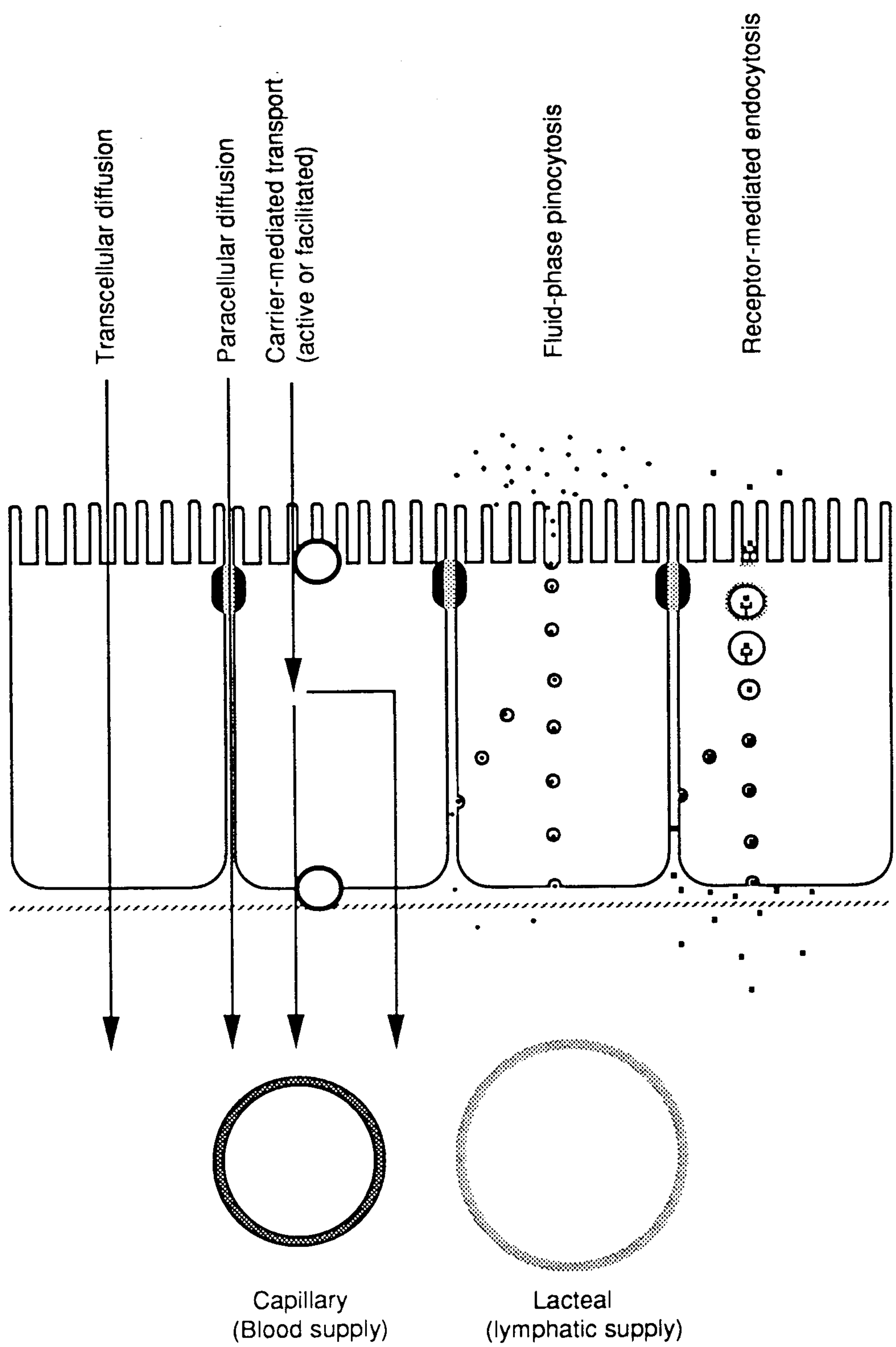

The functional morphology of the intestinal mucosa has been reviewed recently [Carr and Toner, 1984; Madara and Trier, 1987]. The notable features and functions of the most important cell-types are outlined below.

1.3.1 ABSORPTIVE CELLS

Absorptive cells account for approximately 90% of the epithelial cells covering the intestinal villus and are the most important in terms of nutrient and drug transport. The features of absorptive cells are shown schematically in Fig. 1.4.

FIGURE 1.4 *Schematic diagram of a small intestinal absorptive cell.*

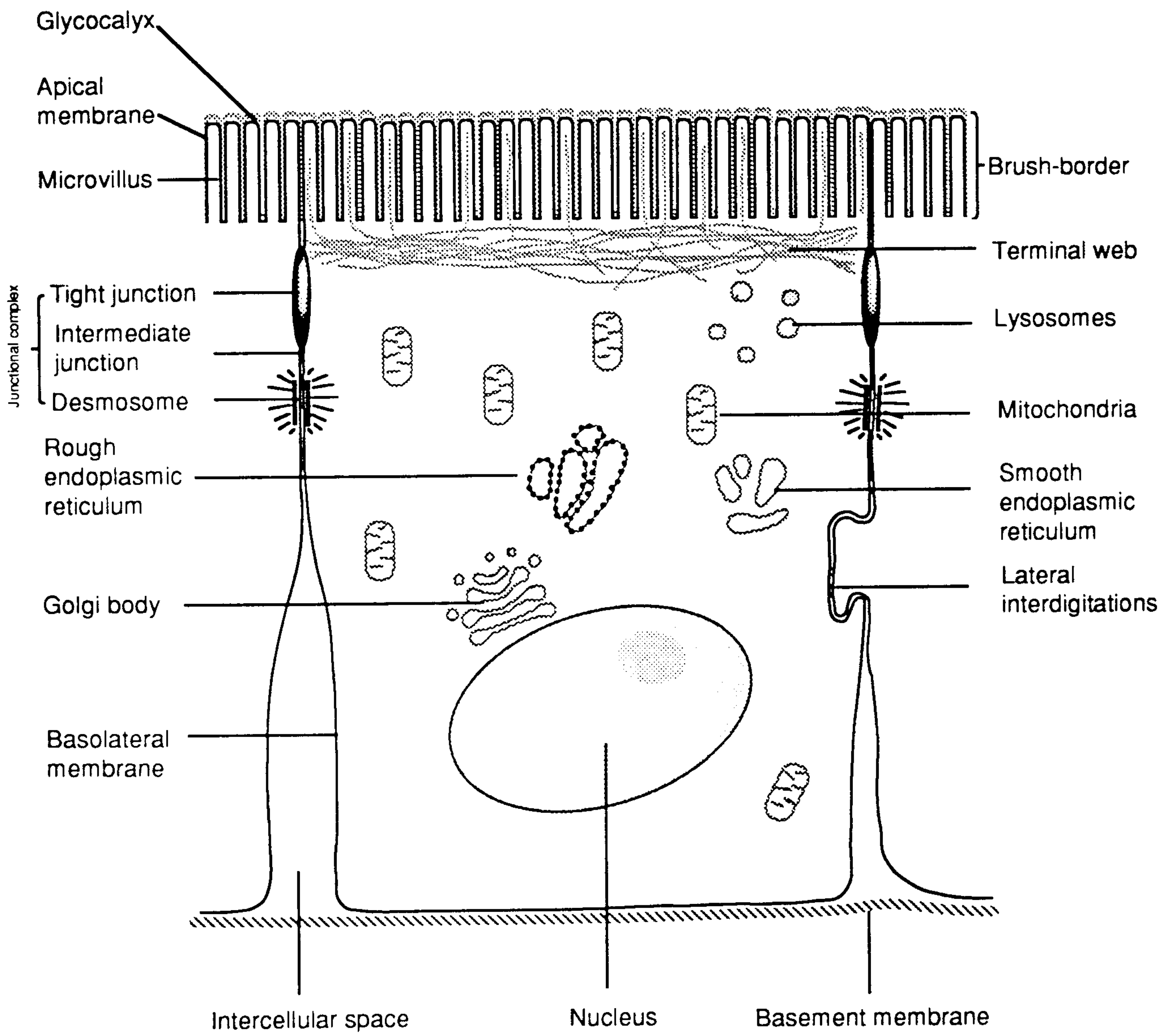

1.3.2 GOBLET CELLS

Discrete goblet cells are present throughout the epithelium acting as a unicellular gland secreting mucus onto the epithelial surface for lubrication and protection. These are easily distinguished from absorptive cells by their cup-shape which results from the apical (Ap) two-thirds of the cell being distended with numerous secretory mucus granules. In addition, they possess sparse and irregular Ap microvilli.

1.3.3 M-CELLS

M-cells [Owen and Jones, 1974] are highly specialised cells present in the epithelium overlying the lymphoid follicles associated with Peyer's Patches. Their apical surface lacks a glycocalyx and is characterised by short and irregular microfolds rather than microvilli. They can be distinguished from absorptive cells at the ultrastuctural level in that they are cuboidal, possess organelles in their terminal webb and have numerous apical vesicles but are deficient in lysosomes. Moreover, a mature M-cell has an indent at its basal membrane forming a central hollow containing one or more intrusive cells which are usually lymphocytes, macrophages or plasma cells.

M-cells have been shown to transport macromolecules (*eg:* ferritin, horseradish-peroxidase), bacteria (*eg:* mycobateria, chlamydia, *Vibrio cholera*) and viruses (*eg:* reoviruses types 1 and 3). These observations have prompted workers to speculate that M cells are involved in trafficking antigens from the gut lumen to the gut-associated lymphoid tissue to stimulate the mucosal immune system [O'Hagan *et al.*, 1987].

1.3.4 PANETH CELLS

Paneth cells are located at the base of the crypts of Lieberkühn. They are truncated pyramidal cells with a basally positioned nucleus and numerous apical eosinophilic secretion granules. The granules are released from the luminal surface with bears a few poorly developed microvilli. The role of the Paneth cells is uncertain. However, the demonstration of lysozyme and immunoglobulin within Paneth cells together with the internalisation and digestion of microorganisms has led to the speculation that they may control microflora in the small intestine, especially within the crypts [Peters and Vantrappen, 1975; Rodning *et al.*, 1976].

1.3.5 TUFT (CAVEOLATED) CELLS

Tuft cells are present on intestinal villi and in crypts. These pear-shaped cells derive their name from a prominent Ap brush-border of microvilli that are longer and wider than those on absorptive cells. The filamentous cores of the Ap microvilli extend well down into the supranuclear cytoplasm. Deep micropinocytotic invaginations of Ap membrane are seen in association with the filamentous bundles. The role of the tuft cells is uncertain, however, it has been speculated from their widespread distribution and ultrastructural specialisations that they may be involved in chemoreception.

Despite the predominance of the absorptive cell-type (≈ 90% of total), the minor cell types may have a disproportionate influence on the transport of certain molecules across the GI epithelium. For instance, M-cells are a minor cell population, however, they may be quantitatively important in the presentation of antigens to the mucosal immune system. Similarly, the absorption of compounds may be limited by the mucus layer [Nimmerfall and Rosenthaler, 1980]. In this case, the minor goblet cell population may indirectly influence the absorption disproportionately. Therefore, a universal absorption model should encompass all cell types in the correct proportions and organisation.

1.4 ABSORPTION MODELS

A major limitation for predicting absorption phenomena in humans is the scarcity of normal tissue and its poor viability upon excision [Trier, 1980]. Consequently, most absorption studies are performed using laboratory animals. However, inter-species variation makes the extrapolation of absorption data in laboratory animals to the human situation inappropriate. Numerous *in vivo, in situ* and *in vitro* models have been used to investigate intestinal absorption mechanisms and to assess oral bioavailabilities of drug molecules. The advantages and disadvantages for some frequently used techniques are surveyed below.

1.4.1 IN VIVO MODELS

1.4.1.1 *THIRY-VELLA FISTULA*

This model was originated by Thiry in 1864 and modified in 1880 by Vella. An intestinal segment, with its blood and lymphatic supply intact, is isolated from the intestinal tract of an anaesthetised animal. One or both ends of the intestinal segment are brought to the skin surface to form a blind ending pocket or loop, respectively. The continuity of the GI tract is restored by end-to-end anastomosis. Absorption studies are performed after a period of post-operative recovery.

A solution of a compound is introduced into the fistula and its rate of luminal disappearance is assumed to equal the rate of absorption. Thiry-Vella absorption studies are most commonly performed using the dog, however, a similar chronic intestinal resection method has been performed in rats [Poelma and Tukker, 1987].

1.4.1.2 *PLASMA APPEARANCE AFTER INTESTINAL ADMINISTRATION*

The plasma appearance of a compound is monitored after the oral administration of a dosage form or following direct instillation of a solution into a specific region of the GI tract. This method has the advantage that it can be used for both laboratory animals and human patients or volunteers. However, human studies cannot be used as a routine research tool as they are expensive, time-consuming and have obvious ethical constraints.

Although this pharmacokinetic approach most closely mimics the *in vivo* situation, only limited mechanistic data can be gained from these studies. For instance, the first order absorption kinetics for baclofen following its oral administration to humans is consistent with diffusion-controlled absorption [Faigle *et al.*, 1981]. Meanwhile, the non-linear absorption kinetics for the angiotensin converting enzyme inhibitor, SQ29852, has indicated the importance of a saturable pathway in its oral bioavailability [Moore *et al.*, 1988].

1.4.2 IN SITU MODELS

The animal is anaesthetised, a midline incision is made and the small intestine is exposed. The intestinal segment in which the drug solution is introduced can either be a closed or open loop. In the closed loop model described by Dolusio *et al.* [1969], the ends of an intestinal segment are cannulated and the cannulae are attached to syringes *via* three-way stopcocks. After the intestinal contents have been flushed out, drug solution is introduced into the lumen with the aid of one syringe. At defined time intervals the drug solution is drawn into the second syringe and sampled before the remaining drug solution is returned. In open loop experiments, the drug solution is perfused through the intestine using a pump. Single-pass, re-circulating and oscillating perfusion techniques may be used. The remaining drug concentration in the perfusate can be assayed after defined time periods.

The *in situ* models typically assume the rate of luminal disappearance of a drug equals its absorption rate. If significant binding or metabolism occurs this assumption is not valid. Therefore, in more sophisticated experiments both luminal disappearance and appearance of a drug in the mesenteric blood are monitored. Furthermore, the volume of the luminal contents may change due to net absorption or secretion of water. Transport can be corrected for changes in the luminal concentration of non-absorbable markers (*eg:* PEG_{4000} or inulin) to account for volume effects.

1.4.3 IN VITRO MODELS

1.4.3.1 *EVERTED SACS*

The everted sac technique was developed by Wilson and Wiseman [1954]. The principle advantage of the everted sac, over the uneverted sac, is that the mucosal surface is exposed to a large volume of oxygenated and well-stirred incubation medium.

Briefly, an intestinal segment is excised and everted over a glass rod. The sac is tied off at both ends and the inside (serosal side) filled with incubation medium. The sac is suspended in a mucosal incubation medium at 37°C, containing the compound of interest. The appearance of the compound inside the sac is determined after a single time point. A modification of this technique, the open loop everted gut, was developed by Crane and Wilson [1958]. In this preparation, one end of the sac is ligated and the other is cannulated with polyethylene tubing. Transport experiments are performed as described above. The advantage of the open everted gut, over closed everted sacs, is that it permits sequential sampling from the serosal compartment with time.

Everted sacs are a simple model for the rapid assessment of absorption phenomena. However, epithelial integrity is maintained for short periods of time (< 5 min) and there is total disruption of epithelial tissue after 1 h [Levine *et al.*, 1970]. Moreover, mucosal-to-serosal transport of a compound reflects permeation of the entire gut wall (epithelial + sub-epithelial tissues). Therefore, everted sacs may underestimate the rate of epithelial transport. Despite these disadvantages, everted sacs have been used to predict the permeability characteristics of drug molecules [Chohan and Amaro, 1977].

1.4.3.2 *INTESTINAL RINGS*

Everted intestine is cut into rings (1 to 5 mm) and suspended in an oxygenated medium containing the compound of interest. Large numbers of rings can be incubated simultaneously and the rate of uptake for the compound into the rings can be determined after defined time intervals. They are useful for demonstrating the concentrative uptake of substrates. However, since all surfaces are exposed to the incubation solution it is not possible to demonstrate transport. Moreover, where multiple transporters are present on both surfaces of enterocytes and different locations within sub-epithelial tissues, the contribution of each cannot be determined. Intestinal rings are further restricted by their limited viability (10 to 20 min) [Osiescka *et al.*, 1985].

Despite these limitations, intestinal rings have been used successfully to study the intestinal uptake of 5-fluorouracil [Hastewell, 1986], histidine [Agar *et al.*, 1954] and peptides [Addison *et al.*, 1972].

1.4.3.3 *INTESTINAL SHEETS*

Transport across intestinal sheets can be studied using Ussing chambers [Ussing and Zerahn, 1951]. Briefly, the gut segment is excised, opened longitudinally and mounted between a mucosal and serosal chamber. Both surfaces of the intestinal sheet are bathed in an incubation medium at 37°C. A mixture of 95% O_2 and 5% CO_2 is continuously bubbled through each chamber to ensure tissue oxygenation and minimise unstirred water layers. Intestinal sheet integrity is monitored by measuring the short circuit current across the tissue. The compound of interest is applied to the mucosal surface and the rate of appearance in the serosal compartment is determined.

As with everted sacs, mucosal-to-serosal flux involves transport across epithelial and sub-epithelial layers, therefore, may underestimate the rate of epithelial transport. This problem can be minimised by stripping the sub-epithelial tissue from the gut wall to leave the epithelium, some mucosal connective tissue and the muscularis mucosae intact. Ussing chamber transport studies can be performed across this mucosal sheet [Field *et al.*, 1971].

1.4.3.4 *MEMBRANE VESICLES*

Brush-border membrane vesicles (BBMV) [Hopfer *et al.*, 1973] are most frequently prepared by calcium-precipitation of a homogenate of mucosal scrapings, followed by differential centrifugation [Kessler *et al.*, 1978]. The specific activities of brush-border marker enzymes (*eg:* sucrase) are enriched and the specific activity of basolateral markers (*eg:* Na^+/K^+-ATPase) are reduced with respect to the initial mucosal homogenate. Furthermore, morphological and immunological studies have shown BBMV to have the correct orientation [Haase *et al.*, 1978].

Basolateral membrane vesicles (BLMV) can also be prepared. Using the method of Scalera [Scalera *et al.*, 1980] a specific enrichment (20-fold) of the basolateral membrane marker, Na^+/K^+-ATPase, over the initial homogenate has been reported. However, the correct orientation of BLMV has not been established.

Membrane vesicles offer a number of advantages over whole tissue *in vitro* experiments and have produced significant advances in the understanding of transcellular transport. Firstly, BBMV and BLMV studies enable brush-border uptake and basolateral events in transcellular transport to be dissected. Secondly, uptake and efflux phenomena can be studied over very short incubation periods from a well stirred extravesicular environment. Thirdly, the initial intravesicular and extravesicular conditions can be precisely controlled for mechanistic studies. Therefore, the intracellular and extracellular driving forces for the operation of transport systems can be determined. Finally, membrane vesicles are devoid of cytoplasmic components, therefore, transport mechanism(s) for substrates that are rapidly metabolised in the intact epithelium can be studied (*ie:* membrane and cytosolic events can be separated). However, membrane vesicles have disadvantages which must be considered. Firstly, membrane vesicles are formed by a long procedure using totally artificial solutions and alterations in membrane permeabilities and/or inactivation of transport systems can occur. Unstirred layers may develop inside the vesicles and driving forces for transport systems (*eg:* extravesicular-to-intravesicular sodium gradient) changes with incubation time. Furthermore, the vesicular approach can only describe the membrane events in transepithelial transport. Membrane vesicles provide no information about the overall transepithelial transport mechanism which involves both transcellular and paracellular routes [Murer and Kinne, 1980].

1.4.3.5 *ISOLATED ENTEROCYTES*

A major disadvantage of intact mucosal preparations, even after stripping of muscle layers, is the unfavourable ratio between epithelial and sub-epithelial tissue. Enterocytes, free from sub-epithelial tissue, can be isolated using a range of physical, enzymatic and/or chemical methods [Dawson and Schwenk, 1989]. In this way, uptake mechanisms into the cells primarily involved in absorption can be studied.

However, isolated enterocytes have considerable disadvantages as an absorption model. They have a limited viability and cannot be used for studies of directional flux. Furthermore, both apical and basolateral membranes are simultaneously exposed to the incubation medium, therefore, it is difficult to predict the quantitative importance of each surface for uptake into the cells.

1.4.3.6 *CELL CULTURE MODELS*

In vitro epithelial cell cultures potentially offer many advantages over conventional absorption models [Audus *et al.*, 1990], including (i) rapid assessment of the epithelial permeability of a compound; (ii) the ability to study metabolism of a compound, or activation of a prodrug, during transepithelial transport; (iii) the opportunity to investigate transport mechanisms under controlled conditions; (iv) rapid evaluation of methods for improving drug absorption (*ie:* formulation factors, penetration enhancers or targeting strategies); (v) the opportunity to perform studies using human cells; and (vi) the prospect of minimising expensive, labour intensive and sometimes controversial animal experiments.

Three different approaches have been employed to obtain a cell culture model of the GI epithelium; (i) the separation and culture of normal epithelial cells; (ii) the maintenance of intestinal explants in organ culture; and (iii) the culture of cell lines derived from intestinal adenocarcinomas [Neutra and Louvard, 1989].

Attempts to establish a differentiated intestinal epithelium in primary culture have not been successful. Epithelial cells are easily obtained, however, in culture they have a limited viability and fail to proliferate or re-establish monolayers [Moyer, 1983]. Therefore, a greater understanding of the factors affecting enterocyte differentiation is required before a primary cell culture model of the GI epithelium is a realistic prospect. Consequently, attention has focused on human intestinal adenocarcinoma cell lines, some of which reproducibly display a number of properties characteristic for differentiated intestinal epithelial cells. Recently, intestinal adenocarcinoma cell lines have been classified according to their degree of differentiation [Chantret *et al.*, 1988]. Type 1 cells spontaneously display a highly differentiated phenotype under standard culture conditions (*eg:* Caco-2). Type 2 cells do not differentiate spontaneously, but can be induced to differentiate by substituting glucose for galactose in the culture-medium (*eg:* HT-29). Type 3 cells are organised into polarised monolayers which form domes but are otherwise undifferentiated. Type 4 cells form multilayers of undifferentiated cells. To date, Caco-2 cells are the only cell line to be assigned type 1 status.

1.5 CACO-2 CELLS

Caco-2 cells were isolated from a moderately well-differentiated colonic tumour in a 72 year old male Caucasian and the cell line established using an explant culture technique [Fogh *et al.*, 1977].

Despite their colonic origin, Caco-2 cells display morphological and functional enterocyte-like differentiation under standard culture conditions [Pinto *et al.*, 1983]. They display asymmetric morphology with discrete apical and basolateral domains separated by tight junctional complexes. The apical membrane is distinguished by a brush-border of microvilli which have two distinct orientations; (i) dense and carpet-like and (ii) flower-like clustered arrangements. The functional enterocyte-like differentiation is characterised be high level expression of brush-border hydrolases. After 19 d of culture, the levels of alkaline phosphatase, aminopeptidase, sucrase isomaltase are approximately 50%, 10% and 50% of those in similar preparations of the human small intestine. In contrast, very low levels of these hydrolases were present in colonic mucosa and undifferentiated HT-29 cells [Pinto *et al.*, 1983]. Subsequently, Caco-2 cells have been shown also to express dipeptidylpeptidase IV, gamma-glutamyltransferase, lactase-phlorizin hydrolase, maltase, and trehalase [Hauri *et al.*, 1985; Blais *et al.*, 1987; Yoshioka *et al.*, 1991]. In addition, they are able to synthesise and secrete lipoproteins [Traber *et al.*, 1987].

Dome formation by post-confluent Caco-2 monolayers [Pinto *et al.*, 1983] provided the first evidence for vectorial transport by these cells. It is generally assumed that dome formation by epithelial cell lines is due to the local accumulation of electrolytes and water between the cell monolayer and culture surface as a result of their polarised transport. This assumption was based on the observations that dome formation by the MDCK cell line was inhibited by ouabain [Leighton, *et al.*, 1970; Abaza, *et al.* 1974] and did not occur on permeable-supports [Leighton, *et al.*, 1970; Abaza, *et al.* 1974; Cereijido *et al.*, 1978; Rabito, *et al.*, 1978]. However, dome formation by Caco-2 monolayers is not ouabain-sensitive and domes can form on 0.015 μm, but not 0.030 μm, permeable-supports. These observations suggest that dome formation by Caco-2 monolayers is not simply due to electrolyte and water transport but probably involves species with an effective hydrodynamic radius between 0.015 and 0.030 μm [Raymond *et al.*, 1985].

In light of their polarised morphology and their ability to form domes, Pinto proposed that the suitability of Caco-2 monolayers as an *in vitro* model of a transporting epithelium should be investigated [Pinto *et al.*, 1983]. Subsequently, a number of specific mechanisms for known substrates of carrier-mediated intestinal absorption have been described in Caco-2 cells. Nutrient carriers include those serving amino acids [Hidalgo and Borchardt, 1990 a; Nicklin, *et al.*, 1992 a; Smith *et al.*, 1991; Souba *et al.*, 1992], bile salts [Hidalgo and Borchardt 1990 b], calcium [Giuliano and Wood, 1991], dipeptide analogues [Dantzig and Bergin, 1990, Dantzig *et al.*, 1992;

Inui *et al.*, 1992], folate [Vincent *et al.*, 1985], hexoses [Blais *et al.*, 1987; Riley *et al.*, 1991], inorganic phosphate [Mohrmann *et al.*, 1986], iron [Alvarez-Hernandez *et al.*, 1991] and vitamin B_{12} (cobalamin, Cbl) [Dix *et al.*, 1990]. Furthermore, amino (and imino) acid, cobalamin, hexose and peptide transport are considered in detail below (see sections 1.5.1, 1.5.2, 1.5.3 and 1.5.4, respectively).

1.5.1 AMINO ACID TRANSPORT

Evidence in the literature suggests that Caco-2 cells express multiple carrier-systems for amino acids. Amino acid transport across Caco-2 monolayers was first demonstrated using electrophysiological techniques [Grasset *et al.*, 1984]. The application of L-alanine to Caco-2 monolayers, cultured on permeable-supports and mounted in Ussing chambers, produced a small concentration-related increase in transepithelial potential difference and short circuit current. This suggests that Caco-2 cells express an electrogenic transport pathway for L-alanine. However, the limiting sensitivity for this technique did not permit a detailed characterisation of the carrier. Subsequently, the high temperature-sensitivity of radiolabelled L-alanine transport across Caco-2 monolayers [Cogburn *et al.*, 1991] has been offered for evidence of its carrier-mediated transport. However, while temperature-dependence is a characteristic of carrier-mediated transport, by itself it cannot be considered conclusive.

The large neutral amino acid, L-phenylalanine, also undergoes carrier-mediated transport across Caco-2 monolayers [Hidalgo and Borchardt 1990 a]. The kinetic parameters for L-phenylalanine transport and its cross-inhibition profile suggest its transporter is distinct from the L-proline carrier (see below). Firstly the Michaelis constant (K_m) for the transcellular transport of L-phenylalanine (0.56 mM) is an order of magnitude greater than that for L-proline (5.28 mM) uptake. Secondly, the activation-energy of 50.4 kJ mol^{-1} for L-phenylalanine transport was lower than that for L-proline uptake. Finally, L-phenylalanine transport is inhibited by other large neutral amino acids (*eg:* L-leucine, L-tryptophan, L-tyrosine), but not by acidic (*eg:* L-aspartate) or small neutral (*eg:* glycine) amino acids. Moreover, the so called Large Neutral Amino Acid (LNAA)-transporter was highly stereoselective. Interestingly, L-phenylalanine transport was reduced 33% by 100 μM ouabain implying a sodium-dependent transport mechanism. However, in an earlier communication the same workers reported that its transport was not reduced from sodium-free (chloine chloride) incubation medium or by 2-5 mM ouabain, suggesting a sodium-independent pathway. Their initial observations agree with results for L-phenylalanine uptake into [Nicklin *et al.*, 1992 a] and transport across [Dr Ian Hassan, Ciba Pharmaceuticals, personal communication] Caco-2 monolayers in independent laboratories.

The anti-hypertensive drug, L-alpha-methyldopa, was shown to inhibit L-phenylalanine transport across Caco-2 monolayers [Hidalgo and Borchardt 1990 a]. Subsequently, the same research group demonstrated it to be a substrate for the LNAA-transporter [Hu and Borchardt, 1990]. The transport of L-alpha-methyldopa was concentration- (K_m = 0.70 to 1.97 mM), energy-, glucose- and pH-dependent and was significantly reduced by L-phenylalanine and L-lysine but not L-aspartate or L-proline. Despite demonstrating the influence of a wide range of variables on L-alpha-methyldopa transport *via* the LNAA-transporter, the requirement for sodium ions or ouabain-sensitivity was not reported.

Recently, the same group have shown that both the Ap and Bl uptake of L-phenylalanine are saturable [Hu and Borchardt, 1992]. The uptake affinity constants for Ap and Bl uptake (2.7 mM, 0.18 mM, respectively) were markedly different and had distinct cross-inhibition profiles. In addition, Ap uptake was sodium-dependent whilst Bl uptake was not. Interestingly, Ap and Bl L-phenylalanine efflux from Caco-2 cells was non-saturable. Kinetic analysis of Ap uptake and Bl efflux events suggests that Bl efflux would be the rate-limiting step in the Ap-to-Bl transepithelial transport of L-phenylalanine.

An amino (and imino) acid carrier which mediates L-proline uptake into Caco-2 cells has been reported [Nicklin *et al.*, 1992 a]. This carrier is sodium-dependent, has an affinity constant for L-proline of 5.28±0.83 mM and an activation-energy of 93.5 kJ mol^{-1}. Furthermore, in cross-inhibition studies L-proline was inhibited by small neutral amino acids (*eg:* L-alanine and L-serine) and the synthetic substrates, alpha-aminoisobutyric acid and MeAIB, but not by acidic (*eg:* L-aspartate) or large neutral (*eg:* L-phenylalanine) amino acids. These uptake characteristics are consistent with L-proline uptake being mediated *via* the A-carrier system. This recent report probably represents a detailed characterisation of the transport pathway which serves L-alanine.

Recently, a sodium-dependent uptake pathway for L-glutamine (K_m = 276±29 μM, V_{max} = 3427±783 pmol (mg protein)$^{-1}$ min^{-1}) has been reported in Caco-2 cells

[Souba *et al.*, 1992]. The sodium-dependent glutamine uptake is reduced by interferon and dexamethasone [Souba *et al.*, 1992].

Finally, a preliminary report has suggested that glycine is actively transported across Caco-2 monolayers *via* the gamma-glutamyl cycle [Smith *et al.*, 1991]. This conclusion was based on the suppression of glycine transport by a known inhibitor of gamma-glutamyl transpeptidase, serine-borate complex. However, this thesis awaits confirmation by further work with a more rigourous experimental design.

1.5.2 COBALAMIN TRANSPORT

Cobalamin (Cbl; vitamin B_{12}) absorption from the GI tract occurs *via* a receptor-mediated process. Cbl is released from dietary sources in the stomach where it binds intrinsic factor (IF) which is secreted by gastric parietal cell. When the IF-Cbl complex reaches the distal ileum, it binds to specific receptors which are located at the intermicrovillus pits of the enterocytes. After a delay of several hours, Cbl appears in the portal circulation bound to transcobalamin II (TCII) [Chanarin *et al.*, 1970]. The formation of the IF-Cbl complex [Allen *et al.*, 1978] and its binding to the ileal receptor [Levine *et al.*, 1984] are well-characterised. However, the subsequent events in transepithelial transport are poorly understood. This is in part due to the lack of a suitable model for mechanistic studies.

Caco-2 cells cultured on plastic specifically bind and internalise IF-[^{57}Co]Cbl complexes in a temperature-dependent fashion. Furthermore, Caco-2 monolayers cultured on permeable-supports specifically transport [^{57}Co]Cbl with an overall vector in an Ap-to-Bl direction. However, the size-exclusion chromatography elution-profile of the [^{57}Co]Cbl entering the Bl receiver-solution was not consistent with IF-[^{57}Co]Cbl which was applied to the Ap surface. In fact, [^{57}Co]Cbl co-elutes with a complex formed between [^{57}Co]Cbl and a Cbl-binding protein secreted from the Bl surface of Caco-2 cells. This Cbl-binding protein was recognised by TCII-antiserum [Dix *et al.* 1990]. The work by Dix *et al.* provided the first direct evidence that cells of intestinal origin take up Cbl at the Ap surface as IF-Cbl but export it from their Bl surface as a Cbl-TCII complex. This significant observation has been confirmed by independent laboratories [Ramanujam *et al.*, 1991].

Subcellular fractionation of Caco-2 cells has identified the endoplasmic reticulum and golgi apparatus as the major biosynthetic compartment for TCII in Caco-2 cells. These studies also showed that TCII is associated with a light-vesicular fraction. It was postulated that these vesicles are important in the trafficking of TCII from the golgi to the basolateral domain for polarised secretion. Indeed, this vesicular pathway may be important in the transcytosis of Cbl [Hassan *et al.* 1991]. These preliminary data from the Caco-2 system suggest it will be a useful experimental tool for elucidating the precise transcellular transport-mechanism of Cbl.

1.5.3 HEXOSE TRANSPORT

Using radiochemical tracer flux measurements of a non-metabolisable D-glucose analogue, alpha-methylglucoside (alpha-AMG), Blais *et al.* [1987] demonstrated the presence of a sodium-dependent hexose-transporter in the Caco-2 cell line. Alpha-AMG uptake, into Caco-2 cells cultured on plastic, was described by a non-saturable, phlorizin-insensitive (diffusional) component and a single saturable pathway (carrier-mediated; $K_m = 3.1 \pm 0.2$ mM and $V_{max} = 13.2 \pm 0.5$ nmol (mg protein)$^{-1}$ (30 min)$^{-1}$). Carrier-mediated alpha-AMG uptake was totally inhibited by equiosmolar substitution of sodium chloride for choline chloride in the incubation medium and by 200 µM phlorizin but only partially (~60%) by 200 µM phloretin. In the same study, workers demonstrated carrier-mediated D-glucose uptake into BBMV prepared from the human foetal colon. This carrier was sodium-dependent and totally inhibited by phlorizin (200 µM) and phloretin (1000 µM). Therefore, Caco-2 cells express a hexose-transporter that shares many properties with that present in the human foetal colon.

Subsequently, D-[^{14}C]glucose was shown to be transported across Caco-2 monolayers at a greater rate than that predicted for passive transport based on its physico-chemical properties [Hilgers *et al.*, 1990]. Furthermore, using electrical measurements, the presence of an electrogenic, sodium-dependent, phlorizin-sensitive and stereoselective D-glucose transport pathway was confirmed [Riley *et al.*, 1991]. This electrogenic transport was only observed following application of D-glucose to the Ap surface of Caco-2 monolayers suggesting the transport system operates in a vectorial fashion. In these studies, the Ap-to-Bl transport affinity constants for three hexoses were reported (glucose, $K_m = 2.44 \pm 0.52$ mM; galactose, $K_m = 8.05 \pm 1.33$ mM and 3-O-methylglucose, $K_m = 22.0 \pm 5.2$ mM) were in the same rank order as reported for transport across the rat jejunum. Interestingly an earlier report, employing similar techniques, failed to show electrogenic D-glucose transport across Caco-2 monolayers [Grasset *et al.*, 1984]. The reason for this discrepancy is not known.

Recently, Caco-2 cells have been shown to express high levels of the facilitated D-glucose transporters GLUT1, GLUT3 and GLUT5. GLUT1 is localised at the basolateral membrane, GLUT3 is localised at the apical membrane whereas GLUT3 is associated with both apical and basolateral membranes [Harris *et al.*, 1992].

1.5.4 PEPTIDE-TRANSPORT

There is a convincing body of evidence that the Caco-2 cell line possesses a small-peptide transporter. The expression of a dipeptide-transporter by the Caco-2 cell line was first postulated by Dantzig and Bergin [1988 a, 1988 b]. They showed that the uptake of the cephalosporin antibiotic, D-cephalexin, was described by a non-saturable (diffusional; K_d = 0.05 nmol min^{-1} (mg protein)$^{-1}$ mM^{-1}) pathway and a single saturable pathway (carrier-mediated; K_m = 15.86±1.5 mM and V_{max} = 5.84±1.5 nmol min^{-1} (mg protein)$^{-1}$). Furthermore, in sodium-free conditions 1 mM D-[^{14}C]cephalexin uptake was inhibited by a range of dipeptides (50 mM; 80 to 90 %), cefaclor (30 mM) and the organic anion p-aminohippurate (50 mM) but not by amino (and imino) acids (50 mM). D-Cephalexin uptake was concentrative (1.8-fold steady state intracellular accumulation), maximal at pH6.0 and stimulated 30 to 40% in the presence of sodium ions. Moreover, the initial rate of D-cephalexin uptake was not inhibited by a pre-incubation with amiloride, oligomycin, ouabain or potassium cyanide. In their subsequent publication, Dantzig and Bergin extended their work on the factors affecting cephalexin uptake into Caco-2 cells but contradicted some of their earlier observations. In agreement with their previous assertions, cephalexin uptake was concentrative (3.5-fold steady state intracellular accumulation), pH-sensitive (maximal at pH6.0) and inhibited by a range of dipeptides (10 mM; 47 to 84%) and cefaclor (30 mM; 76%) but not amino acids (10 mM). L-Cephalexin was a more potent inhibitor than D-cephalexin suggesting the carrier is stereoselective. In addition, kinetic analysis of the concentration-dependent D-cephalexin uptake predicted a single carrier-mediated mechanism superimposed on a non-saturable uptake. However, the kinetic parameters for these pathways were quantitatively different to those reported previously. The diffusional component was approximately 4-times higher (K_d = 0.18±0.01 versus 0.05 nmol min^{-1} (mg protein)$^{-1}$ mM^{-1}) and the carrier-mediated uptake affinity constant was 2-fold higher (K_m = 7.5±2.8 versus 15.86±1.5 mM). Interestingly, the competitive inhibition of p-aminohippurate [Dantzig and Bergin, 1988 a] was not reported in the final publication which states that organic anions do not inhibit cephalexin uptake [Dantzig and Bergin, 1990]. Recently, Dantzig *et al.* have shown that cefaclor uptake into Caco-2 monolayers is mediated by the same proton-dependent dipeptide-carrier as cephalexin [Dantzig *et al.*, 1992].

The carrier-mediated uptake of cephalexin into Caco-2 cells has been confirmed in independent laboratories [Gochoco *et al.*, 1991 a and b]. Moreover, these workers have investigated the factors affecting cephalexin transport. Cephalexin uptake into, and transport across Caco-2 monolayers was pH-sensitive. Steady state accumulation of cephalexin at pH6.0 was approximately 10-fold higher than at pH7.2 [Gochoco *et al.*, 1991 a]. Furthermore, the rate of Ap(pH5.0 to 6.5)-to-Bl(pH7.4) cephalexin transport was twice that of Ap(pH7.0 to 7.4)-to-Bl(pH7.4) transport [Gochoco *et al.*, 1991 a]. Meanwhile, the Ap-to-Bl transport of the passive permeability marker, D-mannitol, was not influenced by pH. Bl-to-Ap cephalexin transport was not pH-dependent. In the presence of an Ap(pH5.5 to 6.0)-to-Bl(pH7.4) proton gradient, the rate of Ap-to-Bl transport occurred at 4-times that of Bl-to-Ap transport [Gochoco *et al.*, 1991 c]. These observations suggest the cephalexin transporter in Caco-2 cells is located at the Ap surface.

Recently, a carrier-mediated uptake and transport of cephradine *via* a peptide-transporter by Caco-2 monolayers has been reported [Inui *et al.*, 1992]. Cephradine uptake occurs preferentially at the Ap surface, is maximal at pH6.0 and is markedly reduced at 4°C. Moreover, uptake is saturable (K_m = 8.3 mM) and is inhibited by a range of peptides, but not glycine. Similarly, cephradine transport is vectorial (Ap-to-Bl > Bl-to-Ap), is pH-dependent (maximal at pH6.0 to 6.5) and is selectively inhibited by a range of dipeptides. These workers also considered the kinetics and polarity of cephradine efflux from pre-loaded Caco-2 cells. Efflux occurs at a greater rate from the Bl pole and is markedly reduced at 4°C. The authors claim this to be the first demonstration of a specific Bl efflux mechanism for cephalosporins, however, further work is required to verify their conclusion.

Thyrotrophin-releasing hormone, TRH, is absorbed from the GI tract of dogs, humans and rats *via* a peptide-transporter [Yokohama *et al.*, 1984 a and b]. A preliminary report proposed a passive paracellular pathway for TRH transport across Caco-2 monolayers [Lundin *et al.*, 1991]. However, in the absence of supportive experimental data this hypothesis was highly speculative. In a more detailed study, evidence for a minor carrier-mediated pathway superimposed onto a major passive transport component was presented [Nicklin *et al.*, 1991]. For instance, TRH transport was saturable (~30%), inhibited by D-cephalexin and vectorial (Ap(pH6.0)-to-Bl(pH7.4) > Bl(pH6.0)-to-Ap(pH7.4)).

One common theme for the carrier-mediated peptides in the Caco-2 model is that the uptake mechanism is more clearly defined than the transport pathway. This probably reflects poor Bl efflux of these small peptides and/or the relative importance of the passive paracellular pathway component compared to the transcellular carrier-mediated transport.

In addition to the study of carrier-mediated peptide transport, Caco-2 monolayers have been employed for mechanistic studies of passive peptide transport. The molecular features controlling the transepithelial transport of peptides has been studied using a series of compounds prepared from one glycine (or equivalent) and one to three D-phenylalanine residues [Conradi *et al.*, 1991]. Whilst there is a correlation between the log distribution-coefficient (Log D) and passive transport across Caco-2 monolayers for low molecular weight, non-peptide, molecules [Artursson and Karlsson, 1991] no such correlation is apparent for this series of peptides. However, a strong correlation between the theoretical hydrogen-bonding potential of peptides in this series and their transport across Caco-2 monolayers was established [Conradi *et al.*, 1991]. This hypothesis was supported by subsequent work with a range of tetrapeptide analogues based on CH_3CO-[D-phe]$_3$-NH_2 and being sequentially methylated at none to all four of its amide nitrogens [Conradi *et al.*, 1992]. N-methylation increased the log distribution coefficient from 2.30 (non-methylated) to 3.24 (tetra-methylated). However, this increase is small in comparison to the >50-fold higher monolayer permeability for the tetra-methylated analogue over the parent oligopeptide. The primary effect of amide-nitrogen methylation in small peptides is to reduce their hydrogen-bonding capacity. This supports the theory that the hydrogen-bonding potential of a peptide molecule to water, hence, its desolvation energy for partitioning into a biological membrane, is an important determinant of peptide transport across epithelia. These studies were performed using a neutral series of closely related peptides, it will be interesting to investigate whether this correlation is true for a diverse range of compounds.

Recently, Burton *et al.* [1993] have demonstrated the presence of a polarised efflux system for peptides in the apical membrane of Caco-2 cells. The rate of Bl-to-Ap transport of AcPhe(MePhe)$_2$NH$_2$ was greater than that for its Ap-to-Bl transport. The rate of Ap-to-Bl transport also increased as the Ap concentration of AcPhe(MePhe)$_2$NH$_2$ was increased. This is consistent with a saturation of efflux-pump which is located at the Ap surface. Moreover, the rate of Ap-to-Bl transport for AcPhe(MePhe)$_2$NH$_2$ is increased by verapamil. These data are consistent with a P-glycoprotein mediated efflux mechanism for peptides in Caco-2 cells.

1.5.5 PASSIVE TRANSPORT ACROSS CACO-2 MONOLAYERS

The ability of a compound to diffuse passively across a Caco-2 monolayer is conveniently expressed as its apparent permeability coefficient (P_{app}). A compound with a rapid flux rate has a high P_{app}. P_{app} values presented in this thesis were calculated according to Equation 1.3 [Artursson and Magnusson, 1990] which can be derived from Fick's Law in the following manner.

EQUATION 1.1 $$dQ/dt = D \cdot A \cdot (C_0 - C_1/dx)$$

where, dQ/dt is the number of moles of a permeant, with a diffusion coefficient D, crossing an area A in the time dt in proportion to a concentration difference (C_0-C_1) over a distance dx. The ratio of the diffusion coefficient (D) to the distance travelled by a permeant (dx) represents the P_{app} [cm s^{-1}], that is;

EQUATION 1.2 $$P_{app} = D/dx$$

Furthermore,if sink conditions prevail and a small proportion of the permeant has been transported, then $C_0 - C_1 \approx C_0$ (initial concentration).

EQUATION 1.3 $$P_{app} = dQ/dt \cdot (1/(A \cdot C_0))$$

Where,	P_{app}	= Apparent permeability coefficient [cm s^{-1}]
	dQ/dt	= Rate of appearance in receiver-solution [moles s^{-1}]
	C_0	= Initial concentration in donor solution [moles ml^{-1}]
	A	= Area of permeable-support [cm^2]

There is significant interest in the potential application of Caco-2 monolayers as a predictive model for the oral bioavailability of new chemical entities to help select suitable drug candidates for development (*ie:* an *in vitro* absorption screen). This attention has stemmed from the relative simplicity, inexpense and rapidity of this technique compared to *in vivo* or *in situ* laboratory animal studies. The first reported correlation between passive transport and the extent of absorption in humans showed that compounds which were well absorbed in humans *in vivo* (*eg:* clonidine, diazepam) were transported across Caco-2 monolayers at a much greater rate than those with very low oral bioavailabilities (*eg:* D-mannitol, PEG_{4000}) [Cogburn *et al.*, 1989]. In addition, a good correlation has been demonstrated between drug absorption rate constants in the Caco-2 model and the *in situ* rat intestinal model for a homologous series of ß-blocking drugs [Artursson, 1990]. Subsequently, a good correlation between the apparent permeability coefficients of a physico-chemically diverse range of drug molecules across Caco-2 monolayers and their oral bioavailabilities in humans has been reported (Fig. 1.5 [Artursson and Karlsson, 1991]). In this correlation, permeants can be classified into three categories. Drugs which are completely absorbed in humans have a permeability coefficient >1.0 x 10^{-6} cm s^{-1}, those which are partially absorbed (1 to <100%) have permeability coefficients between 1.0 x 10^{-7} and 1.0 x 10^{-6} cm s^{-1} and compounds that are very poorly absorbed *in vivo* have permeability coefficients less than 1.0 x 10^{-7} cm s^{-1}. This correlation is reliable for an extended range of compounds [Dr Ian Hassan, Ciba Pharmaceuticals, unpublished observations] suggesting Caco-2 monolayers may be a useful *in vitro* screen for the extent of oral absorption.

FIGURE 1.5 *Correlation between the passive transport of drug compounds across Caco-2 monolayers and their oral absorption in humans.*

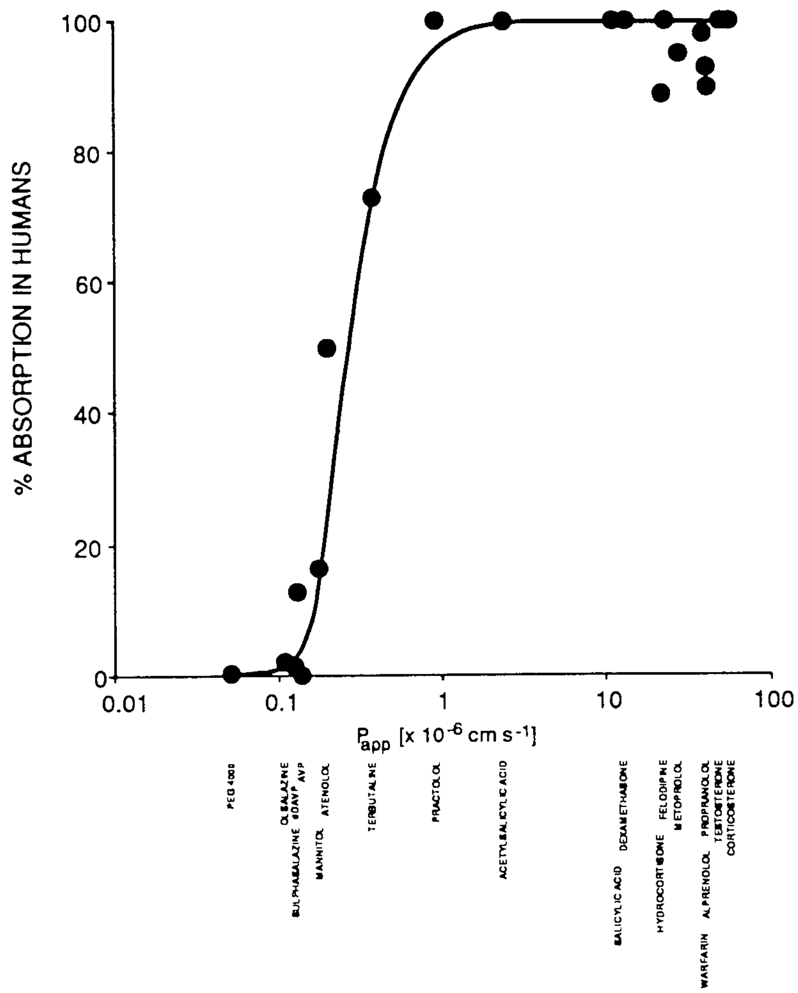

In addition to predicting the extent of absorption, Caco-2 monolayers have been used to dissect the route (*ie:* paracellular versus transcellular) of transcellular transport for drug molecules. Using a calcium-switch technique the permeability of Caco-2 monolayers can be modulated [Artursson and Magnusson, 1990]. Electron microscopy has confirmed that the reduced transepithelial electrical resistance measurements under low calcium conditions results from a reversible separation of the tight junctional complexes between cells. Therefore, under low extracellular calcium conditions the capacity of the paracellular pathway is increased. The calcium switch method had a differential effect on the apparent permeability coefficients for a series of ß-blocking agents with a range of lipophilicities (propranolol (lipophilic; Log D = 1.19 to atenolol (hydrophilic; Log D = -2.14)). The transport of atenolol was increased 7.15-fold in low calcium conditions whereas that of propranolol was unaffected. This suggests that the paracellular pathway is important for atenolol but is of minor importance for propranolol transport. It was concluded that the calcium switch technique could be used to assess the importance of the paracellular pathway in the transepithelial transport of a permeant.

1.5.6 UNSTIRRED WATER LAYER EFFECTS

An unstirred water layer (UWL) adjacent to the surface of the cell membrane can be a significant barrier to the absorption of drugs and nutrients [Barry and Diamond, 1984]. Whether or not the UWL is the rate-determining step in the absorption for a permeant depends on its ability to penetrate the cellular barrier. Permeants that rapidly penetrate the cellular barrier may be wholly or partly controlled by the UWL.

Recently, transport studies have been performed using Caco-2 monolayers cultured on permeable-supports and mounted into side-by-side diffusion cells with gas-lift stirring [Hidalgo *et al.*, 1991]. In these studies, stirring had no influence on the P_{app} of a hydrophilic permeant (D-mannitol) but increased the P_{app} of a lipophilic permeant (testosterone). These observations suggest that the UWL is an important determinant of testosterone transport. The same research group generated corroborative data using a diffusion chamber with mechanical stirring of both donor and receiver chambers [Shah *et al.*, 1990]. However, these two diffusion-systems require specialised apparatus and are more time-consuming than the conventional Caco-2 transport model. Karlsson and Artursson [1991] have developed an alternative method which involves agitating the conventional Caco-2 transport model on an ELISA-plate shaker. Agitation increases the apparent permeability coefficients for rapidly transported lipophilic compounds (*eg:* testosterone, corticosterone and propranolol) but not for poorly transported hydrophilic compounds (*eg:* salicylate, D-mannitol and sulphasalazine). This agitation technique is simple and does not require specialised diffusion cells. Moreover, it can provide useful information about the rate-limiting steps in transepithelial transport. For instance, it can be used to quantify the relative contributions of the cell monolayer (P_c) and UWL (P_{aq}) permeability coefficients in the overall apparent permeability coefficient (P_{app}).

The influence of the UWL on the transport of rapidly transported lipophilic compounds across Caco-2 monolayers has been firmly established. It is envisaged that the use of stirred diffusion-chambers or agitated systems will be used routinely for transport studies with increasing frequency.

1.5.7 METABOLISM

Metabolism is a potentially important determinant of transepithelial transport. Indeed there is evidence that intestinal enterocytes possess the machinery to perform oxidative (phase I) [Kolars *et al.*, 1992] and conjugative (phase II) [Goon and Klaassen, 1990] metabolism.

Early characterisations of Caco-2 cells demonstrated the expression of brush-border hydrolases, including alkaline phosphatase, aminopeptidase N and sucrase-isomaltase [Pinto *et al.*, 1983], suggesting they had catabolic potential. However, most of the compounds used in uptake or transport studies have been selected for their metabolic stability or have been shown to remain intact during uptake or transepithelial transport. Consequently, metabolic transformations of xenobiotics by Caco-2 cells has received relatively little attention.

Most of the metabolic transformations performed by Caco-2 cells have been studied using Caco-2 cell homogenates or enzyme extractions. Using these systems catabolic pathways for thyroxine [Lee *et al.*, 1989] vitamin A [Quick and Ong, 1990] and an inducible metabolism of vitamin D [Tomon *et al.*, 1990] have been reported. Recently, the possibility of phase II metabolic reactions (sulphation and glucuronidation) in by Caco-2 cells has been investigated [Baranczyk-Kuzma *et al.*, 1991]. A temporal-dependent expression of phenol sulphotransferase (EC 2.4.2.1) was reported. This enzyme catalyses the sulphation of p-nitrophenol and catecholamines (*eg:* dopamine). No UDP-glucuronyltransferase (EC 2.4.1.17) activity was detected in Caco-2 cells. Although cell homogenate or enzyme extract experiments are a convenient investigating the metabolism of a compound, their relevance to the metabolism of compounds during transepithelial transport remains to be established.

Reports of metabolism during uptake and transepithelial transport are sparse. Even in the case of peptides, where mucosal metabolism may constitute a formidable barrier to transport, the metabolic capacity of Caco-2 cells has not been investigated in detail. Preliminary results from our laboratories have demonstrated peptidase activity in 21 d Caco-2 monolayers using a specific high-performance liquid chromatography assay for phenylalanylglycine and its constituent amino acids [Holbrook, 1992]. Phenylalanine was detected in the basolateral chamber 1 h the apical application of L-phenylalanylglycine. Therefore, L-phe-gly is hydrolysed during transport across Caco-2 monolayers [Holbrook and Nicklin, Aston University, unpublished observations]. Similarly the degradation of a 40 kDa protein, horse-radish peroxidase (HRP), during transport across Caco-2 monolayers has been reported [Heyman *et al.*, 1990]. Using radionuclide ([^{125}I]HRP) and enzymatic assays in parallel, the total (degraded and intact) and enzymatically active (intact) HRP fluxes across Caco-2 monolayers were quantified. It was concluded that there were two functional pathways for HRP transport; a minor direct pathway allowing transport of intact protein and a major lysosomal degradative pathway. In addition, radiolabelled inulin, a high molecular weight polysaccaride extracellular marker, is degraded by Caco-2 cells during transport so that the radioactivity transported across the monolayers is in the form of monosaccarides [Hassan, 1990]. Therefore, radiolabelled inulin is not suitable as a permeability marker for Caco-2 transport studies. Another marker, radiolabelled polyethylene glycol 4000 (PEG_{4000}), is not degraded therefore is a superior permeability marker.

Clearly, further studies are required to quantify the importance of metabolic transformations by Caco-2 monolayers during transepithelial transport.

1.5.8 LECTIN BINDING

The legume lectins, *Phaseolus vulgaris* agglutinin E4 and L4 (red kidney bean; PHA-E4 and PHA-L4), *Glycine max* agglutinin (soybean; SBA), *Vicia faba* agglutinin (broad bean; VFA) and *Pisium sativum* agglutinin (garden pea; PSA), bind to the apical surface of intact Caco-2 cells and their purified brush-border membranes [Koninks *et al.*, 1992]. These lectins have a range of dissociation constants for binding to purified brush-border membranes (PHA-E4 ($0.11 \pm 0.08 \times 10^{-5}$ M) > PHA-L4 > SBA > VFA > PSA ($1.69 \pm 0.17 \times 10^{-5}$ M)). This sequence correlates with the intensity of fluorescein isothiocyanate (FITC)-conjugated lectin binding to intact Caco-2 cells. FITC-PHA-E4 exhibit dense and localised surface staining, whereas FITC-PSA produces a diffuse staining of low intensity. Interestingly, the dissociation constant for lectin-Caco-2 binding also correlates with the ability of each lectin to influence cellular metabolism (see below). In addition to surface binding, lectins are also internalised by Caco-2 cells [Hendricks *et al.*, 1991]. After a 30 min incubation with ferritin-conjugated PHA-E4 and PHA-L4, ferritin particles can be visualised extracellularly on Caco-2 microvilli and intracellularly in apical invaginations and vesicles.

Lectins are not inert ligands. They induce actin-cytochemical lesions and influence cellular metabolism [Draaijer *et al.*, 1989]. A 48 h incubation of Caco-2 cells with with PHA-E4 increases the globular : filamentous actin ratio (*ie:* actin depolymerisation) and is associated with microvilli shortening and an increase in the incidence of extracellular vesicles adjacent to the brush-border. Interestingly, the legume lectins have a differential ability to cause actin-cytoskeleton lesions. PHA-E4, SBA and VFA incubations result in significant microvilli shortening, whereas PHA-L4 and PSA have no effect. Similarly, lectins have a differential effect on cellular metabolism [Hendricks *et al.*, 1991]. Stimulation of thymidine (DNA turnover), fructose and glucosamine (glycoprotein synthesis) incorporation is observed following exposure to PHA-E4, PHA-L4 and SBA. VFA has no effect, whereas PSA is inhibitory. Clearly, PHA-E4, PHA-L4 and SBA stimulate glycoprotein synthesis. However, since uridine incorporation (RNA synthesis) is not up-regulated in parallel, the cellular effects of lectins must be mediated at the translational, rather than transcriptional, level.

These initial reports describing lectin binding to, uptake into and effects on Caco-2 cells are consistent with *in vivo* data. For instance, lectins induce cytochemical brush-border lesions and experience endocytic uptake in rat intestinal cells [Lorenzsonn and Olson, 1982]. These similarities suggest Caco-2 monolayers may represent a suitable model for investigating the uptake and transport of lectins as well as their metabolic effects on the GI epithelium.

1.5.9 BACTERIAL ADHESION

An important factor in the GI pathogenicity of microorganisms is their ability to adhere to, and colonise, cell surfaces and invade the epithelium. Presently, there is considerable interest in the potential of Caco-2 monolayers for investigating initiation of the pathogenic process during infection of the GI epithelium. Indeed, they have been used to study the pathogenic processes for several bacteria including the adhesion of enteropathogenic *Escherichia coli* (EPEC) [Knutton *et al.*, 1989] and enterotoxic *Escherichia coli* (ETEC) [Darefeuille-Michaud *et al.*, 1990], and invasion by *Listeria monocytogenes* [Gaillard *et al.*, 1987] and *Salmonella typhimurium* [Finlay and Falkow, 1990].

An excellent correlation has been established between adhesion of ETEC strains to the brush-borders of Caco-2 cells and human enterocytes. In one study, adhesion of ETEC strains expressing colonisation factor antigens I, II, III or antigen 2230 to a range of cell lines, HeLa, Hep-G2, HRT 18, HuTu 80, MDBK, MDCK, Vero and Caco-2, was investigated. ETEC strains only adhered to Caco-2 cells. Negative variants, which had been cured of the plasmid encoding the adhesive factor, did not bind to Caco-2 cells. Moreover, pre-treatment of Caco-2 cells with homologous colonisation factor antigen or ETEC with antibodies raised to the adhesive factors prevented adherence [Darefeuille-Michaud *et al.*, 1990]. Therefore, adhesion apparently occurred *via* a specific mechanism and it was proposed that Caco-2 cells express receptors for each of the colonisation factor antigens.

In addition, the Caco-2 model is providing useful information about bacterial invasion and spreading mechanisms during listeriosis. Firstly, pathogenic bacteria (*eg: Listeria monocytogenes* and *Listeria ivanovii*), but not the non-pathogenic *Listeria seeligeri*, *Listeria welshimeri* or *Listeria innocua*, were internalised into a membrane-limiting vacuole. Non-haemolytic strains of *Listeria monocytogenes* are retained within this vacuole and cannot replicate intracellularly. In contrast, the haemolytic variant, which produces a membrane-damaging cytotoxin (listeriolysin-O), is released in the cytoplasm where it replicates rapidly. These reports suggest listeriolysin-O is an important determinant of intracellular replication and virulence [Gaillard *et al.*, 1987]. Once inside the cytoplasm, *Listeria monocytogenes* becomes enveloped in a thick coat of F-actin. These actin filaments are reorganised to form polar tails, which are associated with listerial motility. The bacteria move into deep lateral protrusions into neighbouring cells. Ultimately, a bacterium contained within a limiting double membrane is released into the adjacent cell. Lysis of the limiting-double membrane releases the bacteria into the cytoplasm of its new host cell. It was postulated that the interaction between cytoplasmic *Listeria monocytogenes* with the host-cell microfilament network may permit cell-to-cell tissue colonisation during listeriosis [Gaillard *et al.*, 1987].

Salmonella choleraesuis and *Salmonella typhimurium* have also been shown to exert effects on Caco-2 cells. Both species disrupt the brush-border microvilli and produce cytoplasmic protrusions at the apical surface. The bacteria entered the cells and are enclosed in membrane-bound vacuoles. Finally, transepithelial electrical resistance is abolished at 3-4 h post-infection suggesting a complete loss of monolayer integrity. The morphological effects of *Salmonella choleraesuis* and *Salmonella typhimurium* are similar to those produced in animal infection models [Finlay and Falkow, 1990].

In addition to bacteria, the intestinal parasite *Giardia duodenalis* [Mange *et al.*, 1991] adheres to the apical surface of Caco-2 cells.

1.6 HETEROGENEITY

The wild-type Caco-2 cell line is phenotypically heterogeneous. The expression of sucrase-isomaltase in the parental population is highly variable [Pinto *et al.*, 1983]. Subsequently, a range of clones (Caco-2/1 to 16) have been isolated which express very different levels of sucrase-isomaltase [Beaulieu and Quaroni, 1991]. Clones Caco-2/15 and Caco-2/3 displayed the highest (273±16.9 munits (mg protein)$^{-1}$) and lowest (24.6±6.2 munits (mg protein)$^{-1}$) levels of sucrase-isomaltase expression, respectively. In addition, the clones differed markedly in their growth rates and the amounts of transforming growth factor-alpha /epidermal growth factor-like activity released into the culture medium. The expression of other intestinal markers (aminopeptidase N, dipeptidylpeptidase IV, lactase, alkaline phosphatase and 'crypt cell antigen') had a much lower variability between clones. A range of clones (Caco-2/1 43), and re-clones (Caco-2/40.1 7), which display very different abilities to transport taurocholic acid, have been isolated [Woodcock *et al.*, 1991]. These clones (and the parental population) have identical growth characteristics but display disparate electrical, functional and morphological properties. One clone which has been studied in detail, Caco-2/40, transports taurocholate at a greater rate than the parental cell line, and is morphologically homogeneous. Furthermore, the properties of Caco-2/40 are stable over an extended number of passages.

Since the wild-type Caco-2 cell line is heterogeneous, the overall characteristics of a monolayer is the product of many phenotypes. Therefore, the isolation of stable clones with distinct properties, highlights the prospect of optimising the Caco-2 model for transport studies.

1.7 ARE CACO-2 CELLS ABSORPTIVE CELLS?

Caco-2 cells bear similarities to human small intestinal enterocytes with respect to their morphology and the expression of brush-border membrane hydrolases. Furthermore, they are a population of exponentially dividing undifferentiated cells and differentiation commences upon cessation of cell division. This sequence of the differentiation process mimics the situation present in the small intestine. That is, the dividing intestinal crypt cells are undifferentiated and differentiation occurs during migration of non-dividing cells along the crypt-to-villus axis. This analogy is limited by the fact that Caco-2 cells are malignant and have a colonic origin. It has been proposed that Caco-2 cells are more closely analogous to cells of the normal foetal colon at 15 weeks of gestation [Neutra and Louvard, 1989]. Indeed, Caco-2 membrane hydrolases are expressed in molecular forms typical of those in foetal tissues [Hauri *et al.*, 1985]. Similarly, the pattern of apolipoprotein secretion and levels of glycogen accumulation are consistent with those of the foetal intestine [Traber *et al.*, 1987]. Finally, the electrical resistance and ion-conductance properties of Caco-2 cells resemble those of colonic crypt cells [Grasset *et al.*, 1984]. However, Caco-2 cells express lactase which is present in the adult small intestine but not in the foetal or colonic epithelium. Clearly, despite their superficial enterocyte-like phenotype, Caco-2 cells are not absorptive cell enterocytes. Therefore, a rational evaluation of their properties is required before Caco-2 monolayers are heralded as a relevant *in vitro* model of the adult human GI epithelium.

1.8 CACO-2 AND HT29GlucH CO-CULTURES

Caco-2 cells secrete mucins, however, the level of secretion is low and is further reduced upon cellular differentiation [Niv *et al.*, 1992]. Consequently, during the window for transport studies (15-28 d) Caco-2 monolayers are devoid of a mucin layer. Whilst this simplifies the the model for mechanistic transport studies, the absence of a mucin layer is thought to detract from Caco-2 monolayers as a realistic model of the GI epithelium.

To address this deficiency, Caco-2 cells have been co-cultured with mucin-secreting HT29GlucH cells [Allen, 1992]. In co-culture, both cell types were morphologically differentiated. Caco-2 cells displayed their typical absorptive cell-like morphology whilst the HT29GlucH exhibited a goblet cell-like phenotype. Histochemical analysis of the co-cultured monolayers showed that the HT29GlucH cells synthesised, stored and secreted both neutral and acidic mucins. Tight junction formation was observed between Caco-2 and HT29GlucH cells by transmission electron microscopy and the co-cultured monolayers had a substantial transepithelial electrical resistance of approximately 200 Ω cm^2. However, despite having a lower transepithelial electrical resistance than the standard Caco-2 model (typically 300 - 450 Ω cm^2) the P_{app} for the transport of a number of drug compounds (*eg:* propranolol, testosterone and warfarin) was lower in the co-culture model. In addition, the calculated aqueous boundary layer thickness (h_{aq}) for testosterone and warfarin was greater in the co-culture system than in Caco-2 monolayers. These observations suggest that an additional factor influences the transport of compounds across the co-culture model and it was postulated that a mucin layer may have been responsible.

One potential problem with the co-culture model is that HT29GlucH cells are present as distinct colonies of cells in a sheet of Caco-2 cells. This is not representative of the *in vivo* situation where goblet cells are present as unicellular glands within the GI epithelium. Although this co-culture system is in its infancy, the preliminary results are very encouraging and the model warrants further development.

1.9 OBJECTIVE OF THIS THESIS

The superficial morphological and functional similarities between Caco-2 cells and small intestinal enterocytes has prompted considerable interest in their potential application in absorption studies. Indeed, early reports proposed that Caco-2 monolayers represented a useful *in vitro* model of the human small intestinal epithelium [Hidalgo *et al.*, 1989 and Wilson *et al.*, 1990]. However, these assertions were based on preliminary observations and a non-discerning perspective. The aim of this thesis is to compare and contrast the nutrient transport across Caco-2 monolayers with analogous studies in human and laboratory animal absorption models. The possibility of carrier-mediated drug absorption *via* nutrient carriers will also be investigated. In addition, the pharmaceutical factors affecting passive drug transport will be considered.

It is hoped that this work will provide a realistic appraisal of the opportunities and limitations of the Caco-2 monolayer model for absorption studies.

CHAPTER TWO

GENERAL MATERIALS AND METHODS

ABSTRACT

The materials and methods used routinely throughout this thesis are presented here. Supplementary and modified experimental procedures are described in the relevant sections of subsequent chapters.

2.1 CHEMICALS

All chemicals were cell culture grade or the highest purity available from Sigma Chemical Company (Poole, UK) unless otherwise specified. All cell culture media-components and reagents were purchased from Gibco (Paisley, UK). Radiochemicals were purchased from Amersham (Amersham, UK) or Dupont (New England Nuclear; Germany) unless specified. All reagents were used as received without further purification.

2.2 CELL CULTURE

The preparation of culture-media and the routine techniques used to maintain stock-cultures and prepare Caco-2 monolayers for experiments are described below.

2.2.1 CULTURE-MEDIA

Two media were prepared to culture Caco-2 cells. A maintenance-medium was used to maintain stock-cultures in plastic T-flasks and a plate-medium was used to cultivate cells on six-well clusters or culture-inserts for uptake and transport experiments, respectively. Maintenance-medium comprised Dulbecco's modification of Eagle's medium (DMEM) supplemented with (final concentrations) 10% v/v foetal bovine serum (FBS), 1% v/v non-essential amino acids (NEAA) and 1% v/v glutamine. Permeable-support-medium comprised maintenance-medium supplemented to a final concentration of 1% v/v with penicillin and streptomycin (PS).

FBS (Gibco 011-06290H), L-glutamine (Gibco 043-05030H) and PS (Gibco 043-05140D) were stored at -20°C and thawed according to the manufacturer's directions immediately prior to use. DMEM (Gibco 041-01965M) and NEAA (Gibco 043-01140H) were stored at 4°C. Maintenance- and plate-media were prepared aseptically from pre-sterilised components and were used without further sterilisation. They were stored at 4°C and used within 14 d.

2.2.2 STOCK CULTURES

The Caco-2 cell line was a generous gift from Dr Ian Hassan of Ciba Pharmaceuticals, Horsham, UK. Cells were cultured in 150 cm^2 plastic T-flasks with maintenance-medium. They were incubated at 37°C in a humidified (95%) atmosphere of 10% CO_2 in air. The maintenance medium was renewed every 48 h. Stock-cultures were passaged (1:3) weekly by trypsinisation with a solution containing 0.25% w/v trypsin (Sigma, T-8128) and 0.2% w/v disodium ethylenediamine tetraacetate in phosphate buffered saline, pH7.2 (PBS; Oxoid, UK). Cells were used for experiments between passages 94 and 120.

Frozen stocks of Caco-2 cells (passage 87 onwards) were stored in a liquid nitrogen cell bank in plastic screw-capped cryovials (Costar, UK) using a freezing-medium comprising maintenance-medium and 10% v/v dimethyl sulphoxide. Cells were thawed from frozen stocks and cultured for at least five passages before they were used for transport experiments.

The Caco-2 cells were regularly monitored for mycoplasma contamination using the Hoechst 33258 test [Hessling *et al.*, 1980]. They were cultured with maintenance-medium on sterile glass coverslips, stained (Hoechst 33258) and fixed, then viewed by fluoresence microscopy. Mycoplasma contaminated HGT-1 cells (kindly provided by Dr Peter Hanson, Aston University) were used as a positive control. Mycoplasma contamination results in a diffuse fluorescent halo around the nucleus due to cytoplasmic mycoplasma. In the HGT-1 cells, both the cell nuclei and the cytoplasm were stained (Fig. 2.1 A) whilst in Caco-2 cells, only nuclei were stained (Fig. 2.1 B). The Caco-2 cell line was mycoplasma-negative throughout the work described here.

FIGURE 2.1 *Mycoplasma detection by fluoresence microscopy.*

A) Mycoplasma-positive HGT-1 cells **B)** Mycoplasma-negative Caco-2 cells

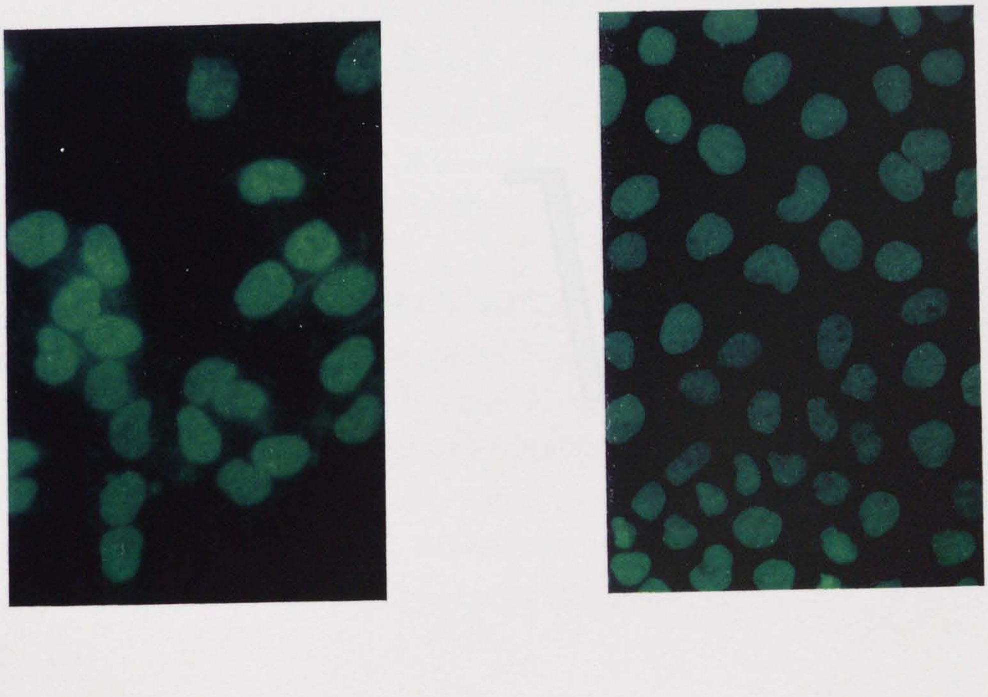

FIGURE 2.2 *Cell culture-inserts used for transport studies.*

A) Nitrocellulose

Millicell-HA insert
Area = 4.20 cm^2
Pore-size = 0.45 μm

B) Aluminium oxide

Nunc Tissue Culture Insert
Area = 4.15 cm^2
Pore-size
Growth surface = 0.20 μm
Counter-growth surface = 0.02 μm

C) Polycarbonate

Transwell
Area = 4.71 cm^2
Pore-size = 0.45 μm

2.2.3 CULTURES FOR UPTAKE STUDIES

For uptake studies, Caco-2 cells were cultured on plastic six-well clusters. Briefly, 2-3 day post-confluent stock-cultures were trypsinised and resuspended in plate-medium. The viable cell-density was measured by haemocytometry using a trypan blue-exclusion test and reduced to 2.0 x 10^5 cells ml^{-1} by dilution with futher plate-medium. Each well was seeded with 5 ml of the diluted cell-suspension (1.0 x 10^6 cells). The six-well clusters were incubated at 37°C in a humidified atmosphere (95%) of 10% CO_2 in air. Plate-medium was renewed every second day. The monolayers received their final change of plate-medium 48 h prior to an uptake study unless otherwise specified.

2.2.4 CULTURES FOR TRANSPORT STUDIES

For transport studies, Caco-2 cells were cultured on a permeable-support in a polystyrene housing (culture-insert). Three types of culture-insert with different geometries, permeable-support matrices and pore-sizes were used in this study (Fig. 2.2). Briefly, stock Caco-2 monolayers were trypsinised and resuspended to 5.0 x 10^5 cells ml^{-1} as described above (section 2.2.3). The Ap chambers of each culture-insert was seeded with 4 ml of the cell suspension (2.0 x 10^6 cells) and 3 ml of plate-medium was added to the Bl chamber. The inserts were not disturbed for the first 72 h, thereafter, the plate-medium was replaced on alternate days. The monolayers received their final change of plate-medium 48 h prior to experimentation.

Caco-2 cells develop a highly polarised morphology when cultured on permeable-supports [Hidalgo *et al.*, 1989; Wilson *et al.*, 1990; Cogburn *et al.*, 1991 and Nicklin *et al.*, 1992 b]. Their apical brush-border of microvilli projects into the inner-chamber of the culture-insert and their basolateral membranes are in contact with the solution in the outer chamber. The inner- and outer-compartments are referred to as the apical (Ap) and basolateral (Bl) chambers, respectively

2.3 UPTAKE AND TRANSPORT EXPERIMENTS

Uptake and transport can be defined as total, non-saturable (passive) or saturable (carrier-mediated). Total uptake or transport represents the radionuclide flux at a low, non-saturating ($<K_m$) radiochemical concentrations. The non-saturable component was estimated by measuring radiochemical flux in the presence of a large, carrier-saturating ($\gg K_m$), concentration of unlabelled ligand. The saturable component is calculated by subtraction of the non-saturable transport from the total radiochemical flux.

Throughout the work described here, a variety of media have been used for uptake and transport experiments. The most frequently employed media are detailed in section 2.3.1. Standard protocols for uptake and transport experiments are given in section 2.3.2 and 2.3.3, respectively. These general methods were subject to minor adaptations as appropriate for each experiment. Such modifications are described in the relevant sections.

2.3.1 TRANSPORT-MEDIA

M1-medium was used for taurocholate transport experiments (Chapter Three). It comprised DMEM supplemented with 10% v/v FBS, 1% v/v L-glutamine and 1% v/v NEAA.

M2-medium was used for L-proline uptake experiments (Chapter Four). It comprised 1% w/v BSA (BSA; Fraction V; Sigma A 7906), 3.2 mM $CaCl_2$, 1.2 mM $MgCl_2$, 4 mM KCl, 150 mM NaCl, 0.01% phenol red and 5 mM D-glucose in double-distilled water, buffered to pH 7.4 with 14 mM HEPES. Sodium-free equivalents were prepared by equimolar substitution of NaCl with choline chloride ($M2_{Choline}$) or LiCl ($M2_{Lithium}$). Similarly, a glucose-free version ($M2_{-Glucose}$) was prepared by omitting D-glucose from the above formula.

M3-medium was used to investigate the anion- and cation-specificities of L-proline uptake (Chapter Four) and L-aspartate transport (Chapter Five) by Caco-2 cells. M3 comprised 140 mM NaCl, 4 mM KH_2PO_4, 5.2 mM K_2HPO_4, 1.2 mM $MgSO_4$, 1.3 mM Calcium gluconate, 0.01% phenol red and 5 mM D-glucose, pH7.4. Chloride-free M3-media were prepared by equimolar substitutions of NaCl with sodium iodide ($M3_{Iodide}$) sodium isethionate ($M3_{Isethionate}$) or sodium thiocyanate ($M3_{Thiocyanate}$). Sodium-free M3-media were prepared by equimolar substitution of NaCl with the chloride salts of choline ($M3_{Choline}$), lithium ($M3_{Lithium}$), potassium ($M3_{Potassium}$), rubidium ($M3_{Rubidium}$) or caesium ($M3_{Caesium}$).

M4-medium was used for the majority of transport studies. It comprised Hanks' balanced salt solution (HBSS) containing 0.1% w/v BSA, 0.01% phenol red, 5 mM D-glucose and buffered with 14 mM HEPES (pH 7.0, 7.4 and 8.0) or MES (pH 5.5, 6.0, 6.5). M4 buffered to pH7.4 was used unless stated otherwise. A sodium-free version was prepared by equimolar substitution of NaCl with choline chloride ($M4_{Choline}$). Similarly, a glucose-free version ($M4_{-Glucose}$) was prepared by omitting glucose from the above formula.

M5-medium comprised Hanks' balanced salt solution (HBSS) containing 0.01% phenol red and 5 mM D-glucose and was buffered to pH7.4 with 14 mM HEPES

These transport-media were adjusted to the appropriate pH using sodium hydroxide (potassium hydroxide from sodium-free solutions) or hydrochloric acid (all Volucon, UK), as appropriate. They were filter-sterilised using a bottle-top filter system (Costar, UK) and stored at 4°C. After the addition of acids (*eg:* L-aspartic acid) or bases (*eg:* thyrotrophin-releasing hormone) in quantities that displaced the pH of these buffered transport-media, the correct pH was restored by the addition of sodium hydroxide, potassium hydroxide or hydrochloric acid, as appropriate.

2.3.2 UPTAKE EXPERIMENTS

For uptake studies, Caco-2 cells were cultured on plastic six-well clusters (Fig. 2.3). The plate-medium was aspirated and the monolayer carefully washed with PBS (2 x 5 ml x 5 min) and finally with the incubation-medium (1 x 2 ml x 5 min). The uptake experiment was initiated by aspirating the final washing-solution and replacing it with a donor-solution (2 ml) containing the radiochemical of interest. Washing- and donor-solutions were equilibrated to 37°C for 1 h prior to use. The monolayers were placed in a dry incubator (37°C) and not disturbed for the duration of the uptake experiment. After the incubation-period, monolayers were transferred to a cold table (0-4°C). The donor-solutions were collected and their radioactive-content determined by liquid scintillation counting (see below, section 2.4.1 A or B). Each monolayer was carefully rinsed (3 x 5 ml x 5 min) with ice-cold PBS-sodium azide 0.05% w/v (PBS-N_3; stop-solution) to terminate the uptake process and remove trace quantities of extracellular radioligand. Following the final PBS-N_3 wash, monolayers were solubilised by shaking (Luckman Recipro-shake) with 0.1% v/v Triton X-100 (TX100; Aldrich Chemical Company, Gillingham, UK) in double-distilled water for 60 min at 25°C. The cell-associated radioactivity was corrected for the radiochemical concentration applied to each monolayer and was normalised to the anticipated DPM (*ie:* 1 μCi ml^{-1} = 2.2 x 10^6 DPM ml^{-1}). This correction cancelled fluctuations in cell-associated radioactivities resulting from minor variations in the radiochemical concentrations applied to each monolayer.

2.3.3 TRANSPORT EXPERIMENTS

The Caco-2 monolayer transport model comprises a cell monolayer, cultured on a permeable-support, separating a donor-chamber from a receiver-chamber (Fig. 2.4). Typically, the donor-solution is placed in the Ap chamber of the culture insert and the receiver-solution in the outer Bl chamber. In this way, the apical-to-basolateral (Ap-to-Bl) flux of a compound can be investigated as described below.

Plate-medium was aspirated from the Ap and Bl chambers and the monolayers washed (1 x (2 ml Ap + 2 ml Bl) x 15 min) with the incubation-medium. The donor and receiver washing- and incubation-solutions, may or may not be identical depending on experimental requirements. The transport experiment was initiated by aspirating the washing-solutions and applying a donor-solution (2 ml) of incubation-medium containing an appropriate concentration of the radiochemical being studied to the Ap chamber. The culture-insert and donor-solution were immediately transferred to a chamber containing 2.5 ml of receiver-solution. All washing- and incubation-solutions were equilibrated to 37°C for 1 h prior to use. Ap-to-Bl transport kinetics were followed by sequentially transferring the culture-insert, complete with its donor-solution, into a new receiver-chamber at defined time intervals. After the final receiver-sample had been collected monolayers were transferred to a cold-table (0-4°C) and the Ap donor-solutions were collected and their radiochemical concentration determined. The radiochemical flux into the receiver-solution for each time interval was corrected for the radiochemical concentration in the Ap donor-solution and was normalised to the anticipated DPM (*ie:* 1 μCi ml^{-1} = 2.2 x 10^6 DPM ml^{-1}) as described for uptake studies (see section 2.3.2). Transport in the reverse direction (*ie:* Bl-to-Ap) was also determined. In this case, the rate of radiochemical flux into the Ap chamber from a Bl donor-solution was monitored.

FIGURE 2.3 *The Caco-2 monolayer uptake model.*

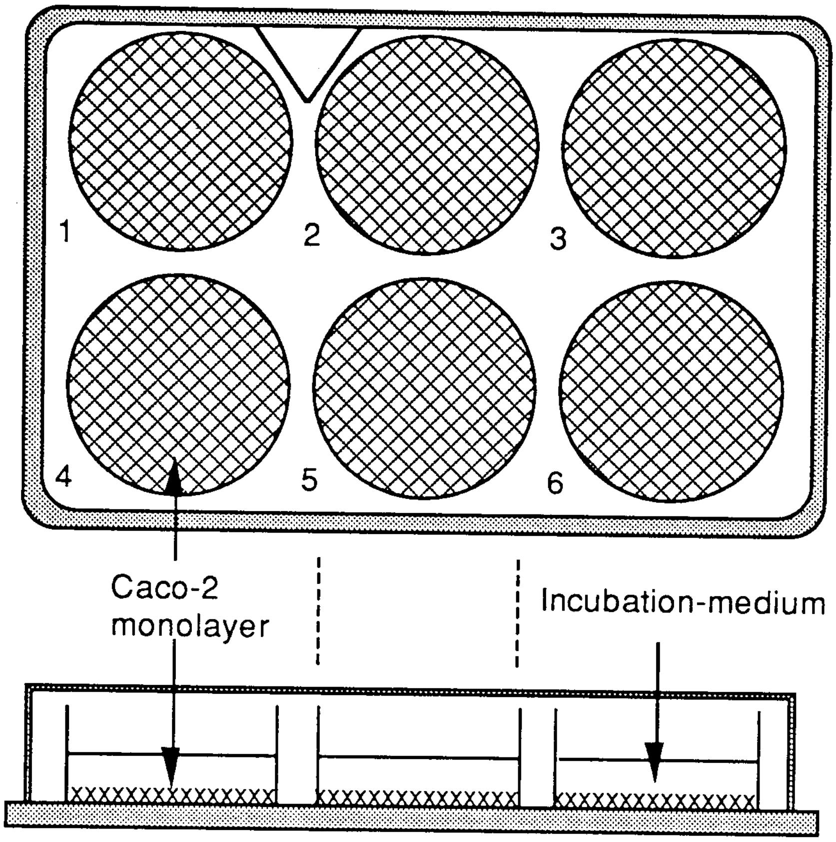

FIGURE 2.4 *The Caco-2 transport model.*

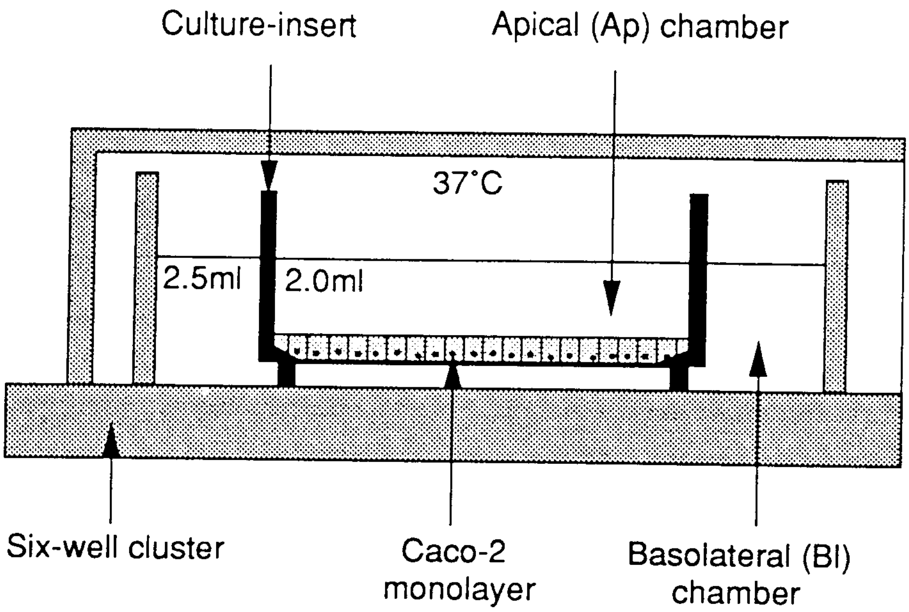

2.4 ANALYTICAL METHODS

2.4.1 LIQUID SCINTILLATION COUNTING

Beta-emitting radionuclides ([^{14}C], [^{3}H], [^{35}S]) were quantified using liquid scintillation spectrophotometry. Two methods were employed;

A) Sample + 10 ml Optiphase HiSafe III (LKB, UK),
Packard Tricarb 2000 CA liquid scintillation analyser,
5 min count-time.

B) Sample + 12 ml Lumagel (Lumac, Netherlands),
Beckman LS1801 liquid scintillation analyser,
10 min count-time.

In both cases, counts per minute (CPM) were converted to decays per minute (DPM) by comparison to standard quench-correction curves.

2.4.2 GAMMA COUNTING

^{125}Iodine was quantified using gamma-radiation spectrophotometry. Samples were counted for 1 min using a LKB Multigamma II gamma-counter and expressed as CPM.

2.5 TRANSEPITHELIAL ELECTRICAL RESISTANCE

Transepithelial electrical resistance (TER) was measured using a medium comprising minimum essential medium (MEM; Gibco 041-02360H) supplemented with 0.1% w/v BSA (TER-medium). Pre-warmed TER-medium was added to the Ap (4 ml) and Bl (5ml) chambers and allowed to equilibrate to 25 or 37°C (see individual experiments). The TER of each monolayer was measured with an epithelial voltmeter using 'chopstick' electrodes (EVOM, World Precision Instruments, USA). The positioning of the electrode was critical in achieving consistent and reliable TER measurements. The chopstick electrode was arranged with its longest electrode in the Bl chamber, against the base of the six-well cluster, and its shorter electrode in the Ap chamber. The mean TER for each monolayer was calculated from three measurements at discrete positions. The intrinsic resistance of the system (permeable-support alone) was subtracted from the total resistance (cell monolayer + permeable-support) to calculate the resistance of the monolayer. The resistance was corrected for surface area of the permeable-support (Aluminium oxide, 4.15 cm^2; nitrocellulose, 4.20 cm^2; polycarbonate, 4.71 cm^2) and the TER expressed in $\Omega\ cm^2$.

2.6 ELECTRON MICROSCOPY

2.6.1 TRANSMISSION ELECTRON MICROSCOPY (TEM)

Caco-2 monolayers were washed with fresh maintenance-medium and fixed with a solution of 2.5% glutaraldehyde and 4% paraformaldehyde (both EM Scope, Ashford, Kent, UK) in 0.1 M cacodylate buffer, pH 7.3 for 2 h at 25°C, then washed in 0.1 M cacodylate buffer. The cells were post-fixed with 1% osmium tetroxide in 0.1 M cacodylate buffer before dehydration through an ascending series of ethanol (70, 80, 90, 95 and 100% to excess). The monolayers, on their permeable-supports, were embedded in Epon resin and cured at 60°C for 48 h. Samples were sectioned on a Reichert OM4 microtome, stained with uranyl acetate and lead citrate then visualised and photographed using a Phillips CM10 electron microscope.

2.6.2 SCANNING ELECTRON MICROSCOPY (SEM)

Cells were fixed and dehydrated using the procedures described above for TEM (see section 2.6.1). At the final 100% ethanol wash, the cells were processed in an Edwards (Cambridge, UK) tissue-processor. Samples were glued onto an SEM-stub and a fine gold film evaporated onto the surface in an Edwards sputter-coater. The monolayers were viewed and photographed using a Cambridge Stereoscan 200 electron microscope.

2.7 OCTANOL-AQUEOUS BUFFER DISTRIBUTION-COEFFICIENTS

The distribution of a radiolabelled compound between n-octanol (High purity for partition-coefficient determinations; BDH, UK) and citric acid(0.1 M)-Na_2HPO_4 (0.2 M) (McIlvaines) buffer was determined and expressed as the log distribution coefficient (Log D) according to Equation 2.1.

EQUATION 2.1 $$\text{Log D} = \text{Log}\,(C_{octanol} / C_{buffer})$$

Briefly, the immiscible phases were pre-saturated with each other by mixing and shaking for 24 h at 37°C (Gallenkamp orbital incubator; 120 rpm). A trace amount of radiolabelled compound (« solubility in either phase) in 1 ml of McIlvaines buffer was vortexed for 1 min with an equal volume of n-octanol. The compound was allowed to distribute between the two phases at 37°C for 24 h with continuous agitation (Gallenkamp orbital incubator; 120 rpm). After distribution, a 500 μl sample was carefully withdrawn from each phase and its radioactive-content determined by liquid scintillation counting (see section 2.4.1).

2.8 DATA PRESENTATION

Uptake values are presented as the moles of compound becoming associated with the a monolayer or 1.0 x 10^6 cells per defined period of time. Transport data are expressed by three methods;

A) Amount entering the receiver-solution per defined time-period,

B) Percentage transported into the receiver-solution per hour,

C) Apparent permeability coefficient (P_{app}; see section 1.5.5).

Data are presented as mean values and experimental errors are expressed as standard deviations (SD) about that mean. Significance testing was performed using an unpaired Student's t-test assuming equal variance.

CHAPTER THREE

PERMEABLE-SUPPORT TYPE INFLUENCES THE MORPHOLOGICAL AND FUNCTIONAL PROPERTIES OF CACO-2 MONOLAYERS

ABSTRACT

The influence of aluminium oxide and nitrocellulose inserts on the uptake and transport of taurocholic acid in Caco-2 cells has been determined. Caco-2 cells grown on nitrocellulose inserts displayed a higher rate of taurocholic acid transport than those grown on aluminium oxide inserts; 59.3 ± 4.1 ng $(4\ h)^{-1}$ $insert^{-1}$ compared to 29.7 ± 4.1 ng $(4\ h)^{-1}$ $insert^{-1}$ at day 14. In addition, Caco-2 cells grown on aluminium oxide and nitrocellulose inserts were not comparable with respect to cell morphology, cell numbers and transepithelial electrical resistance. The low adsorption potential of aluminium oxide inserts, particularly for high molecular weight or lipophilic ligands such as propranolol and testosterone, allowed basolateral uptake events to be studied with a precision not possible with nitrocellulose inserts. In addition, the translucent nature of aluminium oxide inserts offered significant advantages over the nitrocellulose insert in terms of visualising the cells by light microscopy. Caco-2 cells grown on either type of insert appear fully differentiated when observed by light and electron microscopy. Occasional dome-like structures were present when Caco-2 monolayers were grown on aluminium oxide but not nitrocellulose inserts. Cell numbers were significantly lower on aluminium oxide inserts than on nitrocellulose inserts. Moreover, Caco-2 cells grown on aluminium oxide inserts displayed a higher transepithelial electrical resistance than those grown on nitrocellulose inserts; 871 ± 149 $\Omega\ cm^2$ compared to 513 ± 32 $\Omega\ cm^2$ at day 14. Aluminium oxide and nitrocellulose may exert different selection pressures on the heterogeneous parental cell line. It is hypothesised that the functional and morphological differences between Caco-2 monolayers cultured on these two types of permeable-support may reflect their development from distinct sub-populations of the heterogeneous parental cell line.

3.1 BACKGROUND

The Caco-2 transport model comprises a confluent cell monolayer cultured on a permeable-support, separating a donor-chamber from a receiver-chamber (see Fig. 2.4). The apparent permeability coefficient (P_{app}) for a compound across this model reflects permeation of the aqueous boundry-layer (P_{aq}), the cell monolayer ($P_{monolayer}$) and the permeable-support (P_{ps}). Since these diffusional resistances are in series, they are related by the relationship shown in Equation 3.1.

EQUATION 3.1 $$1/P_{app} = 1/P_{aq} + 1/P_{monolayer} + 1/P_{ps}$$

The cell culture approach to transport studies has developed on the premise that transport across a model epithelium can be studied without the complicating effects of sub-epithelial tissue. Therefore, the ideal permeable-support for the Caco-2 monolayer model should promote enterocyte-like differentiation without influencing transport kinetics (*ie:* P_{ps} should be negligible compared to $P_{monolayer}$).

When cultured on nitrocellulose (Millicell HA; see Fig. 2.2 B) permeable-supports, Caco-2 cells display a highly differentiated phenotype [Wilson *et al.*, 1990]. This cell-support combination has been used successfully to study secretion and transport phenomena [Rindler and Traber, 1988; Wilson *et al.*, 1990]. However, the nitrocellulose permeable-support has a large internal volume (150 µm deep; pore size 0.45 µm) and its adsorption of lipophilic-ligands (*eg:* propranolol) may limit its application for transport studies [Wilson *et al.*, 1990; Artursson 1990].

Recently, a culture insert with a permeable-support constructed from aluminium oxide (Nunc Tissue Culture Insert; see Fig. 2.2 A) has been introduced. The aluminium oxide permeable-support has a thin (45 µm deep), high-porosity membrane with a controlled pore-size (0.2 µm at the upper surface and 0.02 µm at the lower surface or 0.2 µm throughout in the case of a specially prepared batch). Its low internal volume and the manufacturer's claim of low ligand-adsorption offer potential advantages over other permeable-supports for transport studies. Moreover, in contrast to the opaque nitrocellulose filter, the aluminium oxide permeable-support is transparent when wet. This transparency allows a visual inspection of cultures on aluminium oxide for monolayer defects prior to transport studies.

The work presented here compares ligand-adsorption to aluminium oxide and nitrocellulose permeable-supports and demonstrates the influence of this adsorption-potential on transport kinetics. In addition, some morphological and functional properties of Caco-2 cells cultured on these two types of permeable-support are compared and contrasted.

3.2 MATERIALS

D-[^{14}C]Mannitol (49.3 Ci mmol^{-1}), L-[^{3}H]Proline (26 Ci mmol^{-1}) and [^{14}C]taurocholic acid (56 mCi mmol^{-1}) were purchased from Amersham, UK. [^{3}H]-Testosterone (80 Ci mmol^{-1}) was obtained from New England Nuclear (Dupont, Germany). DPX mountant, Harris' haemotoxylin and xylene were supplied by BDH (UK).

Aluminium oxide culture-inserts were purchased from Anotec Separations (Banbury, UK) but are presently marketed by Nunc (Nunc Tissue Culture Insert 25; Paisley, UK). Nitrocellulose inserts were obtained from Millipore (Millicell HA; Bedford, MA, USA).

Several of the transport-media described in section 2.3.1 were used for the experiments described below. D-mannitol and testosterone transport experiments were performed using M4-medium. M1-medium was used for taurocholic acid transport experiments and finally M2-medium was used for L-proline transport experiments.

3.3 METHODS

3.3.1 LIGAND ADSORPTION TO PERMEABLE-SUPPORTS

Aluminium oxide and nitrocellulose inserts were conditioned for 2 h in permeable-support-medium. They were washed with PBS before incubation with PBS (1 ml Ap, 1 ml Bl) containing L-[^{3}H]glutamate, [^{125}I]human calcitonin, L-[^{3}H]leucine, D-[^{14}C]mannitol, L-[^{35}S]methionine, [^{14}C]-PEG$_{4000}$, L-[^{3}H]phenylalanine, L-[^{3}H]proline, [^{14}C]taurocholic acid (all Amersham,UK), L-[^{14}C]aspartic acid, [^{14}C]citric acid, [^{3}H]PEG$_{900}$, [^{3}H]-propranolol and [^{3}H]thyrotrophin-releasing hormone (all New England Nuclear, Dupont, Germany) and [^{14}C]Baclofen (Ciba Pharmaceuticals, Basle,Switzerland). After 4 h at 37°C, the filters were washed three times with ice-cold PBS-N$_3$ stop-solution. The residual [^{3}H], [^{14}C] and [^{35}S] radioactivity on the permeable-supports was measured liquid scintillation counting (see section 2.4.1 A or B). Residual [^{125}I] was determined by gamma counting (see section 2.4.2). The radioactivity associated with the permeable-support was expressed as a percentage of the total radioactivity in the incubation chamber.

3.3.2 D-MANNITOL AND TESTOSTERONE TRANSPORT

D-[^{14}C]Mannitol (0.25 μCi ml^{-1}) and [^{3}H]testosterone (1.0 μCi ml^{-1}) in M4-medium were applied to the Ap chamber of on aluminium oxide and nitrocellulose inserts in the presence or absence of a 21 d Caco-2 monolayer. Ap-to-Bl transport kinetics were followed as described previously (see section 2.3.3).

3.3.3 LIGHT MICROSCOPY AND CELL COUNTING

Caco-2 monolayers on aluminium oxide permeable-supports were visualised during culture by phase-contrast light microscopy and photographed (Leitz Labovert, Wild MPS 51S and Photoautomat 45; Fig. 3.1). For cell counting, monolayers cultured on both types of permeable-support were photographed after fixing and staining at days 5, 10, 14, 20 and 25. Briefly, the cells were fixed with 2.5% glutaraldehyde and 4% paraformaldehyde in 0.1 M cacodylate buffer, pH7.3, for 1 h then rinsed with PBS. The monolayers were stained with Harris' haemotoxylin for 5 min, washed with alkaline water (tap water + few drops of 35% ammonia) and finally de-stained with acidified methanol. The cells were dehydrated through an ascending series of 15 min ethanol washes (50, 70, 90, 95 and 100% to excess) and finally rinsed with xylene before mounting onto glass slides with DPX. The fixed and stained monolayers were visualised by light microscopy (Leica Diavert). Six photographs were taken randomly from each sample (Wild MPS 51S and Photoautomat 45). The nuclear counts per unit area were used to calculate the number of cells on each culture-insert.

3.3.4 HORSERADISH PEROXIDASE CYTOCHEMISTRY

The cytochemical localisation of basolaterally-applied horseradish-peroxidase (HRP, Type II; Sigma P8250) was studied in 14 d Caco-2 monolayers cultured on aluminium oxide permeable-supports. HRP (10 mg ml^{-1}) in maintenance-medium was applied to the Bl chamber. Following a 60 min incubation at 37°C, the cells were washed with fresh maintenance-medium then initially fixed using 0.05% glutaraldehyde and 4% paraformaldehyde in 0.1 M cacodylate buffer, pH 7.3, for 1 h at 25°C. The cells were permeabilised overnight in 5% w/v sucrose and washed in 0.1 M cacodylate buffer. The permeabilised-samples were incubated with a reaction mixture (50 mg diaminobenzidine, 34 μl H_2O_2 (30%) in 50 ml of 0.1 M cacodylate buffer, pH 7.3) for 1 h in the dark at 25°C. The cells were rinsed with 0.1 M cacodylate buffer and were processed as described for TEM (see section 2.6.1) but were not stained with uranyl acetate or lead citrate after sectioning. The cells were visualised and photographed using a Phillips CM10 electron microscope.

3.3.5 TRANSEPITHELIAL ELECTRICAL RESISTANCE

TER was measured as described in section 2.5. The monolayers and TER medium were allowed to equilibrate to 25°C for 15 min prior to TER measurement.

3.3.6 TAUROCHOLIC ACID TRANSPORT

Caco-2 monolayers were washed with PBS (1 x (2 ml Ap + 2 ml Bl) x 15 min) before [^{14}C]taurocholic acid (0.1 μCi ml^{-1}; 3.5 μM) in M1-medium was added to the Ap or Bl chamber. They were incubated at 37°C in a humidified atmosphere (95%) of 10% CO_2 in air. Transport kinetics were followed by sequential-transfer of the culture-insert into fresh receiver-solution at 1 h intervals. Alternatively, transport was measured over a single 4 h time point. At the end of each transport experiment the culture-inserts were transferred to a cold table (0-4°C), the Ap and Bl transport media were collected and the monolayers washed three times with ice-cold PBS-N_3 stop-solution. The [^{14}C]-content of each sample was measured by liquid scintillation counting (see section 2.4.1 B). The appearance of [^{14}C] at the opposite side of the monolayer gave total (saturable + non-saturable) transport. The non-saturable transport component was estimated by measuring transport in the presence of a 1,000-fold molar excess (3.5 mM) of unlabelled taurocholic acid. Saturable transport was calculated by subtraction of the total and non-specific transport components. Similarly, [^{14}C]taurocholic acid uptake into the cell-permeable-support composite was measured by removing the permeable-support from its housing using a specialised cutting tool for aluminium oxide (Nunc, UK) or a scalpel for nitrocellulose and its [^{14}C]-content determined by liquid scintillation counting.

3.3.7 PROLINE TRANSPORT

Caco-2 monolayers were washed (1 x (2 ml Ap + 2 ml Bl) x 15 min) with PBS and finally with M2-medium before L-[^{3}H]proline (1.0 μCi ml^{-1}; 44 nM) in M2-medium was added to the apical chamber. After 30 min at 37°C the inserts were transferred to a cold table (0-4°C), the Ap and Bl media collected and assayed for [^{3}H]-content by liquid scintillation counting. The appearance of [^{3}H] in the receiver chamber represented total (saturable + non-saturable) Ap-to-Bl transport. The non-saturable transport component was estimated by measuring transport in the presence of a 1.0 x 10^6 molar excess of L-proline. Saturable transport was calculated by subtraction of the total and non-saturable transport components.

3.4 RESULTS

The percentage of ligand-adsorption to aluminium oxide and nitrocellulose permeable-supports is recorded in Table 3.1. Generally, a much greater adsorption to nitrocellulose than to aluminium oxide was observed. This was notable for the high molecular-weight and/or lipophilic ligands [^{125}I]-human calcitonin, [^{14}C]PEG$_{4000}$, [^{3}H]propranolol and [^{3}H]testosterone. Testosterone is the most striking example with 72.7% binding to the nitrocellulose, whilst less than 0.02% adsorbed to the aluminium oxide insert. This represents a differential binding of over 5000-fold. [^{14}C]-Taurocholic acid binding to nitrocellulose was over 20-fold higher than to aluminium oxide. Significant adsorption to nitrocellulose inserts has been reported previously [Wilson *et al.*, 1990]. In that study, polycarbonate inserts were used in preference to nitrocellulose to reduce the influence of permeable-support binding on transport kinetics. Three compounds, [^{14}C]citric acid, L-[^{14}C]aspartate and L-[^{3}H]glutamate, reverse the general rule and are highly bound to the aluminium oxide insert but have very low binding to nitrocellulose. This preliminary observation that metal-chelating ligands avidly bind to the aluminium oxide permeable-support has been confirmed for other metal-chelating compounds (*personal communication*, Dr Ian Hassan, Ciba Pharmaceuticals, Horsham, UK).

The different adsorption potential of these two permeable-support types is reflected in the transport of D-mannitol and testosterone. D-Mannitol is rapidly transported across both permeable-supports in the absence of a cell monolayer. The presence of a cell monolayer results in a marked reduction in the rate of Ap-to-Bl D-mannitol transport. Therefore, the cell monolayer offers the major barrier to the transport of this hydrophilic compound (Fig. 3.2 A). In contrast, testosterone was rapidly transported across naked aluminium oxide inserts but was transported very slowly across nitrocellulose inserts. Testosterone transport was not significantly reduced in the presence of a cell monolayer on either insert. Caco-2 monolayers, therefore, do not offer a major barrier to transport of the lipophilic ligand testosterone.

Caco-2 monolayers on aluminium oxide inserts can be visualised during culture (Fig. 3.1). This permits a visual inspection of monolayer integrity before transport experiments. Individual Caco-2 cell nuclei become more discrete with time in culture probably reflecting greater monolayer organisation. This was confirmed by light microscopy after fixing and staining (Fig. 3.3). At 5 d, there was poor and diffuse staining of cell nuclei. After 10 d, nuclear staining less diffuse, cell number decreases and the inter-nuclear distance increases. Monolayers became highly organised by 20d. Visually, a lower cell density on aluminium oxide compared to nitrocellulose inserts was apparent. This was confirmed by cell counting (Fig. 3.4). After seeding with 2.0 x 10^6 cells, numbers increased initially to 3.5 x 10^6 in the case on aluminium oxide and 4.3 x 10^6 with nitrocellulose after 10 d. Cell numbers decreased after 10 d to 2.5 x 10^6 and 3.1 x 10^6 after 25 d on aluminium oxide and nitrocellulose inserts, respectively. The decline in cell numbers after 10 d probably reflects cells sloughing from the monolayers, after an initial proliferation, in an organisational phase. The optimal time for transport studies has been reported as 14-25 d post-seeding [Wilson *et al.*, 1990]. Over this window, the cell numbers on aluminium oxide were significantly lower than on nitrocellulose inserts.

A notable feature of Caco-2 monolayers cultured on aluminium oxide permeable-supports was the presence of occasional blister-like domes (Fig. 3.5). These structures were absent on Caco-2 monolayers cultured on nitrocellulose inserts.

Transmission electron micrographs of Caco-2 cells cultured on aluminium oxide and nitrocellulose for 20 d are shown in Figs. 3.6 A and 3.6 B, respectively. Cells cultured on both inserts formed monolayers. On nitrocellulose, Caco-2 cells displayed a highly polarised morphology with good intracellular organisation. The cells were tall (18.6 μm), had a well-developed Ap brush-border and basolaterally positioned nucleus and lipid granules. In contrast, Caco-2 cells cultured on aluminium oxide inserts appeared less polar with a dense, disorganised cytoplasm containing large areas of glycogen accumulation. They were less tall (9.7 μm) and their Ap brush-border was less well developed with fewer and more irregular microvilli. Throughout the culture period, the Bl membrane of the cells on the nitrocellulose insert had permeated into the pores whereas on the aluminium oxide insert cells did not penetrate the insert mesh. Differences in the Ap brush-border on the two inserts seen by transmission electron microscopy were confirmed by scanning electron microscopy (Fig. 3.7). On nitrocellulose, Caco-2 cells displayed both the dense 'carpet-like' and clustered microvilli orientations described previously [Pinto *et al.*, 1983, Wilson *et al.*, 1990]. On aluminium oxide, however, the cells possessed sparse and/or irregular microvilli clusters. Penetration studies showed that the apically positioned tight junctions restricted the Bl-to-Ap transport of horse-radish peroxidase through the paracellular pathway (Fig. 3.8).

The morphometric analysis of Caco-2 cells cultured on both inserts showed differences in cell and microvilli height (Fig. 3.9). On aluminium oxide inserts, cell height remained relatively constant throughout, 10.0±0.7 μm at 5 d to 8.5±1.0 μm after 20 d. On nitrocellulose inserts, cell height increased from 7.7±0.8 μm at 5 d to

17.7±0.6 μm after 20 d. At day 20, Caco-2 cells cultured on nitrocellulose were significantly taller than those cultured on aluminium oxide. Microvilli height remained constant with time for the cell cultured on aluminium oxide 1.4±0.2 μm at 5 d and 1.3±0.1 μm after 20 d. In contrast, the height of microvilli for cells cultured on nitrocellulose decreased with time in culture.

The temporal-dependence of Caco-2 monolayers cultured on both permeable-support types are shown in Fig. 3.10. After 5 d, the TER for Caco-2 monolayers cultured on aluminium oxide and nitrocellulose inserts have similar and substantial TER values, 460.0±26.7 and 454.5±53.4 Ω cm^2, respectively. Therefore, electrically tight monolayers were formed rapidly on both inserts. However, as culture progressed, the Caco-2 monolayers cultured on the two types of insert developed disparate TER characteristics. The TER of monolayers cultured on nitrocellulose inserts increased only slightly remaining between 454.5±53.4 and 524.1±16.0 Ω cm^2. In contrast, the TER of monolayers cultured on aluminium oxide increased up to 14 d (871.2±149.7 Ω cm^2) and remained constant through to 25 d (780.7±42.8 Ω cm^2).

Taurocholic acid transport across Caco-2 monolayers was linear (transport proportional to incubation time) for at least 7 h (Fig. 3.11 A). On both aluminium oxide and nitrocellulose inserts, taurocholic acid transport was highly polar, essentially only occurring in the Ap-to-Bl direction (Fig. 3.11 B). However, higher rates of Ap-to-Bl transport were observed across Caco-2 monolayers cultured on nitrocellulose inserts (14.4±0.8 ng (4h)$^{-1}$ insert^{-1} at 7 d to 126.9±13.2 ng (4h)$^{-1}$ insert^{-1} after 21 d) compared to aluminium oxide inserts (13.2±3.0 ng (4h)$^{-1}$ insert^{-1} at 7 d to 51.5±10.3 ng (4h)$^{-1}$ insert^{-1} after 21 d) ($p<0.001$). The rate of taurocholic acid transport was identical on aluminium oxide inserts with the normal pore size (0.2-to-0.02 μm) and a specially prepared batch where the pore size was 0.2 μm throughout (Table 3.2). Specific Ap uptake into Caco-2 cells increased concomitantly with transport (Fig. 3.12 A) when cultured on nitrocellulose (1.53 ng (4h)$^{-1}$ insert^{-1} at 7 d to 3.2 ng (4h)$^{-1}$ insert^{-1} after 21 d), but remained relatively constant with time on aluminium oxide inserts (0.9 ng (4h)$^{-1}$ insert^{-1} at 7 d to 0.7 ng (4h)$^{-1}$ insert^{-1} after 21 d). Specific Bl uptake of taurocholic acid into Caco-2 cells cultured on the two types of permeable-support is compared in Fig. 3.12 B). On nitrocellulose, the large positive specific Bl uptake probably largely reflects adsorption to the filter rather than cellular uptake (see Table 3.1). However, on aluminium oxide permeable-supports taurocholic acid adsorption is very low and cellular uptake can be determined. For aluminium oxide inserts, the lack of specific Bl uptake is consistent with the lack of Bl-to-Ap transport (see Fig. 3.11 B).

Total, non-saturable and saturable L-proline transport across 14 d Caco-2 monolayers cultured on aluminium oxide and nitrocellulose inserts were not significantly different (Fig. 3.13).

FIGURE 3.1 *Phase-contrast light micrograph of 19 d Caco-2 cells cultured on aluminium oxide permeable-support.*

Scale bar represents 50 μm.

FIGURE 3.2 *The influence of permeable-support type on D-mannitol and testosterone transport.*

The Ap-to-Bl flux of D-mannitol (**A**) and testosterone (**B**) across aluminium oxide (squares) and nitrocellulose (circles) in the presence (closed symbols) or absence (open symbols) of a 21 day Caco-2 monolayer. Data are presented as mean values ± SD for three monolayers.

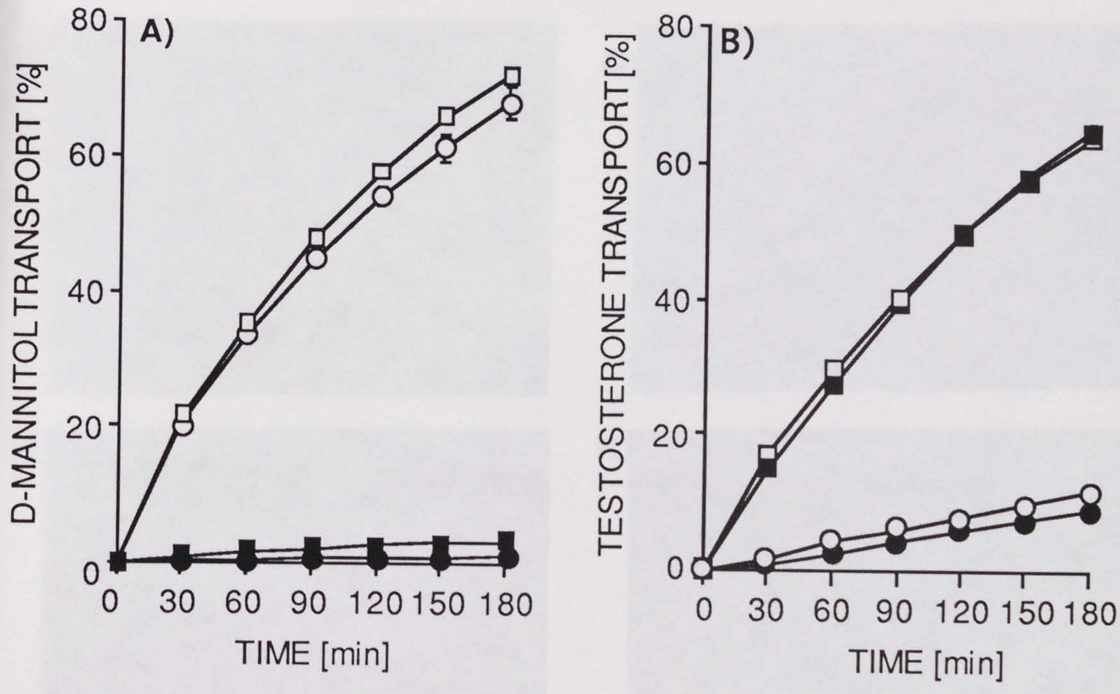

FIGURE 3.3 *Temporal-dependence of Caco-2 monolayer appearance on aluminium oxide and nitrocellulose permeable-supports.*

Caco-2 monolayers cultured on permeable-supports: Aluminium oxide for 10 (**A**), 14 (**B**), 20 (**C**) and 25 (**D**) days; Nitrocellulose for 10 (**E**), 14 (**F**), 20 (**G**) and 25 (**H**) days.

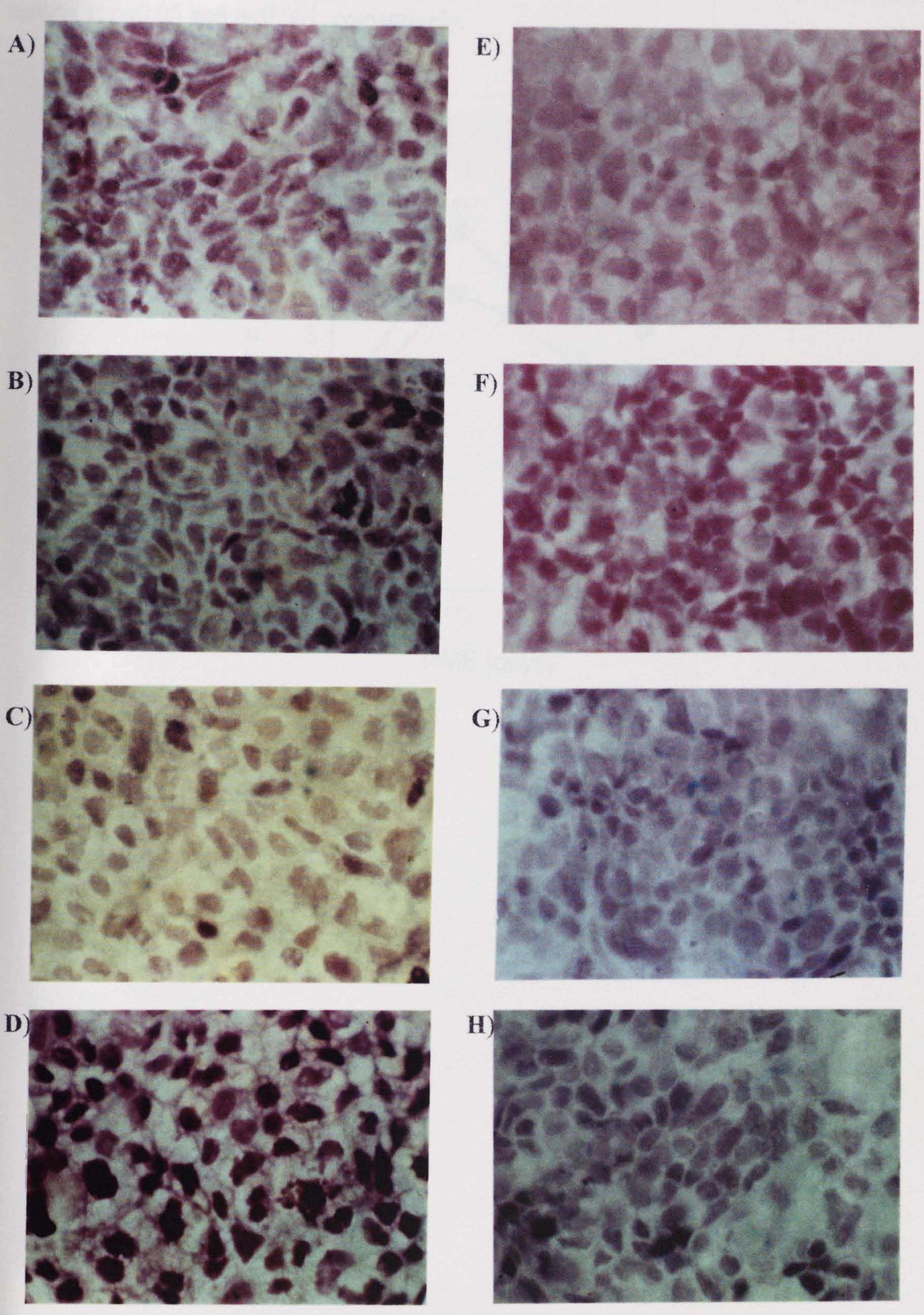

FIGURE 3.4 *Temporal-dependence of Caco-2 cell numbers during culture on aluminium oxide and nitrocellulose permeable-supports.*

Cell counts were performed on Caco-2 monolayers cultured on aluminium oxide (squares) and nitrocellulose (circles) inserts at 10, 14, 20 and 25 d of culture. Data are presented as mean values ± SE for six monolayers. * and ** Denote a significantly greater cell number on nitrocellulose compared to aluminium oxide inserts at $p<0.05$ and $p<0.001$, respectively.

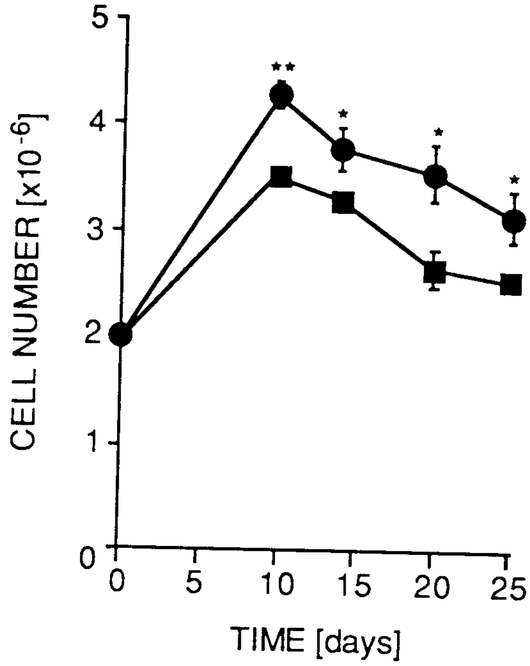

FIGURE 3.5 *Caco-2 monolayer cultured on an aluminium oxide permeable-support for 14 d showing a blister-like dome.*

Scale bar = 5 μm.

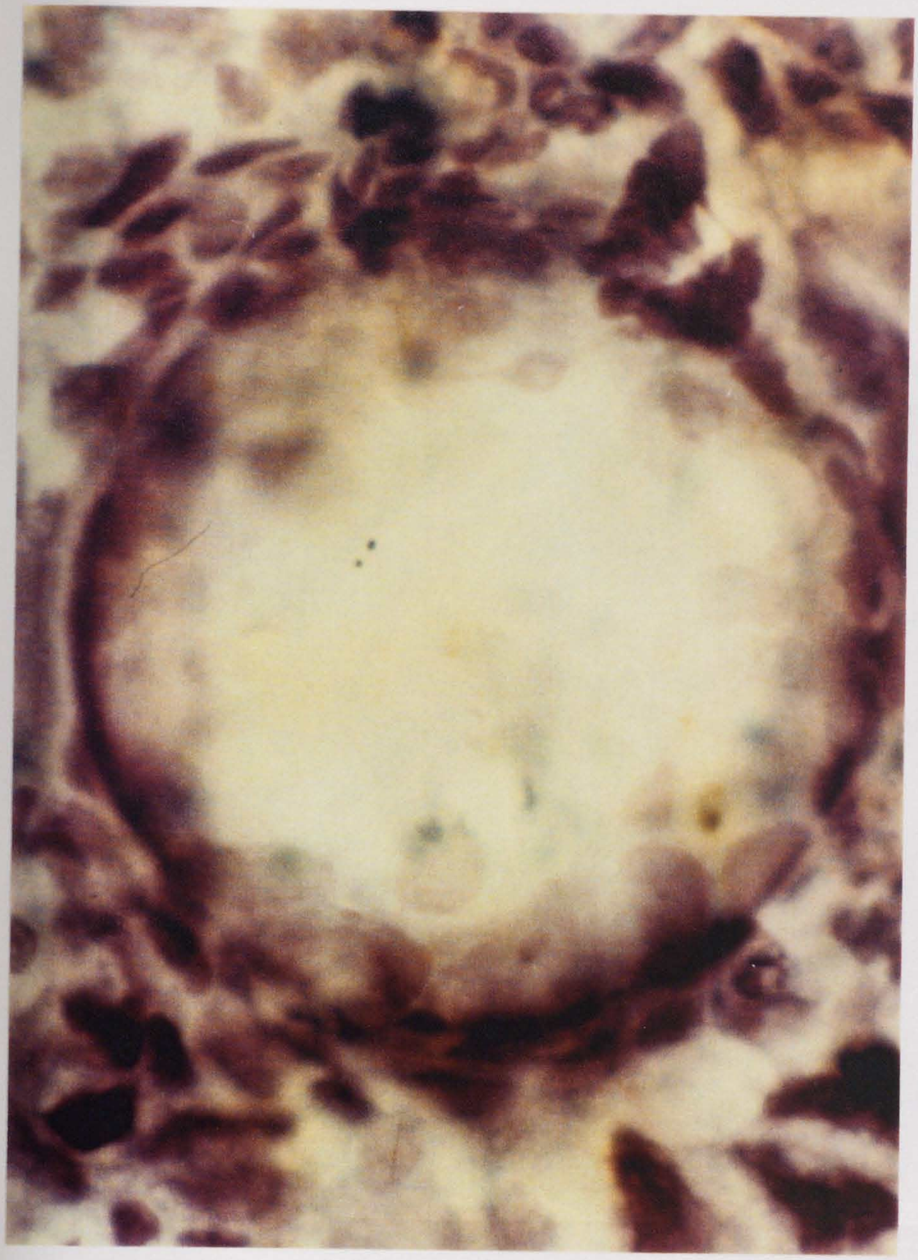

FIGURE 3.6 *Transmission electron micrographs of Caco-2 cells cultured on aluminium oxide and nitrocellulose permeable-supports.*

Caco-2 monolayers cultured on aluminium oxide (**A**) and nitrocellulose (**B**) permeable-supports showing the support (S), glycogen (G), lipid vesicles (L), microvilli (M) and nuclei (N). Scale bar represents 1 μM.

A)

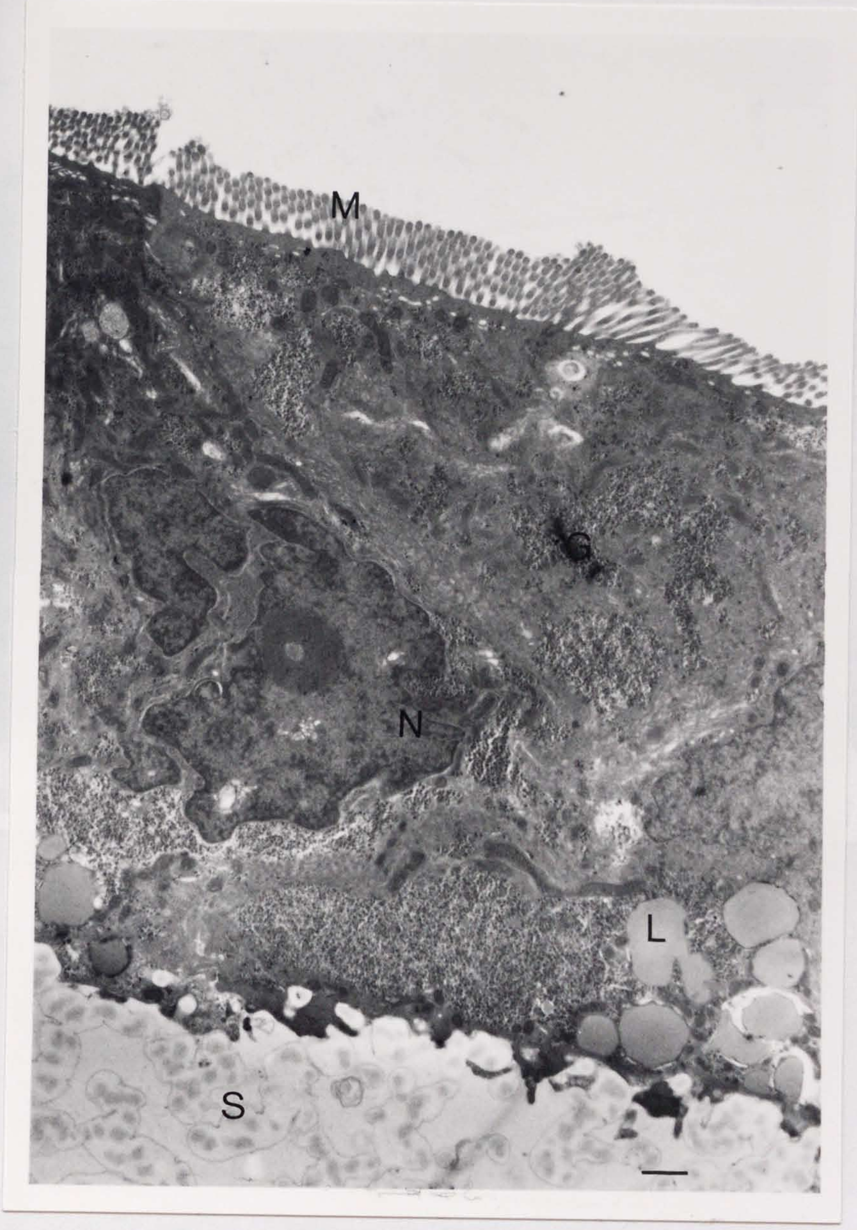

B)

FIGURE 3.7 *Scanning electron micrographs of Caco-2 cells cultured on aluminium oxide and nitrocellulose permeable-supports.*

Caco-2 monolayers cultured on aluminium oxide (**A**) and nitrocellulose (**B**) permeable-supports. Scale bar represents 1 μM.

A)

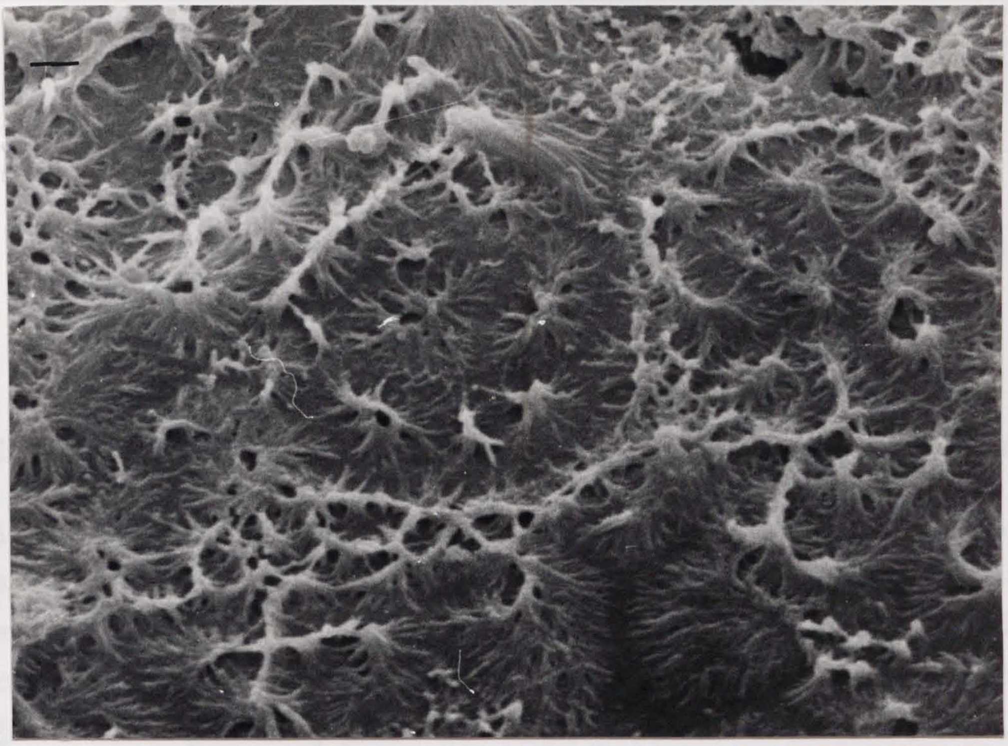

B)

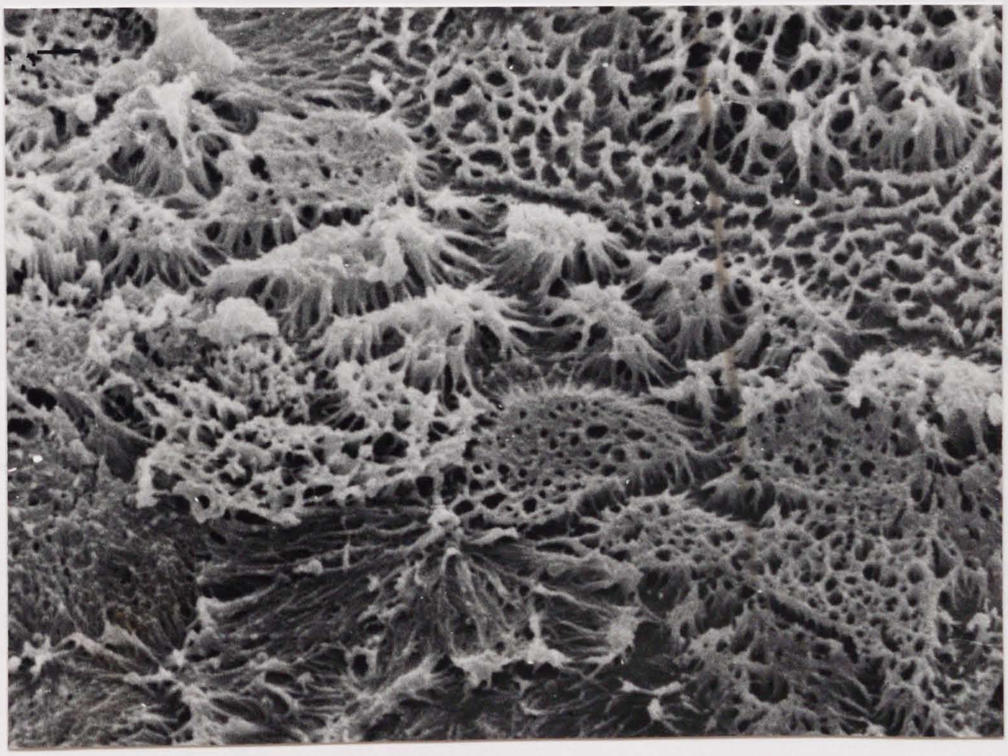

FIGURE 3.8 *Cytochemical localisation of horseradish peroxidase following a 60 min basolateral incubation.*

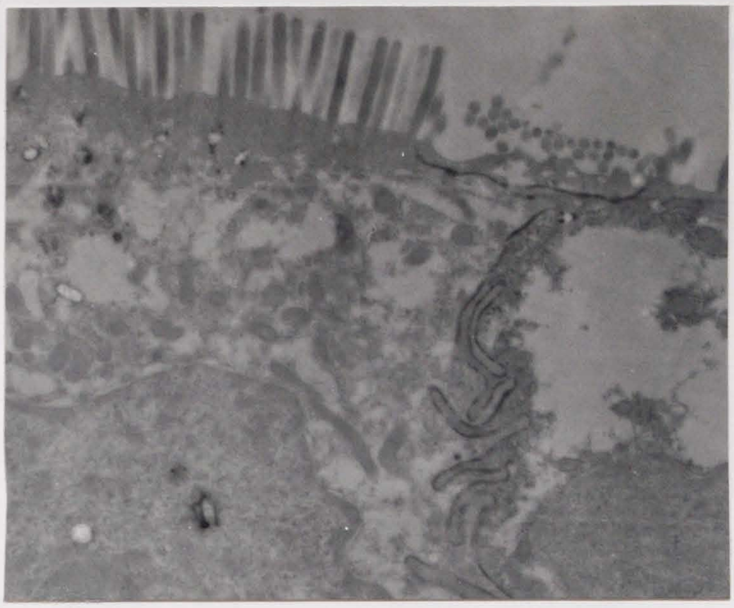

FIGURE 3.9 *Morphometric analysis of Caco-2 cells cultured on aluminium oxide and nitrocellulose permeable-supports.*

Cell (**A**) and microvilli (**B**) height were monitored with time in culture on aluminium oxide (squares) and nitrocellulose (circles) permeable-supports. Measurements were made on micrographs from at least six random areas in the case of cell height and at least eleven random areas in the case of microvilli height. Data are presented as mean ± SE. § Denotes a significantly greater cell height on aluminium oxide at $p<0.05$. * Denotes a significantly greater cell height on nitrocellulose inserts at $p<0.01$.

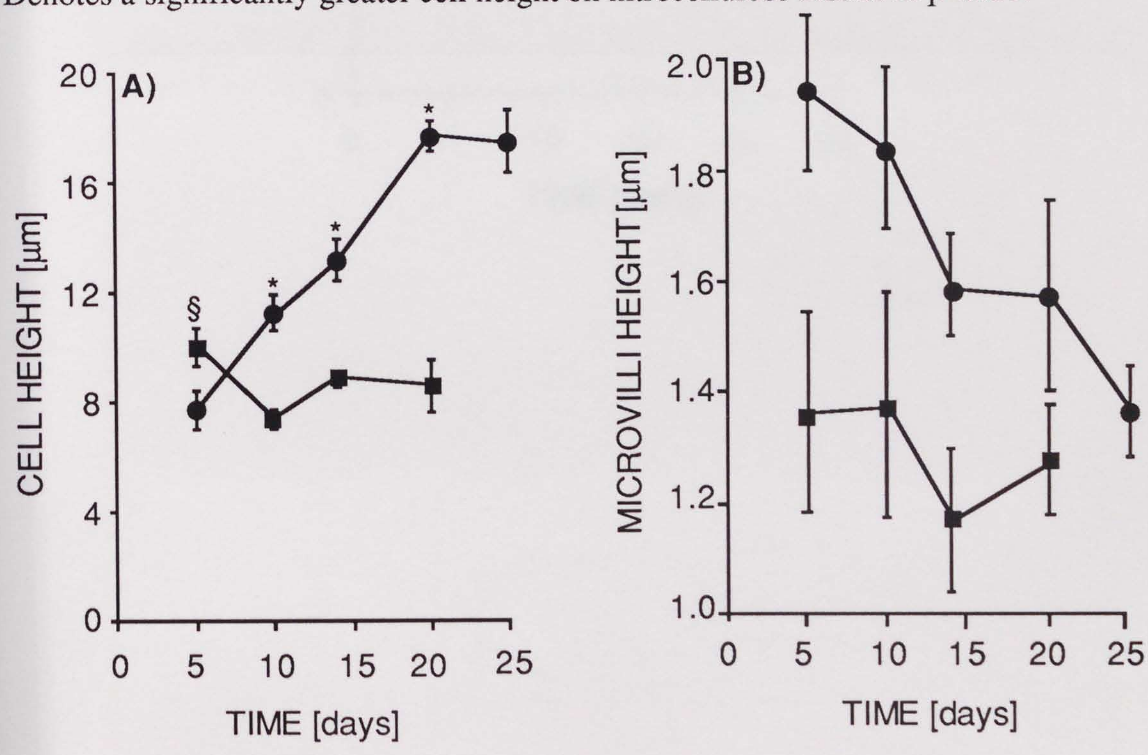

FIGURE 3.10 *Temporal-dependence of transepithelial electrical resistance of Caco-2 monolayers cultured on aluminium oxide and nitrocellulose permeable-supports.*

Data are presented as mean ± SE for three monolayers. * Denotes a significantly higher TER across Caco-2 monolayers cultured on aluminium oxide inserts compared to nitrocellulose at $p<0.01$.

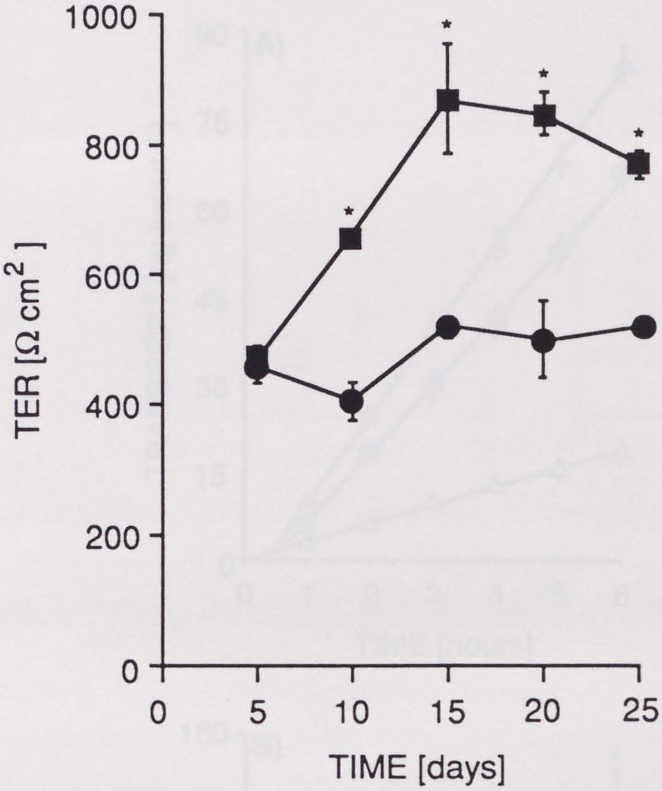

FIGURE 3.11 *Taurocholic acid transport.*

(**A**) *Ap-to-Bl transport kinetics:* Total (closed triangles), non-saturable (open triangles) and saturable (closed circles) Ap-to-Bl transport kinetics across Caco-2 monolayers cultured on nitrocellulose were determined over 7 h. (**B**) *Temporal-dependence of transport polarity:* Saturable transport across Caco-2 monolayers cultured on aluminium oxide (squares) and nitrocellulose (circles) in the Ap-to-Bl (closed symbols) and Bl-to-Ap (open symbols) directions. Data are presented as mean ± SE for three monolayers. * Denotes a significantly higher rate of saturable Ap-to-Bl taurocholic acid transport across Caco-2 monolayers cultured on nitrocellulose compared to aluminium oxide inserts at p<0.01.

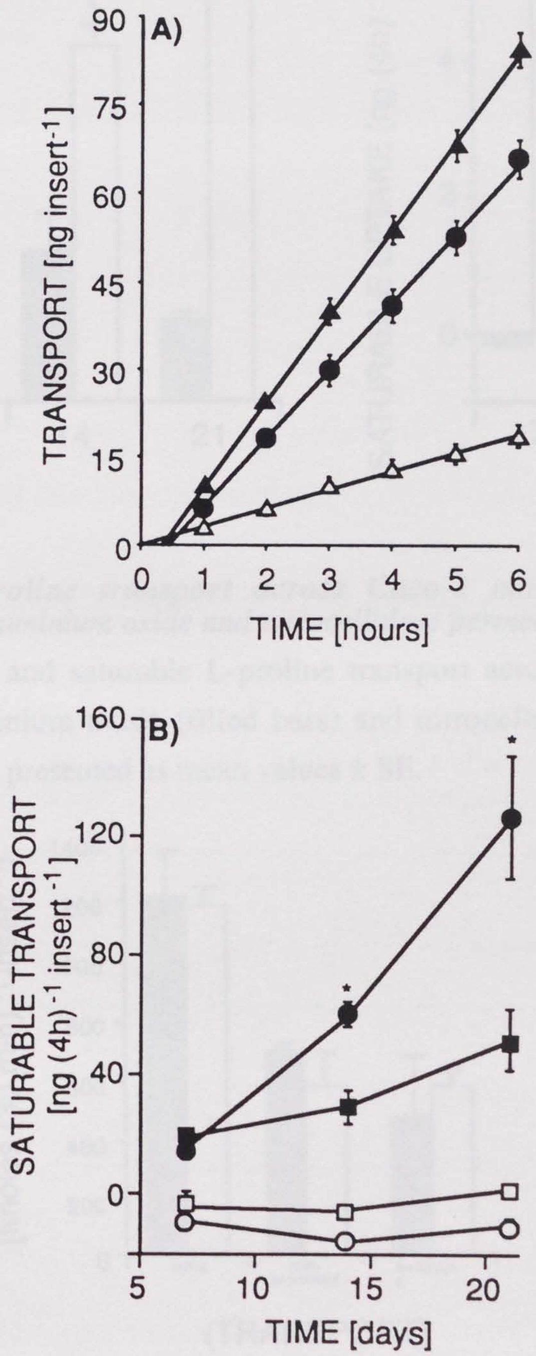

FIGURE 3.12 *Temporal-dependence of apical and basolateral taurocholic acid uptake into Caco-2 monolayers cultured on aluminium oxide and nitrocellulose permeable-supports.*

The saturable Ap (**A**) and Bl (**B**) uptake of taurocholic acid into Caco-2 monolayers cultured on aluminium oxide (closed bars) and nitrocellulose (open bars) were determined. Data are presented as mean values ± SE for three monolayers. * Denotes a significantly higher saturable uptake into Caco-2 monolayers cultured on nitrocellulose compared to aluminium oxide at $p<0.01$.

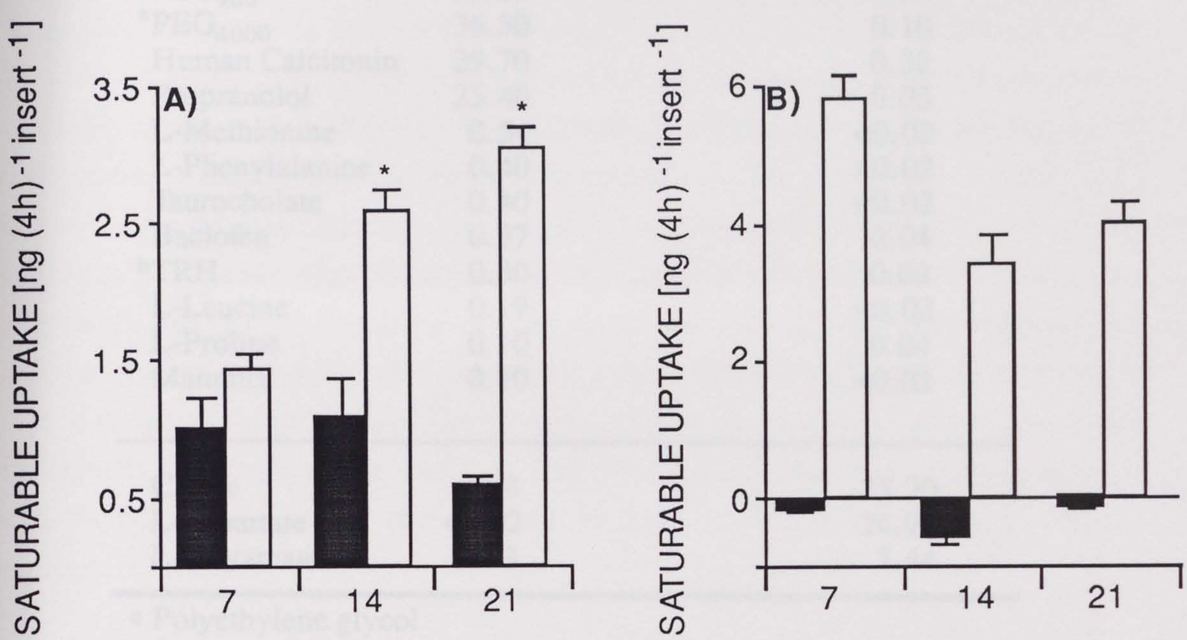

FIGURE 3.13 *Proline transport across Caco-2 monolayers cultured on aluminium oxide and nitrocellulose permeable-supports.*

Total, non-saturable and saturable L-proline transport across Caco-2 monolayers determined on aluminium oxide (filled bars) and nitrocellulose (open bars) were determined. Data are presented as mean values ± SE.

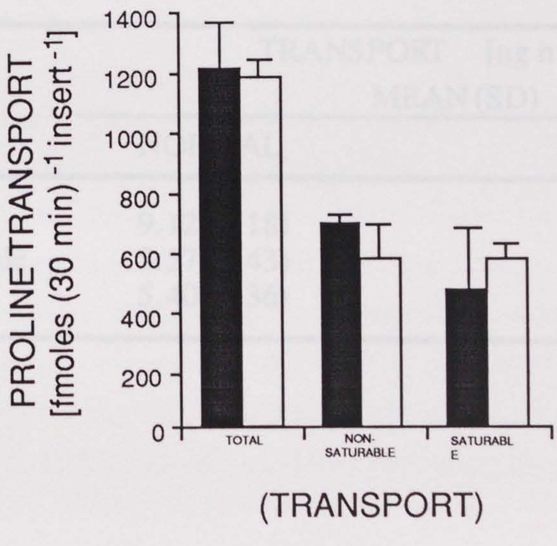

TABLE 3.1 *Ligand adsorption to aluminium oxide and nitrocellulose permeable-supports.*

LIGAND	% ADSORBED	
	NITROCELLULOSE	ALUMINIUM OXIDE
Testosterone	72.70	<0.02
[a]PEG_{900}	59.60	0.07
[a]PEG_{4000}	36.50	0.10
Human Calcitonin	29.70	0.38
Propranolol	25.40	0.05
L-Methionine	0.54	<0.02
L-Phenylalanine	0.40	<0.02
Taurocholate	0.40	<0.02
Baclofen	0.37	0.04
[b]TRH	0.30	0.03
L-Leucine	0.19	<0.02
L-Proline	0.10	0.04
Mannitol	0.10	<0.02
Citrate	0.08	25.20
L-Aspartate	<0.02	24.90
L-Glutamate	0.03	7.44

[a] Polyethylene glycol

[b] Thyrotrophin-releasing hormone

TABLE 3.2 *Taurocholic acid transport across Caco-2 monolayers cultured on aluminium oxide inserts, normal pore-size (0.2 μm upper surface to 0.02 μm lower surface) and special pore-size (0.2 μm throughout).*

	TRANSPORT [ng h^{-1} insert^{-1}] MEAN (SD)	
	NORMAL	SPECIAL
Total	9.12 (0.18)	9.92 (0.39)
Non-saturable	3.57 (0.43)	4.48 (0.14)
Saturable	5.40 (0.36)	5.41 (0.49)

3.5 DISCUSSION

The ideal permeable-support for the Caco-2 monolayer model should promote enterocyte-like differentiation without influencing transport kinetics. In this way, the flux of a compound across the monolayer-permeable support composite predominantly reflects permeation of the cellular barrier. This criterion can only be met by a permeable-support with low ligand adsorption properties. In this respect, the aluminium oxide insert is superior to the nitrocellulose for most compounds. Exceptional ligands were citrate, aspartate and glutamate. The importance of the permeable-support type on transport kinetics is highlighted by its influence on the transport of testosterone. Testosterone flux is rapid across aluminium oxide inserts but slow across nitrocellulose. This difference reflects the large differential in testosterone binding to these permeable-supports. For lipophilic ligands (*eg:* testosterone), transport kinetics are controlled by the permeable-support whilst for hydrophilic ligands (*eg:* D-mannitol) the cellular barrier controls transport. Therefore, the use of aluminium oxide inserts should significantly enhance the versatility of the Caco-2 model for studying the transport properties of compounds with a range of lipophilicities and/or molecular weights. Notable exceptions are compounds that chelate metal cations. One would predict that the transport of citric acid would be retarded by chelation to the aluminium oxide support despite its hydrophilic nature.

Previous studies have shown the properties of Caco-2 monolayers to be dependent on the basement membrane on which they are cultured. For example, Stratford and co-workers [Stratford *et al.*, 1988] showed that 0.3% fluorescein isothiocyanate-dextran was transported across Caco-2 monolayers grown on nitrocellulose permeable-supports coated with Matrigel (a solubilised membrane preparation) compared with 0.04% across those cultured on collagen-coated inserts. The sensitivity of Caco-2 cells towards the surface on which they are cultured was confirmed in the present study.

At the light microscopic level, occasional structures resembling blister-like domes formed by Caco-2 cells cultured on plastic [Pinto *et al.*, 1983] were present only on monolayers cultured on aluminium oxide inserts. Dome formation is characteristic of a polar transporting epithelium. In the MDCK cell line, domes are assumed to result from fluid and electrolyte between the monolayer and an impermeable-support since they are ouabain-sensitive [Leighton, *et al.*, 1970; Abaza, *et al.* 1974] and do not form on permeable-supports [Leighton, *et al.*, 1970; Abaza, *et al.* 1974; Cereijido *et al.*, 1978; Rabito, *et al.*, 1978]. However, dome formation by Caco-2 monolayers is not ouabain-sensitive and can occur on 0.015 μm, but not 0.030 μm polycarbonate permeable-supports. An accumulation of species with a hydrodynamic radius greater than 0.015 μm has been proposed to explain these observations [Raymond *et al.*, 1985]. The counter-growth surfaces of the normal aluminium oxide permeable-supports has a pore-size of 0.02 μm which is comparable to the 0.015 μm pore-size of the polycarbonate filter that stimulated dome formation. These observations suggest that the small pore-size of the normal aluminium oxide permeable-support may encourage dome formation. At the electron microscopic level, Caco-2 cells were highly differentiated on both types of permeable-support. However, the morphology of the cells differed with respect to cell and microvilli height. Moreover, on nitrocellulose inserts, the cells displayed a greater degree of intracellular organisation and the Ap brush-border was more highly developed.

In addition to morphological differences, Caco-2 monolayers differed in their TER and ability to specifically transport taurocholic acid. The TER of cell monolayers cultured on permeable-supports predominantly reflects the resistivity across the tight junction rather than cell membranes [Madara, 1983; Grassett *et al.*, 1984]. Between 14 and 25 d, TER was approximately 350 Ω cm^2 higher for Caco-2 monolayers cultured on aluminium oxide inserts. The lower cell density on the aluminium oxide inserts results in a smaller number of intercellular contacts per unit area of monolayer, thereby increasing the resistance to ion flux. This may partially explain the higher TER of Caco-2 monolayers on aluminium oxide inserts. However, the most likely reason for the disparate electrical properties is selection of different sub-populations from the parental cell line by each support. The parental (wild-type) Caco-2 cell line is heterogeneous and the overall characteristics of the monolayer represent a summation of the properties of a range of cell phenotypes. Recently, the parental Caco-2 cell line has been cloned using a limiting dilution technique [Woodcock *et al.*, 1990]. Several stable clones were established and these showed a wide range of TER profiles, differing with respect to maximal TER (<100 to >1500 Ω cm^2 at 15 d) and the time-scale of TER development. Clearly, selection of different sub-populations by each permeable-support could conceivably explain the disparate electrical properties.

Caco-2 monolayers actively transport taurocholic acid in a saturable and polar fashion when cultured on nitrocellulose [Wilson *et al.*, 1990] or collagen-coated polycarbonate inserts [Hidalgo *et al.*, 1990 b]. The apparent transcellular transport Michaelis constant (K_m) of 42.5±2.8 μM [Wilson *et al.*, 1990] or 49.7 μM [Hidalgo and Borchardt, 1990 b] across Caco-2 cells was comparable to that for its uptake into human brush-border membrane vesicles (37±7 μM) [Barnard and Ghishan, 1987]. Bile acids are also transported across Caco-2 monolayers cultured on aluminium oxide inserts. However, the rate of taurocholic acid transport differs depending on the type of permeable-support. This difference in transport rate can be partially explained in terms of cell numbers although, after correction for this variant, taurocholic acid transport occurs almost twice as rapidly across Caco-2 monolayers cultured on nitrocellulose (35.7±11.2 ng $(4h)^{-1}$ $(10^6$ cells$)^{-1}$) compared to aluminium oxide inserts (19.5±8.3 ng $(4h)^{-1}$ $(10^6$ cells$)^{-1}$). This suggests a functional difference exists between the monolayers cultured on these two permeable-supports. This difference cannot be attributed to the very small pore-size of the normal aluminium oxide permeable-support (0.02 μm) since taurocholic acid transport across Caco-2 monolayers cultured on these and a specially prepared batch with a 0.2 μm pore size (comparable to 0.45 μm of the nitrocellulose) were not significantly different. Interestingly, Caco-2 clones are characterised by having widely different abilities to transport taurocholic acid [Woodcock *et al.*, 1991]. This strengthens the claim that the different properties of Caco-2 monolayers on the two types of insert is related to selection of different sub-populations from the heterogeneous parental cell line.

The correlation between Bl uptake and Bl-to-Ap transport for taurocholic acid is better defined when Caco-2 for monolayers cultured on aluminium oxide inserts. This probably reflects the very low adsorption to the aluminium oxide support allowing cellular uptake events to be studies precisely. Conversely, on nitrocellulose inserts, taurocholic acid adsorption to the support masks Bl cellular uptake. Therefore, aluminium oxide permeable-supports allow Bl uptake events to be studied with a precision not possible with nitrocellulose.

3.6 CONCLUSION

There are significant differences between Caco-2 monolayers cultured on aluminium oxide and nitrocellulose culture inserts. Monolayers cultured on aluminium oxide inserts have a lower cell density, different morphology and form occasional domes. Furthermore, they display a higher TER and lower capacity for taurocholic acid transport. Nevertheless, Caco-2 monolayers cultured on either permeable-support displayed similar abilities to transport L-proline.

The use of inserts for cell culture experiments is increasingly popular. The work presented here shows that the permeable-support type should be an important consideration for transport studies. Furthermore, the influence of permeable-support type on the properties of the cell model should be appraised.

CHAPTER FOUR

PROLINE UPTAKE INTO AND TRANSPORT ACROSS CACO-2 MONOLAYERS

ABSTRACT

Caco-2 monolayers cultured for 6 d on plastic exhibit active and passive uptake systems for L-proline. The active pathway accounts for two thirds of uptake over the nanomolar range, at 37°C and pH7.4. Carrier-mediated uptake is sodium-dependent and is significantly reduced when protein synthesis (cycloheximide), Na^+/K^+-ATPase (ouabain) or cellular metabolism (sodium azide) are inhibited. The temperature-dependence of L-proline uptake followed the Arrhenius model with an apparent activation energy of 93.5 kJ mol^{-1}. The sodium-dependent uptake component followed Michaelis-Menton concentration-dependence with a K_m^{sd} of 5.28 mM and a maximal velocity of 835 pmol min^{-1} (10^6 cells)$^{-1}$. In competition studies, alpha-aminoisobutyric acid, L-alanine and L-serine were potent inhibitors whereas glycine, D-proline and gamma-aminoisobutyric acid were partial inhibitors. Aromatic and branched aliphatic amino acids showed weak (L-valine) or no (L-phenylalanine, L-leucine) inhibition. These data show that L-proline uptake at pH7.4 shares many features with the A-system carrier.

L-Proline uptake exhibits a complex pH-dependence. Within the physiological pH range there was a local pH-optimum at pH7.4 but dramatic increases were noted as pH5.0 was approached. Indeed, the mechanism of L-proline uptake into, and transport across, Caco-2 monolayers cultured for 21 d on permeable-supports demonstrated a pH-dependent heterogeneity. At pH7.4 uptake and transport were energy- and sodium-dependent whereas at pH5.5 they were energy- and sodium-independent. The data presented here suggest that L-proline transport is mediated by different populations of carriers at pH7.4 and pH5.5.

4.1 BACKGROUND

4.1.1 L-PROLINE

Amino acids traverse biological membranes by passive diffusion and a multiplicity of carrier systems. These carriers are classified as sodium-dependent or sodium-independent and sub-classified on the basis of kinetic parameters and cross-inhibition by amino acid pairs. Distinct L-alanine-preferring and L-leucine-preferring amino acid carriers were first defined in the non-epithelial Ehrlich ascites tumour cells, and named the A and L systems, respectively [Oxender and Christensen, 1963]. At least twelve different amino acid carriers have subsequently been characterised in non-epithelial cells of vertebrates [Christensen, 1984; Christensen, 1985]. In addition to a number of these, epithelial cells possess a complement of carriers not present in non-epithelial cells [Stevens *et al.*, 1984]. Delineation of intestinal epithelial amino acid transport is complicated by their overlapping substrate-specificity, regional and inter-species variation [Hopfer, 1987] and the different models employed to study them. This situation is especially true for imino acids.

Early reports described an exclusive imino acid transport-system in the hamster small intestine [Lin, *et al.*, 1962; Hagihira *et al.*, 1962; Spencer and Brody, 1964] whereas in the rat, L-proline (Fig. 4.1 A) shares an uptake system with glycine from which betaine (N-trimethylglycine) is excluded [Newey and Smyth, 1964]. A later report suggested that the imino acid transporter of the rat small intestine resembled the A-system [Munck, 1966]. The involvement of the A system in L-proline uptake has also postulated for the guinea pig ileum. This was based on a 90% inhibition of L-proline uptake by alpha-(methylamino)isobutyric acid (MeAIB) into BBMV [Hayashi *et al.*, 1980], however, in the absence of a comprehensive amino acid cross-inhibition profile, the involvement of other systems cannot be discounted. Indeed, in rabbit jejunal BBMV, the sodium-dependent L-proline uptake can be totally inhibited by MeAIB but it is insensitive to L-alanine and to glycine and excludes ß-alanine [Stevens *et al.*, 1982]. Therefore, uptake occurs *via* a system distinct from the A-mediation and was denoted the IMINO carrier. An equivalent system has been described in intact epithelial preparations from the rabbit distal ileum [Munck, 1985 b]. However, a second sodium-dependent uptake pathway for imino acids which accepts neutral, cationic and non-alpha-amino acids present in the intact preparation [Munck, 1985 a] was not observed in BBMV [Stevens *et al.*, 1982]. The intestinal transport of imino acids and non-alpha-amino acids has been linked in the rabbit and rat but each species has different characteristics [Munck, 1983]. A single study has shown L-proline uptake into adult human ileum is sodium-dependent but this was not extended to analysis of the kinetic parameters or cross-inhibition profiles [Rajendran *et al.*, 1985].

Studies on amino acid uptake into human intestinal tissue have been limited by the scarcity of tissue. Carrier-mediated uptake of L-alanine, L-phenylalanine [Lucke *et al.*, 1977] and dicarboxylic amino acids [Rajendran *et al.*, 1987 b; Harig *et al.*, 1987] into human jejunal brush-border membrane vesicles has been observed. Recently, sodium-dependent carrier-mediated uptake of L-proline into BBMV from human foetal small intestine has been demonstrated [Malo, 1991]. The mechanism of L-proline uptake into the adult human small intestine has not be studied in detail to date. In the present study, the carrier-mediated uptake and transport of the imino acid, L-proline, by monolayers of human intestinal absorptive (Caco-2) cells is investigated.

4.1.2 BACLOFEN

Baclofen (Lioresal; 4-amino-3-(p-chlorophenyl)-butyric acid; Fig. 4.1 B) is the chlorophenyl analogue of gamma-amino isobutyric acid (GABA) an amino acid neurotransmitter in the central nervous system. It is clinically useful as a spasmolytic agent. The possibility of baclofen undergoing amino acid carrier-mediated transport across Caco-2 monolayers is considered.

FIGURE 4.1 *Structures of L-proline (A) and baclofen (B).*

A)

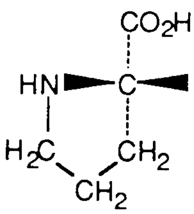

B)

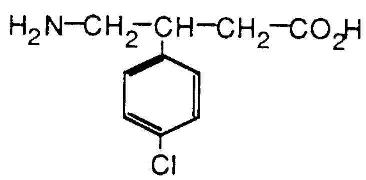

4.2 MATERIALS

4.2.1 CHEMICALS

L-[^{14}C]Arginine (300 Ci mol^{-1}), L-[^{3}H]-proline (26 mCi mmol^{-1}) and L-[^{3}H]-phenylalanine (106 Ci mmol^{-1}) were obtained from Amersham, UK. D-[^{3}H]mannitol (49.3 Ci mol^{-1}) was obtained from New England Nuclear (Dupont, Germany). [^{14}C]Baclofen (1.28 Ci mol^{-1}) and unlabelled baclofen were a gift from Ciba Pharmaceuticals (Basle, Switzerland). Alpha-(Methylamino)isobutyric acid (MeAIB) was obtained from Aldrich Chemical Company (Gillingam, UK).

4.2.2 TRANSPORT-MEDIA

An amino acid-free medium (M2-medium), comprising 1% w/v BSA, 3.2 mM $CaCl_2$, 1.2 mM $MgCl_2$, 4 mM KCl, 150 mM NaCl and 5 mM glucose in double distilled water, buffered to pH 7.4 with 14 mM HEPES, was used for L-proline uptake experiments. Sodium-free amino acid-free media were prepared by equimolar substitution of NaCl with choline chloride ($M2_{Choline}$) or LiCl ($M2_{Lithium}$). Similarly, a glucose-free amino acid-free medium ($M2_{-Glucose}$) was prepared by omitting glucose from the above formula.

A modified amino acid-free medium (M3-medium), comprising 140 mM NaCl, 4 mM KH_2PO_4, 5.2 mM K_2HPO_4, 1.2 mM $MgSO_4$, 1.3 mM Calcium gluconate and 5 mM D-glucose, pH7.4, was prepared in order to to investigate the anion-dependence of L-proline uptake. Chloride-free modified amino acid-free media were prepared by equimolar substitutions of NaCl with sodium iodide ($M3_{Iodide}$)sodium isethionate ($M3_{Isethionate}$) or sodium thiocyanate ($M3_{Thiocyanate}$).

M4-medium, comprising Hanks' balanced salt solution containing 0.1% w/v BSA and buffered with 14 mM HEPES (pH 7.0, 7.4 or 8.0) or MES (pH 5.5, 6.0 or 6.5) was used for L-proline and baclofen transport experiments. M4-medium buffered to pH 7.4 was used unless specified. A sodium-free version was prepared by equimolar substitution of NaCl with choline chloride ($M4_{Choline}$).

4.3 METHODS

4.3.1 CELL CULTURE

For uptake studies, Caco-2 monolayers were cultured for 6 d on plastic six-well plates as described previously (see section 2.2.3). Transport studies were performed using 21 d Caco-2 monolayers unless otherwise specified. They were cultured on aluminium oxide (baclofen studies) or nitrocellulose (L-proline studies) permeable-supports as described previously (see section 2.2.4).

4.3.2 L-PROLINE UPTAKE EXPERIMENTS

L-[^{3}H]Proline uptake experiments were performed in the absence (total uptake) and presence (non-saturable uptake) of a >1.0x10^6 molar excess of L-proline (50 mM), allowing saturable-uptake to be calculated by subtraction.

The permeable-support-medium was aspirated and the Caco-2 monolayer washed with PBS (2 x 5 ml x 5 min) and finally with incubation medium (1 x 2 ml x 15 min). The cells were incubated with L-[^{3}H]proline (1.0 μCi ml^{-1}; 44 nM) in incubation medium, with or without excess (50 mM) L-proline, at 37°C for 20 min. Washing and incubation solutions were equilibrated to 37°C for 1 h prior to use. At the end of the incubation period the medium was removed from each well and its [^{3}H]-content determined by liquid scintillation counting (see section 2.4.1 A). Each monolayer was rinsed carefully three times with ice-cold PBS-azide 0.05% w/v stop-solution and solubilised with 2 ml of 0.1% v/v(aq) TX100. The [^{3}H]-content of each monolayer was determined using a Packard Tri-carb 2000CA liquid scintillation analyser (section 2.4.1 A) and corrected for the L-[^{3}H]-proline concentration in the incubation chamber (see section 2.3.2). A similar procedure was used to quantify L-[^{3}H]-phenylalanine uptake except the [^{3}H]-content using the liquid scintillation protocol described in section 2.4.1.B.

4.3.3 PROLINE TRANSPORT EXPERIMENTS

The Caco-2 monolayers were cultured for 21 d on nitrocellulose permeable-supports as described previously (section 2.2.4). Monolayers were washed with M4-medium pH7.4 or pH5.5 (1 x 2 ml Ap x 15 min) and with M4-medium pH7.4 (1 x 2ml Bl x 15 min). L-[^{3}H]proline (1.0 μCi ml^{-1}; 44 nM) in M4-medium pH7.4 or 5.5 was added to the Ap chamber. Ap(pH7.4)-to-Bl(pH7.4) or Ap(pH5.5)-to-Bl(pH7.4) L-proline transport was determined. The appearance of [^{3}H] in the receiver chamber represented total (saturable + non-saturable) Ap-to-Bl transport. The non-saturable transport component was estimated by measuring transport in the presence of a >1.0 x 10^6 molar excess of L-proline. Saturable transport was calculated by subtraction of the total and non-saturable transport components.

4.3.4 BACLOFEN TRANSPORT EXPERIMENTS

The Caco-2 monolayers were cultured for 21 d on aluminium oxide permeable-supports as described previously (section 2.2.4). Monolayers were washed with M4-medium pH7.4 (1 x 2 ml Ap + 2ml Bl x 15 min). [^{14}C]Baclofen (0.15 μCi ml^{-1}; 44 nM) in M4-medium pH7.4 was added to the Ap chamber. Ap-to-Bl transport kinetics were determined by sequential transfer at 15 min intervals. Alternatively, transport was determined after a single 1 h time point.

4.3.5 PROLINE IDENTIFICATION BY THIN-LAYER CHROMATOGRAPHY

Caco-2 monolayers were incubated with L-[^{3}H]proline (1.0 µCi ml^{-1}; 44 nM) in M2-medium for 30 min at 37°C then washed three-times with ice cold PBS-N_3 stop-solution. The [^{3}H]-loaded cells were scraped off the bottom of each well and resuspended in double-distilled water. The pooled cell-suspensions were homogenised by 10 strokes in a Potter-Elvehjem homogeniser at 2,000 rpm. The proteins in the homogenate were precipitated with trichloroacetic acid (TCA) and pelleted by centrifugation at 11,600 x g for 5 min (MSE minifuge). The supernatant was collected and lyophilised in an Edwards freeze-dryer. The lyophilised residue was reconstituted and spotted onto a cellulose TLC-plate (Whatman, Maidstone, UK). The chromatogram was developed with a mobile phase of butan-1-ol (60%), acetic acid (25%) and double distilled water (15%) run to 12 cm. At completion, the TLC-plate was dried rapidly at 70°C and divided vertically into 1 cm blocks. Each block of cellulose was scraped into a scintillation vial together with 10 ml of scintillation cocktail and its tritium-content determined. A reference sample was made by preparing a non-TCA-precipitable Caco-2 cell fraction as described above but omitting radiolabel from the incubation stage. A tracer of L-[^{3}H]proline was added prior to freeze-drying.

4.4 RESULTS

4.4.1 L-PROLINE UPTAKE

Seeding of 1.0 x10^6 cells per well resulted in a confluent monolayer after 4 days of culture. After 6 days of culture there were 3.4±0.2 x10^6 (n=9) cells per monolayer. Over the incubation-period for all experimental conditions, no cell detachment or alteration of monolayer appearance was observed by phase-contrast microscopy.

Tritium entering the Caco-2 monolayers was positively identified as L-[^{3}H]proline by TLC of the non-TCA precipitable cell fraction (Fig. 4.2). Less than 1% of the tritium was removed by TCA precipitiation of the Caco-2 cell homogenate and this was abolished (>80%) by a 30 minute pre-incubation of the cells with an inhibitor of protein synthesis, 500µM cycloheximide, prior to the addition of L-[^{3}H]proline (results not shown). This indicates that only a small proportion of L-[^{3}H]-proline is assimilated to protein by the cells over the experimental period.

The kinetic profile for L-[^{3}H]proline uptake (Fig. 4.3) shows an initial linear-phase (uptake proportional to incubation time) for at least 20 min, thereafter, uptake tended to a plateau. A distribution-ratio, calculated according to equation 4.1, greater than unity (*ie:* 3.26±0.03 at 45 min) is consistent with L-proline having an active uptake component. This was confirmed by measuring L-[^{3}H]proline uptake in the presence of 50 mM L-proline in order to estimate the passive uptake component. Typically, the non-saturable (passive) uptake component accounted for 32.2±1.1% (n=18) of the total uptake. It is the saturable, carrier-mediated, component which is considered further.

EQUATION 4.1 Distribution ratio = $[\mathrm{Proline}]_{\mathrm{monolayer}} / [\mathrm{Proline}]_{\mathrm{incubation\ medium}}$

Uptake studies, in the presence and absence of sodium ions, showed carrier-mediated uptake to be significantly reduced by replacing sodium chloride with choline chloride (87.7±0.6%; $p<0.001$) and lithium chloride (77.0±0.7%; $p<0.001$). Similarly, pre-incubation with 10 µM ouabain (an inhibitor of the Na^+/K^+-ATPase which generates the inward sodium ion gradient) reduced uptake by (82.6±1.6%; $p<0.001$, Fig. 4.4). Higher ouabain concentrations (up to 5 mM) failed to produce a greater reduction (results not shown). In contrast, L-phenylalanine uptake from $M2_{\mathrm{Choline}}$ was not significantly different from control values.

There is a sigmoidal relationship between the L-proline uptake and the extracellular sodium ion concentration. Uptake initially increased slowly at sodium ion concentrations below 30 mM before increasing rapidly between 30 and 50 mM, but it did not become maximal until much higher sodium concentrations (100 to 140 mM; Fig. 4.5). The saturable L-proline uptake was anion-sensitive (Fig. 4.6). Equimolar substitution of chloride for the more lipophilic anions, iodide and thiocyanate significantly increased L-proline uptake above control levels. In contrast, the replacement of chloride ions with the hydrophilic isethionate anion significantly reduced L-proline uptake. These observations suggest that L-proline uptake is electrogenic and associated with a net influx of positive charge into the cells.

Total L-proline uptake (V^t) in the presence of sodium ions is the sum of sodium-dependent (V^{sd}), sodium-independent (V^{si}) and diffusional (V^d) uptake mechanisms. In the absence of sodium ions, uptake represents the sum of V^{si} and V^d (Fig. 4.7 A). Therefore, subtraction of concentration-dependent uptake profiles performed in the presence and absence of sodium ions provides V^{sd} which depicts Michaelis-Menten saturation-kinetics for the sodium-dependent uptake component (Fig. 4.7 B). An

Eadie-Hofstee analysis of these data (Fig. 4.7 C), according to the transformation shown below (Equation 4.2), predicted a Michaelis constant, K_m^{sd} of 5.28±0.48 mM and maximal velocity, V_{max}^{sd} of 835±48 pmoles min^{-1} (10^6 cells)$^{-1}$.

EQUATION 4.2 $$V^{sd} = (-K_m^{sd} \times V^{sd}) / ([\text{Proline}] + V_{max}^{sd})$$

L-Proline uptake from $M2_{\text{-Glucose}}$ was not significantly different from control levels but was reduced by a pre-incubation with 10 mM sodium azide (Table 4.3; $p<0.05$). In addition, L-proline uptake was significantly ($p<0.001$) reduced by decreasing the temperature below 37°C (77.5±1.8 and 94.3±0.2% reductions at 20 and 4°C, respectively; Fig. 4.8 A). An activation energy (E_a) for L-proline uptake of 95.3 $kJ.mol^{-1}$ was calculated by linear least-squares regression analysis of a plot of Log k against 1/T according to the Arrhenius equation (Fig. 4.8 B and Equation 4.3 below) for these data.

EQUATION 4.3 $$\log k = \log A - E_a / (2.303\ R\ T)$$

To explore the substrate-specificity of the L-proline carrier system, the uptake of 50 µM L-[^{3}H]proline alone, or in the presence of a 100-fold molar excess (5 mM) amino (and imino) acids and three synthetic analogues, alpha- and gamma-amino isobutyric acid and MeAIB, were compared (Table 4.1). A differential ability to inhibit L-proline uptake was observed. The L-aspartate (-1.7±3.0%), did not inhibit L-proline uptake. Similarly, the aromatic amino acids (L-phenylalanine (3.0±1.5%) and L-tryptophan (-5.1±0.8%) and the branched aliphatic side-chain amino acid L-leucine (-0.4±3.7%) failed to significantly interfere with L-proline uptake. L-Valine (10.2±1.1%) showed a small, but significant ($p<0.05$), inhibition. Gamma-amino isobutyrate acid (33.4±7.5%), glycine (30.7±1.4%), and the stereoisomer D-proline (36.9±1.9%), only partially inhibited L-proline uptake ($p<0.01$). Moderate inhibition was observed by amide, basic and sulphur containing amino acids as well as L-hydroxyproline (50.2±5.7%) ($p<0.01$). The most potent inhibitors ($p<0.001$) were alpha-amino isobutyric acid (75.2±5.8%), L-alanine (69.3±4.3%), MeAIB (58.3±2.5%), L-serine (74.1±1.0%) and L-proline (68.3±0.02%) itself.

Expression of the L-proline carrier can be significantly up- and down-regulated by the monolayer feeding regimen (Table 4.2). Uptake in to monolayers that had experienced the normal feeding regimen (48 h; 0.942±0.049 pmoles (20 min)$^{-1}$) was significantly higher than after a recent replacement of permeable-support-medium (12 h; 0.844±0.011 pmoles (20 min)$^{-1}$). This suggests that up- and down-regulation of the L-proline carrier is under some degree of nutritional-control. Similarly, a 24 h incubation in protein-free amino acid-free medium (HBSS+HEPES) produced a marked up-regulation carrier-mediated uptake (1.411±0.069 pmoles (20 min)$^{-1}$). This may again reflect nutritional-control or be caused by the absence of a specific "down-regulating" component present in the permeable-support-medium. The significant inhibition of uptake by the protein synthesis inhibitor, cycloheximide (Table 4.3; 41.5±1.7%), after a 45 min pre-incubation indicates the L-proline carrier may be a protein with a rapid catalytic and synthetic turnover. This would enable a rapid change in L-proline carrier expression in response to environmental stimuli.

L-Proline uptake exhibited a complex pH-dependence (Fig. 4.9 A). Saturable uptake was pH-dependent whereas non-saturable uptake remained relatively constant between pH5.0 and 8.5. At pH-values slightly higher or lower than 7.4, significant reductions in specific L-proline uptake ($p<0.05$ and $p<0.01$ at pH8.5 and 7.0, respectively) were observed. Therefore, under neutral to mildly-alkaline a local pH-optimum occurred at pH7.4. At acidic pH-values, however, specific uptake was stimulated (4.6 fold at pH5.0) but was only 29.4±3.1% sodium-dependent at pH5.0 compared to 87.7±0.6% at pH7.4 (Fig. 4.9 B).

4.4.2 L-PROLINE TRANSPORT

L-Proline uptake was pH-sensitive (Fig. 4.9). Similarly, L-proline transport was dependent on the pH of the Ap donor-solution (Fig. 4.10). Transport was stimulated at acidic pH-values and became maximal at pH5.5. For a 44 nM Ap donor solution, the rate of total (saturable + non-saturable) Ap(pH5.5)-to-Bl(pH7.4) L-proline transport (7.567±0.296 pmoles h^{-1}) was 6.5-fold higher than Ap(pH7.4)-to-Bl(pH7.4) transport (1.17±0.067 pmoles h^{-1} (Fig. 4.11). The non-saturable component of Ap(pH7.4)-to-Bl(pH7.4) and Ap(pH5.5)-to-Bl(pH7.4) L-[^{3}H]proline transport was estimated by performing transport studies in the presence of a >1.0 x 10^6 molar excess (» saturating concentration; 50 mM) of unlabelled L-proline. The non-saturable Ap(pH5.5)-to-Bl(pH7.4) [^{3}H]proline transport (1.882±0.123 pmoles h^{-1}) was 2.7-times higher than that for Ap(pH7.4)-to-Bl(pH7.4) transport (0.686±0.020 pmoles h^{-1}). Saturable transport was calculated by subtraction of the non-saturable component from the total transport. The saturable Ap(pH5.5)-to-Bl(pH7.4) transport (5.685±0.422 pmoles h^{-1}) was 11.7-times that of Ap(pH7.4)-to-Bl(pH7.4) transport (0.486±0.079 pmoles h^{-1}). Furthermore, saturable Ap(pH7.4)-to-Bl(pH7.4) L-proline transport accounted for only 41.5±8.2% of the total ,whereas that for Ap(pH5.5)-to-Bl(pH7.4) transport represented 75.1±6.8% of the total. Passive and carrier-mediated

L-proline transport pathways were quantitatively more important at Ap pH5.5. In addition, the saturable transport component is proportionatly more important at Ap pH5.5.

The mechanism of L-proline transport under acidic conditions was considered. The elevated transport at pH5.5 may reflect stimulation of the same carrier-population that operates at pH7.4 or the activation of a distinct population of carriers which serve L-proline at acidic pH-values. Several observations support the later hypothesis. Firstly, stimulation of the same receptor population would result in a similar time-related expression, however, Ap(pH7.4)-to-Bl(pH7.4) and Ap(pH5.5)-to-Bl(pH7.4) L-proline transport exhibited different temporal-dependencies (Fig. 4.13). Ap(pH7.4)-to-Bl(pH7.4) transport did not increase between 7 and 14 d but increased at 21 d and remained constant through day 28. In contrast, Ap(pH5.5)-to-Bl(pH7.4) transport increased between 7 and 14 d and remained relatively constant thereafter. Secondly, whilst Ap-to-Bl L-proline transport was only slightly vectorial at pH7.4, it was highly vectorial at pH5.5. The rate of total Ap(pH7.4)-to-Bl(pH7.4) L-$[^3H]$proline transport across Caco-2 monolayers was only 1.3-fold higher than Bl(pH7.4)-to-Ap(pH7.4) transport (Fig. 4.14 A). However, the rate of saturable Ap(pH7.4)-to-Bl(pH7.4) was 2.9-times that in the Bl(pH7.4)-to-Ap(pH7.4) direction (Fig. 4.14 A inset). At Ap pH5.5, the total L-proline transport was highly vectorial (Fig. 4.14 B). Ap(pH5.5)-to-Bl(pH7.4) transport occurred at 5.0-times the rate of Bl(pH5.5)-to-Ap(pH7.4). In addition, the differential energy- and sodium-dependencies of L-proline uptake into and transport across Caco-2 monolayers at Ap pH7.4 and pH5.5, are shown in Table 4.4. Uptake into Caco-2 monolayers cultured on nitrocellulose permeable-supports from M4-medium pH7.4 was highly saturable (84.5±1.8%), and the saturable uptake was sodium-dependent (81.0±3.7%), ouabain-sensitive (106.0±1.8%) and reduced by metabolic inhibitors (N_3+2-DG; 101.4±1.4%). Similarly, the saturable Ap(pH7.4)-to-Bl(pH7.4) transport was sodium-dependent (56.4±2.3%), ouabain-sensitive (28.3±13.4) and reduced by N_3+2-DG (32.0±16%). Analogous experiments at Ap pH5.5 also showed uptake to be highly saturable (82.8±1.3%), however, it was sodium-independent and not reduced by metabolic inhibition.

Ap(pH5.5)-to-Bl(pH7.4) L-proline transport across Caco-2 monolayers was concentration-dependent (Fig. 4.14). Total (V^t) L-proline transport is the sum of saturable (carrier mediated; V^{cm}) and non-saturable (diffusional; $V^d = K_d$ x [Proline]) components. The V^t versus L-proline concentration data was fitted to Equation 4.4

and the kinetic parameters for V^{cm} and V^{d} were estimated by non-linear regression analysis (NONREG; Dr W. J. Irwin, Aston University).

EQUATION 4.4 $$v = ((V_{max}^{cm} \times [\text{Proline}]) / (K_m + [\text{Proline}])) + K_d \times [\text{Proline}]$$

The L-proline carrier (pH5.5) had a K_m = 3.0±1.2 mM and V_{max}^{cm} = 0.81±0.14 µmoles h^{-1} $insert^{-1}$. The diffusional rate constant (K_d) was found to be 0.0635±0.0029 µmoles h^{-1} $insert^{-1}$ mM^{-1}.

To examine the substrate-selectivity of the L-proline transporter at pH5.5, the Ap(5.5)-to-Bl(7.4) transport of 50 µM L-[^{3}H]proline alone, or in the presence of a 100-fold molar excess of a range of natural amino (and imino) acids and synthetic analogues was investigated (Table 4.5). L- and D-proline were potent inhibitors of L-[^{3}H]proline transport (81.8±1.0 and 75.0±1.0%, respectively). Similarly, L-alanine (77.2±2.4%) and the synthetic analogues alpha-amino isobutyric acid (70.1±3.2%) and MeAIB (72.6±1.3) were potent inhibitors of transport. Glycine (57.2±3.3%) and L-hydroxyproline (49.1±2.1%) were intermediate inhibitors, whilst the large neutral (L-phenylalanine; 5.4±4.4%) and cationic (L-arginine; 9.1±8.4%) amino acids failed to inhibit L-[^{3}H]proline transport at pH5.5. Interestingly, L-serine, which is a potent inhibitor of L-proline uptake at pH7.4 was only a weak inhibitor (25.2±4.4%) of L-proline uptake at pH5.5.

4.4.3 BACLOFEN

Ap-to-Bl [^{14}C]baclofen transport was linear for at least 90 min (Fig. 4.17). The initial rate of Ap-to-Bl transport was proportional to its Ap concentration from 100 µM to 20 mM (Fig. 4.18). Transport was non-vectorial and (Fig. 4.19) and only marginally influenced by Ap pH (Fig. 4.20). Finally, inhibition studies showed that the transport of baclofen was not reduced in the presence of 250, 2500 and 25000 µM beta-alanine (Table 4.6).

FIGURE 4.2 *Identification of L-[^{3}H]proline post-uptake.*
Thin-layer radio-chromatograms showing [^{3}H]-distribution in the non-TCA-precipitable fraction of L-[^{3}H]proline loaded Caco-2 cells (**A**) and a reference L-[^{3}H]proline-spiked non-TCA-precipitable cell fraction (**B**).

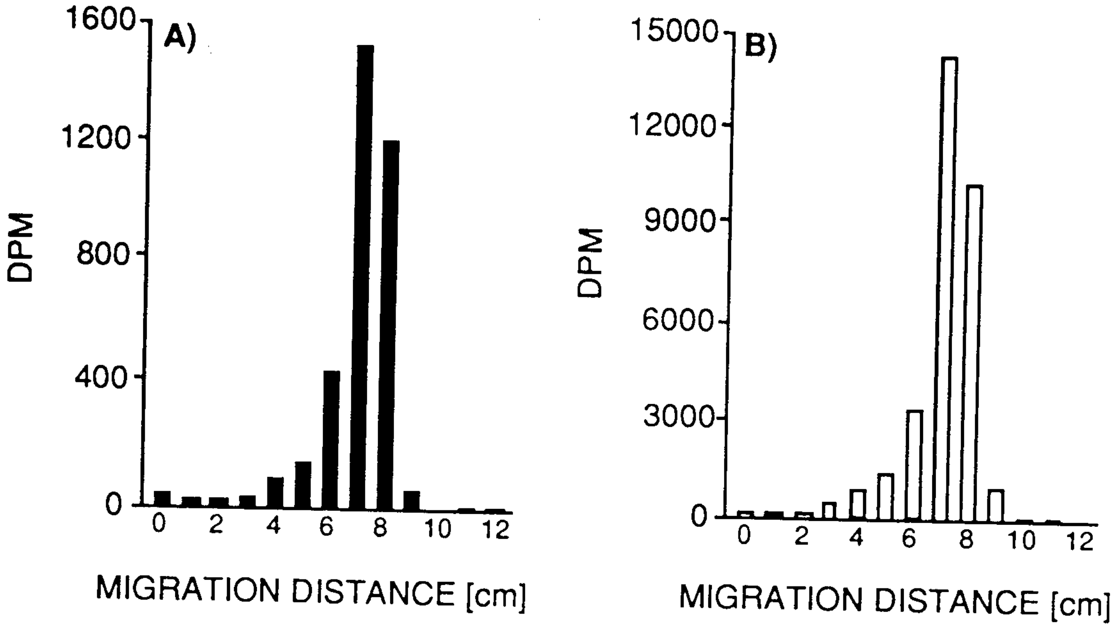

FIGURE 4.3 *Kinetics of L-proline uptake into Caco-2 monolayers.*
Monolayers were washed with PBS (2 x 5 ml x 5 min) followed by M2-medium (1 x 2 ml x 15 min). Total L-[^{3}H]-proline uptake was determined after 1.75, 2.5, 5, 10, 20, 30, and 45 min at 37°C. Data are mean values ± SD for three monolayers.

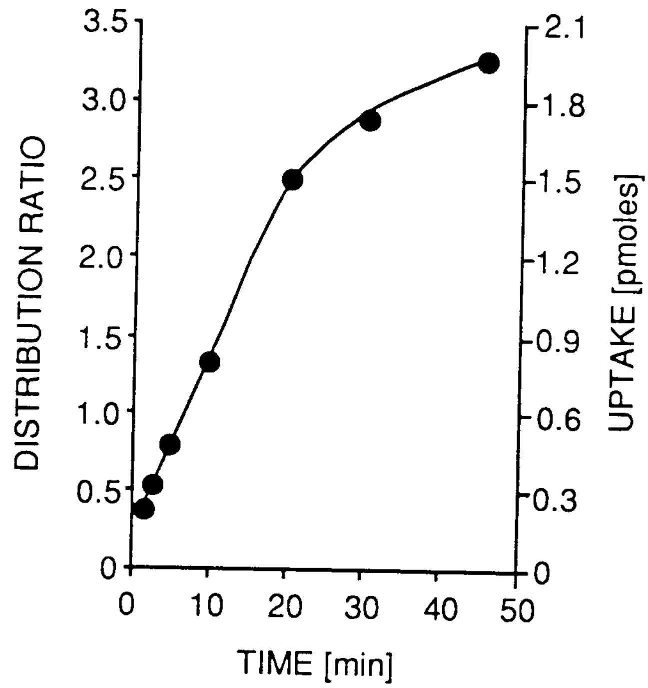

FIGURE 4.4 *Sodium-dependence of L-phenylalanine and L-proline uptake into Caco-2 monolayers.*

Monolayers were washed with PBS (2 x 5 ml x 5 min) then M2-medium (closed bar), $M2_{Choline}$ (open bar) or $M2_{Lithium}$ (shaded bar, L-proline only) as appropriate. The saturable uptake of L-[^{3}H]phenylalanine and L-[^{3}H]-proline were determined from these media. In addition, monolayers were pre-incubated with 10 μM ouabain (1 x 5 ml x 120 min) then washed with M2-medium containing 10 μM ouabain (2 x 2 ml x 5 min). The saturable uptake of L-[^{3}H]proline in the presence of 10 μM ouabain was determined (hatched bar, L-proline only). Data are presented as mean values ± SD for three monolayers. * Denotes significant reduction, $p<0.001$.

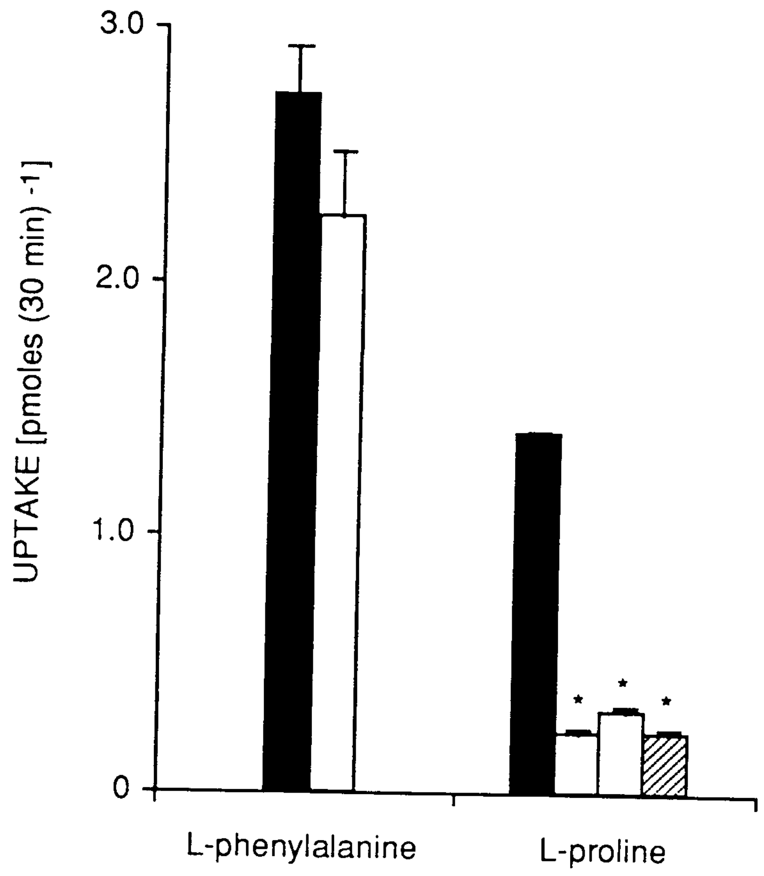

FIGURE 4.5 *Influence of extracellular sodium concentration on L-proline uptake.* Monolayers were washed with PBS (2 x 5 ml x 5 min) then M2-medium containing the appropriate sodium ion concentration (1 x 2ml x 5 min). The uptake of L-[^{3}H]proline The uptake of L-[3H]proline was determined from M2-medium containing 0, 10, 20, 30, 50, 70, 100 and 140 mM sodium ions. Data are presented as mean values ± SD for three monolayers.

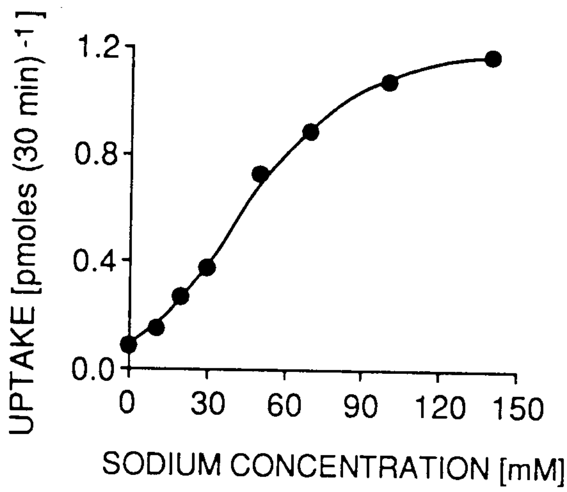

FIGURE 4.6 *Anion-dependence of L-proline uptake.*
Monolayers were washed with PBS (2 x 5 ml x 5 min) then M3-medium containing 140 mM of the appropriate sodium anion concentration (1 x 2ml x 5 min). The uptake of L-[^{3}H]proline was determined from M3-medium, $M3_{Iodide}$, $M3_{Isethionate}$ and $M3_{Thiocyanate}$. Data are presented as mean values ± SD for three monolayers. § Denotes a significant increase from control values at $p<0.05$. * Denotes a significant reduction at $p<0.05$.

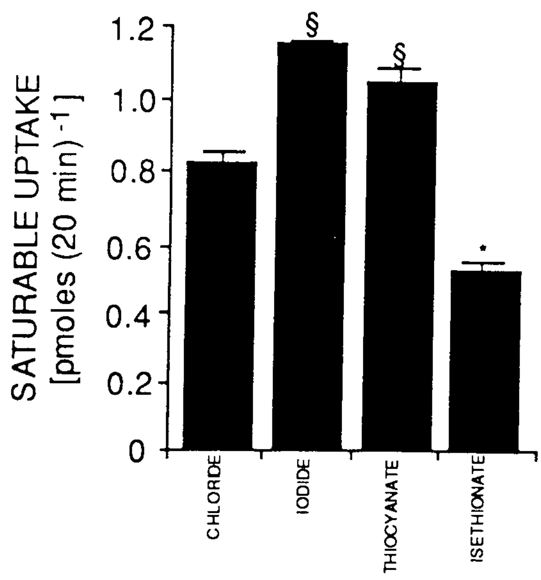

FIGURE 4.7 *Concentration-dependence of L-proline uptake.*
Monolayers were washed with PBS (2 x 5 ml x 5 min) followed by M2-medium or $M2_{Choline}$ (1 x 2 ml x 15 min), then incubated with a range of L-[^{3}H]proline concentrations (0.5 mM to 50 mM), in the presence and absence of sodium ions. The concentration-dependence of L-proline uptake, in the presence (closed circles) and absence of sodium ions (open circles), is shown below (**A**). The difference between the two curves, as a function of concentration (open squares; **B**), was analysed using an Eadie-Hofstee plot (closed squares; **C**). Data are presented as mean values ± SD for three monolayers.

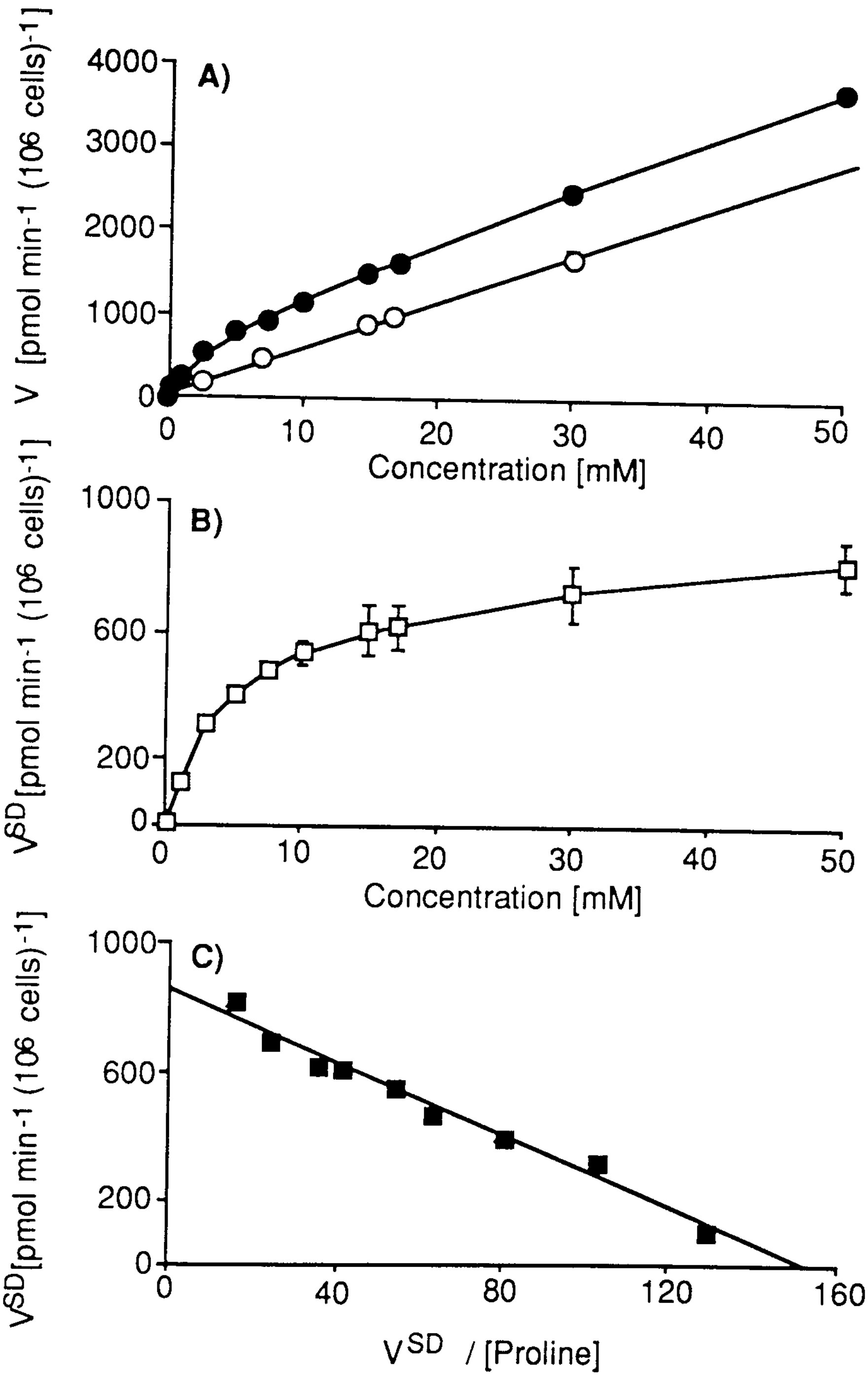

FIGURE 4.8 *Temperature-dependence of L-proline uptake.*
Monolayers were washed with PBS (2 x 5 ml x 5 min) followed by M2-medium (1 x 2 ml x 15 min) pre-equilibrated to 4, 20 or 37°C, as appropriate. Saturable L-[^{3}H]proline uptake at 4, 20 and 37°C was determined (**A**). Data are presented as mean values ± SD for three monolayers. * Denotes significant difference from uptake at 37°C, p<0.001. The uptake activation-energy was calculated from an Arrhenius plot of these data (**B**).

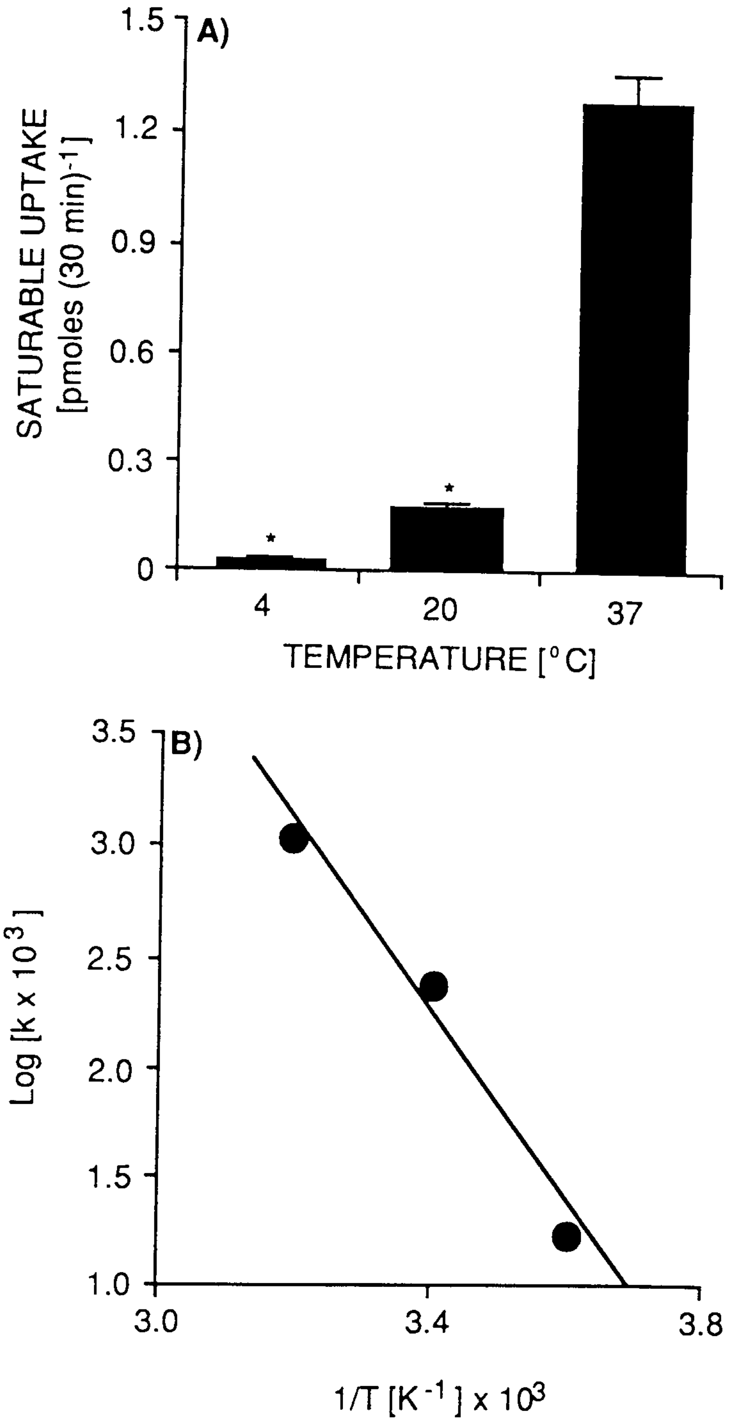

FIGURE 4.9 *The effect of pH on L-proline uptake.*
(**A**) Monolayers were washed with PBS pH7.4 (2 x 5 ml x 5 min) then M2-medium buffered to pH 5.0, 6.0, 7.0, 7.4, 8.0 or 8.5 (1 x 2 ml x 15 min). L-[^{3}H]-proline uptake was determined in the presence (non-saturable, open bar) and absence (total, closed bar) of 50 mM unlabelled L-proline at each pH value. * and ** Denote significantly different uptake to that at pH7.4, $p<0.05$ and $p<0.01$, respectively. (**B**) The effect of sodium-depletion on L-proline uptake at pH5.0. ** Denotes a significant reduction by sodium-depletion $p<0.05$. Data are presented as mean values ± SD for three monolayers.

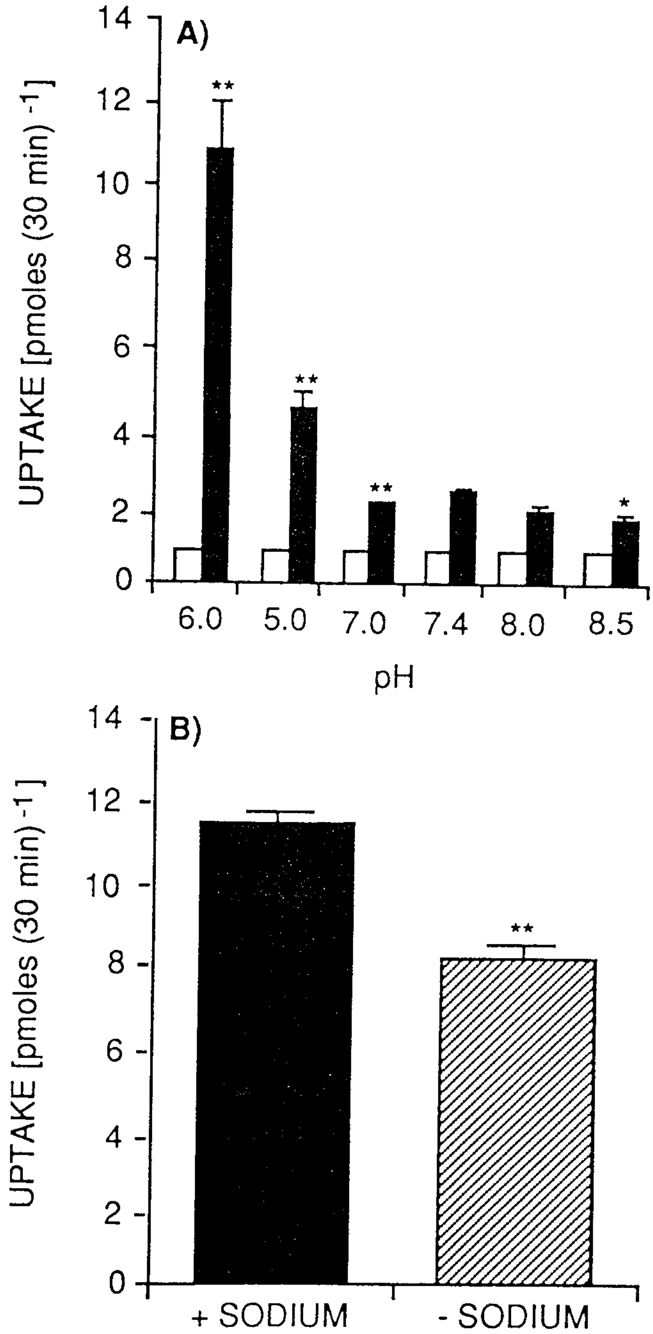

FIGURE 4.10 *pH-dependence of L-proline transport.*
Monolayers were washed (1 x 2ml Ap x 15 min) with M4-medium buffered to the appropriate pH and (1 x 2ml Bl x 15 min) with M4-medium pH7.4. Ap(pH5.0 to 8.0)-to-Bl(pH7.4) L-proline transport was determined. Data are presented as mean values ± SD for three monolayers. * Denotes a significant increase ($p<0.001$) in L-proline transport from that at pH7.2.

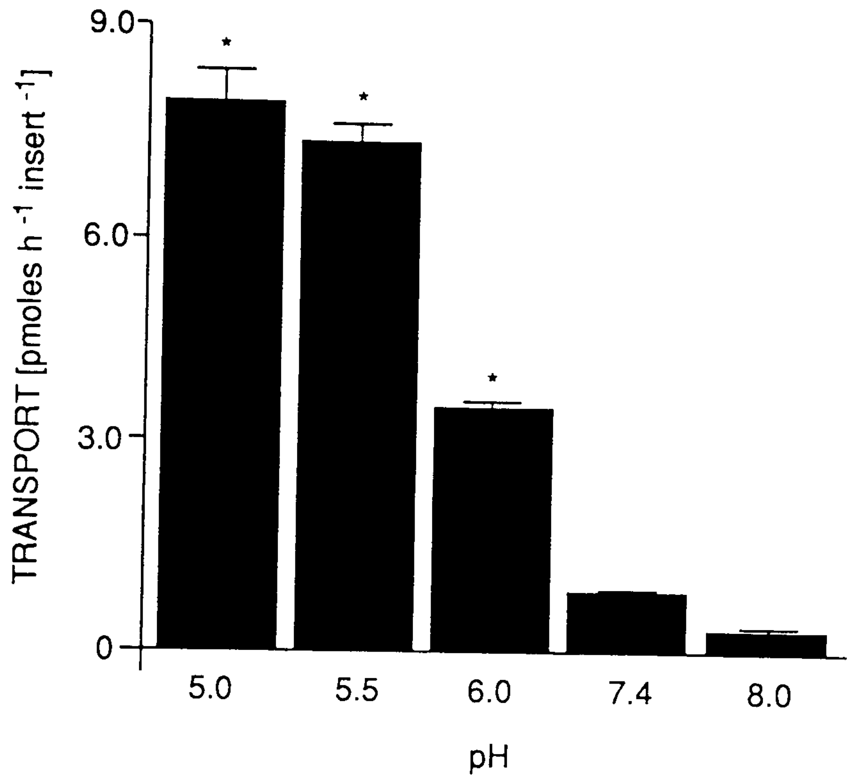

FIGURE 4.11 *Ap-to-Bl L-proline transport kinetics at pH7.5 and pH5.5.*
Monolayers were washed (1 x 2ml Ap x 15 min) with M4-medium buffered to pH7.4 or pH5.5 and (1 x 2 ml Bl x 15 min) with M4-medium pH7.4, as appropriate. Ap-(pH7.4)-to-Bl(pH7.4) (**A**) and Ap(pH5.5)-to-Bl(pH7.4) (**B**) transport kinetics of L-[^{3}H]proline alone (circles, total), or in the presence of 50 mM L-proline (squares, non-saturable) was determined. The saturable transport (triangles) was calculated by subtraction of the non-saturable component from the total transport. Data are presented as mean values ± SD for three monolayers.

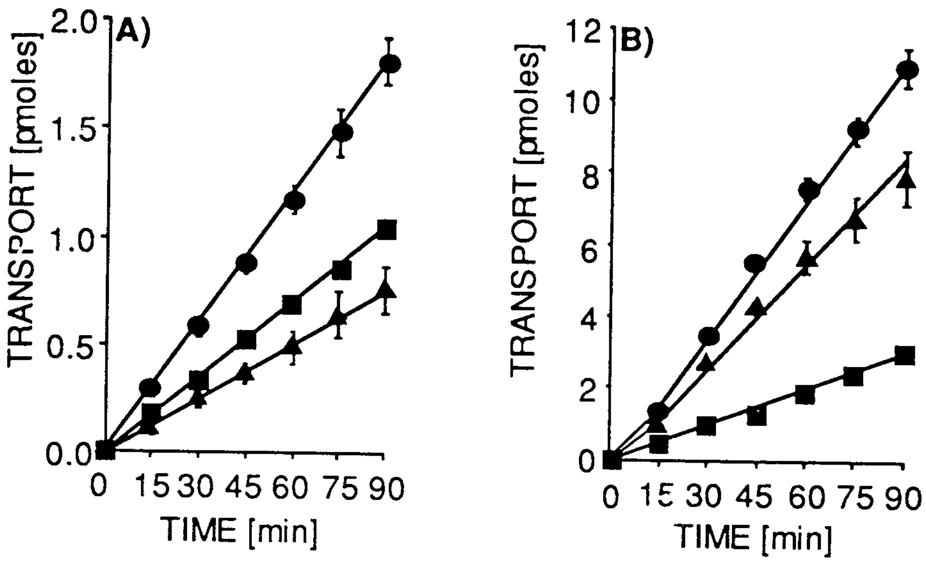

FIGURE 4.12 *Effect of ouabain and metabolic inhibitors on D-mannitol transport.*
Monolayers were pre-incubated for 1 h with M4-medium (pH7.4) alone (control) or containing 50 μM ouabain or N_3+2-DG. Thereafter, monolayers were washed (1 x (2ml Ap + 2ml Bl) x 15 min) with M4-medium (pH7.4). For D-[^{14}C]mannitol transport experiments, the Ap and Bl media were M4 (pH7.4) alone (control), M4 containing 50 μM ouabain or N_3+2-DG. Data are presented as mean % transport ± SD for three monolayers.

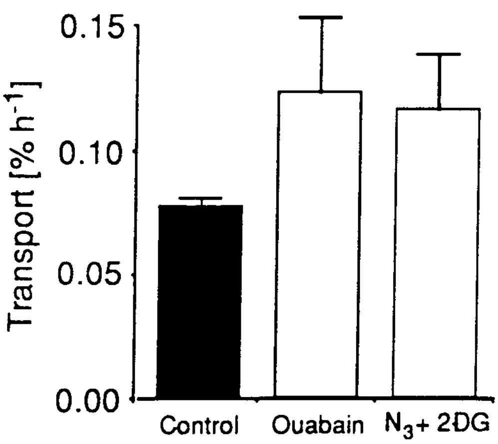

FIGURE 4.13 *Temporal-dependence of L-proline transport (Ap pH7.4 and 5.5).* Monolayers were washed (1 x 2ml Ap x 15 min) with M4-medium buffered to pH7.4 or pH5.5 and (1 x 2 ml Bl x 15 min) with M4-medium pH7.4. Ap(pH7.4)-to-Bl(pH7.4) (open circles) and Ap(pH5.5)-to-Bl(pH7.4) (closed circles) L-proline transport was determined after 7, 14, 21 and 28 d. Data are presented as mean values ± SD for three monolayers. * Denotes a significantly higher Ap(pH5.5)-to-Bl(pH7.4) than Ap(pH7.4)-to-Bl(pH7.4) transport at each culture period ($p<0.01$).

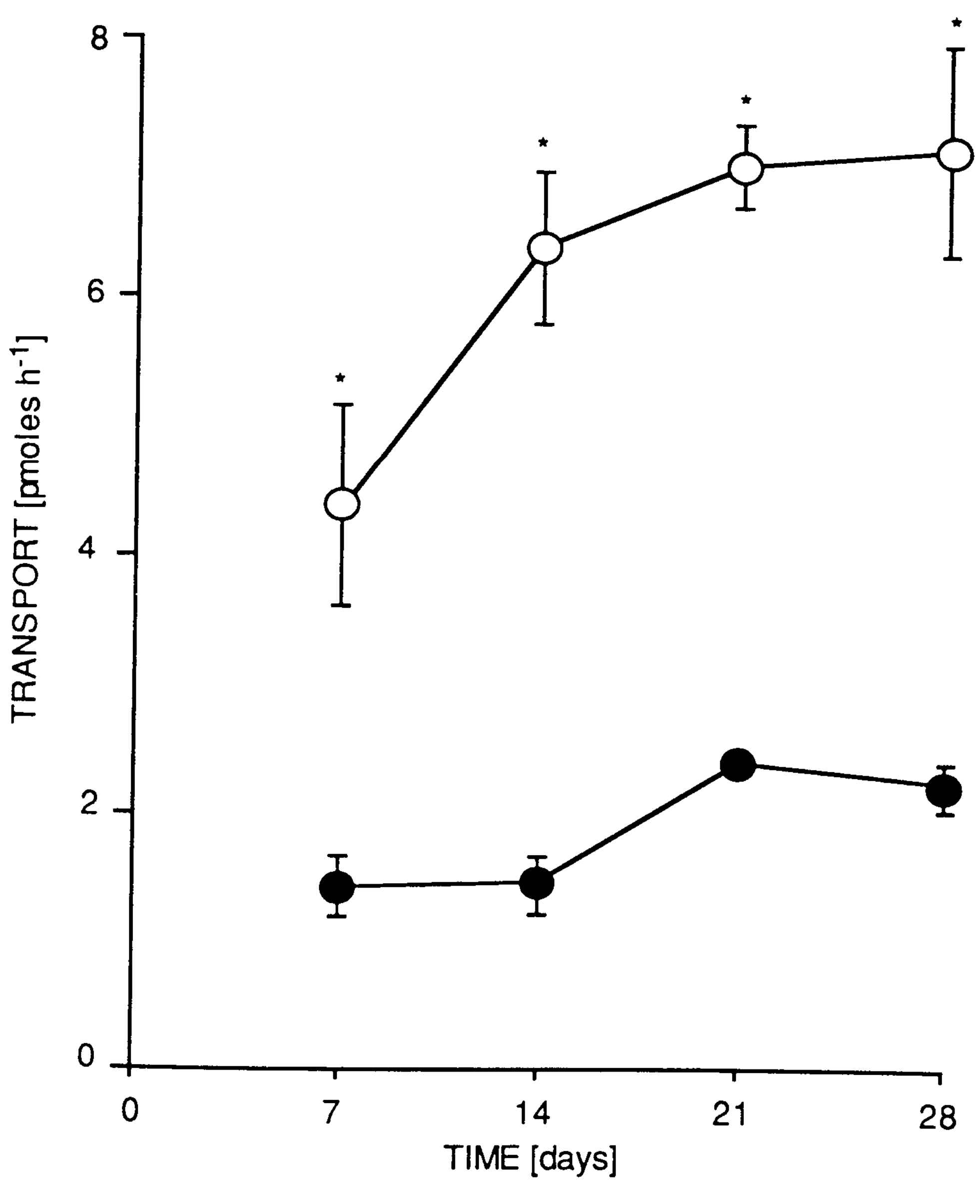

FIGURE 4.14 *Polarity of L-proline transport (Ap pH7.4 and 5.5).*
pH7.4: Monolayers were washed (1 x (2ml Ap + 2ml Bl) x 15 min) with M4-medium pH7.4. L-[^{3}H]Proline alone (total), or in the presence of 50 mM L-proline (non-saturable), was applied to the Ap or Bl surface for Ap-to-Bl (closed bars) or Bl-to-Ap (open bars) transport determined, respectively. The inset shows the saturable Ap-to-Bl and Bl-to-Ap transport components. *pH5.5:* For Ap(pH5.5)-to-Bl(pH7.4) (closed bars)transport experiments, monolayers were washed (1 x 2ml Ap x 15 min) with M4-medium pH5.5 and (1 x 2ml Bl x 15 min) with M4-medium pH7.4. For Bl(pH5.5)-to-Ap(pH7.4) (open bars) transport experiments, monolayers were washed with (1 x 2ml Ap x 15 min) with M4-medium pH7.4 and (1 x 2ml Bl x 15 min) with M4-medium pH5.5. Ap(pH5.5)-to-Bl(pH7.4) and Bl(pH5.5)-to-Ap(pH7.4) L-proline transport were determined. Data are presented as mean values ± SD for three monolayers.

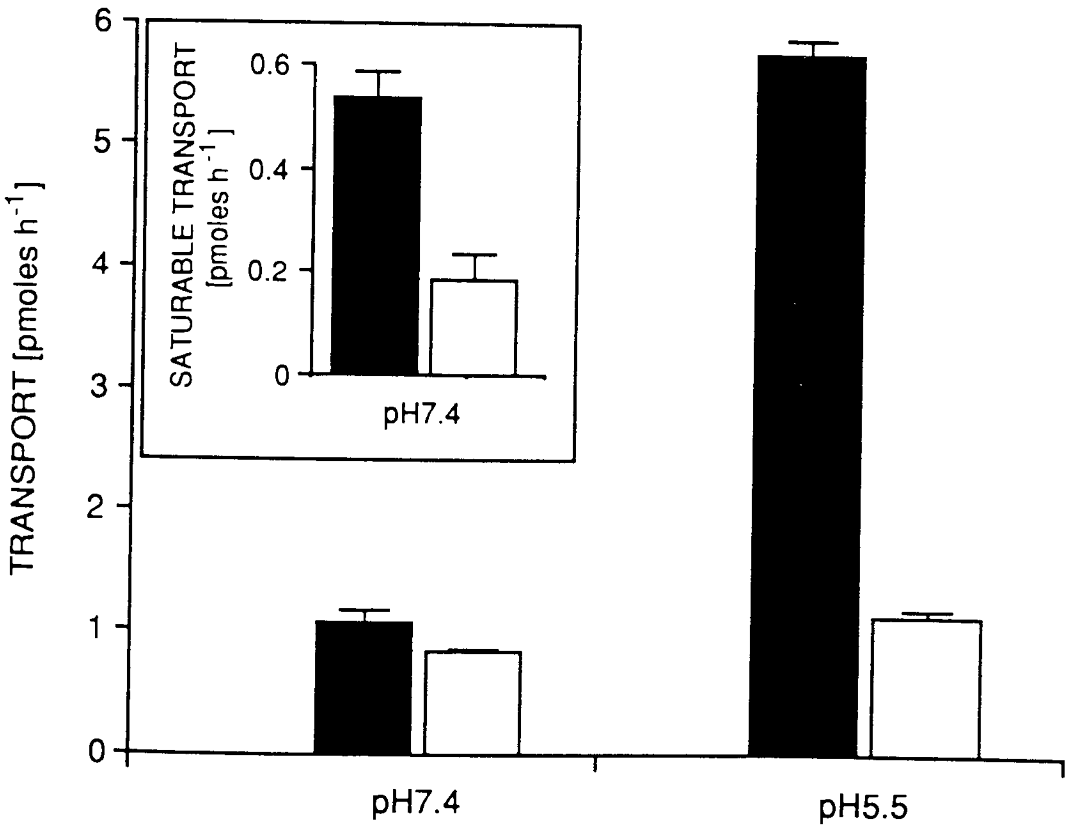

FIGURE 4.15 *Concentration-dependence of L-proline transport (Ap pH5.5).* Monolayers were washed (1 x 2ml Ap x 15 min) with M4-medium pH5.5 and (1 x 2ml Bl x 15 min) with M4-medium pH7.4. Ap(pH5.5)-to-Bl(pH7.4) L-proline transport was determined for a range of Ap concentrations (50 μM to 50 mM). The concentration-dependence profile was resolved into its saturable (K_m = 3.0±1.2 mM, V_{max}^{cm} = 0.81±0.14 μmoles h^{-1} insert^{-1}) and non-saturable (K_d = 0.0635±0.0029 μmoles h^{-1} insert^{-1} mM^{-1}) components by non-linear regression. Data are presented as mean values ± SD for three monolayers.

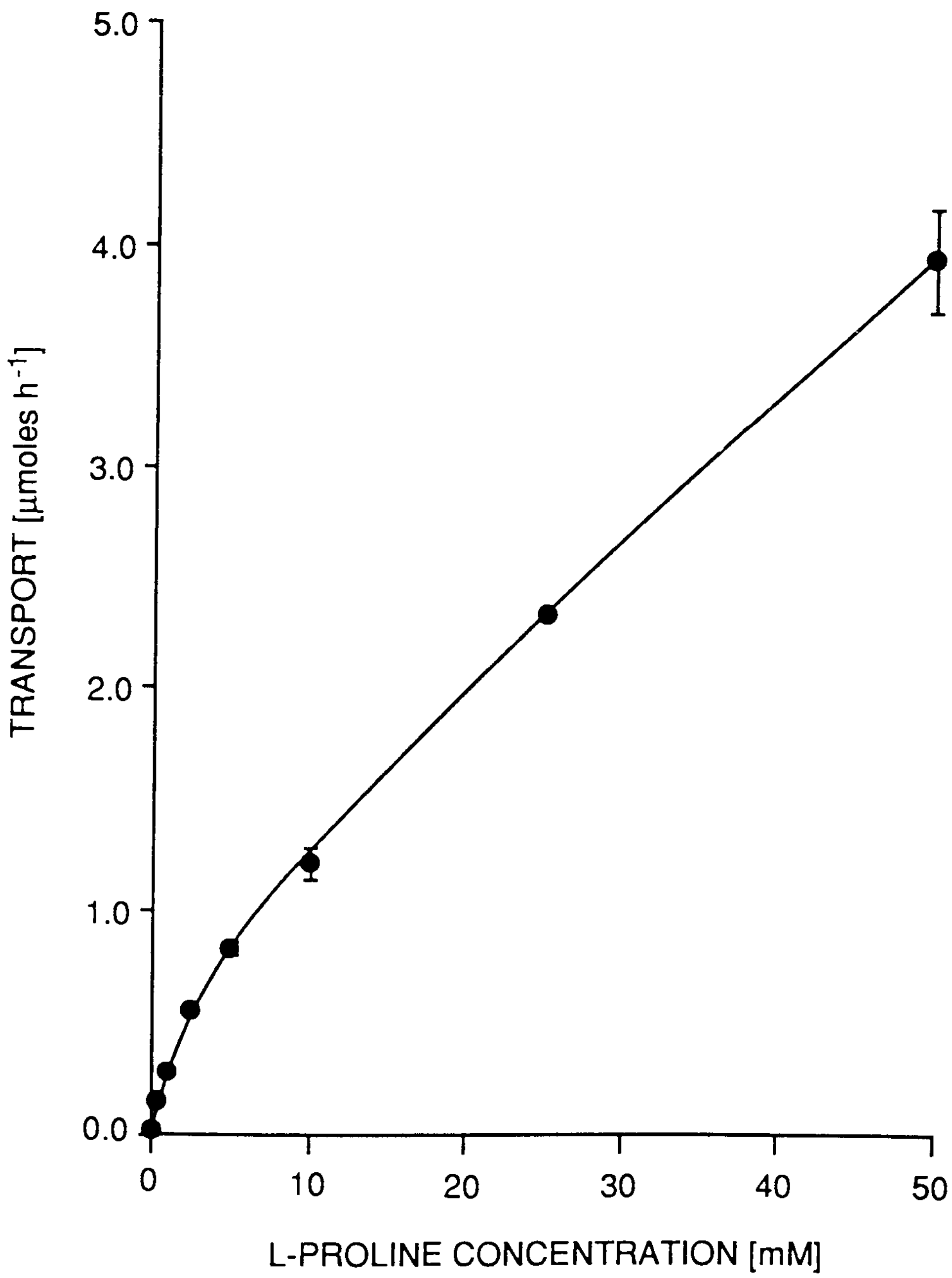

FIGURE 4.16 *pH-dependence of saturable L-[^{14}C]arginine transport.* Monolayers were washed (1 x 2ml Ap x 15 min) with M4-medium pH7.5 or pH5.5 and (1 x 2ml Bl x 15 min) with M4-medium pH7.4. Ap-to-Bl L-[^{14}C]arginine (50 µM) transport was determined in the absence (total) and presence (non-saturable) of 50 mM L-arginine. Saturable transport was calculated by subtraction. Data are presented as mean values ± SD for three determinations.

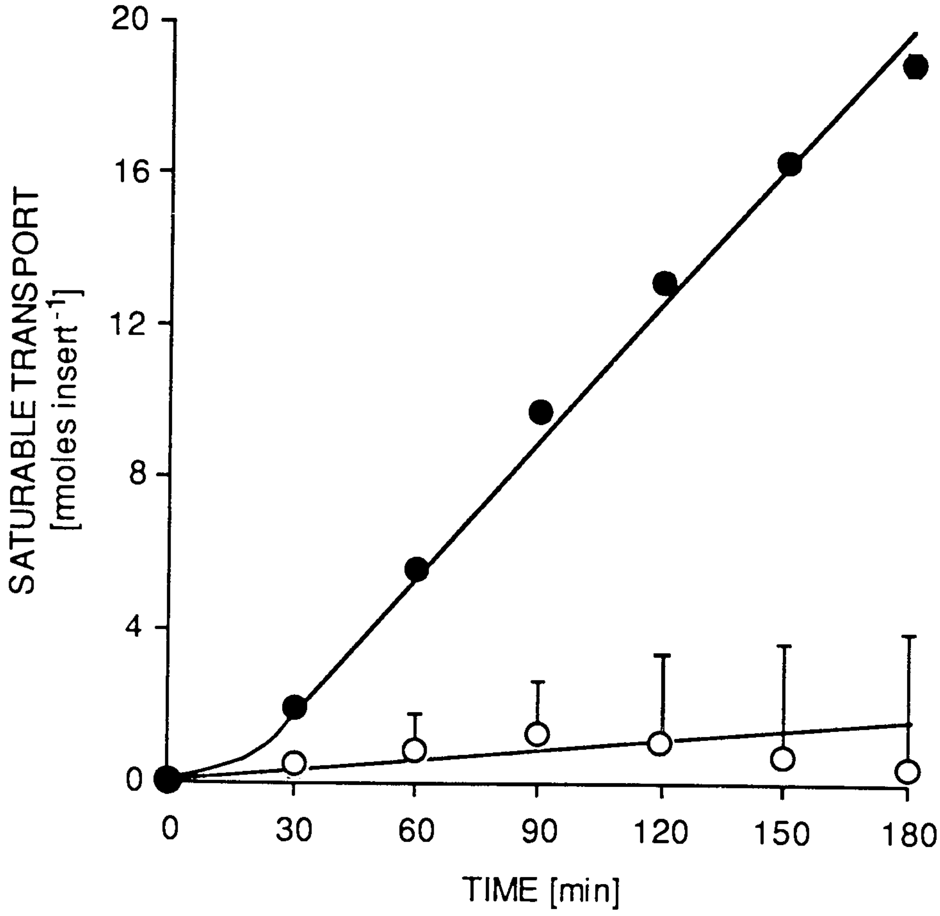

FIGURE 4.17 *Baclofen transport kinetics.*

Monolayers were washed (1 x 2ml Ap+Bl) x 15 min) with M4-medium pH7.2. Ap-to-Bl [^{14}C]baclofen transport was determined over 90 min by sequential transfer at 15 min intervals. Data are presented as mean values ± SD for three monolayers.

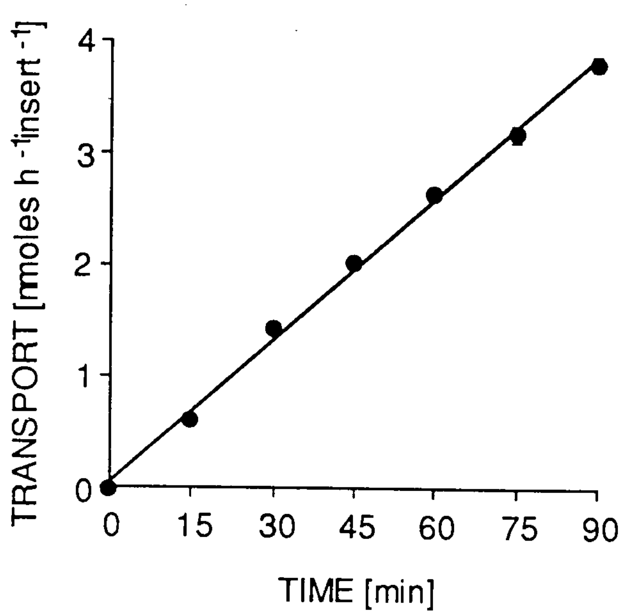

FIGURE 4.18 *Concentration-dependence of baclofen transport.*

Monolayers were washed (1 x 2ml Ap+Bl) x 15 min) with M4-medium pH7.2. Ap-to-Bl [^{14}C]baclofen transport was determined for a range of Ap concentrations. Data are presented as mean values ± SD for three monolayers.

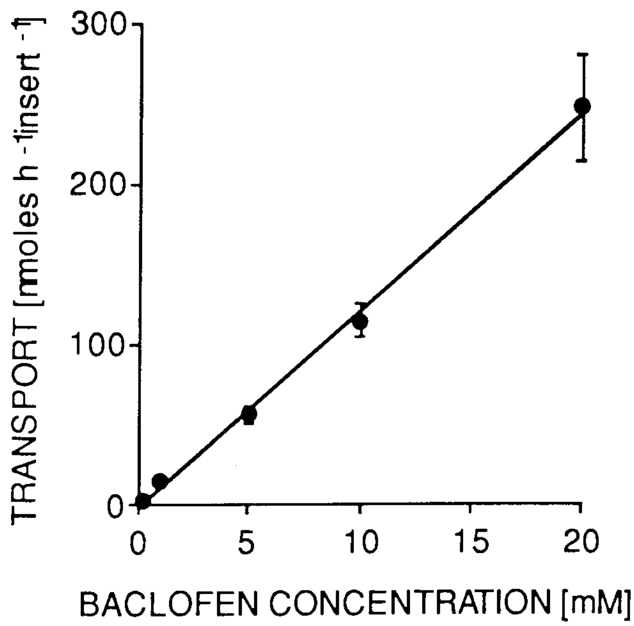

FIGURE 4.19 *Polarity of baclofen transport kinetics.*

Monolayers were washed (1 x 2ml Ap+Bl) x 15 min) with M4-medium pH7.2. Ap-to-Bl and Bl-to-Ap [^{14}C]baclofen transport was determined. Data are presented as mean values ± SD for three monolayers.

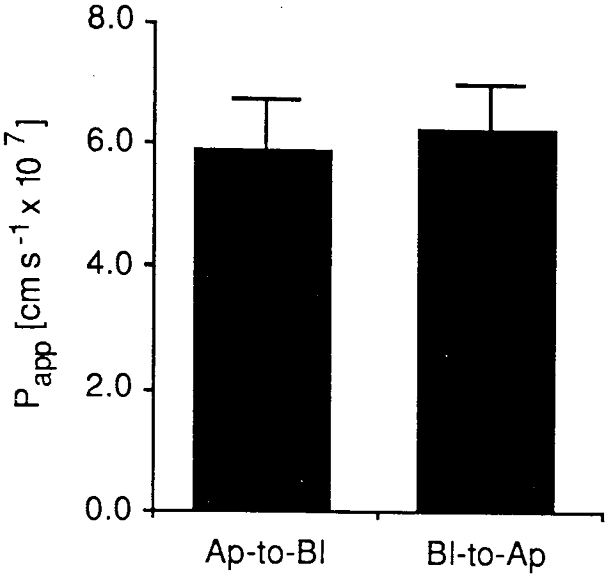

FIGURE 4.20 *pH-dependence of baclofen transport.*

Monolayers were washed (1 x 2 ml Ap x 15 min) with M4-medium buffered to an appropriate pH (5.0, 6.0, 6.8, 7.2, 8.0) and (1 x (2 ml Bl) x 15 min) with M4-medium pH7.4. Ap-to-Bl 50 μM [^{14}C]baclofen transport was determined for a range of Ap pH values (pH 5.0 to 8.5). Data are presented as the mean values ± SD for three monolayers.

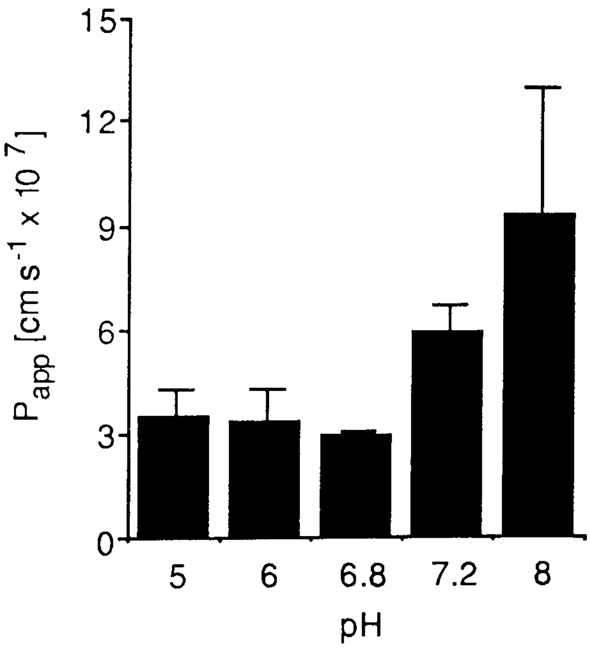

TABLE 4.1 *Inhibition of L-proline uptake by amino acids and their analogues.* Monolayers were incubated with 50 μM L-[^{3}H]-proline alone (control) or in the presence of a 100-fold molar excess (5 mM) of competitor. Data are presented as mean % inhibition of saturable uptake ± SD for three monolayers. *, **, *** Denote significant inhibitions at the $p<0.05$, $p<0.01$ and $p<0.001$ levels, respectively.

COMPETITOR	% INHIBITION OF SATURABLE UPTAKE MEAN (SD)
ACIDIC	
L-Aspartic acid	-1.7 (5.2)
ALIPHATIC	
L-Alanine	69.3 (7.4)***
L-Alanine (50 mM)	104.4 (7.4)***
L-Alanine (50 mM) + MeAIB (5 mM)	104.6 (3.1)***
Beta-Alanine	43.5 (3.6)**
Glycine	30.7 (2.0)**
ALIPHATIC HYDROXYL	
L-Serine	74.1 (1.7)***
AMIDE	
L-Asparagine	51.4 (4.5)***
AROMATIC	
L-Phenylalanine	3.0 (2.6)
L-Tryptophan	-5.1 (1.5)
BASIC	
L-Arginine	32.9 (1.2)**
L-Histidine	50.2 (9.9)**
BRANCHED ALIPHATIC	
L-Leucine	-0.4 (6.4)
L-Valine	10.2 (1.1)*
IMINO	
L-Hydroxyproline	50.2 (6.2)**
L-Proline	68.3 (0.3)***
D-Proline	36.9 (3.3)**
SULPHUR CONTAINING	
L-Cysteine	48.7 (12.1)**
L-Methionine	53.4 (3.8)***
SYNTHETIC ANALOGUE	
Alpha-Aminoisobutyric acid	75.2 (10.0)***
Gamma-Aminoisobutyric acid	33.4 (13.0)**
MeAIB	58.3 (4.3)***

TABLE 4.2 *Influence of feeding-regimen on L-proline uptake.*
After 4 d of the standard culture regimen, monolayers were fed with permeable-support-medium (48 h or 12 h) or with HBSS+HEPES (24 h) prior to experiments. They were washed with PBS (2 x 5 ml x 5 min) followed by M2-medium (1 x 2 ml x 15 min). The uptake of L-[^{3}H]proline was determined from M2-medium. Data are presented as mean values (SD) for three monolayers. * Denotes a significant difference from the 48 h permeable-support-medium feeding-regimen at $p<0.05$.

LAST MEDIUM REPLACEMENT TIME LAPSE (TYPE)	SATURABLE UPTAKE [pmol (20 min)$^{-1}$]
48 h (Plate medium)	0.942 (0.049)
12 h (Plate medium)	0.844 (0.011)*
24 h (HBSS + 14 mM HEPES)	1.411 (0.069)*

TABLE 4.3 *Effect of cycloheximide, glucose depletion and sodium azide on specific L-proline uptake.*
Cycloheximide: Monolayers were pre-incubated for 45 min with 500 μM cycloheximide then washed with M2-medium (1 x 2 ml x 15 min).before the saturable uptake of L-[^{3}H]proline determined. *Glucose-depletion:* Monolayers were washed with PBS (2 x 5 ml x 5 min) then M2-medium or M2$_{\text{-Glucose}}$ (1 x 2 ml x 15 min). The saturable uptake of L-[^{3}H]proline was determined from M2-medium or M2$_{\text{-Glucose}}$. *Sodium azide:* Monolayers were washed with PBS (2 x 5 ml x 5 min) then pre-incubated with M2-medium containing 10 mM sodium azide (1 x 2ml x 30 min). The saturable uptake of L-[^{3}H]proline was determined in the presence of 10 mM sodium azide. Data are presented as mean values (SD) for three monolayers. * Denotes a significant difference from control at $p<0.05$.

CONDITION	SPECIFIC UPTAKE % CONTROL
+ Cycloheximide (500 μM)	58.5 (1.7)*
- Glucose	102.8 (20.6)
+ Sodium azide (10 mM)	41.4 (18.5)*

TABLE 4.4 *Sodium- and energy-dependence of L-proline uptake and transport at pH7.4 and pH5.5.*

Caco-2 cells were pre-incubated for 1 h with M4 alone (**A**,**B**,**C**) or M4-medium containing 50 μM ouabain (**D**) or 10 mM sodium azide and 50 mM 2-deoxyglucose (N_3+2-DG; **E**). Thereafter, monolayers were washed (1 x 2ml Ap x 15 min) with M4-medium or $M4_{Choline}$, buffered to pH7.4 or pH5.5 and (1 x 2ml Bl x 15 min) with M4-medium or $M4_{Choline}$, pH7.4. L-[^{3}H]Proline uptake into, and transport across, Caco-2 monolayers were determined. For transport experiments, the Bl medium was M4 (**A**,**B**), M4 containing 50 μM ouabain (**D**) or N_3+2-DG (**E**) or $M4_{Choline}$ pH (**C**), pH7.4 in all cases. The Ap medium was M4 alone (Total; **A**), M4 containing 50 mM unlabelled L-proline (Non-saturable; **B**), 50 μM ouabain (**D**), N_3+2-DG (**E**) or $M4_{Choline}$ (**C**), buffered to pH7.4 or pH5.5, as appropriate. Data are presented as mean % of the total transport ± SD for three monolayers. Bracketed ([]) data represent the mean % of the saturable transport component (SD) for three monolayers.

CONDITION	% TRANSPORT MEAN (SD)			
	UPTAKE		TRANSPORT	
	7.4	5.5	7.4	5.5
(A) TOTAL	100.0 (1.6)	100.0 (7.0)	100.0 (5.4)	100.0 (3.0)
(B) NON-SATURABLE	25.5 (1.8) [0.0 (1.6)]	17.2 (1.3) [0.0 (1.6)]	19.6 (1.0) [0.0 (1.2)]	61.2 (3.5) [0.0 (9.0)]
(C) - Na^+ ($M4_{Choline}$)	46.0 (3.7) [19.0 (3.7)]	107.0 (17.3) [108.5 (20.9)]	73.0 (1.1) [43.6 (2.3)]	91.7 (7.1) [89.7 (8.8)]
(D) OUABAIN	24.4 (1.6) [-6.0 (1.8)]	NT	89.0 (5.2) [71.7 (13.4)]	NT
(E) N_3 +2DG	21.1 (1.1) [-1.4 (1.4)]	116.2 (10.0) [119.5 (11.9)]	87.6 (6.2) [68.0 (16.0)]	90.3 (3.0) [87.9 (3.75)]

NT = Not Tested

N_3 + 2-DG = Sodium azide (10 mM) + 2-deoxyglucose (50 mM)

TABLE 4.5 *Inhibition of L-proline transport (Ap pH5.5) by natural amino acids, stereoisomers and synthetic analogues.*

Monolayers were washed with M4-medium pH5.5 (1 x 2ml Ap x 15 min) and (1 x 2ml Bl x 15 min) with M4-medium pH7.4. Ap(pH5.5)-to-Bl(pH7.4) L-proline (50 μM) transport was determined alone (control) or in the presence of a 100-fold molar excess (5 mM) of unlabelled competitor. Data are presented as mean % inhibition ± SD for three monolayers. * and ** Denote a significant reduction at $p<0.05$ and $p<0.001$, respectively.

COMPETITOR	% INHIBITION SATURABLE TRANSPORT MEAN (SD)
ALIPHATIC	
L-Alanine	77.2 (2.4)**
Glycine	57.2 (3.3)**
ALIPHATIC HYDROXYL	
L-Serine	25.2 (4.4)*
AROMATIC	
L-Phenylalanine	5.4 (4.4)
L-Tryptophan	30.4 (4.6)*
BASIC	
L-Arginine	9.1 (8.4)
IMINO ACIDS	
L-Proline	81.8 (1.0)**
D-Proline	75.0 (1.0)**
L-Hydroxyproline	49.1 (2.1)**
SYNTHETIC ANALOGUES	
Alpha-aminoisobutyric acid	70.1 (3.2)**
MeAIB	72.6 (1.3)**

TABLE 4.6 *Influence of beta-alanine on [^{14}C]baclofen transport.*
Monolayers were washed with M4-medium (1 x 2ml Ap + Bl x 15 min). Ap-to-Bl [^{14}C]baclofen (250 μM) transport was determined alone (control) or in the presence of 250, 2500 or 25000 μM beta-alanine. Data are presented as mean % inhibition (SD) for three monolayers.

ß-Alanine Concentration [μM]	% Inhibition Baclofen transport
0 (Control)	0.0±2.3
250	1.8±4.3
2500	2.7±3.2
25000	8.0±5.0

4.5 DISCUSSION

4.5.1 L-PROLINE UPTAKE

Coincident L-[^{3}H]-proline reference and post-uptake sample radio-TLC chromatograms shows that L-proline was not appreciably metabolised prior to, during or after uptake over the duration of the experiments. Therefore, [^{3}H]-uptake into Caco-2 monolayers overwhelmingly reflected intact L-[^{3}H]-proline.

The results from the above experiments, which were designed to probe the mechanism of L-proline entry into Caco-2 cells, suggest that uptake predominantly occurred (~70%) *via* carrier-mediation. Firstly, uptake was concentrative. This is consistent with Caco-2 cells being able to actively accumulate L-proline beyond a concentration that can be explained by simple (passive) equilibration across their brush-border membranes. Secondly, uptake was dramatically reduced at temperatures below 37°C. The calculated activation-energy of 95.3 kJ mol^{-1} for L-proline exceeds that anticipated for simple diffusion (<16.8 kJ mol^{-1}) and is within the usual range for carrier-mediated processes (29.4 to 105.0 kJ mol^{-1}) [Hidalgo and Borchardt 1990 a]. Additionally, L-proline uptake was significantly reduced in the presence of 10 mM sodium azide, which inhibits oxidative-phosphorylation, suggesting a reliance on metabolic-energy. The most likely explanation is that sodium azide interrupts the production of metabolic energy required to maintain the inward sodium ion electrochemical-gradient which drives uptake (see later). Furthermore, L-proline uptake was concentration-dependent. This is consistent with the hypothesis that two modes of uptake into Caco-2 cells exist; (i) Saturable uptake *via* a finite number of "carriers" and (ii) non-saturable passive diffusion (uptake proportional to concentration).

Amino (and imino) acid transporters are principally classified according to their reliance on sodium. The sodium-dependence of L-proline uptake was investigated by reducing the inward sodium ion gradient by performing uptake studies from sodium-free amino acid-free incubation medium or in the presence of 10 μM ouabain. Under both experimental conditions, the specific uptake of L-proline was reduced by approximately 85% and is therefore sodium-dependent. This agrees with previous work in other species [Hayashi *et al.*, 1980; Munck, 1985 b] and in brush-border membrane vesicles prepared from adult [Rajendran *et al.*, 1985] and foetal [Malo, 1991] human small intestine which showed that the initial uptake rate of L-proline was reduced in the absence of sodium ions.

The high extracellular concentrations of sodium ions which are required to drive L-proline uptake maximally are consistent with its striking ouabain-sensitivity. Similar uptake experiments for L-[^{3}H]phenylalanine failed to demonstrate significant sodium-dependence. This contests the previously published observation that L-phenylalanine transport across Caco-2 monolayers cultured on permeable-supports is reduced by 33% in the presence of 100 μM ouabain (implying sodium-dependence) [Hidalgo and Borchardt, 1990 a]. Furthermore, an earlier report by the same research group stated that L-phenylalanine transport was not reduced from sodium-free (choline chloride) incubation medium or by 2-5 mM ouabain, suggesting sodium-independent transport [Hidalgo and Borchardt, 1988]. Their earlier observation agrees with the results of L-phenylalanine transport experiments performed within independent laboratories (personal communication, Dr Ian Hassan, Ciba Pharmaceuticals, Horsham, UK).

Uptake was identical in the presence and absence of glucose indicating that the intracellular carbohydrate pool is able to satisfy the energetic demands of the cells over the time-course of the experiment. Clearly, there is no direct interaction between glucose and the L-proline carrier. L-Phenylalanine transport was reduced in the absence of glucose [Hidalgo and Borchardt, 1990 a] but whether this was a result of a reduced availability of metabolic energy or reduced solvent drag through the paracellular shunt pathway in the absence of glucose [Pappenheimer and Reiss, 1987; Madara and Pappenheimer, 1987] was uncertain.

The uptake of L-proline was performed over a range of concentrations (0.5 mM to 50 mM) in the presence and absence of sodium ions. The difference between the uptake profiles (*ie:* the concentration dependence of the sodium-dependent transport component) follows Michaelis-Menten saturation kinetics and the Eadie-Hofstee analysis yields a straight line suggesting a single agency is responsible for the sodium-dependent uptake of L-proline into Caco-2 cells. The Michaelis constant (K_m^{sd}) of 5.28±0.48 mM is an order of magnitude higher than that for brush-border membrane vesicles prepared from guinea pig ileum (K_m =0.67 mM) [Hayashi *et al.*, 1980] and rabbit jejunum (K_m = 0.55 mM) [Stevens *et al.*, 1982]. This discrepancy may be an artefact of the different models used in these studies but more probably reflects functional differences between the uptake systems. Unfortunately, data concerning L-proline uptake into normal human tissues are limited and do not extend to the analysis of kinetic parameters for comparison [Rajendran *et al.*, 1985; Malo, 1991].

The structural requirements of the carrier were investigated by observing the inhibition of carrier-mediated uptake of L-proline by a 100-fold excess of other amino (and imino) acids or synthetic analogues. The inhibition profile for L-proline uptake shows that aliphatic neutral amino acids can effectively compete but branching or aromatic content in the side-chain dramatically reduced its ability to inhibit uptake. L-Proline uptake was inhibited by the non-alpha-amino acid beta-alanine and gamma-amino isobutyric acid but to a lesser extent than by their alpha-analogues. D-proline significantly inhibited L-proline uptake (36.9±1.9%) suggesting that the carrier involved in L-proline uptake has only moderate stereoselectively. The large neutral amino acid (LNAA) transporter in Caco-2 cells displays an opposite substrate specificity preferring neutral amino acids with bulky side chains and being very stereoselective [Hidalgo and Borchardt, 1990 a]. Additionally, glycine inhibits L-proline uptake but failed to influence L-phenylalanine transport across Caco-2 monolayers [Hidalgo and Borchardt, 1990 a]. It is noteworthy that L-phenylalanine did not significantly inhibit L-proline uptake (3.0±1.5%) confirming they are recognised by different carriers in the Caco-2 cell line. These two discrete mediations share the properties of being reduced by basic but not acidic amino acids. The sodium-dependent L-glutamine carrier expressed by Caco-2 cells is strongly inhibited by L-alanine but is not inhibited by L-proline or MeAIB [Souba *et al.*, 1992].

To our knowledge, this is the first detailed characterisation of L-proline uptake using an adult human intestinal preparation, therefore, a comparison of the cross-inhibition profile in Caco-2 cells with those described for other species is merited. In non-epithelial cell types and at the basolateral surface of enterocytes a sodium-dependent, a highly stereo-specific ASC system which excludes MeAIB can serve L-proline [Christensen *et al.*, 1967]. The moderate stereoselectivity, its strong inhibition by MeAIB and alpha-aminoisobutyric acid and the inability of lithium ions to substitute for sodium ions [Edmondson *et al.*, 1979] indicates the ASC system is not responsible for L-proline uptake in Caco-2 cells. Similarly, uptake is not mediated by the IMINO system which serves L-proline and MeAIB but excludes beta-alanine and is insensitive to L-alanine and glycine. This was confirmed by the fact that MeAIB did not inhibit L-proline uptake beyond the L-alanine-sensitive component (Table 4.1). In agreement with observations in the rat small intestine, the cross-inhibition uptake profile for L-proline resembles the A system. Firstly, uptake is sodium-dependent and secondly, it is strongly inhibited by alpha-aminoisobutyric acid, MeAIB and small aliphatic neutral amino acids (*eg:* L-alanine, L-serine) but not by branched or aromatic neutral amino acids (*eg:* L-leucine, L-phenylalanine, L-tryptophan, L-valine). However, this profile is dissimilar in that inhibition potency of non-alpha-amino acids is greater than their alpha-analogues according to the sequence gamma>beta»alpha. This is clearly not the case in Caco-2 cells where the inhibition potency of L-alanine is greater than that of beta-alanine and gamma-aminoisobutyric acid is greater than gamma-aminoisobutyric acid. The rabbit small intestine possesses a high affinity, sodium-dependent carrier of neutral and cationic amino acids which serves imino acids and accepts non-alpha-amino acids according to the sequence alpha>beta>gamma but is more sensitive to L-leucine than the Caco-2 system. The involvement of the A system in L-proline uptake has been postulated for the guinea pig ileum [Hayashi *et al.*, 1980], however, in the absence of cross-inhibition studies, other systems cannot be rejected and its Michaelis kinetic parameters were very similar to the IMINO system of the rabbit jejunum [Stevens *et al.*, 1982]. Variance with observations for imino acid uptake by other species may reflect inter-species heterogeneity or that this system is artificially induced in this tumour cell line. The precise nature of this discrepancy awaits experiments in normal adult human small intestinal preparations.

Under neutral to mildly alkaline conditions, L-proline uptake occurs optimally at pH7.4. This local pH optimum is identical to that of the A system. The ionisation state of L-proline is pH-dependent and is largely cationic at pH values below its isoelectric point, pI=6.3 [Damm, 1966]. The large stimulation of L-proline uptake may be a result of enhanced carrier efficiency, however, the concomitant reduction in sodium-dependence and predicted change in the ionisation state of L-proline suggests another uptake mechanism may prevail at acidic pH values.

We have characterised an amino acid uptake carrier that serves L-proline and which is distinct from the LNAA (L-phenylalanine) [Hidalgo and Borchardt 1990 a] and L-glutamine [Souba *et al.*, 1992] carrier that have been characterised in Caco-2 cells.

Caco-2 monolayers have been proposed as a useful predictive model of the adult human small intestinal epithelium [Wilson *et al.*, 1990; Hidalgo *et al.*, 1989]. However, the major barrier to evaluating this hypothesis is the lack of data for the normal human small intestine, and comparison with other species is inappropriate due to inter-species variation. At best, Caco-2 monolayers only partially explain the intestinal uptake mechanism of imino acids in the normal adult human small intestine. This can be deduced indirectly from our knowledge of clinical disorders of amino acid absorption. Hartnup's disease results from a congenital defect in the absorption of neutral amino acids uptake in which imino acids do not become clinically deficient [Wellner and Meister, 1981]. Therefore, at least one uptake carrier, selective for imino acids and excluding neutral amino acids, must be present in the human small intestine. The predicted exclusive imino acid pathway was not observed in Caco-2 cells. This study, therefore, highlights the caution which should be employed when inferring 'normal' uptake phenomena from the Caco-2 *in vitro* model of the human small intestine.

4.5.2 PROLINE TRANSPORT

The L-proline transport data suggest that there is a pH-dependent heterogeneity in L-proline uptake and transport across Caco-2 monolayers. At Ap pH7.4 and pH5.5, the saturable uptake component represents 74.5±1.8 and 82.8±1.3% of the total, respectively. Therefore, carrier-mediation is the major uptake pathway for L-proline into Caco-2 at both pH values. Similarly, the saturable Ap(pH5.5)-to-Bl(pH7.4) transport component is the major transport pathway and accounts for 80.4±1.0% of the total flux. In contrast, the saturable Ap(pH7.4)-to-Bl(pH7.4) transport represents only 38.8±3.5% of the total flux and the non-saturable (diffusional) mechanism is the major transport pathway. The differential importance of the non-saturable uptake and transport at pH7.4 suggests that the paracellular shunt pathway is proportionatly more important for the transepithelial transport at this pH.

Caco-2 monolayers cultured on permeable-supports are morphologically more differentiated than those cultured on impermeable plastic supports [Hidalgo *et al.*, 1989]. At Ap pH7.4, comparable results were obtained for L-proline uptake into Caco-2 monolayers cultured for 6 d on plastic and those cultivated for 21 d on nitrocellulose permeable-supports. Firstly, uptake was saturable (70-75% of the total in both cases) and the saturable component was highly ouabain-sensitive and energy- and sodium-dependent. Therefore, the L-proline carrier expressed by Caco-2 cells cultured on nitrocellulose permeable-supports is similar to that expressed by Caco-2 cells cultured on an impermeable-support. Similarly, Ap(pH7.4)-to-Bl(pH7.4) L-proline transport is saturable (38.8±3.5%) and the saturable component is sodium-dependent. Transport is apparently less energy-dependent and ouabain-sensitive than uptake. However, since N_3+2-DG and 50μM ouabain increase the Ap-to-Bl transport of D-mannitol, the energy-dependence and ouabain-sensitivity of L-proline transport at pH7.4 may be masked by non-specific effects on monolayer permeability. The saturable component is the major uptake pathway but minor transport pathway at Ap pH7.4.

The data presented here suggest that L-proline transport is recognised by a different transport system at pH5.5 and pH7.4. Firstly, the transport of L-proline displays different temporal-dependence at these two Ap pH values. If the increased L-proline transport at acidic pH values was due to stimulation of the same carrier the temporal-dependencies at pH7.4 and pH5.5 should be displaced but otherwise have identical trends. Secondly, at pH7.4 and pH5.5 the L-proline carriers display different functional properties. At Ap pH7.4, L-proline uptake and transport were energy- and sodium-dependent, meanwhile, at pH5.5 its uptake and transport was energy- and sodium-independent. Finally, there was a subtle shift in cross-inhibition profile. At Ap pH5.5, L-alanine, alpha-AIB and MeAIB are potent inhibitors, whilst the large neutral amino acid, L-phenylalanine, failed to inhibit L-proline uptake. This cross-inhibition pattern is common to L-proline uptake at pH7.4 and transport at pH5.5. However, L-[^{3}H]proline uptake was only partially inhibited by D-proline whilst its transport at pH5.5 is strongly inhibited by both L- and D-proline. Therefore, the L-proline carrier is less stereoselective at pH5.5. Interestingly, whereas L-serine was a potent inhibitor of L-proline uptake at pH7.4 (second only to alpha-AIB) at pH5.5 it was only a weak inhibitor. As mentioned previously, below its isoelectric point (pI = 6.3) L-proline predominantly exists in a cationic form. It is tempting to speculate that under acidic conditions L-proline may be transported *via* a basic amino acid carrier. However, cross-inhibition studies show that L-arginine inhibits L-proline uptake at pH7.4 but it failed to reduce its transport at pH5.5. Furthermore, the saturable transport of L-[^{14}C]arginine is markedly reduced by decreasing the Ap pH from 7.4 to 5.5 (Fig. 4.16). These observations suggest that the population of carriers which transport L-proline at pH5.5 are distinct from that which transport L-arginine.

4.5.3 BACLOFEN TRANSPORT

In pharmacokinetic studies, baclofen had an oral bioavailability of 60 to 70% in man, when administered as a 40 mg tablet formulation. Moreover, the oral bioavailability of baclofen is independent of the dose administered (10 to 30 mg) [Faigle *et al.*, 1981], suggesting a non-saturable (passive) absorption pathway. However, carrier-mediated baclofen absorption from the mid small intestine has been demonstrated using a rat *in situ* luminal perfusion model [Polache *et al.*, 1991]. In addition, baclofen absorption from the rat intestine is partially (up to 64%) inhibited by ß-alanine [Polache *et al.*, 1991]. Taken together, these observations suggest that a quantitatively important proportion of baclofen absorption from the rat intestine is mediated by a carrier which also serves non-alpha-amino acids.

Carrier-mediated baclofen transport across biological barriers is not a novel concept. It has been reported that baclofen inhibits L-phenylalanine transport across monolayers of bovine brain endothelial cells in primary culture [Audus and

Borchardt, 1986]. Furthermore, the transport of baclofen across this model is saturable and temperature-dependent [van Bree *et al.*, 1988]. The authors tentatively concluded that baclofen transport across this blood-brain barrier model is mediated by a LNAA-carrier. These observations have not been verified using a similar porcine brain endothelial cell culture model within our own laboratories (Dr Ian Walker, Drug Development Research Group, Aston University; unpublished observations). Caco-2 monolayers express a LNAA-carrier which serves L-phenylalanine [Hidalgo and Borchardt, 1990 a] and alpha-methyldopa [Hu and Borchardt, 1990].

The data presented here provide no evidence for the involvement of carrier-mediation in the transport of baclofen across Caco-2 monolayers. Indeed, transport across this model is consistent with data from human pharmacokinetic studies. For instance, baclofen transport across Caco-2 monolayers is proportional to concentration (200 μM to 20 mM) and its oral bioavailability is independent of the administered dose (10 to 30 mg). These observations are indicative of a non-saturable (passive) absorption mechanism in both cases. While beta-alanine inhibits baclofen absorption from the rat intestine [Polache *et al.*, 1991] it failed to reduce its transport across Caco-2 monolayers. The reason for this discrepancy between rat and human (Caco-2 monolayers and pharmacokinetics) data is not certain. However, the rat has an unusual capacity to absorb non-alpha amino acids. In the rat, the affinity of carrier-mediated absorption pathways for non-alpha neutral amino acids is greater than their alpha-counterparts (gamma»beta>alpha), this is not the case in other species. Therefore, baclofen (a beta-amino acid analogue) may be a substrate for amino acid carrier in the rat intestine but not the human. This highlights the importance of selecting an appropriate model for absorption studies and the caution which must be employed when extrapolating between species.

4.6 CONCLUSION

The saturable uptake component for L-proline uptake into Caco-2 monolayers cultured for 6 d on a plastic support was predominantly mediated by the A-system. L-Proline uptake was increased at acidic pH values. Similarly, L-proline transport across Caco-2 monolayers cultured for 21 d on a permeable-support was stimulated under acidic conditions and became maximal at pH5.5. This elevated transport resulted from an activation from a carrier population which was distinct from that which operates at pH7.4.

Transport studies with baclofen provided no evidence for the involvement of a carrier-mediated pathway in its transport across Caco-2 monolayers.

CHAPTER FIVE

THE TRANSPORT OF ACIDIC AMINO ACIDS AND THEIR ANALOGUES ACROSS CACO-2 MONOLAYERS

ABSTRACT

Acidic amino acid transport was highly saturable (> 95% at 50 μM), vectorial (Ap-to-Bl » Bl-to-Ap) and sodium-, pH- and temperature-dependent. These data are consistent with a major (saturable) carrier-mediated pathway superimposed onto a minor non-saturable (diffusional) pathway. In addition, L-aspartate was transported against a 10-fold reverse concentration-gradient. The carrier-mediated transport pathway had an absolute sodium-dependence. The Michaelis constants for the sodium-dependent transport component (K_m^{sd}) for L-aspartate and L-glutamate were 55.8±3.3 μM and 65.0±6.3 μM, respectively. Their maximal velocities were 36.0±1.1 nmoles h^{-1} $insert^{-1}$ and 15.0±2.4 nmoles h^{-1} $insert^{-1}$, respectively. Cross-inhibition studies showed that the acidic amino acid carrier had a sharply defined substrate specificity. Potent inhibitors included; L-aspartate, D-aspartate, L-glutamate, *threo*-beta-hydroxy-DL-aspartate, L-cysteate, 2-amino-2-carboxyethylphosphonous acid. Partial inhibitors included, alpha-methyl-DL-aspartate, 2-amino-2-carboxyethylarsonic acid, D-glutamate, L-asparagine, L-proline and L-alanine.

The acidic amino acid carrier expressed by Caco-2 cells is of the generic type X^-_{AG} and it shares many properties with the L-glutamate carrier present in the human jejunum.

CGP40116 and CGP40117 are a stereoisomeric pair of N-methyl-D-aspartate antagonists. Despite their structural similarities to acidic amino acids, they were not substrates for carrier-mediated transport across Caco-2 monolayers.

5.1 BACKGROUND

5.1.1 ACIDIC AMINO ACID TRANSPORT

Gibson and Wiseman [1951] provided the first evidence for the carrier-mediated absorption of acidic amino acids by demonstrating a differential rate for the luminal disappearance of stereoisomer pairs in ligated *in situ* loops of rat intestine. However, interpretation of whole tissue uptake data is complicated by the rapid metabolism of acidic amino acids by cytosolic transaminases in the enterocyte [Ramaswamy and Radhakrishnan, 1963; Ramaswamy and Radhakrishnan, 1970]. The development of the BBMV uptake model has enabled studies of acidic amino acid carriers in the absence of metabolising cytosolic enzymes. Several carrier systems serving acidic amino acids have been identified [Berteloot and Maenz, 1990]. One of these systems, the X^-_{AG} sodium-dependent system, serves both L-aspartate and L-glutamate and is apparently ubiquitous. Whilst X^-_{AG}-carriers from a variety of tissues and species share many properties, subtle mechanistic distinctions suggest these carriers represent a family of closely related, but not identical, transporters [Berteloot and Maenz, 1990].

The existence of a human intestinal acidic amino acid carrier can be deduced indirectly from the clinical observation that dicarboxylic amino acidurea patients have deficient intestinal absorption of L-aspartate and L-glutamate [Teijema *et al.*, 1974]. Secondly, human jejunal BBMV accumulate acidic amino acids in a concentration-, pH- and sodium-dependent manner [Rajendran *et al.*, 1987 b; Harig *et al.*, 1987]. However, the scarcity of human tissue, and its rapid loss of integrity upon excision [Trier, 1980], has restricted our knowledge of the human acidic amino acid-transporter.

5.1.2 ACIDIC AMINO ACIDS IN THE CENTRAL NERVOUS SYSTEM (CNS)

It was first reported that the topical application of L-aspartate and L-glutamate to the mammalian cerebral cortex produced cortical seizure activity in 1952 [Hayashi, 1952]. Furthermore, the iontophoretic application of L-aspartate and L-glutamate to the spinal cord results in neuronal depolarisation and increased generation of nerve action-potentials [Curtis *et al.*, 1959]. Subsequently, a convincing body of evidence that the acidic amino acids and/or very closely related endogenous substances are the major class of excitatory neurotransmitters in the CNS. However, it is only in the last decade that specific agonists and antagonists have been developed and an understanding of the receptors that mediate the excitatory effects of these substances has evolved. Receptors for excitatory amino acids have been classified into three major subgroups on the basis of specific effects of conformationally restricted synthetic analogues. These consist of receptors activated by N-methyl-D-aspartate (NMDA), kainate and quisqualate [Watkins and Evans, 1981]. In parallel with the developments in receptor-pharmacology, the (patho)physiological importance of L-glutamate and related substances has emerged. For instance, intracerebral injection of the receptor-specific agonists kainic acid, quisqualate and NMDA results in a perikaryal-specific, axon-sparing lesion [Coyle, 1987]. It was hypothesised that they killed neurons by persistent depolarisation of L-glutamate receptors on their dendrites and cell bodies. Accordingly, these compounds have been termed *excitotoxins*. As L-glutamate and related substances are thought to be excitatory neurotansmitters at over one third of the synapses in the mammalian brain, it can be anticipated that these systems could play a role in neurological and psychiatric disorders. By virtue of their excitatory nature it has been postulated that L-aspartate and L-glutamate may be involved in epilepsy [Sloviter, 1986]. Consistent with this hypothesis, glutamate-specific receptor agonists exhibit potent convulsant effects when injected intracerebrally [Coyle, 1987] and several glutamate-receptor antagonists have anticonvulsant activity [Meldrum, 1985]. Furthermore, the intrastriatal injection of kainic acid to rodents and primates reproduces many of the synaptic, neurochemical, histopathological and behavioural aspects of Huntington's disease [Coyle, 87]. The pre-clinical pharmacology of glutamate-receptor antagonists suggests these compounds may be useful as anticonvulsants, analgesics, anaesthetics and possibly as protectors of hypoxaemic brain damage [Robinson and Coyle, 1987].

Many of the acidic amino acid antagonists are highly charged, very hydrophilic and have a molecular weight in excess of 200 Da. All of these factors mitigate against efficient transepithelial transport and consequently their oral bioavailabilities are low. CGP37849 is a NMDA antagonist (Ciba Pharmaceuticals, Basle, Switzerland) which is a mixture of two stereoisomers, CGP40116 and CGP40117 (see Fig. 5.1). The bioavailability of CGP37849 following oral administered as a simple solution to rats or dogs is low (~15% and ~30%, respectively). Interestingly, when CGH37849 is administered orally, only CGP40116 achieves systemic availability (Dr Ian Hassan, Ciba Pharmaceuticals; personal communication). There are two likely explanations for this phenomenon, either stereo-specific transport across the GI epithelium and/or stereo-selective first-pass metabolism. Because of the structural similarity of CGP37849 to glutamate and the presence of a stereo-selective acidic amino acid carrier in the human small intestine (see above) the possibility of carrier-mediated absorption of CGP40116 was considered. This was investigated by characterising acidic amino acid transport across the Caco-2 monolayer model and comparing this with the transepithelial transport properties of CGP40116 and CGP40117.

FIGURE 5.1 *Structures of acidic amino acids and their analogues.*

L-Aspartic acid

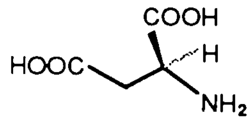

L-Glutamic acid

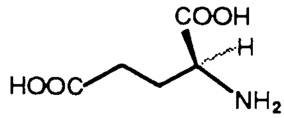

CGP40116

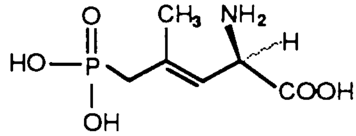

CGP40117

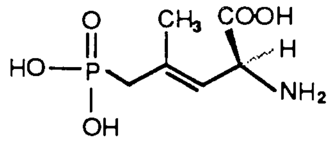

Cysteic acid

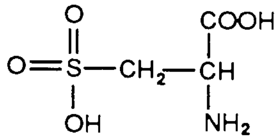

2-Amino-2-carboxyethylphosphonous acid

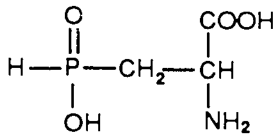

2-Amino-2-carboxyethylphosphonic acid

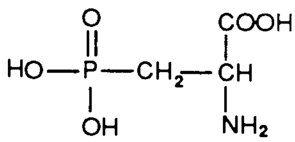

2-Amino-2-carboxypropylphosphonic acid

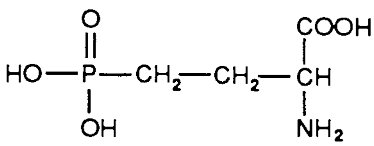

2-Amino-2-carboxyethylarsonic acid

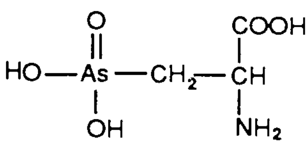

2-Amino-2-carboxypropylarsonic acid

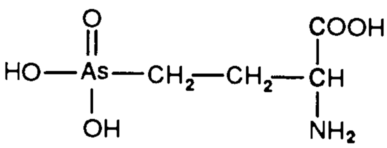

5.2 MATERIALS

5.2.1 CHEMICALS

L-[^{3}H]Aspartate (25 Ci mmol^{-1}) and L-[^{14}C]aspartate (220.4 Ci mol^{-1}) were purchased from New England Nuclear (Dupont, Germany). L-[^{3}H]Glutamate (45 Ci mol^{-1}) was obtained from Amersham, UK. [^{14}C]CGP37849 (3.2 mCi mmol-1), [^{14}C]CGP40116 (1.6 mCi mmol^{-1}) and [^{14}C]CGP40117 (1.6 mCi mmol-1) and their unlabelled counterparts were a gift from Dr A. Probst (Ciba Pharmaceuticals, Basle, Switzerland). 2-Amino-2-carboxyethylphosphonous acid was synthesized by Dr Sally Freeman (Drug Development Research Group, Aston University, UK). 2-Amino-2-carboxyethylarsonic acid, 2-amino-2-carboxypropylarsonic acid and 4-amino-4-carboxybutylphosphonic acid were a gift from Dr Hal Dixon (Cambridge University, UK). Cycloheximide was purchased from the Aldrich chemical company.

5.3 METHODS

5.3.1 CELL CULTURE

Transport studies were performed using Caco-2 monolayers cultured for 21 d on nitrocellulose (L-asparate and L-glutamate studies) or polycarbonate (CGP37849, CGP40116 and CGP40117 studies) culture-inserts. For uptake studies, cells were cultured for 6 days on six-well clusters.

5.3.2 TRANSPORT MEDIA

M4-medium was used for the majority of acidic amino acid transport experiments. It comprised Hanks' balanced salt solution (HBSS) containing 0.1% w/v BSA, 0.01% phenol red, 5 mM D-glucose and buffered with 14 mM HEPES (pH 7.0, 7.4 or 8.0) or MES (pH 5.5, 6.0 or 6.5). M4-medium buffered to pH7.4 was used unless specified. A sodium-free version was prepared by equimolar substitution of NaCl with choline chloride ($M4_{Choline}$).

M3-medium was used to investigate the cation- and anion-dependence of L-aspartate transport across Caco-2 monolayers. It comprised, 140 mM NaCl, 4 mM KH_2PO_4, 5.2 mM K_2HPO_4, 1.2 mM $MgSO_4$, 1.3 mM Calcium gluconate, 0.01% phenol red and 5 mM D-glucose, pH7.4. Chloride-free M3-media were prepared by equimolar substitutions of NaCl with sodium iodide ($M3_{Iodide}$) sodium isethionate ($M3_{Isethionate}$) or sodium thiocyanate ($M3_{Thiocyanate}$). Sodium-free M3-media were prepared by equimolar substitution of NaCl with the chloride salts of choline ($M3_{Choline}$), lithium ($M3_{Lithium}$), potassium ($M3_{Potassium}$), rubidium ($M3_{Rubidium}$) or caesium ($M3_{Caesium}$).

5.3.3 TRANSPORT EXPERIMENTS

Permeable-support-medium was aspirated from the Ap and Bl chambers and the monolayers washed (1 x (2 ml Ap + 2 ml Bl) x 15 min) with the incubation-medium. The donor and receiver washing- and incubation-solutions were dependent on experimental requirements. The transport experiment were initiated by aspirating the washing-solutions and applying a donor-solution (2 ml) of incubation-medium containing 50 μM of L-[^{3}H]aspartate (1.0 μCi ml^{-1}), L-[^{14}C]aspartate (0.25 μCi ml^{-1}), L-[^{3}H]glutamate (1.0 μCi ml^{-1}), [^{14}C]CGP37849 (0.1625 μCi ml^{-1}), [^{14}C]CGP40116 (0.1625 μCi ml^{-1}) or [^{14}C]CGP40117 (0.1625 μCi ml^{-1}). The culture-insert and donor-solution were immediately transferred to a chamber containing 2.5 ml of receiver-solution. All washing- and incubation-solutions were equilibrated to 37°C for 1 h prior to use. Ap-to-Bl transport kinetics were followed by sequentially transferring the culture-insert into a new receiver-chamber at defined time intervals. After the final receiver-sample had been collected, monolayers were transferred to a cold-table (0-4°C) and the Ap donor-solutions were collected. The radiochemical flux into the receiver-solution for each time interval was corrected for the radiochemical concentration in the Ap donor-solution and was normalised to the anticipated DPM (*ie:* 1 μCi ml^{-1} = 2.2 x 10^6 DPM ml^{-1}, 0.25 μCi ml^{-1} = 0.55 x 10^6 DPM ml^{-1}, 0.1625 μCi ml^{-1} = 0.36 x 10^6 DPM ml^{-1}) as described previously (see section 2.3.2).

Transport in the reverse direction (*ie:* Bl-to-Ap) was also determined. The rate of radiochemical appearance in the Ap chamber from a Bl donor-solution was monitored with time. Briefly, at defined time-intervals the culture-insert was removed from the Bl donor-solution and the entire Ap receiver-solution collected then carefully replaced with fresh transport-medium and the culture-insert returned to the donor-solution. After the final Ap receiver-sample had been collected, monolayers were transferred to a cold table (0-4°C) and the Bl donor-solutions collected and their radiochemical concentrations determined. The radiochemical flux into the Ap receiver-solution was determined at each time interval and corrected for the radiochemical concentration applied to each monolayer. The corrected radiochemical fluxes at each time interval were summed and expressed as cumulative-flux with respect to time.

5.3.4 EXPERIMENTAL CONDITIONS

The standard acidic amino acid transport protocol (see section 5.3.4) was modified to probe their transport mechanism. These modified experimental conditions are summarised below and are described in detail in the appropriate figure legends.

5.3.4.1 ACIDIC AMINO ACIDS

Acidic amino acid transport investigated over a range of concentrations (50 μM to 50 mM), Ap pH values (5.5 to 8.5), sodium-concentrations (0 to 140 mM) and temperatures (4, 20 and 37°C). In addition, the influence of a 10-fold reverse concentration gradient and inhibitors for the Na^+/K^+-ATPase (ouabain), oxidative-phosphorylation (10 mM sodium azide + 50 mM 2-deoxyglucose; N_3+2-DG) or protein synthesis (500 μM cycloheximide) on transport were investigated. Inhibition of L-aspartate or L-glutamate (50 μM) transport by a 20-fold excess of unlabelled analogues (1 mM) was used to examine the substrate-specificity of the acidic amino acid-transporter.

5.3.4.2 CGP37849, CGP40116 AND CGP40117

The Ap-to-Bl transport kinetics of CGP37849, CGP40116 and CGP40117 were compared. In addition, the polarity (Ap-to-Bl versus Bl-to-Ap) and concentration- and temperature-dependence of CGP40116 and CGP40117 were investigated.

5.3.5 IDENTIFICATION OF POST-TRANSPORT RADIOCHEMICALS

Samples were analysed for L-[^{3}H]-aspartate by ion-exchange high-performance liquid chromatography. Briefly, proteins in the Bl (receiver) sample (2.5 ml) were precipitated with 40% w/v (aq) trichloroacetic acid (100 μl) and pelleted by centrifugation at 11,600 x g (MSE minifuge). The supernatant (20 μl) was injected onto a cation exchange column (Partisil SCX, 250 mm x 4.6 mm) and eluted with 0.01M potassium phosphate buffer (pH 3.0) at a flow-rate of 1.5 ml min^{-1}. Eluant fractions were collected at 1 min intervals (Gilson, model 204) and analysed for [^{3}H]-content by liquid scintillation counting. An L-[^{3}H]-aspartate reference sample in M4-medium was prepared then processed and analysed as described above.

5.3.6 INHIBITION CONSTANT (K_i) CALCULATION

The Inhibition constant (K_i) was calculated from the % inhibition of carrier-mediated L-aspartate or L-glutamate transport by a range of compounds, using the following method.

EQUATION 5.1 $\quad$ % inhibition, $R_{100} = 100\,((V_o - V_i) / V_o)$

Where, V_o = Transport velocity in the absence of an inhibitor

V_i = Transport velocity in the presence of an inhibitor

Therefore,

EQUATION 5.2 $\quad$ $V_o / V_i = 100 / (100 - R_{100})$

V_o / V_i was used to calculate the K_i for each competitor using equation 5.3.

EQUATION 5.3

$$K_i = (K_m^{sd} \times [\text{Competitor}]) / ((V_o / V_i) \times (K_m^{sd} + [\text{Substrate}])) - (K_m^{sd} + [\text{Substrate}])$$

This calculation assumes that the compounds inhibit transport competitively.

5.4 RESULTS

5.4.1 ACIDIC AMINO ACID TRANSPORT

Tritium in the non-TCA precipitable fraction of the Bl (receiver) solution co-eluted with the reference L-[^{3}H]-aspartate sample (Fig. 5.2). Only 0.54±0.22% of the total [^{3}H]- was present in the TCA precipitable and this was not significantly reduced by a 45 min pre-incubation with 500 μM cycloheximide, 0.47±0.16%. Therefore, L-aspartate was not appreciably metabolised over the duration of these experiments and [^{3}H]- assays overwhelmingly reflect intact L-[^{3}H]aspartate.

L-Aspartate showed an Ap-to-Bl transepithelial lag-time of 7 5±0.6 min followed by a linear-phase (transport proportional to time; 7.0±0.1 nmoles h^{-1} insert^{-1}) which continued for at least 60 min (Fig. 5.3 A). At low concentrations it was rapidly transported across Caco-2 monolayers, 83.8±1.4% of apically applied L-aspartate was transported into the Bl compartment after 180 min. The reduction in transport-rate at extended time periods (*ie:* between 60 to 180 min) probably reflects depletion of L-aspartate in the Ap chamber. The Ap-to-Bl transport rate for 50 μM L-[^{3}H]aspartate was markedly reduced (>64-fold) by a 1,000-fold molar excess (50 mM) of unlabelled L-aspartate (Fig. 5.3 B). Bl-to-Ap L-aspartate transport occurred at a much slower rate and was linear over at least 180 min (Fig. 5.4).

The initial rate of Ap-to-Bl transport increased from day 7 (3.63±0.12 nmoles h^{-1} insert^{-1}) to day 14 (5.98±0.78 nmoles h^{-1} insert^{-1}) of culture then remained constant through to day 28. Meanwhile, Bl-to-Ap transport decreased steadily between day 7 (0.69±0.02 nmoles h^{-1} insert^{-1}) and day 21 (0.45±0.01 nmoles h^{-1} insert^{-1}) before increasing slightly at day 28 (0.65±0.10 nmoles h^{-1} insert^{-1}). The rate of Ap-to-Bl L-aspartate flux was significantly higher ($p<0.001$) than that in the Bl-to-Ap direction at each time-point but was most polar after 21 days of culture when Ap-to-Bl transport occurred at 12.1±1.0 times the rate of Bl-to-Ap transport (Fig. 5.5).

The non-saturable (passive) transport component of L-[^{3}H]aspartate (50 μM) was estimated by performing transport in the presence of a 1000-fold molar excess of unlabelled L-aspartate (50 mM). The difference between total and non-saturable transport represented the saturable (carrier-mediated) component. In sodium-free conditions ($M4_{Choline}$), L-[^{3}H]aspartate (50μM) transport was reduced to passive-flux rates (Fig. 5.6 A). The saturable transport component was stimulated at low concentrations of extracellular sodium ions. A half-maximal stimulation of L-aspartate transport occurred at an extracellular sodium-concentration of approximately 20 mM whilst maximal transport was only achieved at concentrations of 100 mM and above (Fig. 5.6 B). Despite an absolute dependence on extracellular sodium ions, L-aspartate uptake into, and transport across, Caco-2 monolayers was only partially reduced by ouabain. Cellular uptake was reduced by 32.3±1.3% ($p<0.01$) by 50 μM ouabain compared with a reduction of 80.6±3.9% ($p<0.001$) from $M4_{Choline}$ (Fig. 5.7 A). Similarly, transport was reduced 16.2±4.3% ($p<0.05$) by 50 μM ouabain, but 97.9±0.7% ($p<0.001$) from $M4_{Choline}$ (Fig. 5.7 B). The requirement of carrier-mediated L-aspartate transport for extracellular sodium ions was specific. Equimolar replacement of extracellular Na^+ with K^+, Rb^+ or Cs^+ failed to significantly stimulate L-aspartate transport above passive transport-fluxes. Li^+ produced a small, but significant ($p<0.05$), stimulation of transport compared to choline chloride conditions. In contrast, L-aspartate transport was not anion-sensitive (Table 5.1).

Total acidic amino acid transport (V^t) is the sum of the sodium-dependent (V^{sd}) and sodium-independent (V^{si}) pathways. In the absence of sodium ions, transport only occurs by the sodium-independent (diffusional) pathway. Therefore, subtraction of concentration-dependent transport profiles, performed in the presence and absence of sodium ions, provides (V^{sd}) which depicts Michaelis-Menten saturation kinetics for the sodium-dependent transport components for L-aspartate and L-glutamate (Fig. 5.8 A and B). Eadie-Hofstee plots of these data were used to calculate the Michaelis constant ($K_m{}^{sd}$) and maximal transport velocity ($V_{max}{}^{sd}$) (Fig. 5.8 C and D). The kinetic parameters for the sodium-dependent L-aspartate and L-glutamate are given in Table 5.2.

The rate of Ap-to-Bl L-aspartate transport against a 10-fold reverse concentration-gradient was indistinguishable from that in the absence of a gradient (Table 5.3). L-aspartate transport was significantly ($p<0.05$) reduced by a 45 min pre-incubation with 500 μM cycloheximide (Fig. 5.9). In addition, there was a bell-shaped relationship pH-dependence with a broad pH-optimum between pH6.5 (4.89±0.21 nmoles h^{-1} $insert^{-1}$) and 7.5 (4.80±0.34 nmoles h^{-1} $insert^{-1}$) and was significantly reduced outside this range at pH6.0 (3.73±0.03 nmoles h^{-1} $insert^{-1}$) and at pH8.0 (3.14±0.16 nmoles h^{-1} $insert^{-1}$); p<0.01; Fig. 5.10). Finally, L-aspartate transport was significantly reduced at temperatures below 37°C (67.6±1.1% and 99.0±0.1% at 20 and 4°C, respectively; p<0.001; Fig. 5.11 A). An activation energy (E_a) for L-aspartate transport across Caco-2 monolayers of 101.6±1.0 kJ mol^{-1} was calculated by linear least-squares regression analysis of an arrhenius plot for these data (Fig. 5.11 B).

Cross-inhibition transport studies between radiolabelled L-aspartate or L-glutamate (50 μM) and a 20-fold molar excess (1 mM) of unlabelled compounds showed the acidic amino acid carrier to have stringent structural-requirements for competing ligands (Tables 5.4 and 5.5). L- and D-aspartate were equally effective and potent inhibitors (92.1±3.5% and 88.0±1.7%, respectively; p<0.001) of L-aspartate transport (Table 5.4). Interestingly, L-glutamate was a strong inhibitor (74.8±0.7%; p<0.001) whilst its stereoisomer D-glutamate was only a weak inhibitor (23.5±8.8%; p<0.05) of transport. Similarly, L-aspartate, D-aspartate and L-glutamate are potent inhibitors of L-glutamate transport whilst D-glutamate was a weak inhibitor. The small neutral amino acids (L-alanine, L-asparagine and L-proline) were weak inhibitors whilst large neutral amino acids (L-methionine and L-phenylalanine) failed to significantly inhibit L-aspartate transport. The organic anions, 4,4'-diisothiocyanatostilbene-2,2'-disulphonate, *p*-aminohippurate and succinate did not significantly reduce L-aspartate transport.

Synthetic analogues of acidic amino acids showed a differential ability to inhibit L-aspartate and L-glutamate transport (Table 5.5). Potent inhibition of acidic amino acid transport was retained after minor structural modifications of L-aspartate and L-glutamate. Insertion of a hydroxyl-group in the *threo*-configuration at the beta-position of the L-aspartate side-chain does not impair inhibition-potency (*Threo*-beta-hydroxy-DL-aspartate, 90.7±0.6%; p<0.001). Some substitutions of side-chain carboxylate functionality preserved inhibition properties. L-Cysteate and 2-amino-2-carboxyethylphosphonic acid were strong inhibitors of acidic amino acid transport. The arsono analogue of L-aspartate (2-amino-2-carboxyethylarsonic acid) partially inhibited L-aspartate (32.5±1.7%; p<0.01) and L-glutamate (44.2±7.6%; p<0.01) transport. However, the arsono-analogue of glutamate (3-Amino-3-carboxypropylarsonic acid) failed to significantly inhibit L-aspartate transport. Whilst 2-amino-2-carboxyethylphosphonous acid (89.8±0.5%; p<0.001) is a potent inhibitor of L-aspartate transport, the phosphono-analogue of aspartate (2-amino-2-carboxyethylphosphonic acid, 13.9±2.7%) did not inhibit transport. The phosphono-analogue of glutamate failed to significantly inhibit acidic amino acid transport.

Methylation at the alpha-carbon halved inhibition-potency (alpha-methyl-DL-aspartate, 40.0±2.4%; $p<0.01$) whilst methylation at the amino group abolished inhibition (N-methyl-DL-aspartate, 14.2±7.1%). A range of centrally active acidic amino acid analogues (N-methyl-DL-aspartate, 2-amino-5-phosphonovalerate, DL-alpha-amino-3-hydroxy-5-methylisoxazole-4-propionate (AMPA), CGP37849, CGP40116, Kainate and quisqualate) failed to significantly inhibit L-aspartate transport.

5.4.2 TRANSPORT OF CGP37849, CGP40116 AND CGP40117

Ap-to-Bl transport of acidic amino acids across Caco-2 monolayers occurs in a saturable fashion when cultured on nitrocellulose or polycarbonate permeable-supports. Furthermore, the level of acidic amino acid carrier expression by Caco-2 cells cultured for 15 d on nitrocellulose (4.20 cm^2) and polycarbonate (4.71 cm^2) inserts was indistinguishable when expressed as apparent permeability coefficients which corrects for the surface area available for transport (Table 5.7).

A 20-fold molar excess (1 mM) of CGP37849 or CGP40116, failed to significantly inhibit the Ap-to-Bl transport of 50 μM L-[^{14}C]aspartate (Table 5.5). This result indicated that the transport of these compounds was not mediated to any extent by the acidic amino acid carrier.

The Ap-to-Bl transport kinetics for the radiolabelled CGP37849, and its two stereoisomers are shown in Fig. 5.12. The apparent permeability coefficients for [^{14}C]CGP37849, [^{14}C]CGP40116 and [^{14}C]CGP40117 were 3.458±0.221, 1.247±0.001 and 0.558±0.001 x 10^{-7} cm s^{-1}, respectively. These slow transport rates represent another notable difference with the acidic amino acids which are rapidly transported across Caco-2 monolayers ($P_{app(50\mu M)}$ for L-aspartate = 122±8.0 x 10^{-7} cm s^{-1} and L-glutamate = 28±0.5 x 10^{-7} cm s^{-1}). The higher transport rate of CGP37849 is surprising and may be related to the presence of radiochemical impurities (Table 5.8). However, despite the identical and absolute radiochemical purities of CGP40116 and CGP40117 these compounds exhibited different transport properties. At 37°C, the rate of Ap-to-Bl transport for [^{14}C]CGP40116 was 1.52-fold higher than for [^{14}C]CGP40117 (Fig. 5.13; $p<0.01$). A 100-fold molar excess of unlabelled compound failed to reduce the transport of [^{14}C]CGP40116 and

[^{14}C]CGP40117 and the differential transport rates were maintained (Fig. 5.13). Despite being non-saturable Ap-to-Bl transport was temperature-dependent. Interestingly, at 20 and 4°C the transport rates for CGP40116 and CGP40117 were not significantly different (Fig. 5.14 A). CGP40116 transport was non-vectorial, that is, it occurred at an identical rate in Ap-to-Bl and Bl-to-Ap directions. Interestingly, the rate of CGP40117 transport in the Bl-to-Ap direction was greater than in the Ap-to-Bl direction. Indeed, the Bl-to-Ap transport of CGP40117 occurred at the same rate as Ap-to-Bl and Bl-to-Ap transport of CGP40116 (Fig. 5.15).

FIGURE 5.2 *Identification of post-transport L-[^{3}H]aspartate*

Radio-HPLC chromatograms showing the post-transport tritium-distribution in the non-TCA precipitable fraction of 60 min post-transport Bl receiver-solution (**A**) and a reference sample spiked with L-[^{3}H]aspartate (**B**).

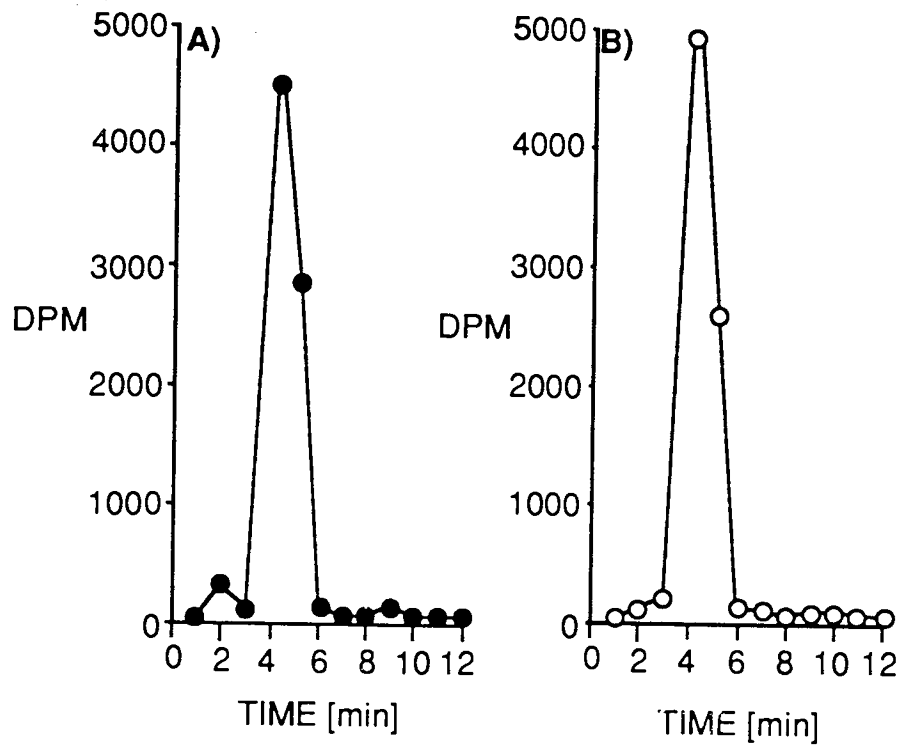

FIGURE 5.3 *Ap-to-Bl transport kinetics of L-[^{3}H]aspartate.*
Monolayers were washed (1 x (2 ml Ap + 2 ml Bl) x 15 min) with M4-medium before 50 µM L-[^{3}H]aspartate was applied to the Ap surface of Caco-2 monolayers. Ap-to-Bl L-[^{3}H]aspartate (50 µM) transport kinetics (closed circles) were determined by sequential transfer at 10 min (**A**) and 30 min (**B**) intervals. Ap-to-Bl transport kinetics of 50 µM L-[^{3}H]aspartate in the presence of a 1000-fold molar excess (50 mM) was also monitored (**B**; open circles).

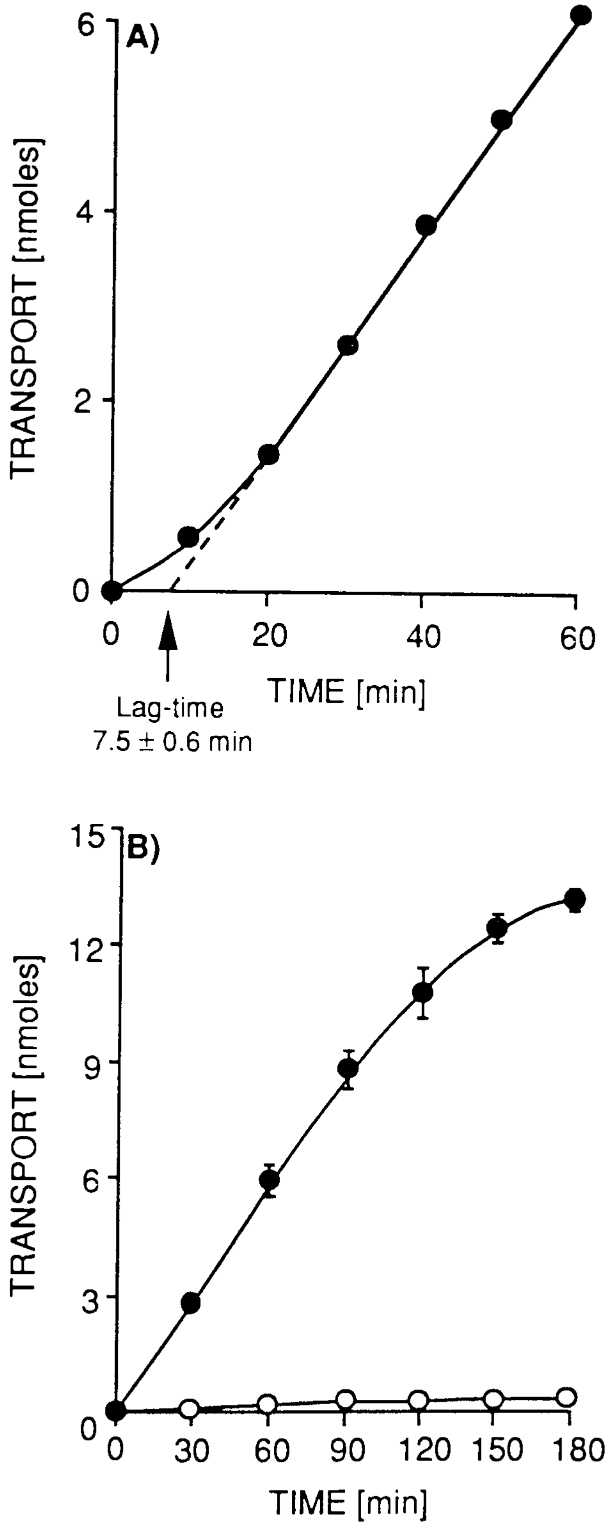

FIGURE 5.4 *Polarity of L-aspartate transport at 21d of culture.*
Monolayers were washed (1 x (2 ml Ap + 2 ml Bl) x 15 min) with M4-medium before 50 μM L-[^{3}H]aspartate was applied to the Ap or Bl surface of Caco-2 monolayers. The kinetics of Ap-to-Bl (closed circles) and Bl-to-Ap (open circles) were monitored by collecting the receiver solutions at 30 min intervals. Data are presented as mean values ± SD for three monolayers.

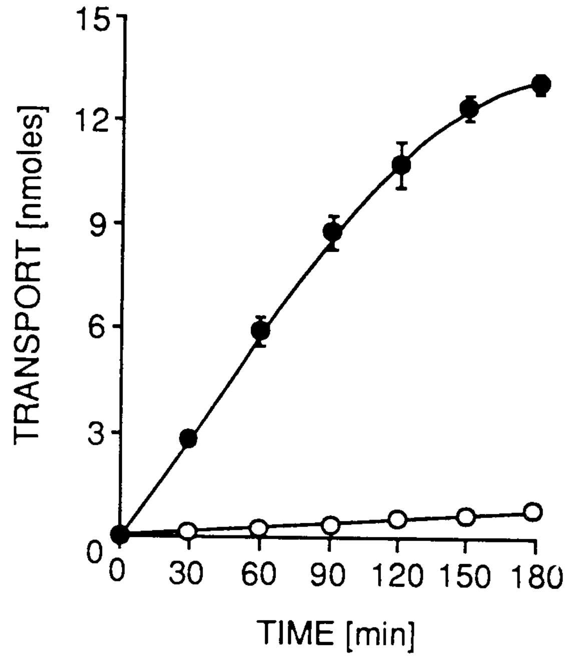

FIGURE 5.5 *The temporal-dependence of L-aspartate transport.*
Monolayers were washed (1 x (2 ml Ap + 2 ml Bl) x 15 min) with M4-medium before 50 μM L-[^{3}H]aspartate was applied to the Ap or Bl surface of Caco-2 monolayers. The initial rate of Ap-to-Bl (closed circles) and Bl-to-Ap (open circles) transport was determined after 7, 14, 21 and 28 d of culture. Data are presented as mean values ± SD for three monolayers. * Denotes a significantly higher Ap-to-Bl than Bl-to-Ap transport of L-aspartate at $p<0.001$.

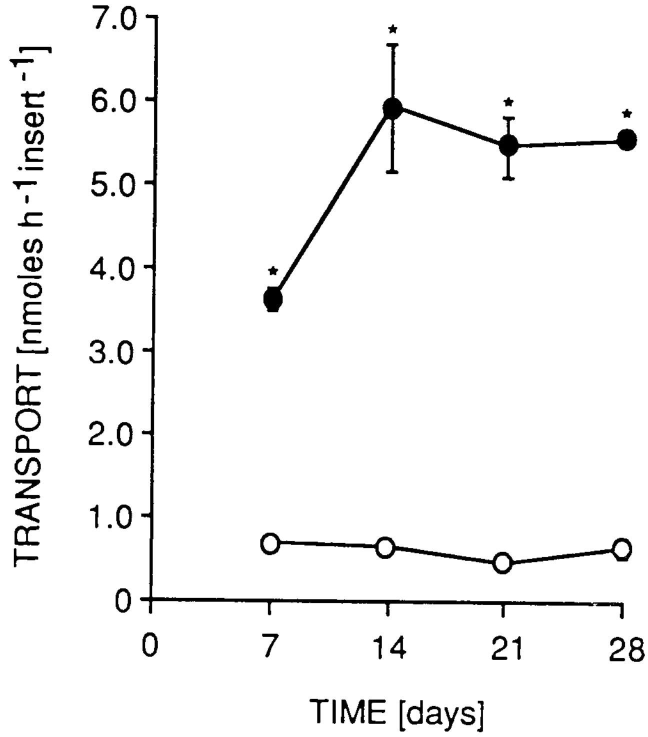

FIGURE 5.6 *Sodium-dependence of Ap-to-Bl L-[^{3}H]aspartate transport.*
(A) Monolayers were washed (1 x (2 ml Ap + 2 ml Bl) x 15 min) with M4-medium or $M4_{Choline}$, as appropriate. Ap-to-Bl transport of L-[^{3}H]aspartate (50 μM) alone, or in the presence of a 1000-fold molar excess of L-aspartate (50 mM) of unlabelled L-aspartate, was determined in the presence and absence of extracellular sodium ions. * Denotes a significant reduction in L-[^{3}H]aspartate transport at $p<0.001$. **(B)** Monolayers were washed (1 x (2 ml Ap + 2 ml Bl) x 15 min) with M4-medium containing the appropriate sodium ion concentration. The initial rate of Ap-to-Bl transport of L-[^{3}H]aspartate (50 μM) was determined in the presence (Ap and Bl) of 0, 10, 20, 30, 50, 70, 100 and 140 mM sodium ions. Data are presented as mean values ± SD for three monolayers.

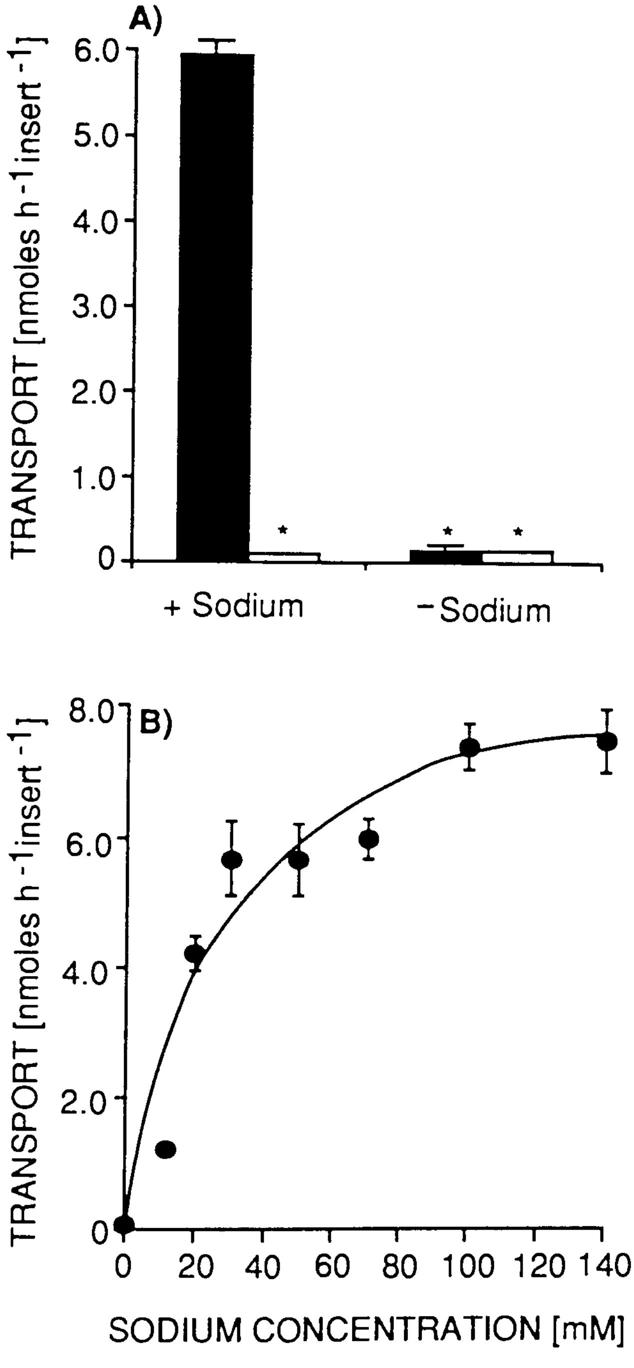

FIGURE 5.7 *Ouabain-sensitivity and energy dependence of L-aspartate uptake and transport.*

(A) *Transport;* Monolayers were pre-incubated (2 ml Ap + 2 ml Bl) for 60 min with M4-medium, $M4_{Choline}$, M4 containing 50 µM ouabain or M4 containing N_3+2-DG, as appropriate. The initial rate of Ap-to-Bl L-[^{3}H]aspartate transport was determined from M4, $M4_{Choline}$, M4 containing 50 µM ouabain or M4 containing N_3+2-DG. **(B)** *Uptake;* Monolayers were pre-incubated with M4-medium, $M4_{Choline}$, M4 containing an appropriate concentration of ouabain. L-[^{3}H]aspartate (50 mM) uptake over 10 min was determined from M4-medium, $M4_{Choline}$ and M4 containing 10, 50, 100, 1000 or 5000 µM ouabain. Data are presented as mean values ± SD for three monolayers.* and ** Denote significant reductions from control values at $p<0.01$ and $p<0.001$, respectively.

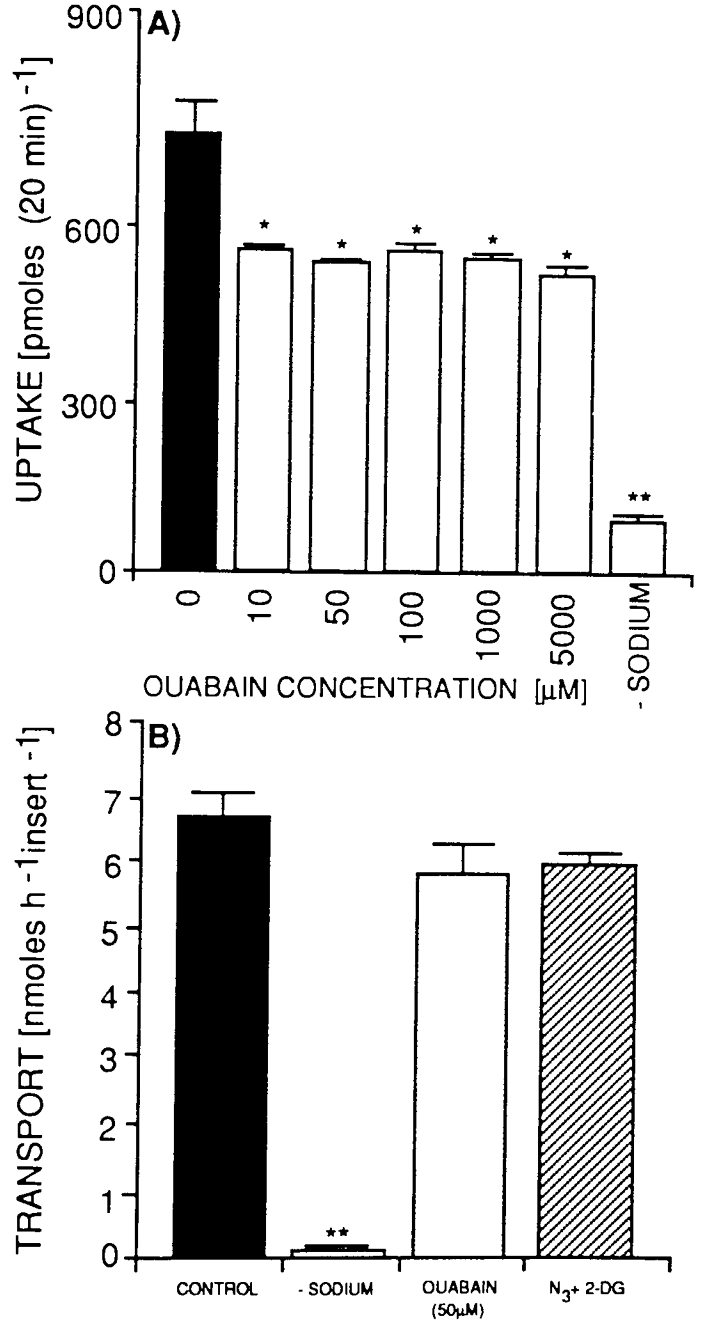

FIGURE 5.8 *Concentration-dependence of L-aspartate and L-glutamate transport.* Monolayers were washed (1 x (2 ml Ap + 2 ml Bl) x 15 min) with M4 or $M4_{Choline}$, as appropriate. The initial rate of Ap-to-Bl L-aspartate (**A**) and L-glutamate (**B**) transport were determined over a range of Ap concentrations in the presence or absence of extracellular sodium ions. The sodium-dependent transport component (dashed line) was calculated by subtraction of sodium-independent transport (solid line) from the total transport (dotted line). Data are presented as mean values ± SD for three monolayers. The kinetic parameters for the saturable transport component for L-aspartate (**C**) and L-glutamate (**D**) transport were estimated from Eadie-Hofstee plots of these data.

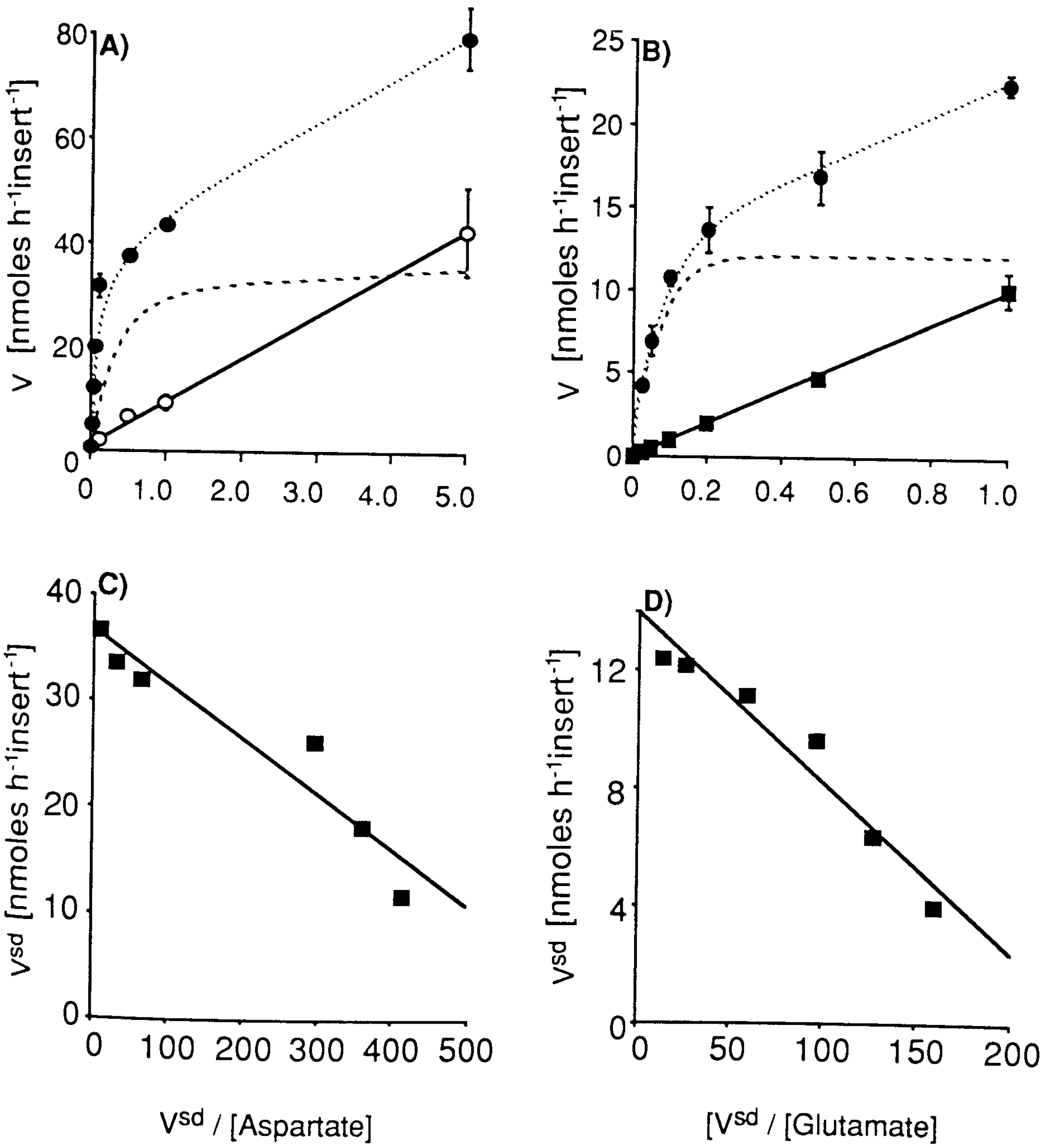

FIGURE 5.9 *Effect of cycloheximide on L-aspartate transport.*
Monolayers were pre-incubated for 45 min M4-medium alone (control) or M4-medium containing 500 µM cycloheximide, then the Ap-to-Bl transport of 50 µM L-aspartate compared. Data are presented as mean values ± SD for three monolayers. * Denotes a significant reduction $p<0.05$.

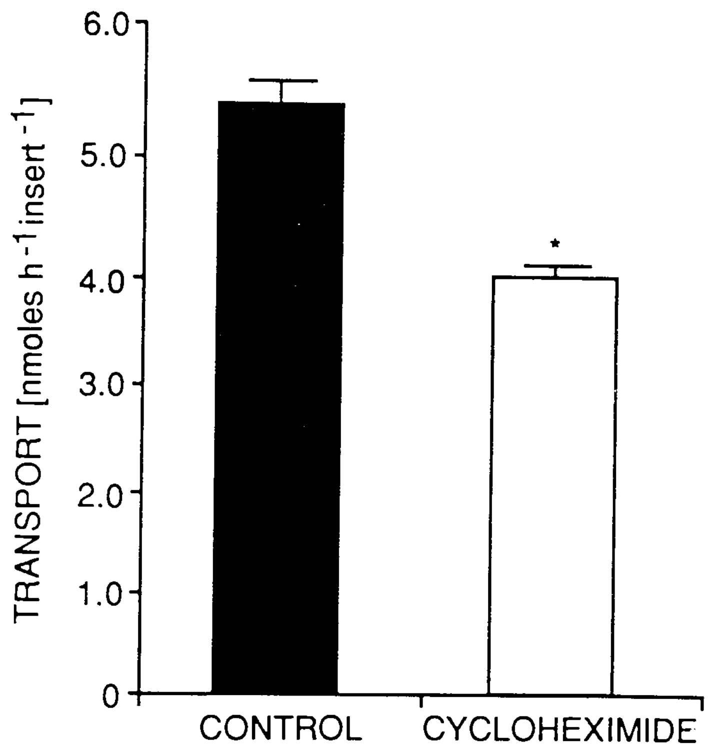

FIGURE 5.10 *pH-dependence of L-aspartate transport.*
Monolayers were washed (1 x 2 ml Ap x 15 min) with M4-medium buffered to an appropriate pH (5.5, 6.0, 6.5, 7.0, 7.5, 8.0) and (1 x (2 ml Bl) x 15 min) with M4-medium pH7.4. The initial rate of Ap-to-Bl 50 μM L-aspartate transport was determined for a range of Ap pH values (pH 5.5 to 8.0). Data are presented as the mean ± SD for three monolayers. * Denotes a significant reduction from L-aspartate transport at pH6.5.

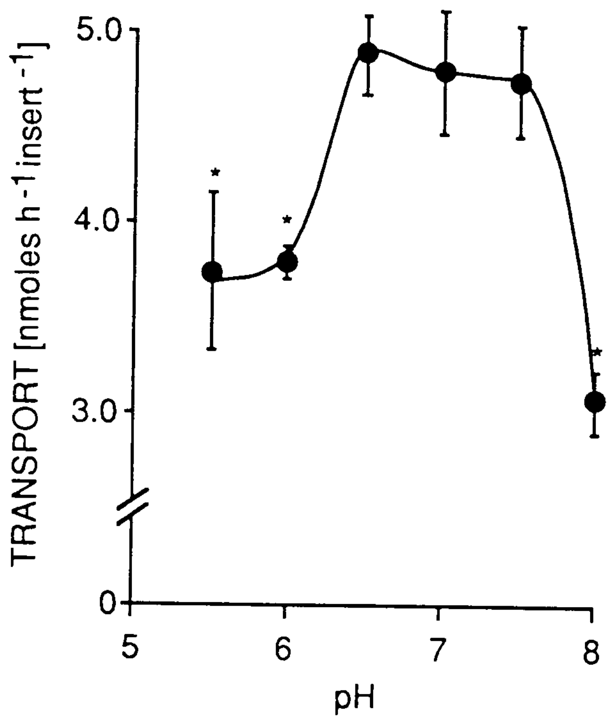

FIGURE 5.11 *Temperature-dependence of Ap-to-Bl L-aspartate transport.*
(A) Monolayers were washed (1 x (2 ml Ap + 2 ml Bl) x 15 min) with M4-medium pre-equilibrated 4, 20 or 37°C, as appropriate. L-[^{3}H]Aspartate (50 μM) was applied to the Ap surface of Caco-2 monolayers. The initial rate of Ap-to-Bl transport was determined at 4, 20 and 37°C. Data are presented as mean values ± SD for three monolayers. * Denotes a significant reduction in L-aspartate at p<0.001. **(B)** The activation-energy for Ap-to-Bl transport was calculated from an Arrhenius plot of these data.

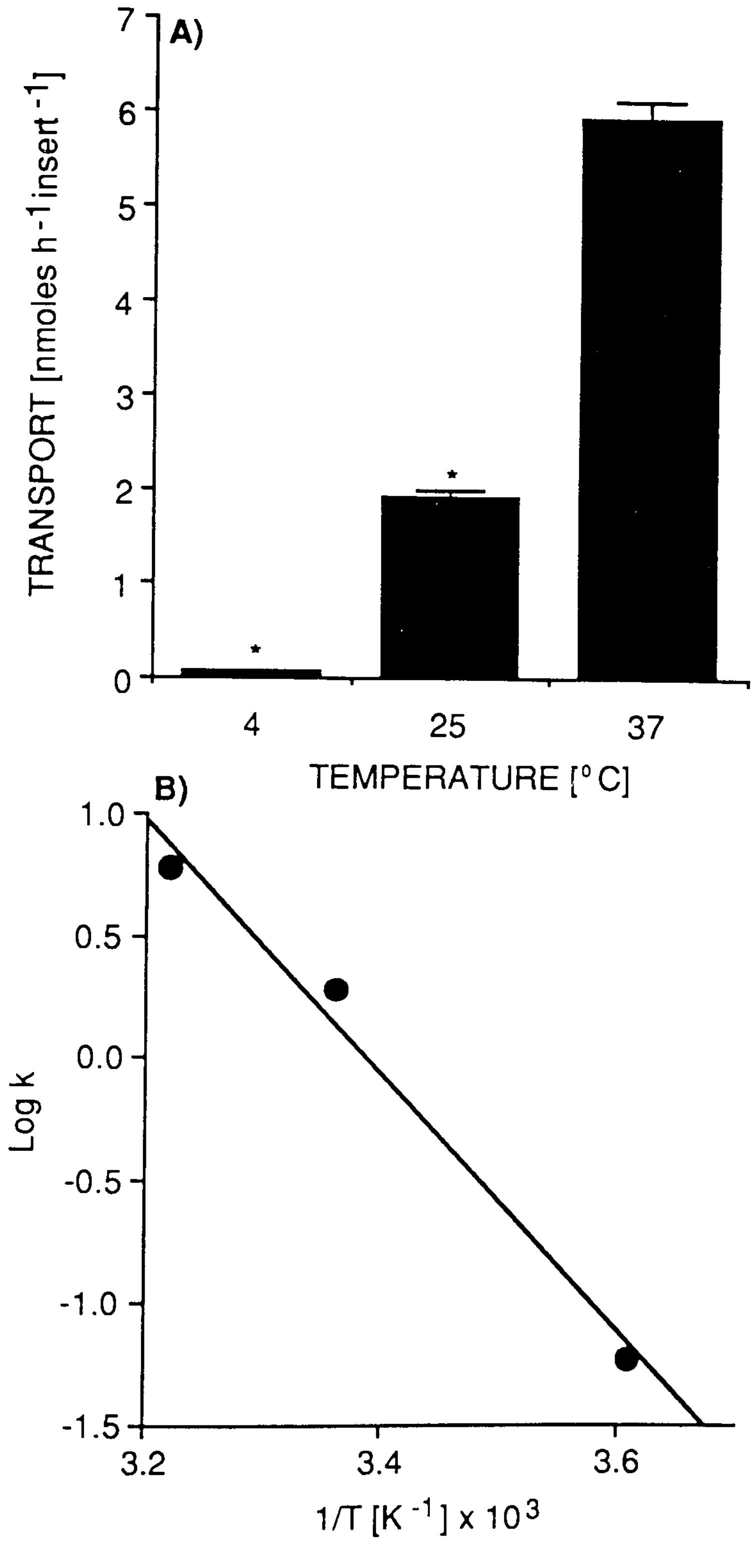

FIGURE 5.12 *Ap-to-Bl transport kinetics for [^{14}C]CGP37849, [^{14}C]CGP40116 and [^{14}C]CGP40117.*

Monolayers were washed (1 x (2 ml Ap + 2 ml Bl) x 15 min) with M4-medium before 50 µM of [^{14}C]CGP37849 (open triangles), [^{14}C]CGP40116 (closed circles) or [^{14}C]CGP40117 (open circles) was applied to the Ap surface of Caco-2 monolayers and Bl samples collected at 30 min intervals. Data are presented as mean values ± SD for six monolayers.

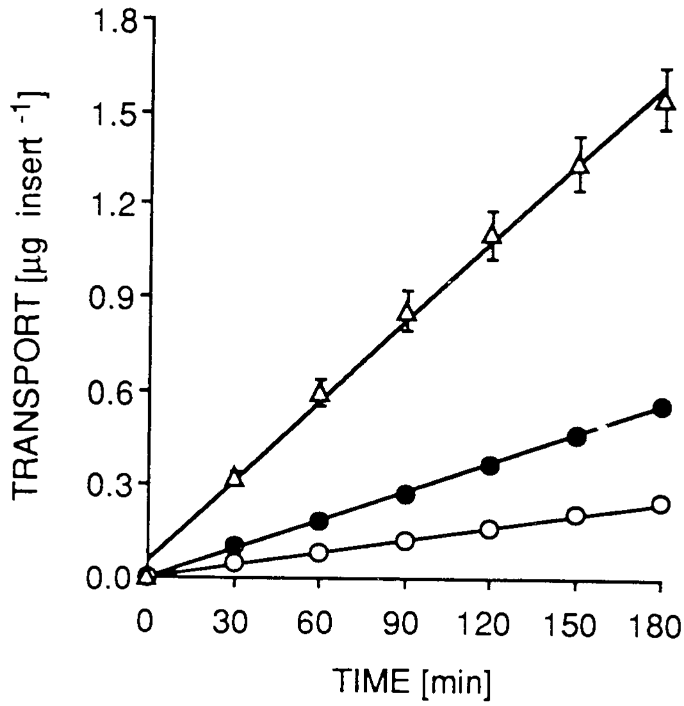

FIGURE 5.13 *Effect of 5 mM CGP40116 and CGP40117 on 50 μM [¹⁴C]CGP40116 and [¹⁴C]CGP40117 transport.*

The transport of 50 μM [^{14}C]CGP40116 or [^{14}C]CGP40117 alone (closed bars) or in the presence of a 100-fold molar excess (5 mM; open bars) of CGP40116 or CGP40117, respectively. Data are presented as mean values ± SD for six monolayers. * Denotes a significantly lower transport of CGP40117 compared to CGP40116 at $p<0.01$.

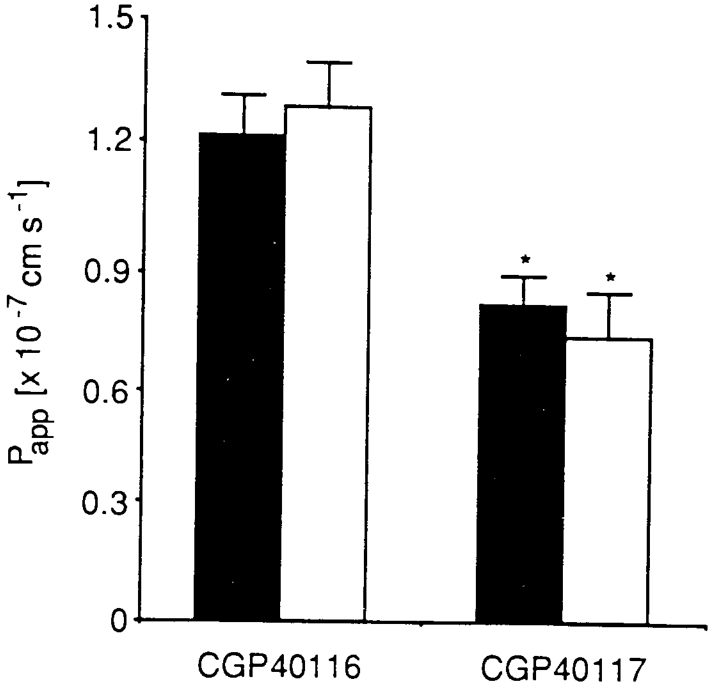

FIGURE 5.14 *Temperature-dependence of CGP40116 and CGP40117 transport.* Monolayers were washed (1 x (2 ml Ap + 2 ml Bl) x 15 min) with M4-medium pre-equilibrated 4, 20 or 37°C, as appropriate. (**A**) 50 μM [^{14}C]CGP40116 or [^{14}C]CGP40117 was applied to the Ap surface of Caco-2 monolayers. The initial rate of Ap-to-Bl transport was determined at 4, 20 and 37°C. * Denotes a significant reduction in transport compared to that at 37°C. (**B**) TER was determined at 4, 20 and 37°C. Data are presented as mean values ± SD for three monolayers.

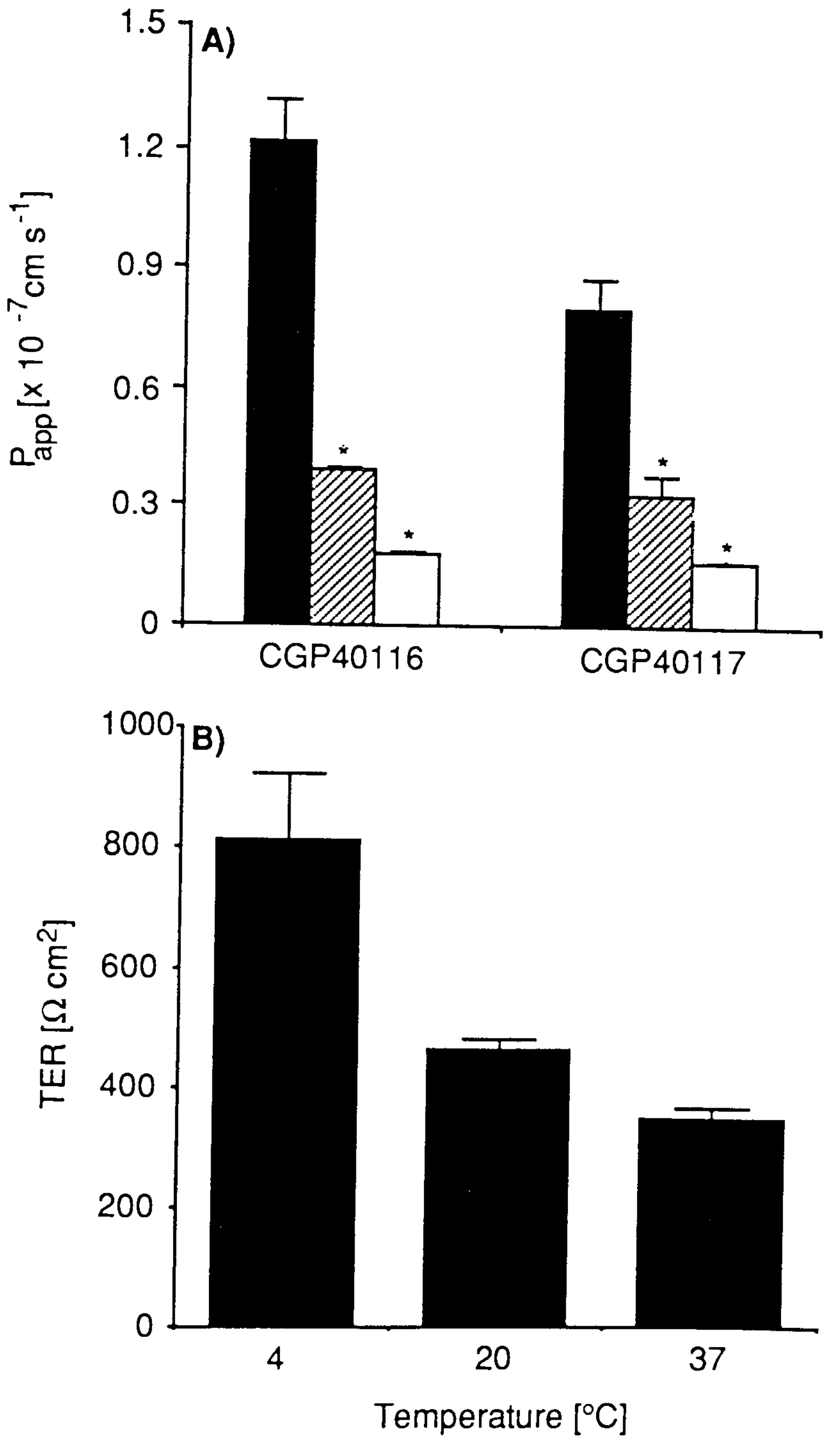

FIGURE 5.15 *Ap-to-Bl and Bl-to-Ap CGP40116 and CGP40117 transport.* Monolayers were washed (1 x (2 ml Ap + 2 ml Bl) x 15 min) with M4-medium before 50 μM of [^{14}C]CGP40116 or [^{14}C]CGP40117 was applied to the Ap or Bl surface of Caco-2 monolayers. The initial rate of Ap-to-Bl (closed bars) and Bl-to-Ap (open bars) transport was determined. Data are presented as mean values ± SD for three monolayers.

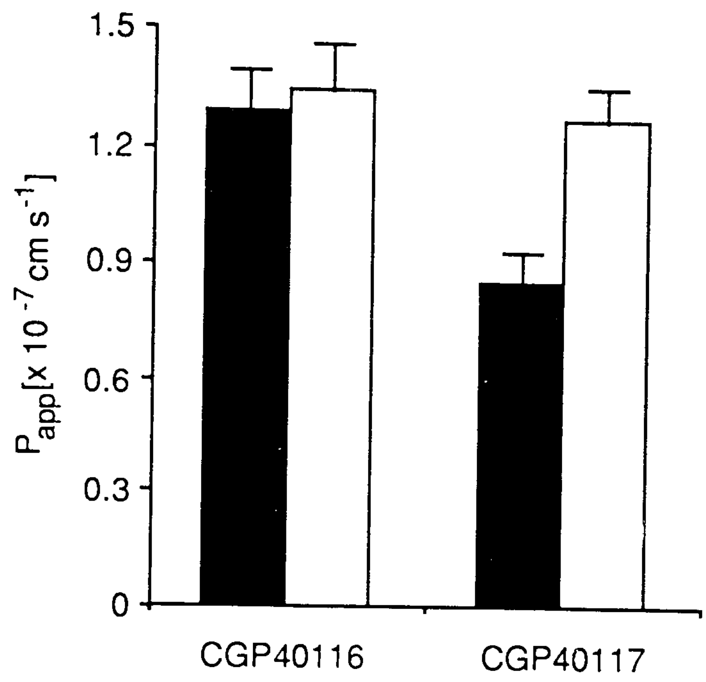

TABLE 5.1 *Cation- and anion-dependence of L-aspartate transport.*
The initial rate of Ap-to-Bl L-aspartate (50 μM) transport was determined from M3-medium containing the cation-anion salts shown below. Data are presented as mean values ± SD for three monolayers. * Denotes a significant reduction in L-aspartate transport from that in sodium chloride. § and §§ denote a significant stimulation of transport from that in choline chloride at $p<0.05$ and $p<0.001$, respectively.

CATION	ANION	L-ASPARTATE TRANSPORT % CONTROL (SD)
Sodium	Chloride	100.0 (3.0) §§
Sodium	Isethionate	100.3 (1.0) §§
Sodium	Thiocyanate	90.8 (3.2) §§
Lithium	Chloride	23.4 (2.2)* §
Potassium	Chloride	14.8 (3.1)*
Rubidium	Chloride	16.0 (2.4)*
Caesium	Chloride	12.3 (1.0)*
Choline	Chloride	12.5 (0.7)*

TABLE 5.2 *Kinetic parameters for acidic amino acid transport.*

Substrate	K_m^{sd} [μM] Mean (SD)	V_{max}^{sd} [nmoles h $^{-1}$ insert $^{-1}$] Mean (SD)
L-Aspartate	55.8 (3.3)	36.0 (1.1)
L-Glutamate	65.0 (6.3)	15.0 (2.4)

TABLE 5.3 *L-Aspartate transport against a 10-fold concentration-gradient*
Monolayers were washed (1 x (2 ml Ap + 2 ml Bl) x 15 min) with M4-medium before 50 μM L-[^{3}H]aspartate was applied to the Ap chamber. In the control group the receiver-solution comprised M4-medium alone and in the test group the receiver-solution comprised M4-medium supplemented with 500 μM unlabelled L-aspartate. Data are presented as mean values ± SD for three monolayers.

	TRANSPORT [nmoles] MEAN (SD)				
TIME [min]	30	60	90	120	150
Control	2.29(0.07)	5.95(0.11)	8.64(0.24)	10.86(0.12)	12.10(0.12)
Gradient	2.10(0.16)	5.59(0.19)	8.37(0.32)	10.42(0.25)	11.63(0.30)

TABLE 5.4 *Inhibition of acidic amino acid transport by natural amino acids.* Monolayers were washed (1 x (2 ml Ap + 2 ml Bl) x 15 min) with M4-medium. They were incubated with 50 μM acidic amino acid alone or in the presence of 1 mM of competitor. Data are presented mean % inhibition ± SD for three monolayers. * and ** Denote significant inhibition at p<0.01 and p<0.001, respectively.

COMPETITOR	% INHIBITION MEAN (SD)	
	L-Aspartate	L-Glutamate
NATURAL AMINOACIDS		
L-Aspartate	92.1 (2.0)**	73.9 (14.8)**
L-Glutamate	74.8 (0.4)**	70.1 (3.8)**
L-Asparagine	26.2 (5.5)*	NT
L-Proline	22.0 (3.1)*	NT
L-Alanine	17.2 (1.7)*	NT
L-Cysteine	14.5 (3.0)	NT
L-Histidine	12.8 (1.7)	NT
L-Phenylalanine	8.1 (1.4)	NT
L-Methionine	6.3 (4.5)	NT
L-Serine	-0.2 (5.3)	NT
Glycine	-6.6 (4.1)	NT
STEREOISOMERS		
D-Aspartate	88.0 (1.0)**	85.5 (1.9)**
D-Glutamate	23.5 (5.1)*	24.5 (6.1)*
ORGANIC ANIONS		
p-Aminohippurate	13.6 (6.4)	NT
4,4'-Diisothiocyanatostilbene-2,2'-disulphonate	6.5 (1.6)	NT
Succinate	2.8 (2.4)	NT

** P<0.001, * P<.01.
NT = Not Tested

TABLE 5.5 *Inhibition of acidic amino acid transport by synthetic analogues.* Monolayers were washed (1 x (2 ml Ap + 2 ml Bl) x 15 min) with M4-medium. They were incubated with 50 μM acidic amino acid alone or in the presence of 1 mM of competitor. The inhibition of acidic amino acid transport is expressed as a percentage of control (SD) for three monolayers. * and ** Denote significant inhibition at $p<0.01$ and $p<0.001$, respectively.

COMPETITOR	% INHIBITION MEAN (SD)	
	L-Aspartate	L-Glutamate
SYNTHETIC ANALOGUE		
Threo-ß-hydroxy-DL-aspartate	90.7 (0.6)**	NT
2-Amino-2-carboxyethylphosphonous acid	89.8 (0.5)**	88.0 (0.3)**
L-Cysteic acid	89.2 (0.7)**	89.0 (0.5)**
Alpha-methyl-DL-aspartate	40.0 (1.4)*	NT
2-Amino-2-carboxyethylarsonic acid	32.5 (1.7)*	44.2 (7.6)*
N-Methyl-DL-aspartate	14.5 (4.1)	NT
2-Amino-2-carboxyethylphosphonic acid	13.9 (2.7)	NT
Quisqualate	13.3 (8.1)	NT
L-3,4-Dihydroxyphenylalanine	5.1 (4.2)	NT
Alpha-(methylamino)isobutyrate	3.4 (5.3)	NT
2-Amino-2-carboxypropylarsonic acid	2.7 (1.5)	NT
Alpha-aminoisobutyrate	1.8 (4.6)	NT
DL-2-Amino-5-phosphonovalerate	1.5 (6.6)	NT
CGP40116	1.2 (4.1)	NT
AMPA	0.7 (2.2)	NT
Kainate	0.3 (7.4)	NT
2-Amino-2-carboxypropylphosphonic acid	-2.5 (0.6)	NT
CGP 37849	-2.4 (6.5)	NT

AMPA = DL-Alpha-amino-3-hydroxy-5-methylisoxazole propionate
** P=0.001, * P=0.01.
NT = Not Tested

TABLE 5.6 *Estimated K_i values for a range of competitors of L-aspartate transport.*

COMPETITOR	K_i [μM]
D-Aspartate	72
L-Glutamate	178
D-Glutamate	1720
L-Asparagine	1547
L-Proline	1874
L-Alanine	2544
Threo-ß-hydroxy-DL-aspartate	54
2-Amino-2-carboxyethylphosphonous acid	60
L-Cysteic acid	64
Alpha-methyl-DL-aspartate	793
2-Amino-2-carboxyethylarsonic acid	1101
N-Methyl-DL-aspartate	3116
2-Amino-2-carboxyethylphosphonic acid	3274

TABLE 5.7 *The influence of the permeable-support on P_{app} of acidic amino acids.* L-[^{3}H]aspartate or L-[^{14}C]glutamate (50 μM) alone or in the presence of a 1000-fold molar excess (50 mM) of unlabelled ligand was applied to the Ap surface of 15 d Caco-2 monolayers cultured on aluminium oxide or polycarbonate culture-inserts. Ap-to-Bl fluxes are expressed as apparent permeability coefficients to correct for the different surface area of these two permeable-support types. Data are presented as mean values ± SD for three monolayers

CONCENTRATION [μM]	P_{app} x 10^6 [cm s^{-1}] MEAN (SD)			
	Nitrocellulose		Polycarbonate	
	L-Aspartate	L-Glutamate	L-Aspartate	L-Glutamate
50	12.4 (0.50)	4.75 (0.34)	12.2 (0.80)	5.10 (0.40)
5000	0.20 (0.02)	0.12 (0.05)	0.28 (0.05)	0.12 (0.03)

TABLE 5.8 *The radiochemical purities of ^{14}C]CGP37849, [^{14}C]CGP40116 and [^{14}C]CGP40117.*

COMPOUND	PURITY	P_{app} [cm s^{-1}]
[^{14}C]CGP37849	98.0	3.458±0.221 x 10^{-7}
[^{14}C]CGP40116	99.9	1.247±0.002 x 10^{-7}
[^{14}C]CGP40117	100.1	0.558±0.001 x 10^{-7}

Analysis performed by thin-layer chromatography
(Dr A. Probst, Ciba Pharmaceuticals, Basel, Switzerland).

5.5 DISCUSSION

5.5.1 ACIDIC AMINO ACIDS

Caco-2 monolayers have been proposed as a useful *in vitro* model of the normal human small intestinal epithelium [Hidalgo *et al.*, 1989; Wilson *et al.*, 1990]. Two amino acid transport pathways expressed by Caco-2 cells have been described in detail, however, a major obstacle to evaluating the relevance of these systems is the paucity of comparative data for the normal human small intestine. Whilst the similarity of L-phenylalanine transport in the Caco-2 model and humans is uncertain, the uptake of L-proline by Caco-2 monolayers can at best only partially explain our knowledge of imino acid absorption from the normal human intestine [Nicklin *et al.*, 1992 a]. In comparison with other systems, the uptake of acidic amino acids into human jejunal BBMV is well-characterised [Rajendran *et al.*, 1987 b; Harig *et al.*, 1987]. Furthermore, the intestinal brush-border acidic amino acid carrier has been studied extensively in the chick [Lerner and Steinke, 1977; Wingrove and Kimmich, 1987], rabbit [Berteloot, 1984], rat [Corcelli *et al.*, 1982; Corcelli and Storelli, 1983]. Therefore, a rigourous comparison between acidic amino acid transport in the Caco-2 model and human or laboratory animals is possible.

Gibson and Wiseman [1951] provided the first evidence that the intestinal absorption of acidic amino acids occurs *via* carrier-mediation. They showed that, in the rat small intestine, the rates of luminal disappearance for L-aspartate and L-glutamate were greater than their D-stereoisomers. However, in a later study, using an everted rat intestine preparation, Wiseman was unable to show mucosal-to-serosal transport against a concentration-gradient or accumulation of acidic amino acids within the intestinal mucosa. These observations were attributed to rapid mucosal metabolism of L-aspartate and L-glutamate [Wiseman, 1953]. Indeed, Ramaswamy and Radhakrishnan [1963] have shown that mucosal homogenates from the human and rat small intestine are rich in glutamic-aspartic transaminase and glutamic-alanine transaminase. Low levels of aspartic-alanine transaminase were also present. Furthermore, metabolism of acidic amino acids during mucosal-to-serosal transport across everted sacs from the rat intestine has been reported. One hour after administering L-[^{14}C]aspartate to the mucosal surface only 80% of the radioactivity entering the serosal compartment was present as intact L-aspartate [Ramaswamy and Radhakrishnan 1970]. This rapid metabolism of acidic amino acids in whole tissue preparations has prohibited detailed studies of their transport mechanisms using the early absorption models. The development of intestinal BBMV, which are devoid of cytosolic enzymes, has proved an important milestone in elucidating uptake mechanisms across the brush-border membrane. However, BBMV do not give any information about the rates of basolateral efflux or paracellular transport and therefore provide little information about the overall mechanism of transepithelial transport. Despite this severe limitation, they have been used extensively since, at present, there are no suitable models for studying the transport mechanisms for acidic amino acids across the GI epithelium.

Interestingly, during a 1 h study of D-aspartate uptake into a cell culture model of the porcine proximal tubule epithelium (LLC-PK_1 monolayers), no metabolism was detected [Rabito and Karish, 1983]. Although this observation may reflect the relative metabolic stability of D-aspartate, it also highlights the possibility that cell culture models may be useful in studying acidic amino acid transport without significant interference by metabolism. Indeed, the stability of L-[^{3}H]aspartate towards metabolism and assimilation into protein during transport across Caco-2 monolayers supports this hypothesis (see Fig. 5.2). In light of the degradation of L-aspartate during its transport across everted sacs of rat gut, this metabolic stability during transport across Caco-2 monolayers may appear surprising. Nevertheless, there are several possible explanations. Firstly, during mucosal-to-serosal transport across the everted rat intestine, L-aspartate must traverse multiple cell barriers (including muscle layers) but in the Caco-2 model the transport-barrier is a single layer of epithelial cells. Clearly, there is a greater potential for metabolic-transformation during transport across the whole tissue preparation. Secondly, the human intestinal epithelium may have a lower metabolic capacity for L-aspartate than the rat intestine. Interestingly, the specific transaminase-activity in the human small intestine is considerably lower than that of rats [Ramaswamy and Radhakrishnan, 1963]. A third possibility is that the Caco-2 cell line has a lower metabolic capacity for L-aspartate than normal enterocyte.

On the basis of L-aspartate remaining intact during its passage across Caco-2 monolayers, the transport mechanism of acidic amino acids across this model was investigated. The results from several experiments provided evidence that L-aspartate transport across Caco-2 monolayers was predominantly transcellular and carrier-mediated (>95%). Firstly, a 10-fold reverse concentration-gradient had no effect on the rate of Ap-to-Bl transport. This observation is significant since the early experiments in whole tissue preparations failed to show transport against a concentration-gradient. Secondly, L-aspartate and L-glutamate transport was concentration-dependent and the saturable transport component had an absolute sodium-dependence. Thirdly, the pH-dependence of L-aspartate transport did not reflect the pH-effects on the passive permeability of Caco-2 monolayers or a shift in the ionic speciation of L-aspartate. In addition, L-aspartate transport was vectorial. Moreover, the activation-energy (E_a) for L-aspartate transport across Caco-2 monolayers (101.6±1.0 kJ mol^{-1}) exceeds that anticipated for simple diffusion (<16.8 kJ mol^{-1}) and is within the usual range for carrier-mediated transport processes (29.4 to 105.0 kJ mol^{-1}) [Hidalgo and Borchardt, 1990 a]. Finally, cross-inhibition studies show L-aspartate and L-glutamate transport can be inhibited by a narrow range of closely related structural analogues. The substrate-specificity identified the acidic amino acid transport pathway as being of the generic classification X^-_{AG}, since it was sodium-dependent and served L-aspartate, D-aspartate and L-glutamate but not D-glutamate. Subtle inter-species differences in X^-_{AG} carriers suggest they are a family of closely related, but not identical, transporters. Experiments were designed to compare and contrast the Caco-2 acidic amino acid transporter with that present in the human and laboratory animal small intestine.

The saturable transport component of acidic amino acid transport across Caco-2 monolayers had an absolute sodium-dependence. In the absence of extracellular sodium ions, L-aspartate and L-glutamate fluxes were reduced to passive diffusion levels and transport was proportional to concentration. An absolute sodium-dependence has also been reported for the uptake of acidic amino acids into LLC-PK_1 cells [Rabito and Karish, 1983], cells isolated from chicken small intestine [Wingrove and Kimmich, 1987] and BBMV prepared from human [Rajendran *et al.*, 1987 b; Harig *et al.*, 1987], rabbit [Berteloot, 1984] and rat [Corcelli *et al.*, 1982]. Interestingly, a half-maximal stimulation of L-aspartate transport across Caco-2 monolayers occurred at low extracellular sodium ion concentrations (≈20 mM), whereas maximal stimulation only occurred at sodium ion concentrations exceeding 100 mM. In BBMV, an inward (*ie:* extravesicular > intravesicular) sodium-gradient is required to maximally stimulate uptake. However, in the presence of sodium ions, but the absence of an inward gradient (*ie:* extravesicular = intravesicular) an acceleration and partial overshoot of acidic amino acid uptake is observed in the presence of an outward (*ie:* intravesicular > extravesicular) potassium-gradient [Rajendran *et al.*, 1987 b; Berteloot, 1984]. It was postulated, from the sodium-stimulation in the absence of an inward sodium-gradient, that there is a direct coupling of sodium ion(s) and acidic amino acids in the translocation mechanism [Corcelli *et al.*, 1982]. These observations may explain the marked stimulation of L-aspartate transport across Caco-2 monolayers at low extracellular sodium ion concentrations, where one might anticipate an outward potassium-gradient without an inward sodium-gradient.

Moreover, the transport of L-aspartate across Caco-2 monolayers is cation(sodium)-specific. In the presence of extracellular sodium chloride (140 mM) the rate of L-aspartate transport was at least 6.25-times that in the presence of an equal concentration of the chloride salts of K^+, Rb^+, Cs^+ or choline. A small but significant stimulation of transport by Li^+, above the choline chloride baseline value, suggests this cation can partially substitute for sodium ions. Similarly, in rat intestinal BBMV the initial rate of L-aspartate uptake in the presence of an inward 100 mM cation chloride-gradient is at least 4-times greater in the presence of sodium compared to other cations [Corcelli *et al.*, 1982]. However, the partial stimulation by Li^+ was not observed. Unfortunately, the cation-specificity of acidic amino acid uptake into human jejunal BBMV has not been reported.

Higher extracellular sodium ion concentrations are required to drive L-proline uptake into Caco-2 cells (half-maximal ≈ 50 mM; maximal ≥ 140 mM) [Nicklin *et al.*, 1992 a]. Therefore, an inward sodium-gradient, rather than just the presence of sodium ions, is probably required for the sodium-dependent carrier-mediated uptake of L-proline. This observation may explain the greater ouabain-sensitivity of L-proline uptake by Caco-2 monolayers (82.6±2.8% reduction by 10 µM ouabain) compared to that of L-aspartate (29.1±1.9% reduction by 10 µM ouabain).

To investigate any direct anion-dependence or the possibility of an electrogenic transport, L-aspartate transport experiments were performed using incubation medium containing the sodium salts of anions having a range of permeabilities (thiocyanate > chloride > isethionate). Glucose uptake into human jejunal BBMV is electrogenic and increased by replacing chloride anions in the incubation medium with the more lipophilic thiocyanate [Rajendran *et al.*, 1987 b]. In the same study, L-glutamate uptake into human jejunal BBMV was not anion-sensitive suggesting an electroneutral transport mechanism. Similarly, L-aspartate transport across Caco-2 monolayers is anion-insensitive which is consistent with an electroneutral process. In rat BBMV, acidic amino acid uptake is sensitive to chloride ions. L-aspartate and L-glutamate is reduced (≥60%) by equimolar substitution of a 100 µM inward sodium chloride gradient for a sodium thiocyanate [Corcelli and Storelli, 1983]. This chloride-sensitivity has not been demonstrated in other species.

One of the most striking inter-species, and inter-absorption model, differences in acidic amino acid transport is the number and affinities of sodium-dependent carriers that have been presented in the literature. Using a tissue accumulation method in isolated segments of chick intestine, Lerner and Steinke [1977] described a single high-affinity (K_m = 4-8 μM) sodium-dependent L-glutamate uptake mechanism. Meanwhile, Wingrove and Kimmich [1987] using isolated intestinal epithelial cells from the same species have reported both high- (K_m = 16 μM) and low- (K_m = 2.7 mM) affinity sodium-dependent uptake pathways for L-aspartate. A single high affinity (K_m = 30 μM) and sodium-dependent uptake system is expressed in the LLC-PK_1 cell line. In BBMV prepared from the rat intestine, Corcelli and co-workers [1982] have reported a single sodium-dependent carrier with K_m values of 1.0 mM and 1.5 mM for L-aspartate and L-glutamate, respectively. A single high-affinity (K_m = 91 μM) carrier (see Fig. 5.8 C and D) has been reported in human jejunal BBMV [Rajendran *et al.*, 1987 b]. Similarly, kinetic analysis of the sodium-dependent transport of acidic amino acids across Caco-2 cells suggests that at pH7.4 it is controlled by a single high-affinity carrier. The affinity constant for L-glutamate transport across Caco-2 monolayers was 65.0±6.3 μM which is comparable to that for uptake into human jejunal BBMV. L-Aspartate had a higher affinity (K_m = 55.8±3.3 μM) for the Caco-2 acidic amino acid-transporter. This higher affinity for L-aspartate transport is reflected in the cross-inhibition studies. A 20-fold molar excess of unlabelled L-aspartate inhibited 50 μM L-[^{3}H]aspartate transport by 92.1±2.0 whereas L-glutamate resulted in only a 74.8±0.4 % inhibition.

A bell-shaped pH-dependence between the uptake of 50 μM L-glutamate into both human [Harig *et al.*, 1987] and rabbit [Berteloot, 1984] jejunal BBMV has been reported. Optimum pH conditions were slightly acidic (pH6.5) and non-acidic (pH7.0 to 7.5) for the human and rabbit BBMV, respectively. The pH-dependence cannot be explained by a shift in the ionic speciation of L-glutamate and probably represents a titration of the transporter rather than the substrate. The pH-profile for the Ap-to-Bl transport of L-aspartate across Caco-2 monolayers has a skewed bell-shape (maximum = pH6.5). This pH-dependence is strikingly similar to that for L-glutamate uptake into human jejunal BBMV [Harig *et al.*, 1987] and provides support for the conclusion that Caco-2 monolayers are a suitable tool for studying the human X^-_{AG} transporter. Recently, a pH-dependent heterogeneity in acidic amino acid uptake into rabbit jejunal BBMV has been reported [Maenz *et al.*, 1992]. At pH8.0 both D-aspartate and L-glutamate are served by a single high affinity system (K_m = 30 μM). However, under acidic conditions (pH6.0) D-aspartate was transported by the high affinity system alone whereas L-glutamate transport was mediated by both a high and low (K_m = 25 mM). This affinity-shift in the uptake pathway at pH6.0 was accompanied by a change in the cross-inhibition profile. This interesting observation pH-dependent heterogeneity of acidic amino acid transport has yet to be confirmed in other species and models.

Acidic amino acids are transported across Caco-2 monolayers by an X^-_{AG} carrier, that is, it is sodium-dependent and serves L-asparate and L-glutamate equally. Potent inhibition of X^-_{AG} carriers by L-aspartate, L-glutamate and D-aspartate, but not D-glutamate has been reported previously in the human [Rajendran *et al.*, 1987 b], rabbit [Maenz *et al.*, 1992] and rat [Corcelli *et al.*, 1982] intestinal BBMV, LLC-PK_1 [Rabito and Karish, 1983] and H35 (Hepatoma) [Christensen and Makowske, 1983] cell lines, cultured rat hepatocyte and skin fibroblasts [Gazzola *et al.*, 1981]. Gazzola *et al.* [1981] have shown that radiolabelled cysteate uptake into cultured rat hepatocytes was strongly inhibited by L-aspartate, L-glutamate, D-aspartate and 3-aminoglutarate but not D-glutamate. Inhibition by 3-aminoglutarate indicates that the amino group does not have to be at the alpha-position to the carboxylate functionality for recognition. Consequently, it was postulated that the anomalous stereo-selectivity of the X^-_{AG} carriers results from the ability of L-aspartate, but not D-glutamate to bind backwards, with respect to their L-stereoisomers, in the carrier recognition site [Gazzola *et al.*, 1981; Christensen and Makowske, 1983]. That is, the alpha- and beta-carboxylate groups of aspartate can bind in alpha, beta (L-aspartate) and beta, alpha (D-aspartate) orientations and the alpha- and gamma-carboxylate groups of glutamate bind in alpha, gamma (L-glutamate) but rarely in gamma, alpha (D-glutamate) orientations. A refinement to this reverse-binding hypothesis is proposed and shown schematically in Fig. 5.16. It is proposed that the acidic amino acid carrier has four recognition domains, two positive centres and two negative centres. For substrate recognition, at least three of the four sites need to be satisfied. This model accounts for the recognition of L-aspartate (Fig. 5.16 A), D-aspartate (Fig. 5.16 B), L-glutamate (Fig. 5.16 C) and 3-amino-glutarate (Fig. 5.16 E). D-glutamate (Fig. 5.16 D) only satisfies two recognition domains, therefore, would not be a good substrate. The model predicts that $H_2OC(NH_2)CHCH(NH_2)CO_2H$ would be a potent inhibitor of acidic amino acid transport (see Fig. 5.16 F), however, this awaits experimental verification.

FIGURE 5.16 *Proposed recognition of acidic amino acids by the X^{-}_{AG} carrier.*

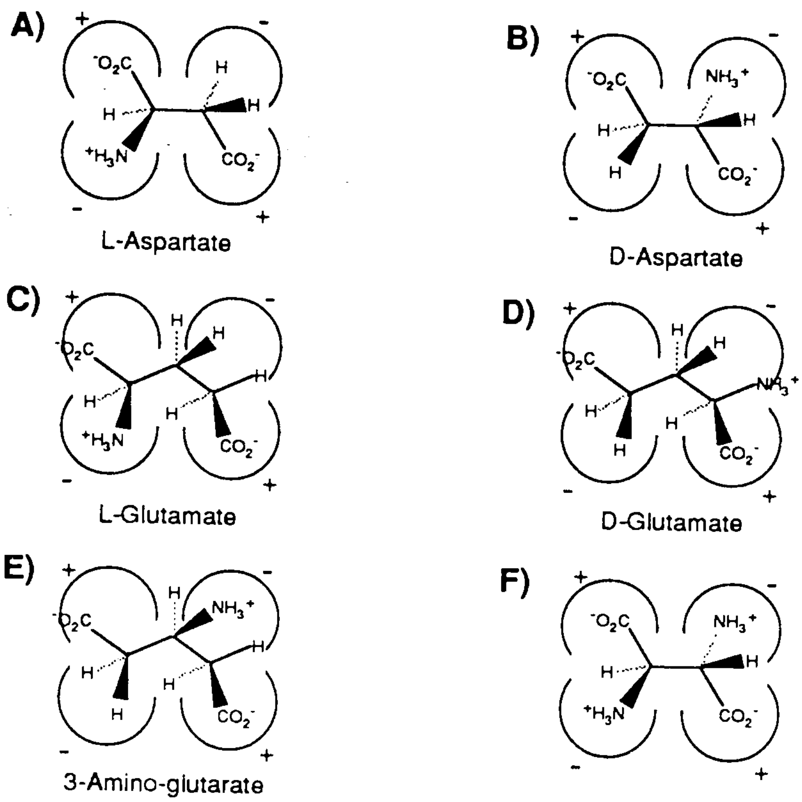

To probe the structural requirements of the Caco-2 acidic amino acid carrier, the transport of radiolabelled L-aspartate or L-glutamate was competed with a 20-fold molar excess of unlabelled amino acids, organic anions, stereoisomers or synthetic analogues. The carrier displayed an exacting substrate-specificity with only very close analogues of L-aspartate and L-glutamate being potent transport-inhibitors. The inability of 4,4'-Diisothiocyanatostilbene-2,2'-disulphonate and *p*-aminohippurate to reduce L-aspartate transport suggest it is not transported *via* a general organic anion-transporter. Moreover, the failure of succinate ($^{-}O_2CCH_2CH_2C_2O^{-}$) to inhibit L-aspartate transport suggests that an amino functionality is required for recognition. L-Alanine, L-asparagine and L-proline were weak inhibitors of L-aspartate transport across Caco-2 monolayers. Unfortunately, cross-inhibition studies for L-glutamate uptake into human jejunal BBMV did not extend to small neutral amino acids for comparison. However, partial inhibition of acidic amino acid transport by L-alanine, L-leucine and L-proline has been reported in cells isolated from the chick intestine [Wingrove and Kimmich, 1987]. Whilst cross-inhibition studies are a useful exercise, they cannot discriminate between a carrier-substrate and non-transported inhibitor. Therefore, if a compound inhibits L-aspartate transport it does not follow that it is transported *via* the L-aspartate transporter. For instance, it is known from previous studies that the sodium-dependent L-proline uptake by Caco-2 monolayers is not inhibited by L-aspartate. Furthermore, the L-proline uptake mechanism has a very different cross-inhibition profile [Nicklin *et al.*, 1992 a] to that for L-aspartate transport. Therefore, although L-proline inhibits L-aspartate transport, L-proline itself is not transported *via* the acidic amino acid carrier. One possible explanation is that small neutral amino (and imino) acids may reversibly dock into the recognition site of the acidic amino acid carrier without activating the transport process, thereby reducing the probability of L-aspartate transport (*ie:* L-proline acts as a partial competitive antagonist of L-aspartate transport). Large neutral amino acids may be sterically excluded from the recognition site and therefore are not able to competitively antagonise L-aspartate transport.

Despite the exquisite substrate specificity, some side-chain modifications are permitted without the loss of inhibition-potency. Firstly, insertion of a hydroxyl-group in the *threo* configuration at the beta-carbon (*threo*-beta-hydroxy-DL-aspartate) does not reduce inhibition-potency. Secondly, substitution of the beta-carboxylate group for the mono-anionic sulphono (L-cysteic acid; MWt = 169) or phosphino (2-amino-2-carboxyethylphosphonous acid; MWt = 154) functionalities maintained inhibition-potency. This suggests that the recognition site for the beta-carbon anionic-functionality has a degree of geometric tolerance since it accepts the planar carboxylate and tetrahedral sulphonate or phosphinate groups. The K_i values for *threo*-beta-hydroxy-DL-aspartate, L-cysteic acid and 2-Amino-2-carboxyethylphosphonous acid were comparable to the K_m^{sd} values for L-aspartate transport suggesting that they are nearly as good substrates as the natural ligand (Table 5.6). In contrast, a similar substitution with a phosphono (2-amino-3-phosphonopropionic acid; MWt = 169) functionality abolished inhibition. The pKa values of the phosphono group are approximately, 1.83 and 7.43. Since transport experiments were performed at pH7.4, approximately 50% of 2-amino-3-phosphonopropionic acid exists as the di-anionic form. This suggests that a single negative charge on the side chain is optimum and a double negative charge markedly reduces the inhibition-potency of a competing ligand. Interestingly, the mono-anionic 2-amino-2-carboxyethylarsonic acid (MWt = 215) was a partial inhibitor whereas 2-amino-2-carboxypropylarsonic acid (MWt = 228) failed to inhibit L-aspartate or L-glutamate transport. These two competitors have high molecular weights but the extra methylene group in the side-chain of 2-amino-2-carboxypropylarsonic acid must prevent it inhibiting the acidic amino acid carrier. It is noteworthy that 2-Amino-2-carboxyethylphosphonous acid and 2-Amino-2-carboxyethylarsonic acid are novel inhibitors of acidic amino acid transporters.

Finally, modification of the functional groups about the chiral alpha-carbon reduced inhibition-potency. Methylation of the alpha-carbon (alpha-methyl-DL-aspartate) halved inhibition-potency. This may be due to the steric bulk of the methyl group reducing its affinity for the recognition-site. Alternatively, alpha-methyl-DL-aspartate is a racemic mixture and insertion of the methyl group may impart stereo-selection such that one stereoisomer is still a potent inhibitor and the other inactive. This later possibility would halve the inhibition potency for a given concentration of the racemate. N-Methylation (N-methyl-DL-aspartate) abolishes inhibition-potency. Therefore, replacement of an amino hydrogen with a methyl group sterically restricts docking to the amino group recognition-site.

The X^-_{AG} carrier described here is distinct from the other amino acid carriers characterised in the Caco-2 cell line. Firstly, the transport K_m values for L-aspartate (K_m = 55.8±3.3 μM) and L-glutamate (K_m = 65.0±6.3 μM) are 5-fold lower than that for L-glutamine (K_m = 276 μM) [Souba *et al.*, 1992], one order of magnitude lower than for L-phenylalanine (K_m = 560 μM) by the LNAA transporter [Hidalgo and Borchardt, 1990 a] and two orders of magnitude greater than the uptake K_m for L-proline uptake (K_m = 5480 μM) *via* the A-system [Nicklin *et al.*, 1992 a]. Secondly, the acidic amino acid transport pathway has a different cross-inhibition profile to the LNAA and A-system pathways. Acidic amino acid transport is only strongly inhibited by close analogues of L-aspartate and L-glutamate. Small neutral (and imino) acids partially inhibited L-aspartate transport whereas large neutral amino acids failed to inhibit transport. L-aspartate failed to interfere with L-proline uptake [Nicklin *et al.*, 1992 a] or L-phenylalanine transport [Hidalgo and Borchardt, 1990 a] across Caco-2 monolayers. Finally, whilst acidic amino acid transport across Caco-2 monolayers has an absolute sodium-dependence, L-phenylalanine is at best only partially (≈33%) sodium-dependent [Hidalgo and Borchardt, 1990 a].

Whilst the relevance of the L-phenylalanine and L-proline transport pathways to amino acid absorption from the human GI tract is uncertain, there is a good correlation between our knowledge of intestinal acidic amino acid uptake and their transport across Caco-2 monolayers. Moreover, the characteristics of the Caco-2 acidic amino acid transporter more closely resemble those of the human compared to laboratory animals. These studies suggest that Caco-2 monolayers represent a useful experimental tool for studying the transport of acidic amino acids across the human GI epithelium.

5.5.2 CGP37849, CGP40116 AND CGP40117

The oral bioavailability of CGP37849 is low (≈15% and 30% in rats and dogs, respectively). Interestingly, after oral administration of CGP37849 only CGP40116 reaches the systemic circulation (Dr Ian Hassan, Ciba Pharmaceuticals; personal communication). The Caco-2 monolayer model was employed to characterise the epithelial transport properties of CGP37849, CGP40116 and CGP40117. The possibility of stereo-selective absorption *via* an acidic amino acid pathway was considered.

The experimental results provide no evidence for the carrier-mediated transport of CGP37849, CGP40116 or CGP40117 across Caco-2 monolayers. Firstly, a 20-fold molar excess of unlabelled CGP37849 and CGP40116 failed to inhibit L-[^{14}C]aspartate transport across Caco-2 monolayers suggesting that these molecules are not substrates for the X^{-}_{AG} carrier. Nevertheless, from these cross-inhibition studies, one cannot exclude the possibility that these compounds are transported *via* another carrier-mediated pathway. The Ap-to-Bl transport of CGP40116 and CGP40117 were non-saturable at pH7.4. Despite a non-saturable transport mechanism, the apparent permeability coefficients for CGP40116 and CGP40117 were temperature-dependent. However, temperature-dependent flux of passively transported molecules (*eg:* D-mannitol) across Caco-2 monolayers has been reported previously [Cogburn *et al.*, 1991]. Furthermore, the TER of Caco-2 monolayers is temperature-dependent indicating that the transport capacity of the paracellular pathway is reduced at temperatures below 37°C [Fig. 5.14 B]. Therefore, temperature-dependence alone is not an indicator of carrier-mediated transport. Nevertheless, once it has been established that the passage of a compound occurs predominantly by carrier-mediation, the transport activation-energy can be a useful characteristic of the carrier.

The transport of CGP40116 is non-vectorial (indicating a passive transport mechanism) and the rates for Ap-to-Bl and Bl-to-Ap CGP40116 transport and Ap-to-Bl CGP40117 transport were indistinguishable. However, the rate of CGP40117 transport in the Bl-to-Ap direction was greater than in the Ap-to-Bl direction. These data highlight the possibility of a selective retardation of CGP40117 transport in the Ap-to-Bl direction although the mechanism for such an effect is not clear.

The P_{app} for [^{14}C]CGP37849 (1.15×10^{-7} cm s^{-1}) predicts an oral bioavailability of up to 70% in humans according to the correlation described by Artursson and Karlsson (see Fig. 1.5) [Artursson and Karlsson, 1991]. This predicted value in humans exceeds the observed bioavailabilities in rats (≈15%) and dogs (≈30%). However, for molecules with a low P_{app}, (*ie:* $\leq 1.0 \times 10^{-7}$ cm s^{-1}), efficient transport of even minor radiochemical impurities may artificially increase the measured apparent permeability coefficient of the parent radiochemical. Therefore, the 1.8% undefined [^{14}C]-impurities may have falsely increased the P_{app} of [^{14}C]CGP37849 and consequently the predicted oral bioavailability of CGP37849 would be overestimated. The apparent permeability coefficients for CGP40116 and CGP40117 were lower ($<5.0 \times 10^{-8}$ cm s^{-1}) and predict an oral bioavailability between 15 and 30% in humans. By virtue of their superior radiochemical purities, compared to [^{14}C]CGP37849, this value must be considered more reliable. Indeed, the data for these compounds agree more closely with the *in vivo* data from the animal absorption models and suggest that these molecules would have low oral bioavailabilities. The P_{app} for [^{14}C]CGP40116 transport across Caco-2 monolayers is greater than that for [^{14}C]CGP40117, predicting a greater oral bioavailability for CGP40116. It is tempting to speculate that this observation explains the stereo-selective absorption of CGP40116 following the oral administration of CGP37849 in whole animal studies. However, the *in vivo* data suggests that systemic bioavailability is exclusive to, rather than preferentially for, CGP40116. Therefore, the possibility of selective hepatic extraction for first-pass metabolism of CGP40117 cannot be eliminated from these studies. For this reason, the possibility of stereo-selective first pass hepatic elimination for these stereoisomers should be considered.

5.6 CONCLUSION

To summarise, CGP40116 and CGP40117 are not transported across Caco-2 monolayers by an acidic amino acid carrier. Since the properties of the X^-_{AG} carriers expressed by Caco-2 cells and the human jejunum are very similar, these NMDA-antagonists are unlikely to experience carrier-mediated absorption in man. Because of the exacting substrate specificity of the acidic amino acid carrier, this observation is not surprising. However, it is hoped that the information generated during these studies may highlight some opportunities for designing NMDA-antagonists with good oral bioavailabilities. In particular, cross-inhibition studies suggest that the phosphono side-chain on CGP40116 and CGP40117 would preclude these molecules from the acidic amino acid absorption pathway. Since 2-amino-2-carboxyethylphosphonous acid is a potent inhibitor of L-aspartate transport, one possibility is to design analogues of aspartate and glutamate with phosphino side-chain functionality. Clearly, the design of acidic amino acid analogues with good oral bioavailabilities which retains potent NMDA-antagonistic activity remains an exciting challenge.

CHAPTER SIX

PEPTIDE TRANSPORT ACROSS CACO-2 MONOLAYERS

ABSTRACT

The transport of thyrotrophin-releasing hormone, SQ29852 and cyclosporin A across Caco-2 monolayers has been studied.

TRH transport across Caco-2 monolayers was characterised by a minor saturable (carrier-mediated, approximately 25%) pathway superimposed onto a major non-saturable (diffusional) pathway. Transport was selectively inhibited by small peptides and cephalexin suggesting a peptide-transporter may be responsible for the minor saturable pathway.

SQ29852 uptake into Caco-2 monolayers is described by a major saturable-mechanism (K_m = 0.91 mM) superimposed onto a minor passive component. However, the initial-rate transport of SQ29852 is consistent with a passive transepithelial transport mechanism. Therefore, these data highlight the possibility that its basolateral efflux is severely retarded such that the passive paracellular transport dictates the overall transepithelial transport characteristics.

A model suitable for investigating the transepithelial transport of cyclosporin A has been developed.

6.1 BACKGROUND

The active transport of peptides in the small intestine was first demonstrated by Addison in 1972 [Addison *et al.*, 1972]. An excellent review of the history and current knowledge of peptide-transport has recently been provided by Matthews [Matthews, 1991]. The intestinal peptide-transporter serves di- and tripeptides but excludes tetrapeptides and above. The transporter is stereoselective, preferring L-amino acid or glycine compared to D-amino acid residues. Substitution of peptides at their amino (*eg:* methylation, acetylation) or carboxy (*eg:* amidation, esterification) termini reduces their affinity for the peptide-transporter. Meanwhile, methylation at the nitrogen of the peptide bond(s) does not significantly interfere with carrier affinity. It is now accepted that the energy required to drive the active transport of peptides into enterocytes is generated from an inward proton gradient [Matthews, 1991]. However, peptide transport in the absence of a proton-gradient has been reported [Rajendran *et al.*, 1987 a].

The current knowledge of peptide uptake and transport by Caco-2 monolayers is summarised in Chapter One (see section 1.5.4).

6.1.1 THYROTROPHIN-RELEASING HORMONE

The oral administration of thyrotrophin-releasing hormone (L-pyroglutamyl-L-histidyl-L-proline amide, TRH; Fig. 6.1) to humans [Haigler *et al.*, 1972] elicits a release of thyroid stimulating hormone. These observations suggest that physiologically relevant quantities of TRH can be absorbed from the GI tract. Indeed, oral bioavailabilities of 12.6, 2.0 and 1.5% have been recorded in dogs, humans and rats, respectively [Yokohama *et al.*, 1984 a].

TRH is hydrophilic and has structural features which usually mitigate against recognition and transport by the small peptide-transporter (*ie:* it is substituted at amino and carboxy termini), therefore, it was postulated that absorption probably occurs by non-mediated transport *via* the paracellular route [Matthews and Payne, 1980]. Subsequently, TRH has been shown to be a substrate for the intestinal small peptide-transporter [Yokohama *et al.*, 1984 a ; Yokohama *et al.*, 1984 b]. Region-specific TRH absorption has been demonstrated in the rat intestine using *in situ* (ligated loop) and *in vitro* (everted sac) models [Yokohama *et al.*, 1984 b]. The transport rate was greatest in the upper small intestine where it was vectorial (mucosal-to-serosal > serosal-to-mucosal) and dose-dependent. Furthermore, transport is markedly reduced by the co-administration of an oligopeptide mixture and by some ß-lactam antibiotics, but not by an amino acid mixture. Similarly, in beagle dogs, the oral bioavailability is dose-dependent and reduced by food ingestion [Yokohama *et al.*, 1984 a]. These observations are consistent with TRH absorption being mediated *via* a small peptide-transporter.

The uptake and transport of TRH by Caco-2 monolayers was investigated to probe the possibility of a carrier-mediated mechanism.

6.1.2 ANGIOTENSIN CONVERTING ENZYME INHIBITORS

Angiotensin-converting enzyme (ACE) is responsible for converting angiotensin I to angiotensin II which is a potent vasoconstrictor and stimulator of aldosterone secretion. ACE inhibitors lower blood pressure by reducing the peripheral vascular resistance and by reducing aldosterone-mediated sodium-reabsorption. They are clinically useful in the management of hypertension and congestive heart failure.

The ACE inhibitor captopril has an oral bioavailability of 60 to 75% in man [Kubo and Cody, 1985]. Moreover, its bioavailability in humans [Duchin *et al.*, 1982] is dose-independent suggesting a passive uptake mechanism. However, captopril absorption is reduced 35% in the presence of food [Singhvi *et al.*, 1982]. This later observation prompted a detailed investigation of the absorption mechanism(s) of captopril. Using an *in situ* rat intestine luminal perfusion technique, Hu and Amidon have shown that rate of luminal disappearance for captopril is concentration-, energy-, pH- (optimum = pH7.0) and sodium-dependent [Hu and Amidon, 1988]. Furthermore, captopril absorption is inhibited by a range of dipeptides and the ß-lactam antibiotic, cephradine [Hu and Amidon, 1988]. These observations are consistent with a carrier-mediated absorption pathway (*via* the small peptide-transporter) for captopril from the GI tract. It was postulated that the products of dietary protein digestion could compete with captopril for the small peptide-transport pathway and thereby reduce its bioavailability [Hu and Amidon, 1988]. This would explain the reduced absorption after food. Subsequently, using the same model, Amidon and co-workers have demonstrated uptake pathways for several ACE inhibitors. Enalapril, an orally active (60-70% [Kubo and Cody 1985]) ACE inhibitor has a saturable (K_m = 0.07 mM) uptake component which is inhibited by L-tyrosyl-glycine (L-tyr-gly) and cephradine, but not by amino acids [Friedman and Amidon, 1989 a]. In the same study, the uptake of a heavily substituted ACE inhibitor, fosinopril, was shown to occur *via* a non-saturable (passive) mechanism. Finally, two ACE inhibitors of the lysyl-proline class, Lisinopril and SQ29852, undergo carrier-mediated absorption from the rat intestine [Friedman and Amidon, 1989 b].

SQ29852 ((S)-1-(6-amino-2-([hydroxy(4-phenylbutyl)-phosphinyl]oxy)-1-oxohexyl)-L-proline) is an ACE inhibitor currently under development by Bristol-Myers Squibb, USA. It is a potent inhibitor *in vitro* (IC_{50} = 36 nM) and *in vivo* following intravenous (ED_{50} = 0.063 µmol kg^{-1}) or per oral (ED_{50} = 0.53 µmol kg^{-1}) administration to rats [Karanewsky *et al.*, 1988]. After oral administration of SQ29852 to human volunteers, its plasma appearance occurs slowly ($t_{max} \approx 4$ h) and is dose-dependent [Moore *et al.*, 1988]. Moreover, its luminal disappearance from the *in situ* rat intestine has passive and carrier-mediated (K_m = 0.08 mM) components. Its disappearance is also inhibited by the dipeptide L-tyrosyl-glycine and the ß-lactam antibiotic, cephradine, but not amino acids [Friedman and Amidon, 1989 b]. This observation was corroborated using intestinal rings prepared from the rat intestine [Stewart *et al.*, 1990]. It has been hypothesised that a carrier-mediated uptake mechanism probably accounts for the non-linear absorption kinetics in humans [Friedman and Amidon, 1989 b], however, a direct interaction between SQ29852 and the human peptide-transporter has not been established.

The present study was designed to investigate the possibility of carrier-mediated SQ29852 uptake into monolayers of human intestinal absorptive (Caco-2) cells and the importance of this mechanism in its transepithelial transport.

6.1.3 CYCLOSPORIN

Cyclosporin A (CsA) is a cyclic undecapeptide isolated from the fungus *Tolypocladium inflatum Gams*. It is a potent immunosuppressive agent used clinically to prevent graft rejection following organ transplantation. The clinical usefulness of CsA has been promoted by the development of an orally active formulation. Although CsA has a low oral bioavailability of 30% in humans [Beveridge *et al.*, 1981; Frey *et al.*, 1988; Ptachcinski *et al.*, 1986], compared to other peptide drugs, the extent of absorption is high. This has prompted considerable interest in the mechanism of CsA absorption and the factors affecting its oral bioavailability.

Despite numerous studies the mechanism of CsA absorption from the GI tract is not certain. The highly lipophilic nature (octanol-water distribution coefficient of approximately 1000) of CsA and its molecular mass of 1201 suggests that transcellular lipid diffusion would be the most likely absorption mechanism. However, several experimental observations provide indirect evidence against a passive transport mechanism. Firstly, using an *in vivo* rat model Cefalu and Pardridge

[1985] showed that CsA traverses the blood brain barrier very slowly. This observation is contrary to the anticipated result if passive lipid partitioning is the GI absorption mechanism. Secondly, CsA is predominantly absorbed from the small intestine in humans [Drewe *et al.*, 1992 a]. Finally, the appearance of CsA in the blood of healthy volunteers following oral administration is described by zero-order (absorption rate independent of dose) model [Grevel *et al.*, 1986]. A passive absorption process would classically follow first-order kinetics (absorption proportional to dose). The zero-order systemic appearance is consistent with a carrier-mediated absorption mechanism operating under saturation conditions. A second possibility is that the release of CsA from its non-aqueous, self-emulsifying, formulation is the rate-limiting step for absorption and occurs in a zero-order fashion. Alternatively, the very limited aqueous solubility of CsA may retard release of CsA from the large drug reservoir in the formulation and produce pseudo-zero order absorption kinetics. Interestingly, CsA uptake into monolayers of LLC-PK_1 cells (porcine kidney proximal tubule cell line) is saturable (K_m = 17.1 μM) and is inhibited by Cyclosporin C and D and by verapamil but not metabolic inhibitors. Moreover, cyclosporin uptake and efflux are strongly temperature-dependent [Takayama, *et al.*, 1991]. Although this work does not refer to intestinal absorptive cells it may be the first direct evidence for carrier-mediated cellular uptake of cyclosporin A. However, the very limited aqueous solubility of CsA dictates that extreme caution must be employed when interpreting uptake data and further experiments are required to verify this observation.

The absorption of CsA from the GI tract is further complicated by the effect of a range of physiological and pharmaceutical factors. CsA absorption is influenced by bile [Mehta *et al.*, 1988], co-administration of drugs [Wadhwa *et al.*, 1987], food [Ptachcinski *et al.*, 1985], and formulation [Johnston *et al.*, 1986] resulting in high inter- and intra-subject variability [Lindholm *et al.*, 1988]. Recent reports have suggested that CsA metabolism occurs within human and rat small intestinal enterocytes [Kolars *et al.*, 1992]. In rat enterocyte microsomes, the cytochrome P450IIIA system was responsible for this metabolism. It was proposed that this observation may partly explain the the low oral bioavailability of CsA. In addition, this may explain some of the drug interactions that alter the oral bioavailability of CsA. For instance, the bioavailability of CsA is increased by the co-oral administration of a known inhibitor of P450IIIA, erythromycin [Gupta *et al.*, 1988].

The debate over a carrier-mediated versus a passive absorption pathway for CsA and the mechanism by which many of the above factors influence CsA bioavailability remain unresolved. This partly stems from the lack of an *in vitro* model which is suitable for mechanistic studies. The objective of this work was to optimise the Caco-2 monolayer model for a detailed CsA transport experiments.

FIGURE 6.1 *Structures of thyrotrophin-releasing hormone (A), SQ29852 (B) and cyclosporin A (C).*

A) Thyrotrophin-releasing hormone

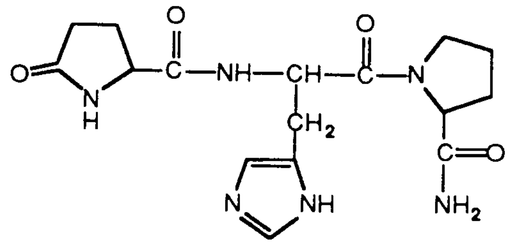

B) SQ29852

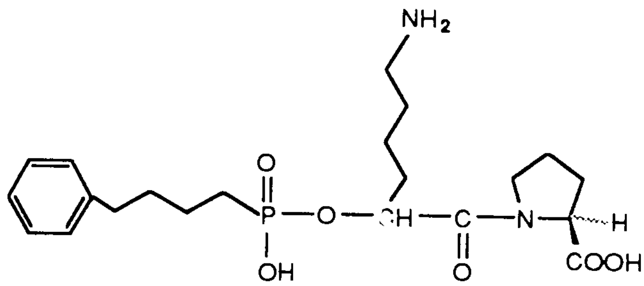

C) Cyclosporin A

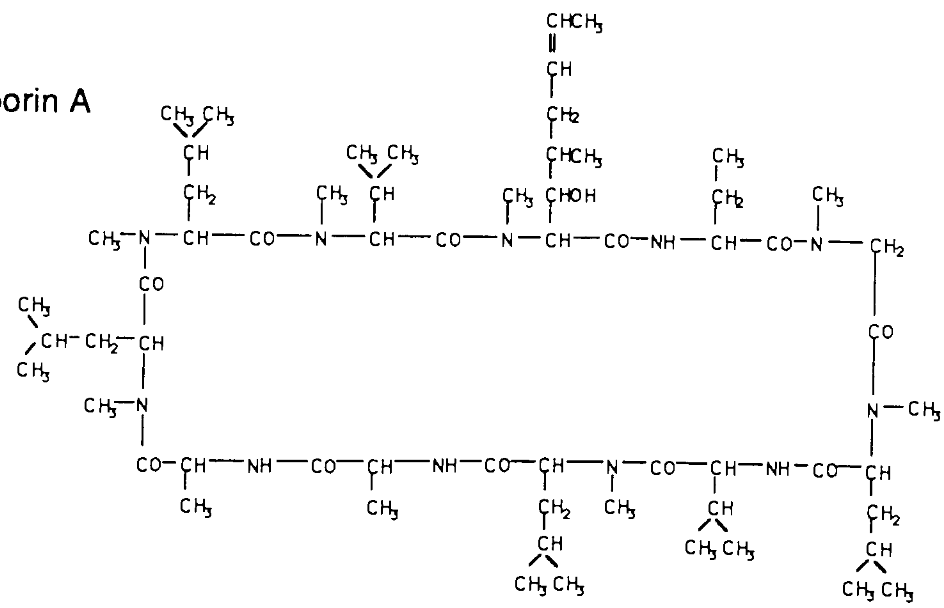

6.2 MATERIALS

[^{3}H]TRH (119.2 Ci mmol^{-1}), D-[^{14}C]mannitol (49.3 Ci mol^{-1}) and [^{3}H]testosterone (80 Ci mol^{-1}) were purchased from New England Nuclear (Dupont, Germany). TRH was obtained from Aldrich Chemical Company (Gillingham, UK). SQ29852 and cephradine were supplied by Dr. P. Timmins (Bristol-Myers Squibb, UK). SQ29852 and the SQ29852 radioimmunoassay (RIA) kit were provided by Bristol-Myers Squibb, USA. [^{3}H]CsA (10 Ci mmol^{-1}) was purchased from Amersham UK. Dimethyldichlorosilane solution (2% in 1,1,1-trichloroethane) was obtained from Fisons, UK. Powdered milk substitute (Marvel™, Cadbury's, Bournville, UK) and semi-skimmed UHT cows milk were purchased from a general retail store. Human blood was collected into lithium heparinised serological tubes 15 min prior to use and maintained at 37°C throughout.

6.3 METHODS

6.3.1 THYROTROPHIN-RELEASING HORMONE

6.3.1.1 *UPTAKE EXPERIMENTS*

For uptake experiments, Caco-2 monolayers were cultured for 6 to 18 d as described previously (see section 2.2.3). Monolayers were initially washed (2 x 5 ml x 5 min) with PBS and finally (1 x 2 ml x 15 min) with M4 pH6.0 before 100 μM [^{3}H]-TRH (0.25 μCi ml^{-1}) M4 pH6.0 was applied to their surface. After a 30 min incubation at 37°C, the donor solution was collected and the monolayers carefully rinsed (3 x 5 ml x 5 min) with ice-cold PBS-sodium azide stop-solution. The monolayers were solubilised by shaking (Luckman Recipro-shake) with 0.1% v/v TX100 in double-distilled water for 60 min at 25°C. The cell-associated radioactivity was corrected for the radiochemical concentration applied to each monolayer and was normalised to the anticipated DPM (*ie:* 0.25 μCi ml^{-1} = 5.5 x 10^5 DPM ml^{-1}). This correction cancelled fluctuations in cell-associated radioactivities resulting from minor variations in the radiochemical concentrations applied to each monolayer. Uptake experiments were performed from donor-solutions containing 100 μM TRH alone (control) and in the presence of an excess of unlabelled competitor.

6.3.1.2 *TRANSPORT EXPERIMENTS*

TRH transport studies were performed using Caco-2 monolayers cultured for 21 d on nitrocellulose permeable-supports (see section 2.3.4). Briefly, 21 d Caco-2 monolayers were washed (1 x (2ml Ap M4(pH6.0) + 2ml Bl M4(pH7.4)) x 15 min) before TRH donor-solution (0.5 μCi ml^{-1} in M4 pH6.0) was applied to the Ap surface. Ap(pH6.0)-to-Bl(pH7.4) transport was determined at 15 min intervals for kinetic studies or after a fixed 1 h time-point. After the final receiver-sample had been collected, monolayers were transferred to a cold-table (0-4°C) and the Ap donor-solutions were collected and their radiochemical concentration determined. The radiochemical flux into the receiver-solution for each time interval was corrected for the radiochemical concentration in the Ap donor-solution and was normalised to the anticipated DPM (*ie:* 0.5 μCi ml^{-1} = 1.1 x 10^6 DPM ml^{-1}) as described for uptake studies (section 2.3.2).

6.3.1.3 HPLC ANALYSIS

Samples were analysed for [^{3}H]TRH by reversed-phase high-performance liquid chromatography. Briefly, donor solutions were collected and pooled (total = 4.5 ml) following a 60 min incubation at 37°C, on the Ap surface of 21 d Caco-2 monolayers. Proteins in the donor solutions were precipitated with 40% w/v TCA (100 μl) and pelleted by centrifugation at 11,600 x g (MSE minifuge). The supernatant was collected and freeze dried. The sample was reconstituted with 500 μl of double distilled water and 20 μl was injected onto a μ-Bondopak C_{18} column (250 mm x 4.6 mm; Waters, UK) and eluted with a mobile phase comprising 80% 0.01 M potassium phosphate buffer (pH 7.5), containing 0.1% diethylamine, and 20% methanol at a flow rate of 1.5 ml min^{-1}. Eluant fractions were collected at 20 s intervals (Gilson, model 204) and assayed for [^{3}H]-content by liquid scintillation counting (see section 2.4.1 A). A reference sample was prepared by incubating dono. solutions for 60 min at 37°C in the absence of Caco-2 cells and processing it as described above.

6.3.2 SQ29852

6.3.2.1 *UPTAKE EXPERIMENTS*

SQ29852 uptake experiments were performed using Caco-2 monolayers cultured on impermeable plastic supports (see section 2.2.3). Briefly, 18 d Caco-2 monolayers were initially washed (2 x 5 ml x 5 min) with PBS and finally (1 x 2 ml x 15 min) with M4 pH6.0 before the SQ29852 in M4 pH6.0 was applied to their surface. After a 15 min incubation at 37°C, the donor solution was aspirated and the monolayers carefully rinsed (3 x 5 ml x 5 min) with ice-cold PBS-sodium azide stop-solution. Each Caco-2 monolayer was solubilised by shaking (2 min) with 1 ml of 0.1% v/v TX100 in double distilled water followed by 10 μl of 4.0 M sodium hydroxide. The solubilised monolayers were neutralised by 10 μl of 4.0 M hydrochloric acid. The SQ29852 concentration in the solubilised Caco-2 monolayers was determined by radioimmunoassay, as described in section 6.3.2.3.

6.3.2.2 *TRANSPORT EXPERIMENTS*

SQ29852 transport studies were performed using Caco-2 monolayers cultured for 21 d on nitrocellulose permeable-supports (see section 2.3.4). Briefly, 21 d Caco-2 monolayers were washed (1 x (2ml Ap M4 pH6.0 + 2ml Bl M4 pH7.4) x 15 min) before SQ29852 in M4 pH6.0 was applied to the Ap surface. Ap(pH6.0)-to-Bl(pH7.4) transport was determined at 30 min intervals for kinetic studies or after a fixed 1 h time-point. SQ29852 concentration was determined in the receiver-solution by radioimmunoassay, as described in section 6.3.2.3.

6.3.2.3 *SQ29852 RADIOIMMUNOASSAY*

SQ29852 was quantified by radioimmunoassay. The standard protocols for SQ29852 determination in human plasma or urine were modified slightly to reflect the assay-media used in these experiments. The RIA protocol is summarised in Fig. 6.2 and Table 6.1.

FIGURE 6.2 *SQ29852 Radioimmunoassay.*

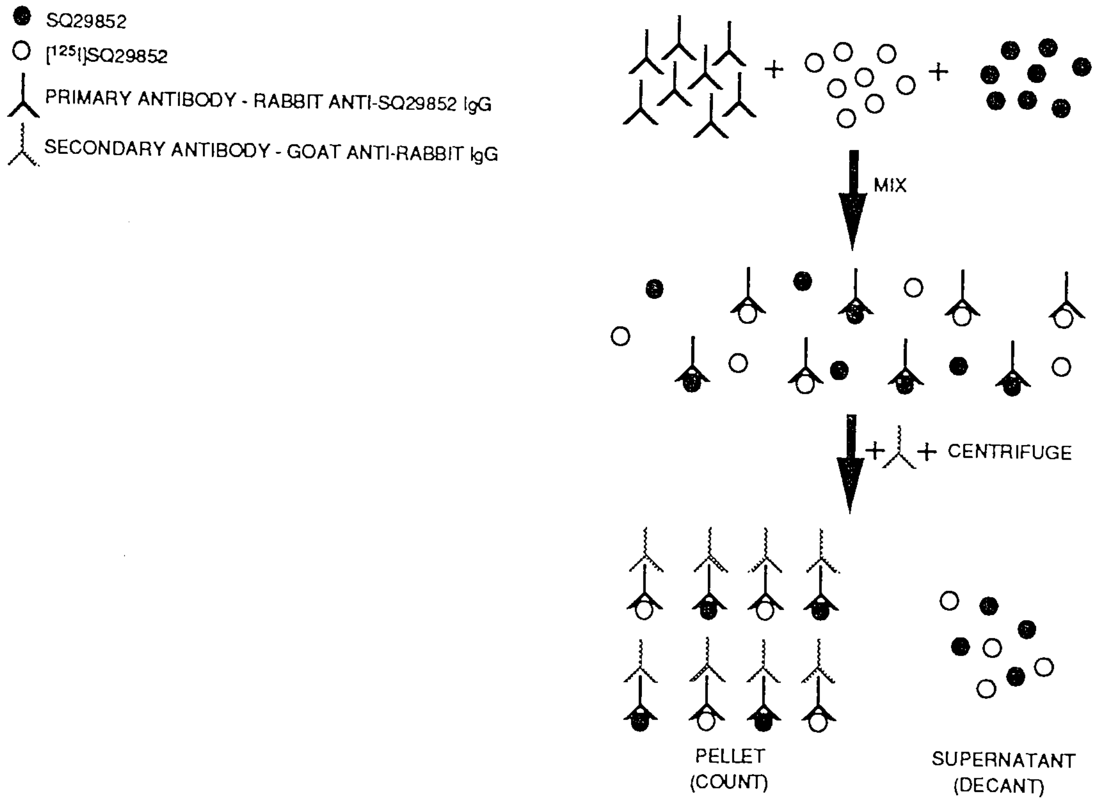

TABLE 6.1 *SQ29852 radioimmunoassay protocol.*

TUBES	STEP 1	STEP 2	STEP 3	STEP 4
	ASSAY MEDIUM	SAMPLE	[125]I-SQ29852	SQ29852 ANTISERUM
TOTALS				
1,2	NONE	NONE	200 µl	NONE
STANDARD CURVE				
3,4	10 µl; AM	10 µl; 0 ng ml^{-1}	200 µl	100 µl
5,6	10 µl; AM	10 µl; 1 ng ml^{-1}	200 µl	100 µl
7,8	10 µl; AM	10 µl; 5 ng ml^{-1}	200 µl	100 µl
9,10	10 µl; AM	10 µl; 10 ng ml^{-1}	200 µl	100 µl
11,12	10 µl; AM	10 µl; 25 ng ml^{-1}	200 µl	100 µl
13,14	10 µl; AM	10 µl; 50 ng ml^{-1}	200 µl	100 µl
15,16	10 µl; AM	10 µl; 100 ng ml^{-1}	200 µl	100 µl
17,18	10 µl; AM	10 µl; 250 ng ml^{-1}	200 µl	100 µl
19,20	10 µl; AM	10 µl; 500 ng ml^{-1}	200 µl	100 µl
CONTROL SAMPLES				
21,22	10 µl; AM	10 µl; control 1	200 µl	100 µl
23,24	10 µl; AM	10 µl; control 2	200 µl	100 µl
SAMPLES				
25,26	10 µl; SDil	10 µl; sample 1	200 µl	100 µl
N, N+1	10 µl; SDil	10 µl; sample 2	200 µl	100 µl

AM = Assay-medium
SDil = Standard diluent = potassium phosphate buffer

For uptake studies, monolayer-associated SQ29852 was assayed following a 15 min incubation. Therefore, the assay-medium used for the calibration standards and control samples (tubes 3 through 24) comprised Caco-2 monolayers solubilised by 0.1% v/v TX100 in double distilled water. This was prepared from Caco-2 monolayers cultured for 18 d in an identical manner to those used for uptake experiments. These Caco-2 monolayers were initially washed (2 x 5 ml x 5 min) with PBS and finally (2 x 2 ml x 15 min) with M4 pH6.0 at 37°C. The M4 pH6.0 was aspirated and the monolayers carefully rinsed (3 x 5 ml x 5 min) with ice-cold PBS-sodium azide stop-solution. The monolayers were solubilised by shaking (2 min) with 1 ml of 0.1% v/v TX100 in double distilled water followed by 10 μl of 4.0 M sodium hydroxide. The solubilised monolayers were neutralised by the addition of 10 μl of 4.0 M hydrochloric acid and used as the assay-medium for the SQ29852 RIA. For transport studies, the receiver-solution was assayed for SQ29852 content. Therefore, M4 pH7.4 was used as the assay-medium for the calibration standards and control samples (tube 3 through 24).

Tubes (polyethylene LP3, Luckman, UK) 1 and 2 represent the total counts, tubes 3 through 20 constitute a standard curve (0 to 500 ng ml^{-1}) and tubes 21, 22 and 23, 24 are sample controls I and II, respectively. Two additional tubes were required for a duplicate assay of each SQ29852 sample. Briefly, 10 μl of receiver-medium (solubilised Caco-2 monolayer or M4 pH7.4, for uptake or transport studies, respectively) was added to tubes 3 through 24 and an equal volume of standard diluent to each sample tube. 200 μl of $[^{125}I]$SQ29852 was added to each tube followed by 100 μl of diluted SQ29852-antiserum to tubes 3 onwards. The tubes were vortexed gently and incubated overnight at 4°C. The SQ29852 bound to the primary antibody was separated from unbound SQ29852 by specifically precipitating the SQ29852-primary antibody complex with 1.0 ml of separant (1% v/v goat anti-rabbit IgG in 7.5% w/v polyethylene glycol in potassium phosphate buffer; 4°C). Each tube was gently vortexed and incubated at 4°C for 10 min. Tubes 3 onwards were centrifuged at 3000 rpm for 10 min at 4°C (Chilspin, Fisons, UK.) to pellet the precipitate. The supernatant (containing the unbound SQ29852 fraction) was decanted and the tube inverted for 10 min on absorbent paper. Excess supernatant on the walls of each tube was removed with a wick of absorbent paper. The $[^{125}I]$-content of each pellet (which represented the bound $[^{125}I]$SQ29852) was determined by gamma counting (see section 2.4.2).

Standard calibration-curves were prepared using assay-medium comprising Caco-2 monolayers solubilised with 0.1% v/v TX100 in double distilled water (uptake studies) or M4 pH7.4 (transport studies), as appropriate. In both cases, a cubic function (*ie:* $y = a + bx + cx^2 + dx^3$) could be fitted to the standard curve of pellet-associated CPM *versus* log [SQ29852] profile (Fig. 6.8). Sample concentrations were calculated using the equation which described the best fit through the standard curve data.

6.3.3 CYCLOSPORIN

Lipophilic ligands (*eg:* testosterone) are avidly bound onto nitrocellulose permeable-supports but have low adsorption to aluminium oxide (see Table 3.1). Therefore, CsA transport experiments were performed across Caco-2 monolayers cultured on aluminium oxide culture inserts. Initial transport experiments were performed using identical Ap (donor) and Bl (receiver) solutions comprising M4-medium buffered to pH7.4. Under these conditions, the Bl appearance of tritium from an Ap donor-solution containing [^{3}H]CsA (0.5 μCi ml^{-1}; 50 nM) was low and erratic (Fig. 6.12 A). Furthermore, total [^{3}H]-recovery in these preliminary experiments was only 47.2±3.0%. The radiochemical loss was attributed to [^{3}H]CsA adsorption to surfaces during experimental handling. This was confirmed by measuring the [^{3}H]-content in ethanol washes of plastic pipette tips, solution vials and culture plastics.

The loss to plastic surfaces could have been reduced by increasing the concentration of CsA in the Ap donor solution. However, for this series of experiments the biological events controlling CsA absorption are the primary interest. The aqueous solubility of CsA is extremely low (0.04 mg ml^{-1}, Sandoz data sheet), therefore, as its concentration is increased physical phenomena would begin to distort its transepithelial transport kinetics. To simplify interpretation of transport data, an alternative approach of minimising the surface adsorption of [^{3}H]CsA at low concentrations was adopted. Firstly, siliconised pipette tips and glass vials were prepared for all [^{3}H]CsA handling procedures. They were immersed in dimethyldichlorosilane solution for 5 min then dried under vacuum for 30 min. This treatment reduced [^{3}H]CsA adsorption to pipette tips and vials by 10.5- and 5.8-fold, respectively. Secondly, the volume of Ap donor-solution was reduced from 2.0 ml from 1.0 ml to minimise the area of contact between the donor-solution and the polystyrene housing of the aluminium oxide permeable-support. Finally, alternative receiver-solutions were screened for their ability to prevent CsA adsorption to the walls of the receiver chambers (six-well clusters). Briefly, 2ml of [^{3}H]CsA (0.5 μCi ml^{-1}; 50 nM) in each medium (Hanks' balanced salt solution alone and supplemented with 0.1 or 5% BSA, milk substitute, semi-skimmed UHT cows milk or human blood) was applied to a receiver chamber. After 60 min at 37°C, the total volume of receiver-medium was collected and the fraction of [^{3}H]CsA remaining in solution was determined by liquid scintillation counting (see section 2.4.1 A). For [^{3}H]-content determinations in whole human blood, a 100 μl aliquot was de-colourised with an equal volume of 30% H_2O_2 then diluted with 1.8 ml of double distilled water before being assayed by liquid scintillation counting. Each chamber was subsequently washed (2 x 1 ml x 15 min at 25°C) with 100% ethanol. The [^{3}H]-content of these washings were measured and taken as the bound fraction.

In addition, the influence of these Bl receiver-solutions on the Ap-to-Bl transport of a hydrophilic (D-[^{14}C]mannitol) and hydrophobic ([^{3}H]testosterone) permeability marker was assessed.

6.4 RESULTS

6.4.1 THYROTROPHIN-RELEASING HORMONE

The coincident sample and reference [^{3}H]-elution profiles indicate that [^{3}H]TRH was not metabolised at the Ap surface of Caco-2 monolayers under the experimental conditions used in these studies (Fig. 6.3). This agrees with the observations of other workers who failed to detect metabolism of TRH during transport across Caco-2 monolayers [Lundin *et al.*, 1991]. Indeed, in this later study, the apparent permeability coefficients for [^{3}H]TRH (determined by [^{3}H]-flux measurements) and unlabelled TRH (determined by HPLC) were identical. These combined observations suggest that [^{3}H]-flux measurements reflect the transport of intact [^{3}H]TRH.

[^{3}H]TRH showed an Ap-to-Bl transepithelial lag time of 25 min followed by a linear phase (transport proportional to time, 1.30±0.10 pmoles insert^{-1} h^{-1}) which continued for at least 120 min (Fig. 6.4). The P_{app} of 2.28±0.17 x10^{-6} cm s^{-1}, calculated from the linear phase of transport, agrees with that previously reported (1.41 x 10^{-6} cm s^{-1} [Lundin *et al.*, 1991]).

The proportion of TRH transported in the Ap(pH6.0)-to-Bl(pH7.4) direction decreased with increasing Ap concentration. Increasing the TRH concentration in the Ap donor solution from 2 nM to 20 mM decreased the percentage transported by 24.5±0.5% from 2.29±0.05% h^{-1} to 1.73±0.06% h^{-1} (Fig. 6.5). The polarity of TRH transport across Caco-2 monolayers was temperature-dependent (Fig. 6.6). At 37°C, Ap(pH6.0)-to-Bl(pH7.4) [^{3}H]TRH transport was 25.5±0.9% higher than in the Bl(pH6.0)-to-Ap(pH7.4) direction. At 4°C, [^{3}H]TRH flux was reduced in both directions and vectorial transport was abolished.

TRH uptake into, and transport across, Caco-2 monolayers was selectively inhibited by small peptides. The inhibition of TRH uptake into Caco-2 cells by a range of potential inhibitors is summarised in Table 6.2. TRH uptake into 10 d Caco-2 monolayers was significantly ($p<0.05$) inhibited by the dipeptides, carnosine ($16.1\pm1.4\%$) and L-phe-gly ($18.2\pm2.0\%$), and the ß-lactam antibiotic, D-cephalexin ($17.5\pm2.6\%$). This effect was specific to small peptides (and analogues) since the amino acids, glycine and L-histidine, and the imino acid, L-proline, failed to inhibit uptake. TRH uptake was not reduced in the presence of a 100- and 500-fold molar excess of D-mannitol. Inhibition of TRH uptake was dependent on the concentration of the competing peptide. For instance, 10 and 50 mM carnosine produce a $16.1\pm1.4\%$ and $28.6\pm4.3\%$ inhibition, respectively. Furthermore, inhibition of TRH uptake exhibited a temporal-dependence. Carnosine (50 mM) reduced uptake by 28.6 ± 4.3, 37.0 ± 2.0 and $50.4\pm3.6\%$ after 10, 14 and 18 d of culture, respectively. TRH transport across Caco-2 monolayers was also significantly inhibited by carnosine, cephalexin and L-tyrosyl-glycine ($p<0.05$) (Table 6.3).

The transport of TRH into Caco-2 monolayers was pH-dependent and maximal at pH7.0 (Fig. 6.7 A). This reflected the pH-dependence for the log distribution coefficient (log D) of [^{3}H]TRH between octanol and McIlvaine buffer (Fig. 6.7 B). TRH is a hydrophilic peptide, its Log D value remained constant at -2.5 as the buffer pH increased from 2.5 to 4.5. As pH increased further, the Log D increased to a maximum at pH7.4 then remained constant through to pH8.5 (-2.01 ± 0.01). These values were in good agreement with values reported previously [Moss *et al.*, 1990]. The pKa of TRH can be calculated from the pH at which the half-maximal pH-dependent change in the Log D occurs (see equation 6.1). The derived pKa value for TRH was 5.923 ± 0.124. This values is comparable to the pKa of the imidazole group of L-histidine (6.04) and agrees with the proposed pKa of 5.9 for TRH [Ho *et al.*, 1990].

EQUATION 6.1 $\quad \mathrm{pKa} = \mathrm{Log}\, D_1 + ((\mathrm{Log}\, D_2 - \mathrm{Log}\, D_1) / 2)$

6.4.2 SQ29852

The Ap(pH6.0)-to-Bl(pH7.4) transport kinetics, from Ap donor-solutions containing 100 µM and 500 µM SQ29852, are shown in Figures 6.9 A and 6.9 B, respectively. Transport was bi-phasic. Transport was proportional to time through 60 min, thereafter, the rate of transport increased. The initial phase has no lag-time and a rate-constant k_1 (100 µM = 0.83 ± 0.02 ng insert^{-1} min, 500 µM = 4.17 ± 1.01 ng insert^{-1}

min^{-1}). The second phase has a lag-time for transepithelial transport (100 µM = 48.7 min, 500 µM = 59.3 min), and a rate-constant k_2 (100 µM = 1.65±0.08 ng insert^{-1} min, 500 µM = 8.53±1.17 ng insert^{-1} min^{-1}).

SQ29852 uptake into Caco-2 monolayers was concentration-dependent (10 µM to 5 mM; Fig. 6.10 A). Total SQ29852 uptake was resolved into saturable and non-saturable components by least-squares non-linear regression analysis (NONREG, Dr W.J. Irwin, Aston University). The saturable component had a K_m of 0.91±0.11 mM and a V_{max} of 538±46 ng (10^6 cells)$^{-1}$ (20 min)$^{-1}$. The non-saturable component had a K_d of 32.3±6.6 ng (10^6 cells)$^{-1}$ (20 min)$^{-1}$ mM^{-1}. Despite this highly saturable uptake-mechanism, Ap(pH6.0)-to-Bl(pH7.4) SQ29852 transport was proportional to its concentration in the Ap donor solution between 50 µM and 10 mM (Fig. 6.10 B).

Inhibition of SQ29852 uptake into, and transport across, Caco-2 monolayers by a range of small peptides or ß-lactam antibiotics was investigated (Table 6.4). SQ29852 uptake was significantly inhibited ($p<0.05$) by L-alanyl-L-proline, L-phenylalanyl-glycine, L-tryptophanyl-glycine and L-tyrosyl-glycine but not cephalexin or cephradine. Interestingly, SQ29852 transport was not significantly inhibited by any potential competitor.

6.4.3 CYCLOSPORIN

The percentage of [^{3}H]CsA remaining in solution, and that bound to the walls of the receiver chamber, for a range of potential receiver-solutions is given in Table 6.5. The greatest surface adsorption (96.3%) occurred from HBSS alone. The addition of 0.1% w/v BSA reduced the percentage bound slightly to 57.8%, but it was not reduced further by additional BSA (63.5% bound at 5% w/v BSA). Surface adsorption was considerably lower from receiver solutions comprising 10% w/v milk substitute (15.8%), milk (4.5%) or human blood (3.6%). Milk and human blood exhibited a similar and potent ability to inhibit [^{3}H]CsA adsorption. The adsorption to plastic surfaces was specific to CsA (Log D = 3.0 [Cefalu and Pardridge, 1985]) since significant binding of [^{3}H]testosterone (3.3 [Artursson and Karlsson, 1991]) and D-[^{14}C]mannitol (-3.1 [Artursson and Karlsson, 1991]) was not observed from any receiver solution tested.

Replacement of the HBSS receiver solution for 10% w/v milk substitute, milk or human blood influenced the Ap-to-Bl transport of testosterone and D-mannitol (Fig. 6.11). The Ap-to-Bl transport of the lipophilic transport marker, testosterone, into milk substitute, milk or human blood was higher than into HBSS. One can speculate that testosterone would partition more rapidly from the cell monolayer into these alternative receiver-solutions compared to HBSS, thereby facilitating its Ap-to-Bl transport. Transport of the hydrophilic marker, D-mannitol, was also elevated by milk substitute, milk or human blood compared to HBSS. Semi-skimmed UHT milk was selected as the Bl receiver-medium for transport experiments as it maintained monolayer integrity, it prevented CsA adsorption and was convenient to use.

Ap-to-Bl [^{3}H]CsA transport into semi-skimmed UHT cows milk was determined from an Ap donor-solution comprising HBSS with or without 0.1% w/v BSA under stagnant or agitated conditions (Fig. 6.12). Transport was sensitive to the conditions of the transport experiment and greatest (3.76±0.91 % h^{-1}; P_{app} = 1.98±0.53 x 10^{-6} cm s^{-1}) from an Ap solution of Hanks' balanced salt solution containing 0.1% w/v BSA under agitating conditions.

FIGURE 6.3 *Identification of post-incubation [^3H]TRH.*

Radio-HPLC chromatograms showing the tritium-distribution in the non-TCA precipitable fraction of the post-incubation Ap donor-solution (**A**) and a reference sample spiked with [^{3}H]TRH (**B**).

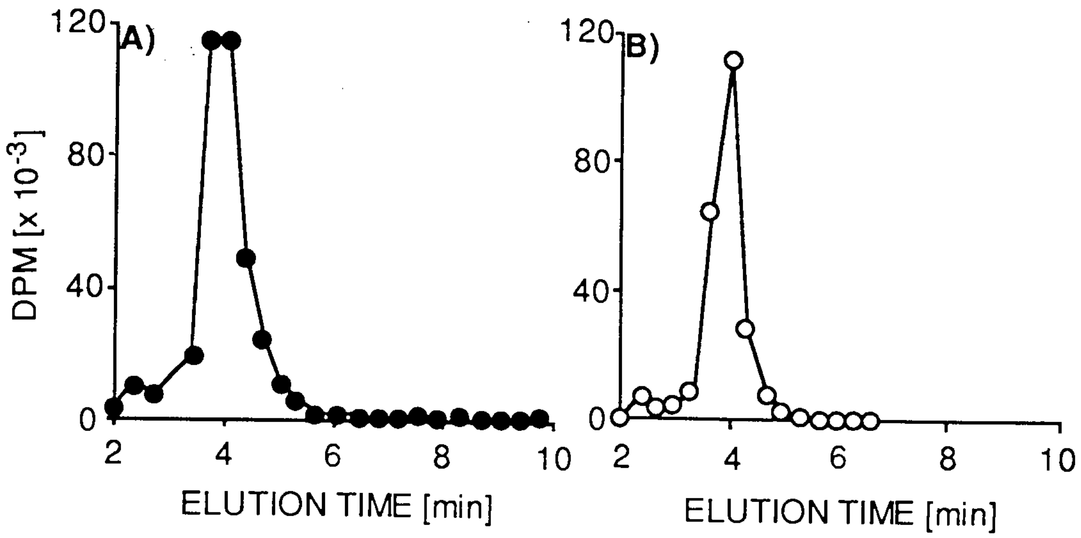

FIGURE 6.4 *Ap(pH6.0)-to-Bl(pH7.4) transport kinetics of [^3H]TRH.*

Monolayers were washed (1 x 2ml Ap x 15 min) with M4 pH6.0 and (1 x 2ml Bl x 15 min) with M4 pH7.4 before [^{3}H]TRH was applied to their Ap surface. Ap(pH6.0)-to-Bl(pH7.4) transport kinetics were followed by sequential transfer at 15 min intervals. Data are presented as mean values ± SD for three monolayers.

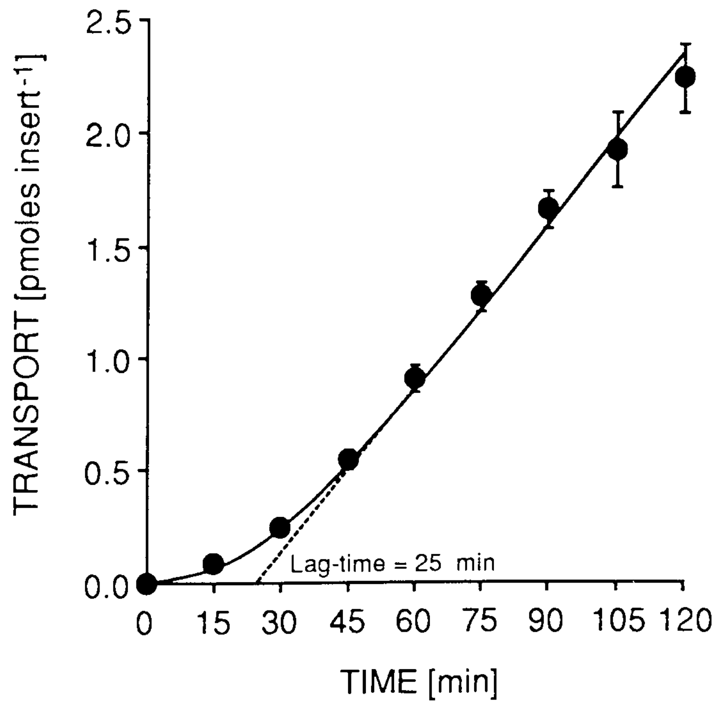

FIGURE 6.5 *Concentration-dependence of TRH transport.*
Monolayers were washed (1 x 2ml Ap x 15 min) with M4 pH6.0 and (1 x 2ml Bl x 15 min) with M4 pH7.4). Ap(pH6.0)-to-Bl(pH7.4) TRH transport was determined for a range of Ap concentrations (2 nM to 20 mM). Data are presented as mean values ± SD for three monolayers.

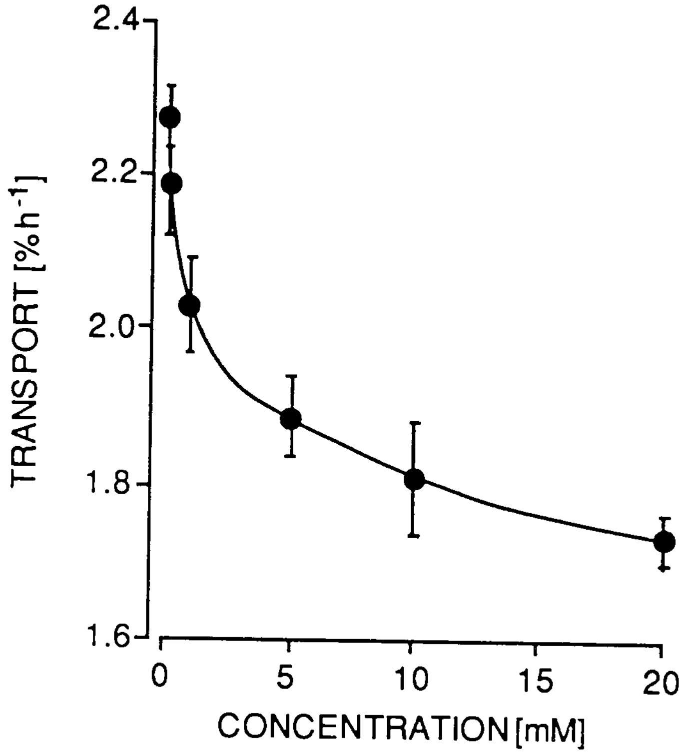

FIGURE 6.6 *Temperature-dependent polarity of TRH transport.*
For Ap(pH6.0)-to-Bl(pH7.4) transport experiments, monolayers were washed (1 x 2ml Ap x 15 min) with M4 pH6.0 and (1 x 2ml Bl x 15 min) with M4 pH7.4. For Bl(pH6.0)-to-Ap(pH7.4) transport experiments, monolayers were washed (1 x 2ml Ap x 15 min) with M4 pH7.4 and (1 x 2ml Bl x 15 min) with M4 pH6.0). [^{3}H]TRH (0.5 µCi ml^{-1}) in M4 pH6.0 was applied to the donor chambers. The washing and transport media were equilibrated to 37 or 4°C as appropriate. Ap(pH6.0)-to-Bl(pH7.4) (closed bars) and Bl(pH6.0)-to-Ap(pH7.4) (open bars) TRH transport were determined at 37 and 4°C. Data are presented as mean values ± SD for three monolayers. * Denotes a significantly lower Bl-to-Ap transport compared to Ap-to-Bl transport at the same temperature.

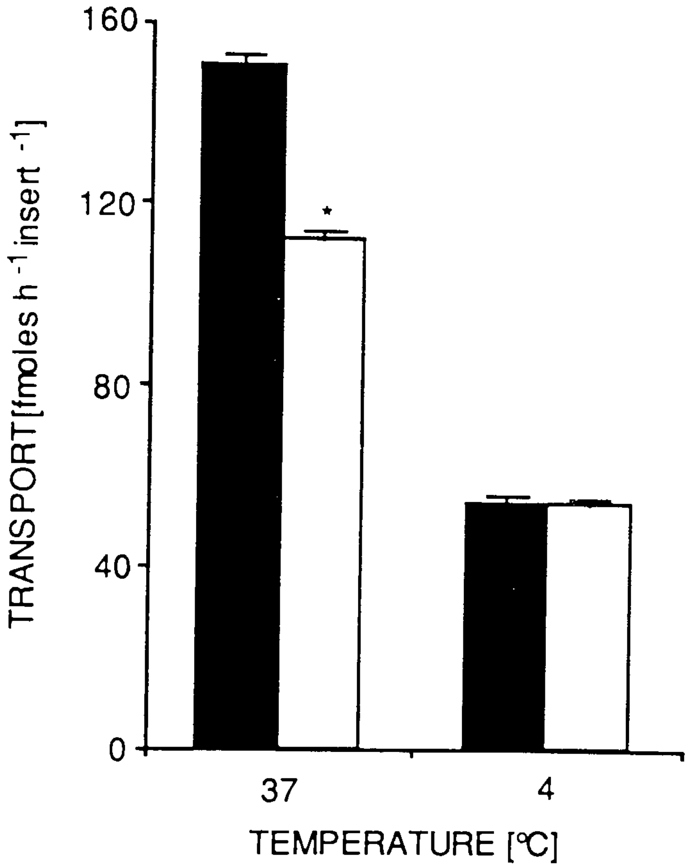

FIGURE 6.7 *pH-dependence of TRH transport and octanol-buffer Log D.*
(**A**) *Transport:* Monolayers were washed (1 x 2ml Ap x 15 min) with M4 buffered to the appropriate pH and (1 x 2ml Bl x 15 min) with M4 pH7.4. Ap(pH5.0 to 8.0) Bl(pH7.4) TRH transport were determined. Data are presented as mean values ± SD for three monolayers. (**B**) *Log D:* Data are presented as mean values ± SD for three determinations.

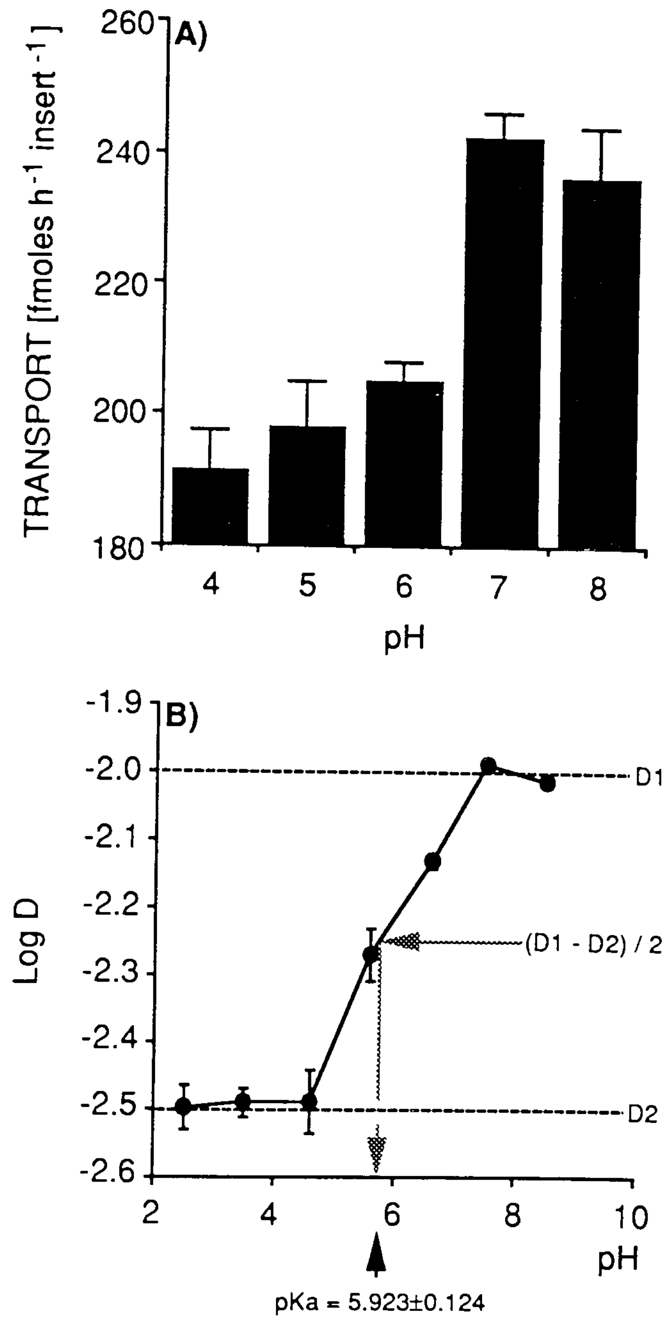

FIGURE 6.8 *SQ29852 radioimmunoassay standard curve.*

Typical standard curves of the SQ29852 radioimmunoassay in the presence (open circles) and absence (closed circles) of 0.1% TX100.

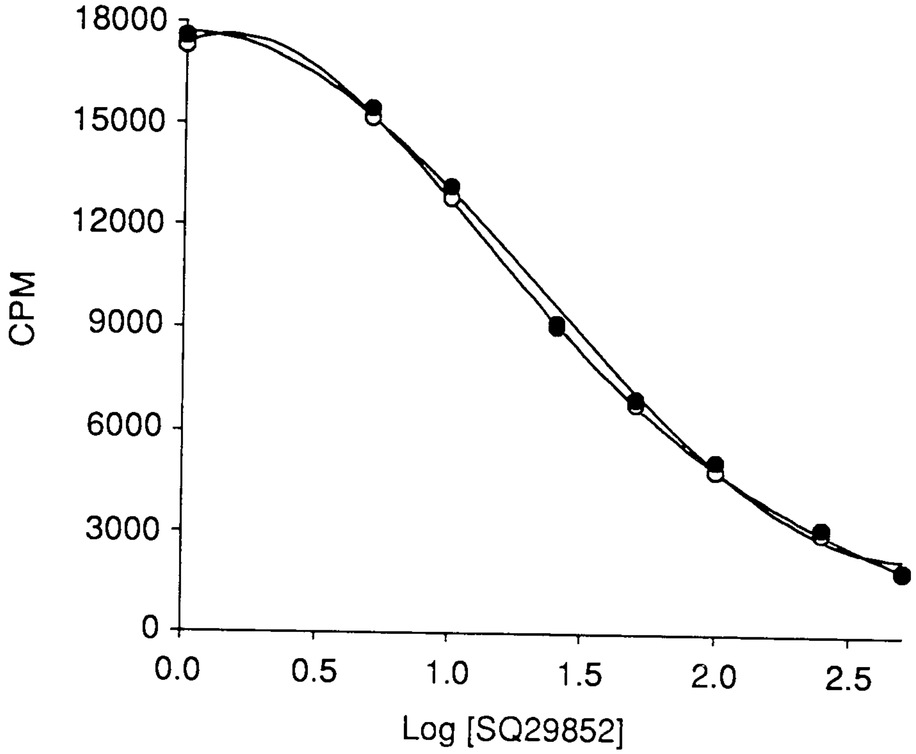

○ + 0.1% TX100
y = 1.7361e+4 + 316.22x - 6430.9x^2 + 1563.6x^3   R^2 = 0.998

● - 0.1% TX100
y = 1.7661e+4 + 271.08x - 6420.0x^2 + 1556.8x^3   R^2 = 0.997

FIGURE 6.9 *SQ29852 transport kinetics.*

Caco-2 monolayers were washed (1 x 2ml Ap x 15 min) with M4 pH6.0 and (1 x 2 ml Bl x 15 min) with M4 pH7.4. 100 μM (**A**) or 500 μM (**B**) SQ29852 in M4 pH6.0, was applied to their Ap surface and its appearance in the Bl receiver-solution was determined at 30 min intervals. Data are presented as mean values ± SD for three monolayers.

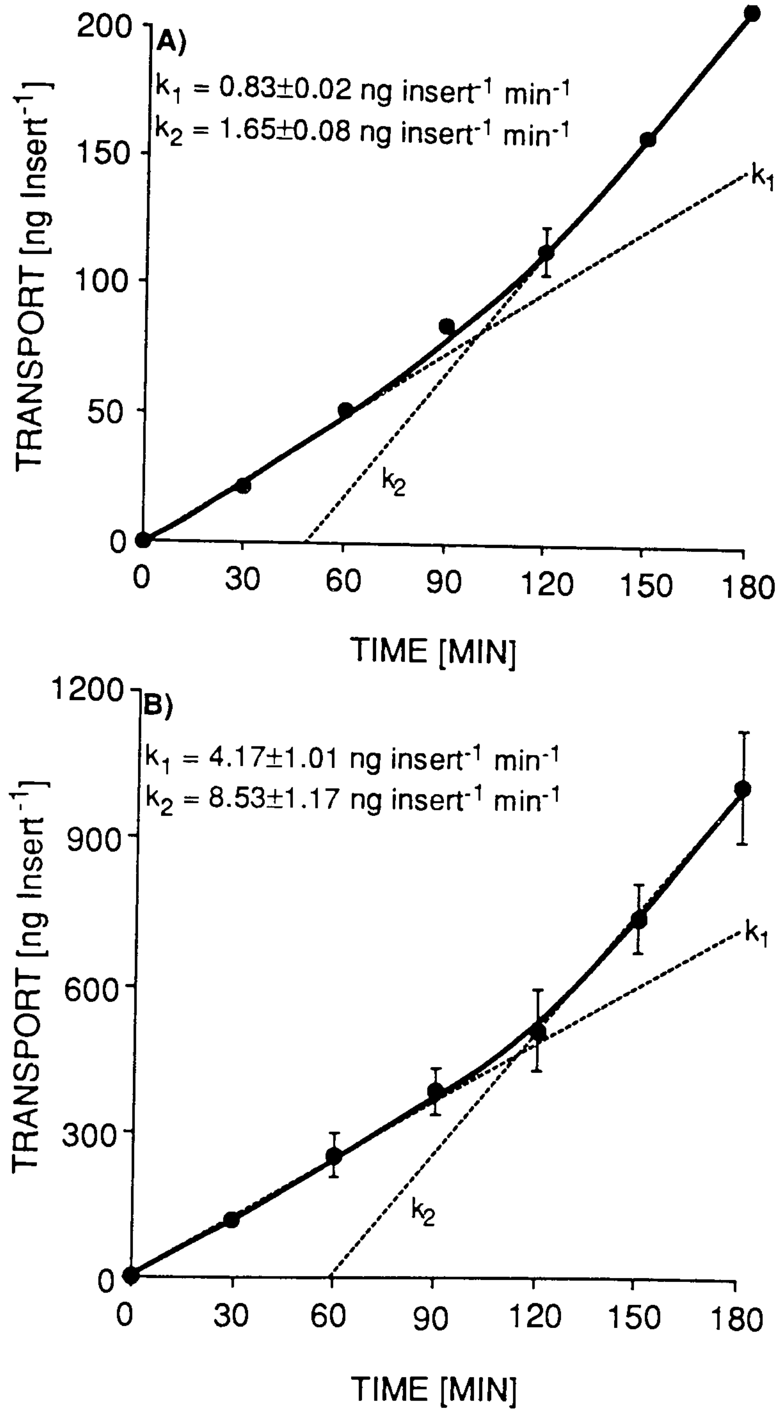

FIGURE 6.10 *Concentration-dependence of SQ29852 uptake and transport.* **(A)** *Uptake:* Caco-2 monolayers were washed (1 x 2ml Ap x 15 min) with M4 (pH6.0). SQ29852 uptake was determined for a range of Ap concentrations (10 μM to 5 mM). The total uptake was resolved into saturable (K_m = 0.91±0.11 mM; V_{max} of 538±46 ng $(10^6$ cells$)^{-1}$ (20 min$)^{-1}$) and non-saturable (K_d of 32.3±6.6 ng $(10^6$ cells$)^{-1}$ (20 min$)^{-1}$ mM^{-1}) components by non-linear regression analysis. **(B)** *Transport:* Caco-2 monolayers were washed [1 x 2ml Ap x 15 min] with M4 pH6.0 and (1 x 2 ml Bl x 15 min) with M4 pH7.4. Ap(pH6.0)-to-Bl(pH7.4) SQ29852 transport was determined for a range of concentrations (50 μM to 10 mM). Data are presented as mean values ± SD for three monolayers.

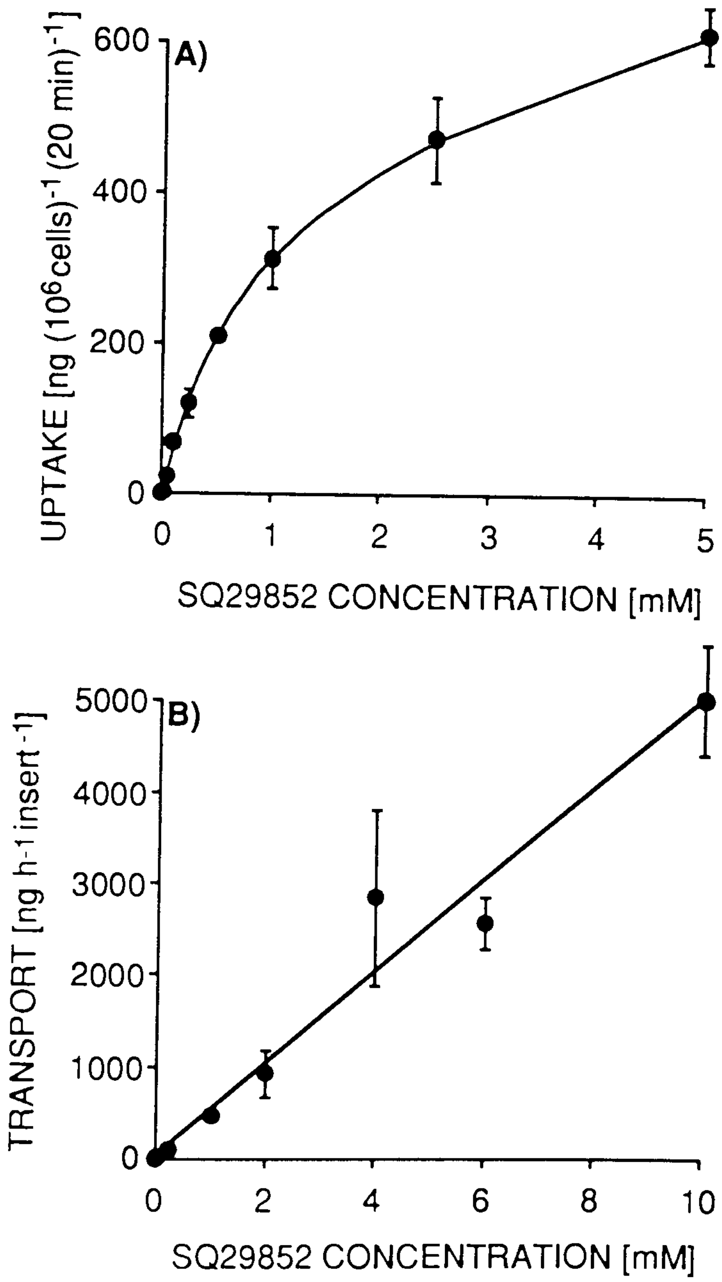

FIGURE 6.11 *Influence of alternative receiver-media on D-mannitol and testosterone transport.*

Monolayers were washed (1 x 2ml Ap + Bl x 15 min) with M5 pH7.4. [^{3}H]testosterone (1.0 μCi ml^{-1}) (**A**) or D-[^{14}C]mannitol (0.25 μCi ml^{-1}) (**B**) in HBSS were applied to their Ap surface. Their Bl appearance into HBSS, 10% w/v milk substitute in HBSS, semi-skimmed UHT milk or human blood was determined. Data are presented as mean values ± SD for three monolayers. * Denotes a significant increase above in flux above HBSS values at $p<0.05$.

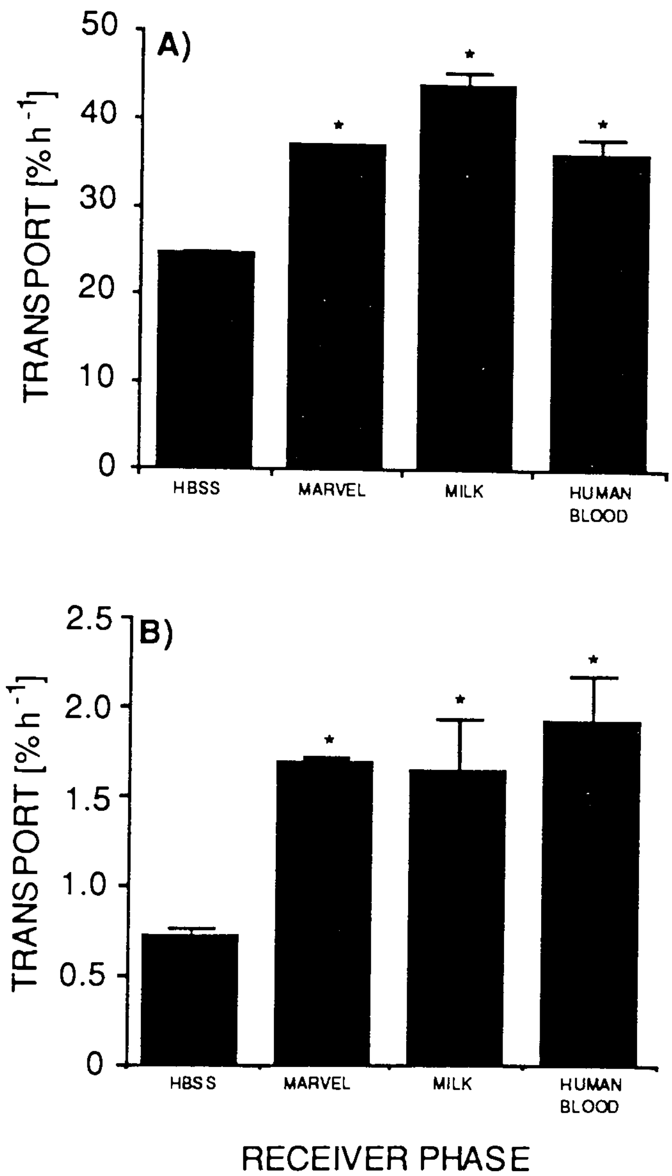

FIGURE 6.12 *[^{3}H]CsA transport*

(**A**) [^{3}H]CsA (0.5 μCi ml^{-1}) in HBSS was applied to their Ap surface and its Bl appearance into HBSS was determined. (**B**) [^{3}H]CsA (0.5 μCi ml^{-1}) in HBSS with (squares) or without (circles) 0.1% w/v was applied to their Ap surface. Its Bl appearance into semi-skimmed UHT milk was determined in stagnant (open symbols) and stirred (closed symbols) conditions. Data are presented as mean values ± SD for three monolayers.

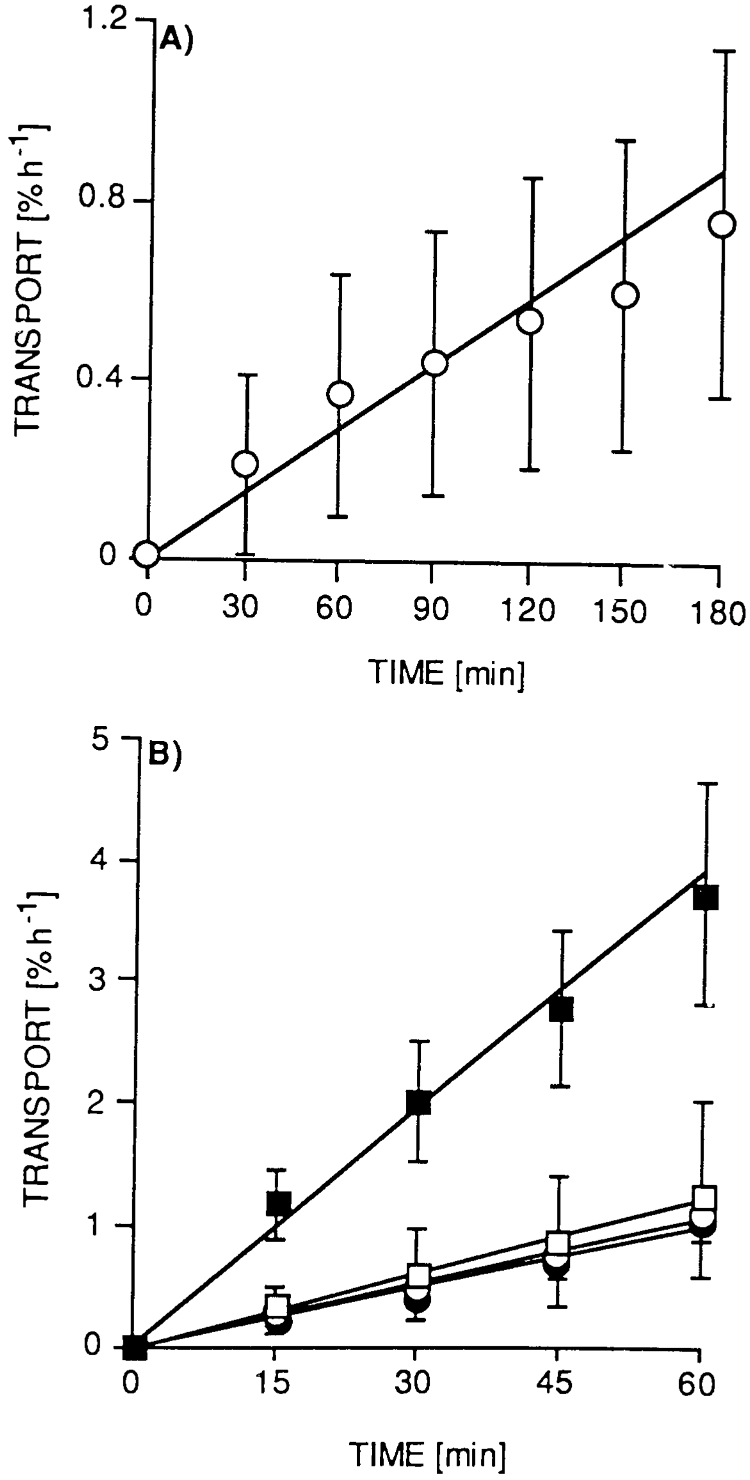

TABLE 6.2 *Cross-inhibition of TRH uptake.*

Data are presented as mean values ± SD for three monolayers. * and ** Denote a significant inhibition from control values at $p<0.05$ and $p<0.01$.

COMPETITOR	[mM]	% INHIBITION OF UPTAKE MEAN (SD) 6 d	10 d	14 d	18 d
Carnosine	10	NT	16.1 (1.4)*	19.4 (0.9)*	NT
	50	NT	28.6 (4.3)**	37.0 (2.0)**	50.4 (3.6)**
Cephalexin	10	14.1 (0.7)*	17.5 (2.6)*	18.5 (0.8)*	NT
L-Phe-gly	10	NT	18.2 (2.0)*	NT	NT
	50	NT	22.3 (1.5)*	NT	NT
Glycine	10	NT	2.7 (1.9)	NT	NT
L-Histidine	10	NT	-15.9 (9.5)	NT	NT
L-Proline	10	NT	-2.4 (12.9)	NT	NT
D-Mannitol	10	NT	5.5 (1.4)	NT	NT
	50	NT	4.7 (6.6)	NT	NT

NT = Not Tested

TABLE 6.3 *Cross-inhibition of TRH transport.*
Data are presented as mean values ± SD for three monolayers. * Denotes a significant inhibition from control values at $p<0.05$.

COMPETITOR	% INHIBITION MEAN (SD)
Carnosine	21.2 (2.9)*
Cephalexin	16.5 (1.7)*
L-Trp-gly	20.4 (3.4)*
L-Trp-gly-gly	17.2 (6.0)
L-Proline	0.6 (5.4)

NT = Not Tested
L-Trp-gly = L-Tryptophanyl-glycine
L-Trp-gly-gly = L-Tryptophanyl-glycyl-glycine

TABLE 6.4 *Cross-inhibition of SQ29852 uptake and transport.*
Data are presented as mean values ± SD for three monolayers. * Denotes a significant inhibition from control values at $p<0.01$.

COMPETITOR	% INHIBITION MEAN ± SD	
	UPTAKE	TRANSPORT
L-Alanyl-L-proline	75.3 (9.4)*	3.6 (38.1)
Cephalexin	6.3 (1.3)	14.9 (10.9)
Cephradine	14.3 (5.2)	29.1 (10.5)
L-Phenylalanyl-glycine	70.1 (5.5)*	30.2 (55.6)
L-Phenylalanyl-glycyl-glycine	NT	30.9 (10.9)
Thyrotrophin-releasing hormone	NT	-6.7 (17.8)
L-Tryptophanyl-glycine	55.6 (4.5)*	39.1 (33.4)
L-Tryptophanyl-glycyl-glycine	NT	13.3 (14.8)
L-Tyrosyl-glycine [a]	57.3 (9.4)*	NT

[SQ29852] = 100 μM, [COMPETITOR] = 10 mM,
a = [L-Tyrosyl-glycine] = 2 mM,
NT = Not Tested,

TABLE 6.5 *Inhibition of [^3H]CsA surface adsorption by receiver-media.*

	% IN SOLUTION	% BOUND
CYCLOSPORIN		
HBSS	3.7	96.3
HBSS+0.1% BSA	42.2	57.8
HBSS+5.0% BSA	36.5	63.5
MILK SUBSTITUTE	84.2	15.8
MILK	95.5	4.5
HUMAN BLOOD	96.4	3.6
TESTOSTERONE		
HBSS	95.4	4.6
MILK SUBSTITUTE	96.4	3.6
MILK	77.7	2.3
MANNITOL		
HBSS	98.9	1.1
MILK SUBSTITUTE	98.7	1.3
MILK	98.8	1.2

6.5 DISCUSSION

6.5.1 THYROTROPHIN-RELEASING HORMONE

The present study demonstrates that TRH flux across Caco-2 monolayers predominantly (≥75%) occurs by non-saturable passive transport. However, there was evidence for a minor carrier-mediated transport component (up to 25%). Firstly, the proportion of TRH transported across Caco-2 monolayers decreased as its concentration increased. The proportion transported decreased by 24.5±0.5% as the TRH concentration increased from 2 nM to 20 mM. Secondly, TRH transport in the Ap-to-Bl direction was 25.5±0.9% higher than in the Bl-to-Ap direction. This vectorial transport was abolished at 4°C. Finally, TRH transport was significantly reduced by a range of di- and tripeptides and the ß-lactam antibiotic cephalexin, but not L-proline. In addition, TRH uptake into Caco-2 monolayers was reduced by a range of small peptides and cephalexin, but not by amino acids or D-mannitol. This cross-inhibition profile is consistent with the involvement of the small peptide-transporter. Indeed there is a substantial body of evidence suggesting that Caco-2 cells express a small peptide-transporter (see section 1.5.4) which serves cephalexin [Dantzig and Bergin, 1990], cefaclor [Dantzig *et al.*, 1992] and cephradine [Inui *et al.*, 1992].

Cephalexin uptake into Caco-2 cells was maximal at pH6.0 [Dantzig and Bergin, 1990]. This is consistent with numerous observations suggesting that the intestinal small peptide-transporter is energised by a inwardly-directed proton-gradient [Okano *et al.*, 1986 a and 1986 b; Sugawara *et al.*, 1991]. Similarly, cephradine uptake into Caco-2 cells is maximal at pH6.0, however, the pH optimum for transport occurs between pH6.0 and 6.5 and is less well-defined [Inui *et al.*, 1992]. Interestingly, whilst TRH transport across Caco-2 monolayers is pH-dependent, it reflects the Log D *versus* pH profile rather than a typical pH-titration of the small peptide-transporter. This may result from the predominance of the passive transport mechanism and the fact that transport rather than uptake was being monitored.

The involvement of the small peptide-transporter in the transepithelial transport of TRH across Caco-2 monolayers is consistent with its dose-dependent oral bioavailability in dogs, rats [Yokohama *et al.*, 1984 a]. Moreover it is congruent with the region-specific, concentration-dependent and vectorial transport of TRH across the rat intestine [Yokohama *et al.*, 1984 b]. In addition, TRH transport across the rat intestine is inhibited by the co-administration of an oligopeptide mixture and by some ß-lactam antibiotics, but not by an amino acid mixture [Yokohama *et al.*, 1984 a]. This is similar to the cross-inhibition profile for TRH uptake into, and transport across, Caco-2 monolayers. Whilst the work presented here corroborates the observations of TRH transport in whole animal and tissue preparations other workers have failed to demonstrate any evidence for the carrier-mediated transport of TRH across Caco-2 cells [Thwaites *et al.*, 1992]. The reason for this discrepancy is not clear, however, the heterogeneous nature of this cell line means that their properties are susceptible to variation between laboratories.

6.5.2 SQ29852

The data presented here show that SQ29852 uptake into Caco-2 monolayers is saturable and is inhibited by a range of di- and tripeptides. This is compatible with observations in the rat intestine, which suggest that SQ29852 is a substrate for the intestinal peptide-transporter [Friedman and Amidon, 1989 b; Stewart *et al.*, 1990]. Paradoxically, the initial rate (0-to-60 min) of Ap-to-Bl SQ29852 transport across Caco-2 monolayers is proportional to its concentration (between 50 μM to 10 mM) and is not significantly inhibited by a range of small peptides. Therefore, despite carrier-mediated uptake of SQ29852 into Caco-2 cells, its overall transepithelial transport characteristics are consistent with a passive mechanism.

SQ29852 is hydrophilic (Log D less than -3.0 at pH7.0) and has a molecular weight of 440.48 [Ranadrive *et al.*, 1992]. Therefore, in the absence of a carrier-mediated basolateral export mechanism, the passive efflux of SQ29852 across the Bl lipid membrane would be expected to occur very slowly. Indeed, these data highlight the possibility that SQ29852 enters Caco-2 cells *via* an apical peptide-transporter but that its basolateral efflux may be severely retarded such that the passive paracellular transport dictates the overall transepithelial transport characteristics.

Following the oral administration of SQ29852 to humans, the maximal plasma-concentration is achieved only after 4 h [Moore *et al.*, 1988]. Therefore, its absorption from the GI tract occurs very slowly. Moreover, the oral bioavailability of SQ29852 is dose-dependent. This observation provided direct evidence for the importance of a saturable pathway in the oral absorption of SQ29852. However, initial rate (*ie*: 0-to-60 min) transport data, suggest that carrier-mediation does not make a major contribution to the overall flux of SQ29852 across Caco-2 monolayers. However, Ap(pH6.0)-to-Bl(pH7.4) SQ29852 transport across Caco-2 monolayers was bi-phasic. The initial rate (from a 100 μM Ap donor-solution; $k_1 = 0.83 \pm 0.02$ ng min^{-1}) had a zero lag-time which is consistent with a passive paracellular mechanism. The terminal rate ($k_2 = 1.65 \pm 0.08$ ng min^{-1}) had a very long lag-time of approximately 60 min. Lag-times are a characteristic feature of carrier-mediated transcellular transport. Therefore, it is tempting to speculate that the bi-phasic kinetics results from distinct paracellular (k_1) and transcellular (k_2) transport pathways. The possibility that the putative transcellular transport occurs *via* carrier-mediation cannot be excluded. However, experiments studying SQ29852 transport across Caco-2 monolayers over extended time-periods are required to test this hypothesis.

The K_m for carrier-mediated SQ29852 uptake in the rat intestine (0.08 mM) [Friedman and Amidon 1989 b; Stewart *et al.*, 1990] is an order of magnitude lower than that in the Caco-2 model (0.91±0.11 mM). This discrepancy may represent an inter-species difference. In addition, the cross inhibition profiles for SQ29852 uptake in the rat [Friedman and Amidon, 1989 b; Stewart *et al.*, 1990] and Caco-2 models are dissimilar. The rate of luminal disappearance of 10 µM SQ29852 in the *in situ* rat intestine perfusion model is significantly reduced by a 1000-fold molar excess (10 mM) of the ß-lactam antibiotic, cephradine, and the dipeptide, L-tyrosyl-glycine [Friedman and Amidon, 1989 b]. These observations were corroborated by cross-inhibition studies of SQ29852 uptake into intestinal rings prepared from rat intestine [Stewart *et al.*, 1990]. Similarly, the uptake of SQ29852 into Caco-2 monolayers was inhibited by a 20-fold molar excess of L-tyrosyl-glycine. However, uptake was not significantly reduced in the presence of a 100-fold molar excess (10 mM) of the ß-lactam antibiotics, cephalexin and cephradine. The failure of cephradine to inhibit SQ29852 uptake into Caco-2 monolayers may be due to a lower molar excess being used in these experiments or represent an inter-species difference. Interestingly, previous reports of carrier-mediated peptide uptake and transport by Caco-2 monolayers have described ß-lactam antibiotic-sensitive pathways. However, SQ29852 uptake was cephalexin- and cephradine-insensitive. Therefore, these results provide preliminary evidence for second peptide-carrier in the Caco-2 cell line. This pathway serves SQ29852, a L-lysyl-L-proline analogue, and is inhibited by a range of naturally occurring peptides (L-alanyl-L-proline, L-phenylalanyl-glycine, L-tryptophanyl-glycine and L-tyrosyl-glycine), but not ß-lactam antibiotics.

Despite an oral bioavailability of 67% in humans [Foley *et al.*, 1988], SQ29852 is very poorly transported across Caco-2 monolayers. Indeed, its $P_{app(0\ to\ 60\ min)}$ of $1.3\pm0.4\times10^{-8}$ cm s^{-1} is less than that of PEG_{4000} (3.6±0.1 cm s^{-1}) and predicts a low oral bioavailability (<1%) in man according to the correlation described by Artursson and Karlsson [1991]. There are many possible explanations for this apparent deviation from this established correlation. Firstly, the P_{app} value for SQ29852 transport was calculated from initial-rate (*ie:* 0-to-60 min) transport. However, there is evidence for a second transport pathway with a very long lag-time which increases the rate of transepithelial transport after 120 min. Therefore, SQ29852 flux measurements over prolonged time-periods may increase its P_{app} and consequently its predicted oral bioavailability. Secondly, deviation from the correlation may be anticipated for a compound if carrier-mediation is an important factor in its oral bioavailability *in vivo*. For instance, the number of peptide-transporters expressed per cell may be different in Caco-2 cells and normal absorptive cells *in vivo*. Consequently, a carrier-mediated transport mechanism may be quantitatively important *in vivo* whilst it does not play a major role in the *in vitro* Caco-2 model, or *visa-versa*. Alternatively, there is the possibility that efficient carrier-mediated basolateral efflux mechanisms are present in normal absorptive cells but are absent in Caco-2 cells.

Clearly, SQ29852 illustrates a general concern that the Caco-2 monolayer model may be qualitatively useful for identifying drug candidates that recognise carrier-mediated transport pathways, but it may quantitatively unreliable for predicting the extent of absorption for these molecules.

6.5.3 CYCLOSPORIN

The conventional Caco-2 monolayer transport model has been successfully modified for CsA transport experiments. Ap-to-Bl CsA transport was proportional to time for at least 60 min and was dependent on the Ap donor-solution. In the absence of Ap BSA, the rate of Ap-to-Bl transport was not influenced by agitation at 60 rpm. Secondly, in the non-agitated system, CsA transport was not influenced by the presence of 0.1% w/v in the Ap donor-solution. However, the rate of Ap-to-Bl CsA transport was markedly increased in the presence of 0.1% w/v BSA under agitated conditions. The reason for the marked increase flux under this specific set of conditions is not certain but demonstrates the importance of the mode of CsA presentation to a model epithelium on its rate of transepithelial transport. This is in keeping with the observation that the bioavaliability of CsA is dependent on formulation factors [Johnston *et al.*, 1986; Drewe *et al.*, 1992 b].

The P_{app} calculated from the maximal rate of Ap-to-Bl CsA transport (Ap donor solution = 0.1% in HBSS, agitated at 60 rpm) was $1.98 \pm 0.53 \times 10^{-6}$ cm s^{-1}. The slowest rate of transport (Ap donor solution = HBSS, agitated at 60 rpm) was $0.61 \pm 0.09 \times 10^{-6}$ cm s^{-1}. Because the Caco-2 monolayer model has been adapted for CsA transport studies care must taken when predicting % absorption figures from the correlation with P_{app} values [Artursson and Karlsson, 1991]. However, even the

This suggests that the transepithelial transport of CsA does not limit its oral bioavailbility *in vivo*. Therefore, formulation factors or first pass metabolism may be responsible for the partial oral bioavailability of CsA in man.

These preliminary observations highlight the potential application for Caco-2 monolayers for detailed studies on the mechanism of, and factors affecting, CsA absorption. However, further work is required to confirm this assertion.

CONCLUSION

TRH transport across Caco-2 monolayers is characterised by a minor saturable (carrier-mediated, approximately 25%) pathway superimposed onto a major non-saturable (diffusional) pathway. Transport was selectively inhibited by small peptides and cephalexin suggesting a peptide-transporter may be responsible for the minor saturable pathway.

SQ29852 uptake into Caco-2 monolayers is described by a major saturable-mechanism (K_m = 0.91 mM) superimposed onto a minor passive component. However, the initial-rate transport of SQ29852 is consistent with a passive transepithelial transport mechanism. Therefore, these data highlight the possibility that its basolateral efflux is severely retarded such that the passive paracellular transport dictates the overall transepithelial transport characteristics.

CHAPTER SEVEN

CALCIUM AND MAGNESIUM IONS RETARD THE TRANSEPITHELIAL TRANSPORT OF PAMIDRONATE

ABSTRACT

The oral absorption of some drug molecules is limited by interactions with di- and trivalent metal cations within the lumen of the GI tract. Progress in understanding these absorption-interactions has been restricted by the absence of a suitable *in vitro* model.

A modification of the conventional Caco-2 model has been developed which has a Ca^{2+}-free Ap donor-solution and a Bl receiver-solution containing the minimum Ca^{2+} concentration required to maintain monolayer integrity (100 μM). The influence of Ca^{2+} and Mg^{2+} on the absorption of [^{14}C]pamidronate was evaluated by comparing its transport across the conventional and minimum calcium Caco-2 models. The passive permeability of each monolayer was assessed using D-[^{3}H]mannitol as a transport marker.

In the conventional Caco-2 transport model the ratio of D-mannitol : pamidronate flux was 5:1, meanwhile, in the minimum calcium model, this ratio was reduced to 3:1. These data suggest that under minimum calcium conditions the transepithelial transport of pamidronate is increased to a greater degree than can be explained by minor changes in the passive permeability of Caco-2 monolayers. It was concluded that Ap Ca^{2+} and Mg^{2+} ions retard the Ap-to-Bl flux of pamidronate across Caco-2 monolayers.

7.1 BACKGROUND

7.1.1 BISPHOSPHONATES

Bisphosphonates are potent inhibitors of osteoclastic bone resorption. They bind strongly to hydroxyapatite crystals and inhibit the formation and dissolution of these crystals *in vitro* [Fleisch, 1987]. *In vivo*, the inhibition of osteoclastic bone activity may be due to binding of bisphosphonates to the bone mineral [Flanagan and Chambers, 1988]. Bisphosphonates are increasingly being used in a variety of bone disorders including Paget's Disease [Cantrill and Anderson, 1990], bone metastases [Dodwell *et al.*, 1990], tumour induced hypercalcaemia [Coleman and Rubens, 1987] and osteoporosis [Papapoulos *et al.*, 1992].

The oral bioavailability of this class of compounds is low. For example, Daley-Yates *et al.* [1991] using pamidronate (3-amino-1-hydroxypropylidene-1,1-diphosphonate; Fig. 7.1) in patients with breast cancer and bone metastases, estimated the bioavailability to be 0.3% for a 300 mg oral dose. In a volunteer study, the bioavailability of clodronate (dichloromethylene diphosphonate) was 1-2% [Yakatan *et al.*, 1982]. The bioavailability of of radiolabelled etidronate (ethane-1-hydroxy-1,1-diphosphonate) in man was shown to be low and variable [Fogelman *et al.*, 1986].

FIGURE 7.1 *Pamidronate (CGP23339a)*

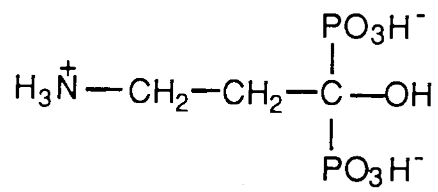

The factors which limit the absorption of bisphosphonates from the GI tract have not been determined The ability of pamidronate to chelate calcium and magnesium ions is well recognised and it has been used as an additive in detergents to prevent the precipitation of insoluble calcium- and magnesium-detergent salts from hard water [Francis and Centner, 1978]. This chelation potential highlights the possibility that complexation with these ions in the lumen of the GI tract may retard its absorption.

We have used the Caco-2 monolayer model to determine the influence of calcium and magnesium ions on the transepithelial transport of pamidronate.

7.1.2 MINIMUM CALCIUM MODEL

Calcium plays an important role in the maintenance of Caco-2 monolayer integrity [Artursson and Magnusson, 1990]. Total removal of calcium from the external bathing-solutions results in a complete disruption of the junctional complexes between cells. In the minimum calcium model Caco-2 cells are incubated with a calcium- and magnesium-free Ap donor-solution and a Bl receiver-solution containing the minimum calcium and magnesium concentrations to maintain monolayer integrity. In this way the influence of Ap calcium and magnesium ions on transepithelial transport can be investigated.

7.2 MATERIALS

[^{14}C]CGP23339a (8.86 Ci mol^{-1}) and CGP23339a were provided by Ciba Pharmaceuticals (Basle, Switzerland). D-[^{3}H]mannitol (30.0 Ci mol^{-1}) was purchased from New England Nuclear (Dupont, Germany). Citric acid was supplied by BDH (Poole, UK). 7-Nitro-2,1,3-benzoxadiazol-4-yl-ceramide (C_6NBD-ceramide) and propidium iodide were obtained from Molecular Probes (USA) and Sigma Chemical Company (UK), respectively.

M4-medium was used for transport studies. It comprised Hanks' balanced salt solution (HBSS; Gibco, Paisley, UK; 042-04180 H) containing 0.1% w/v BSA, 0.01% phenol red, 5 mM D-glucose and buffered with 14 mM HEPES. A calcium- and magnesium-free version ($M4_{-Ca}$) was prepared using HBSS without calcium and magnesium salts (Gibco, Paisley, UK; 076-01200 N). M4-media were also prepared containing intermediate concentrations of calcium and magnesium ions by appropriate dilutions of M4-medium (calcium = 1260 µM; magnesium = 811 µM) with $M4_{-Ca}$ (*ie:* 100 µM was prepared by a 12.6-fold dilution of M4-medium with $M4_{-Ca}$). Although $M4_{-Ca}$ is devoid of both calcium and magnesium ions it will be subsequently referred to as calcium-free throughout this chapter. Similarly, the media containing intermediate concentrations of calcium and magnesium will be referred to by their calcium concentration.

7.3 METHODS

7.3.1 CELL CULTURE

Caco-2 monolayers were cultured on Transwell™ polycarbonate culture inserts (see Fig. 2.2) for 15 d as described previously (see section 2.2.4).

7.3.2 TITRATION OF MINIMUM CALCIUM CONCENTRATION

The minimum Bl calcium concentration required to maintain Caco-2 monolayer integrity was titrated. Monolayers were washed with $M4_{-Ca}$ (1 x 2 ml (Ap+Bl) x 15 min), then $M4_{-Ca}$ containing citrate (pH7.4) 1 mM (1 x 1 ml (Ap+Bl) x 1 min) to chelate residual extracellular calcium ions. Finally, monolayers were washed with $M4_{-Ca}$ (1 x 2 ml Ap x 15 min) and M4 containing the appropriate concentration of calcium (1 x 2 ml Bl x 15 min). Thereafter, transport experiments were performed using $M4_{-Ca}$ as the Ap donor-solution and M4 containing the appropriate calcium concentration as the Bl receiver-solution.

7.3.3 TRANSEPITHELIAL ELECTRICAL RESISTANCE

TER was measured at 37°C as described previously (see section 2.5) using TER-medium containing 1260 μM calcium and 814 μM magnesium ions. TER measurements were made at defined periods after transport experiments (30, 60 and 90 min) or simple incubations under test conditions.

7.3.4 LASER-SCANNING CONFOCAL MICROSCOPY

For laser-scanning confocal fluorescence microscopy, monolayers were washed with $M4_{-Ca}$ (1 x 2 ml (Ap+Bl) x 15 min), then $M4_{-Ca}$ containing citrate (pH7.4) 1 mM (1 x 1 ml (Ap+Bl) x 1 min) to chelate residual extracellular calcium ions. Finally, monolayers were washed with M4 (1260 μM calcium; control), $M4_{-Ca}$ (calcium-free) (both 1 x 2 ml (Ap+Bl) x 15 min) or $M4_{-Ca}$ (1 x 2 ml Ap x 15 min) and M4 containing 100 μM calcium (1 x 2 ml Bl x 15 min) (minimum calcium). Monolayers were incubated for 60 min with M4, $M4_{-Ca}$ or $M4_{-Ca}$ (Ap) and M4 containing 100 μM calcium (Bl) then fixed with 4% formaldehyde and 0.25% glutaraldehyde in 0.1 M cacodylate buffer. The cells were subsequently stained for 30 min with C_6NBD-ceramide (10 μg ml^{-1}; lipid stain) and propidium iodide (10 μg ml^{-1}; nuclear stain) in PBS. The permeable-support (with monolayer) was removed from its polystyrene housing using a scalpel and mounted on a glass slide (Fig. 7.2) using Permafluor mountant (Biogenesis, Bournemouth, UK). The samples were viewed using a BioRad 500 laser-scanning confocal microscope. They were excited at 514 nm and the emitted fluorescence resolved by filters into 540 nm (lipids) and 570 nm (nuclei) and represented as green and red images, respectively.

Since laser-scanning confocal microscopy allows optical sectioning of the sample, the lipid and nuclear staining pattern depends on the focal plane through the cells. Therefore, to permit valid comparison between samples, each was visualised and photographed in the optical plane with the most subjectively intense nuclear signal.

FIGURE 7.2 *Sample mounting for confocal microscopy*

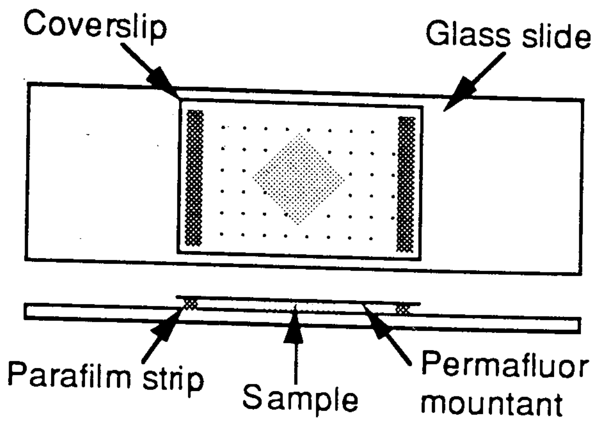

7.3.5 CGP23339a TRANSPORT EXPERIMENTS

Caco-2 monolayers were washed with $M4_{-Ca}$ (1 x 2 ml (Ap+Bl) x 15 min), then $M4_{-Ca}$ containing citrate (pH7.4) 1 mM (1 x 1 ml (Ap+Bl) x 1 min) to chelate residual extracellular calcium ions. Finally, monolayers were washed with M4 (1 x 2 ml (Ap+Bl) x 15 min)(conventional model), $M4_{-Ca}$ (1 x 2 ml (Ap+Bl) x 15 min)(calcium-free model) or $M4_{-Ca}$ (1 x 2 ml Ap x 15 min) and M4 containing 100 µM calcium (1 x 2 ml Ap x 15 min)(minimum calcium model). The transport experiment was initiated by applying a donor solution of M4 (conventional model) or $M4_{-Ca}$ (calcium-free and minimum calcium models) containing 0.44 µCi ml^{-1} (50 µM) [^{14}C]CGP23339a and 0.50 µCi ml^{-1} D-[^{3}H]mannitol to the Ap chamber. The culture-insert was immediately transferred to a receiver-chamber containing 3.0 ml of M4 (conventional model), $M4_{-Ca}$ (calcium-free model) or M4 containing 100 µM calcium (minimum calcium model) receiver-solutions. Ap-to-Bl transport kinetics were followed by sequentially transferring the culture-insert into a fresh receiver-solution at 30 min intervals. After the final receiver-sample had been collected monolayers were transferred to a cold-table (0-4°C) and the Ap donor-solutions were collected and their radiochemical concentration determined. [^{14}C]CGP23339a flux across each monolayer was corrected for the amount applied to the Ap donor-solution.

7.4 RESULTS

The influence of calcium ions on Caco-2 monolayer integrity was assessed by three methods, the transport of permeability markers ([^{14}C]PEG_{4000} and D-[^{3}H]mannitol), post-transport TER and by visual inspection using laser-scanning confocal microscopy.

Preliminary results showed that TER across Caco-2 monolayers under uniform calcium-free conditions (112.1±3.2 Ω cm^2) was 3.9-fold lower than in the presence of calcium ions (control; 432.4±15.0 Ω cm^2). Moreover, in the absence of Ap calcium ions, but the presence of 1260 μM Bl calcium, TER (422.5±30.7 Ω cm^2) was comparable to control values (Fig. 7.3). Therefore, the Ap-to-Bl transport of drug molecules can be studied across an intact monolayer from a calcium-containing and calcium-free donor-solution. However, the use of 1260 μM calcium as the Bl receiver-solution with a calcium-free Ap donor-solution establishes a large Bl-to-Ap concentration-gradient. Flux in proportion to this gradient may result in significant levels of calcium appearing in the Ap donor-solution over the duration of the transport experiment. This would complicate interpretation of the transport data, therefore, Bl-to-Ap calcium flux should be minimised. The minimum concentration of calcium required in the Bl receiver-solution to maintain monolayer integrity was titrated. By using a low Bl calcium concentration, the passive Bl-to-Ap calcium flux would be minimised by reducing the concentration-gradient.

All monolayer permeability indices were dependent on the Bl calcium concentration Ap-to-Bl $[^{14}C]PEG_{4000}$ transport (Fig. 7.4 A and B) remained constant as the Bl calcium concentration was reduced from 1260 μM (0.32±0.02 % h^{-1}) to 75 μM (0.40±0.07 % h^{-1}). Thereafter, further small decreases produced significantly elevated fluxes (50 μM = 0.54±0.03 % h^{-1}, $p<0.05$; 25 μM = 0.91±0.27 % h^{-1}, $p<0.05$). At concentrations of 10 μM and below, high rates of Ap-to-Bl $[^{14}C]PEG_{4000}$ fluxes were observed suggesting a complete loss of monolayer integrity. Correspondingly, D-$[^3H]$mannitol transport (Fig. 7.4 C and D) showed a similar dependency on the Bl calcium concentration. As the Bl calcium concentration decreased below 1260 μM, Ap-to-Bl D-$[^3H]$mannitol flux remained constant through to 75 μM, thereafter its transport was increased. At concentrations of 10 μM and below, high rates of Ap-to-Bl D-$[^3H]$mannitol fluxes were observed suggesting a complete loss of monolayer integrity.

Following a 60 min transport experiment, the Ap and Bl donor solutions were aspirated and replaced with TER-medium containing 1260 μM calcium and 814 μM magnesium. Post-transport TER-determinations are presented as a function of the Bl calcium-concentration during the transport experiment (Fig. 7.4 E and F). Post-transport TER was inversely related to $[^{14}C]PEG_{4000}$ and D-$[^3H]$mannitol transport. The 30 min post-transport TER increased as the Bl calcium-concentration increased from 0 μM (139.6±12.2 Ω cm^2) to 100 μM (398.9±11.8 Ω cm^2). Thereafter, the 30 min post-transport TER remained constant despite further increases in Bl calcium-concentration. At 100 μM Bl calcium the post-transport TER was not significantly different from control values (398.9±21.7 Ω cm^2). Interestingly, there was no evidence for a recovery in post-transport TER values after 60 and 90 min (Fig. 7.4 E). This suggests that the loss in Caco-2 monolayer integrity induced by a 60 min exposure to a low extracellular calcium-concentration is not rapidly reversible upon the replacement of calcium ions.

The percentage changes in the above permeability indices were calculated at each Bl calcium concentration and compared to calcium-free conditions (defined as 100% response) (Fig. 7.5 A). The mean % response for all indices was calculated and plotted as a function of Bl calcium concentration (Fig. 7.5 B). The half-maximal increase in Caco-2 monolayer permeability occurs between 15 and 20 μM Bl calcium.

Based on the above observations, the following conditions were used for the minimum calcium model; $M4_{-Ca}$ as the Ap donor solution and M4 containing 100 μM calcium as the Bl receiver-solution. Under these conditions, the transport of permeability markers and post-transport TER were consistently indistinguishable from control values.

In the uniform presence of calcium ions, Caco-2 cell nuclei were well-defined. In addition, the inter-nuclear distance was small and the inter-nuclear spaces stained green indicating the presence of lipids (Fig. 7.6 A). This appearance is consistent with a monolayer formed from closely opposed cells with tight inter-cellular junctions. Under calcium-free conditions, cell nuclei were poorly defined and closely associated with lipids. Moreover, the inter-nuclear spaces were substantially devoid of lipid staining (Fig. 7.6 B). Large numbers of cells were present on the permeable-support under calcium-free conditions suggesting that the inter-cellular gaps were formed by separation of inter-cellular contacts and not cells sloughing from the polycarbonate filter. Under minimum calcium conditions the monolayer appearance was indistinguishable from that of the control sample (Fig. 7.6 C). Therefore, laser-scanning confocal microscopy confirmed that under minimum calcium conditions Caco-2 monolayer integrity is maintained.

The Ap-to-Bl transport of [^{14}C]CGP23339a and D-[^{3}H]mannitol across Caco-2 monolayers were compared in the uniform presence and absence of calcium and in the minimum calcium model (Fig. 7.7). In the uniform presence of calcium ions, CGP23339a transport was slow (142.6±12.0 nmoles h^{-1}) and linear for at least 180 min. In the total absence of calcium ions, CGP23339a transport was rapid (initial rate

= 12611±176 nmoles h^{-1}) and linear for at least 120 min. This represents a 88.4-fold increase in the rate of [^{14}C]CGP23339a transport. D-mannitol transport was increased 15.0-fold by removing calcium ions.

The ratios of D-mannitol to CGP23339a transport across Caco-2 monolayers in the presence and absence of calcium ions were 4.892 and 1.078, respectively (Table 7.1). These data indicate that intact Caco-2 monolayers are approximately five times more permeable towards D-mannitol than CGP23339a, but that this differential flux is abolished when monolayer integrity is compromised by calcium removal. In the minimum calcium model, the rate of CGP23339a transport is 1.92-times greater control levels. Meanwhile, D-mannitol flux across the minimum calcium model was only slightly (1.22-fold) above control levels. The ratio of D-mannitol to CGP23339a transport was reduced from 4.892 in the uniform presence of calcium to 3.095 in the minimum calcium model (Table 7.1). Therefore, in the absence of Ap calcium ions, CGP23339a transport is increased to a greater extent than that of D-mannitol. The apparent permeability coefficients for CGP23339a transport in the conventional and minimum calcium models were 7.90±0.68 x 10^{-8} cm s^{-1} and 2.11±0.25 x 10^{-7} cm s^{-1}, respectively.

Finally, the proportion of [^{14}C]CGP23339a transported into the Bl receiver-solution in the minimum calcium model was dependent upon its concentration in the Ap donor-solution (Fig. 7.8 A). At 50 μM and 5000 μM, 0.35±0.04 and 0.59±0.06 % h^{-1} of apically applied [^{14}C]CGP23339a was transported. Therefore, a 100-fold molar increase in concentration increased the proportion of [^{14}C]CGP23339a transport 1.7-fold. This increase in Ap-to-Bl flux was not specific since the transport of D-mannitol was concomitantly increased by 2.2-fold. In addition, a 60 min incubation of the minimum calcium Caco-2 model with an Ap donor solution containing 5000 μM CGP23339a significantly reduced TER values below reference levels (327.4±13.6 versus 437±28.6 Ω cm^2; $p<0.05$). This effect was abolished by the use of an Ap donor solution containing 1260 μM calcium ions (Table 7.2).

FIGURE 7.3 *Influence of the distribution of calcium and magnesium ions on TER.* Caco-2 monolayers were incubated in uniform calcium (**A**; control), Bl calcium (**B**) or uniform calcium-free conditions (**C**). After 60 min these incubation media were replaced with TER-medium and the TER measured at 15, 30 and 60 min. Data are presented as mean values ± SD for six monolayers. * Denotes a significant reduction from control values at $p<0.01$.

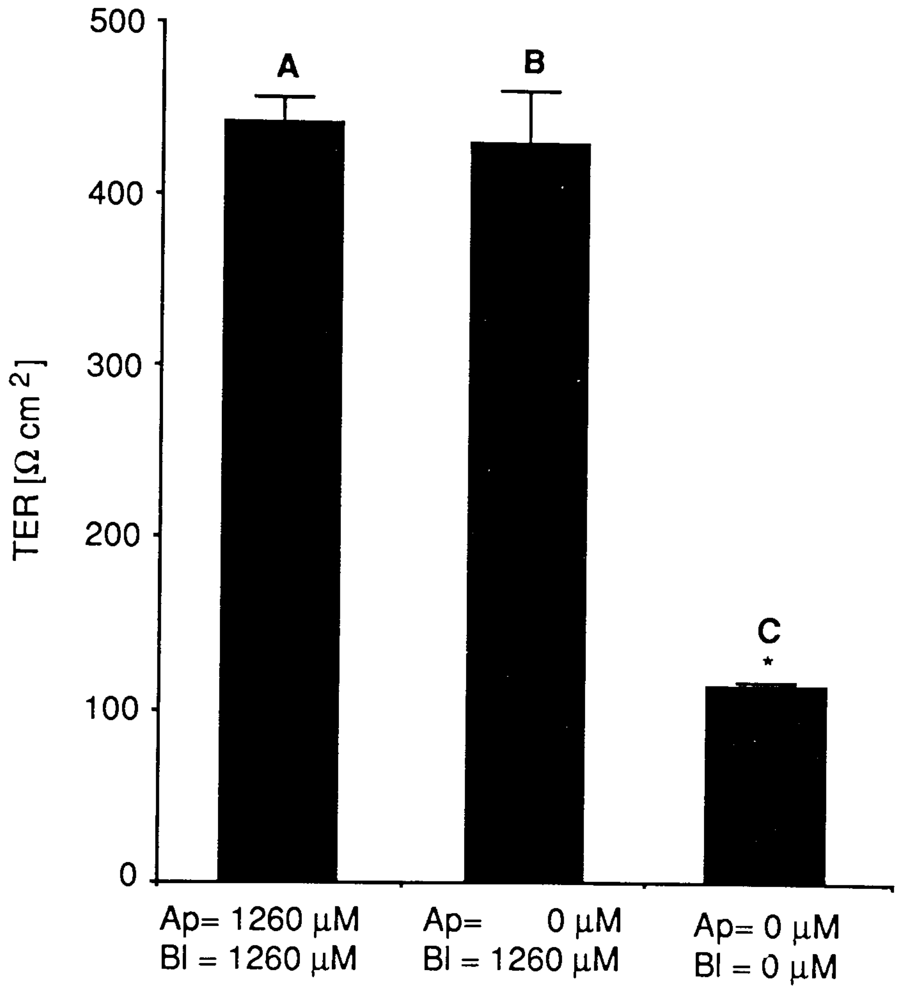

FIGURE 7.4 *The influence of Bl calcium concentration on Caco-2 monolayer integrity.*

Data are presented as mean values ± SD for three monolayers as a function of Bl calcium concentrations. * and ** Denote significant difference from control values at $p<0.05$ and $p<0.001$, respectively.

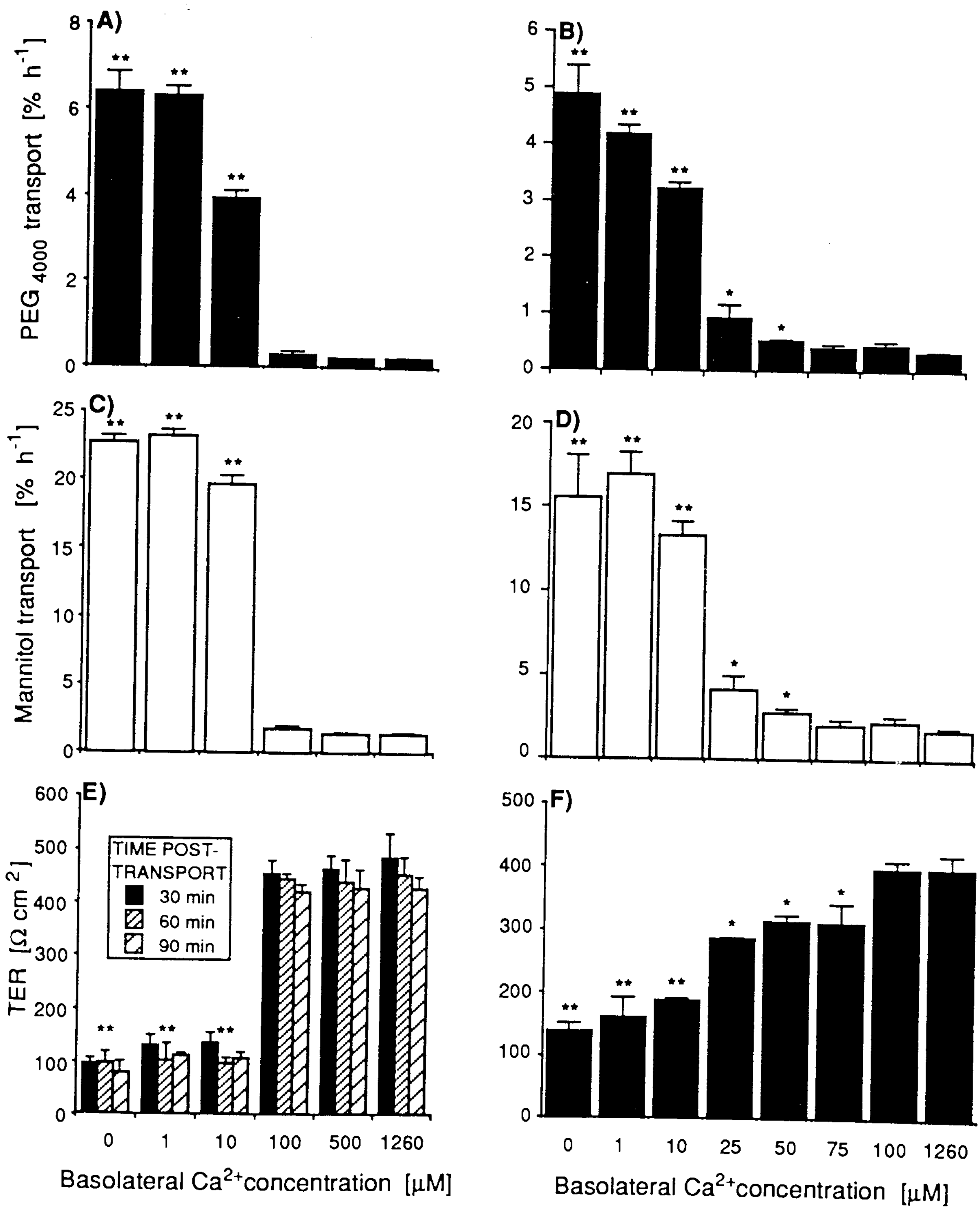

FIGURE 7.5 *Dose-response curves for permeability indices as a function of Bl calcium concentration.*

(A) *% Response;* The % response of each permeability index (D-mannitol transport = open circles; PEG_{4000} transport = closed circles and TER = closed squares) are individually plotted as a function of Bl calcium concentration where a 100% response is defined as the difference between values at 1260 and 0 μM Bl calcium. **(B)** *Mean % response;* The mean % response of all permeability indices was calculated and plotted as a function of Bl calcium concentration.

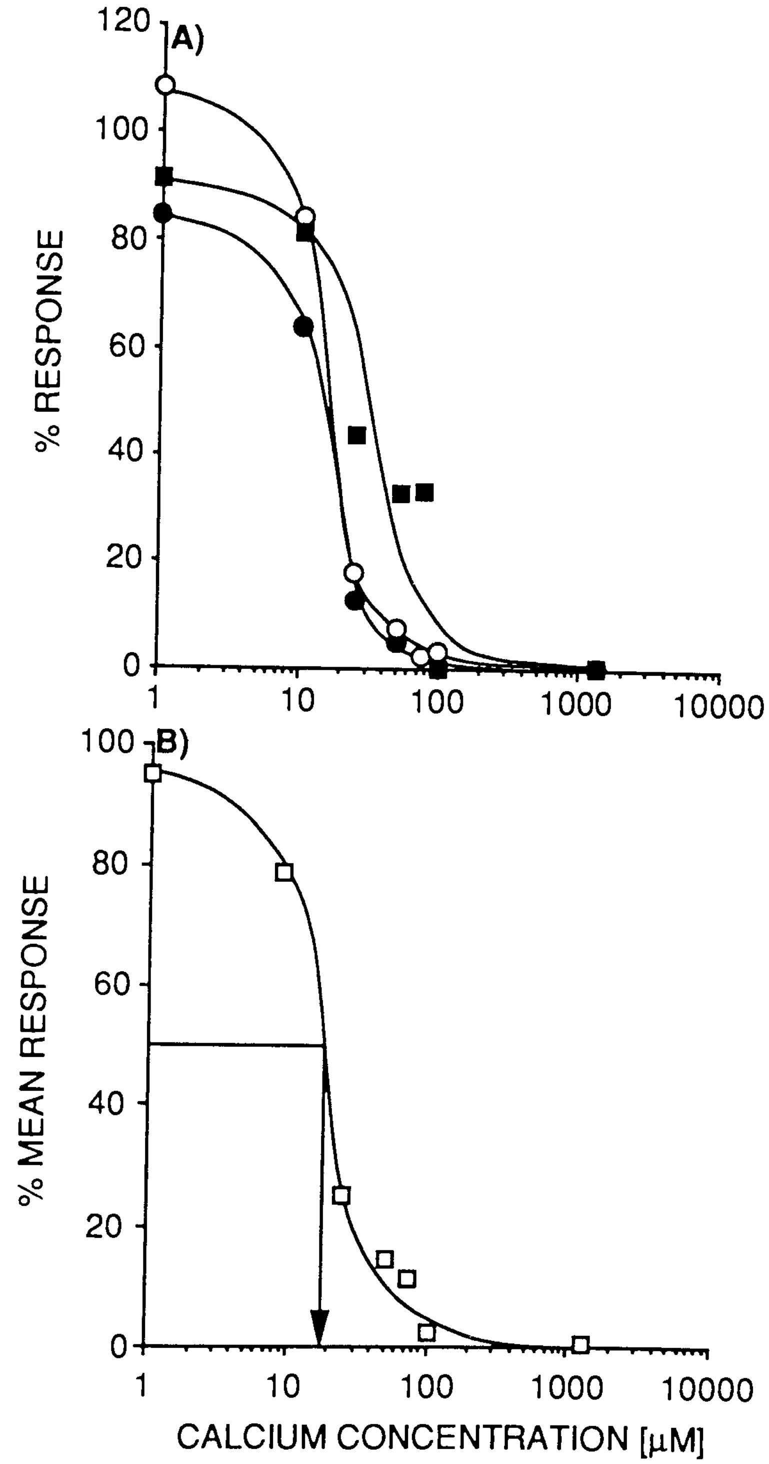

FIGURE 7.6 *Effect of calcium on Caco-2 monolayer appearance.*

Caco-2 monoloayers were incubated for 60 min under uniform calcium (**A**), uniform calcium-free (**B**) or 100 μM Bl calcium alone (**C**). Scale bar = 25 μm.

A)

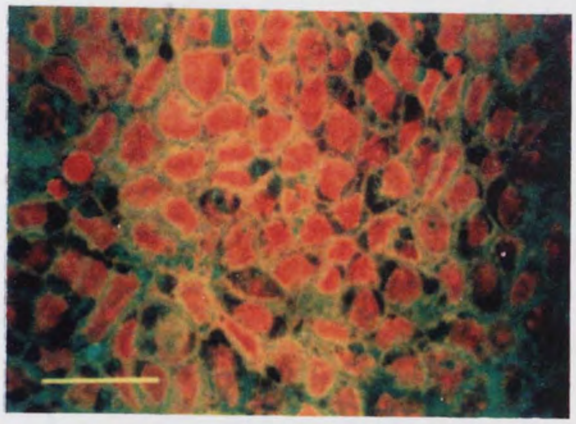

B)

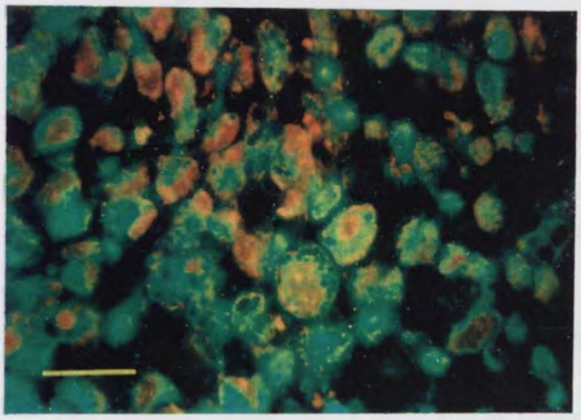

C)

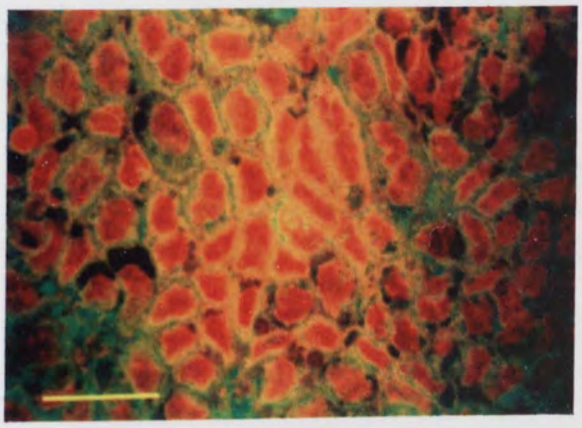

FIGURE 7.7 *Effect of calcium removal on CGP23339a and D-mannitol transport.* The kinetics of Ap-to-Bl CGP23339a (**A**) and D-mannitol (**B**) transport in the uniform presence (open circles) and absence (closed circles) of calcium ions was determined. Data are presented as mean values ± SD for three monolayers.

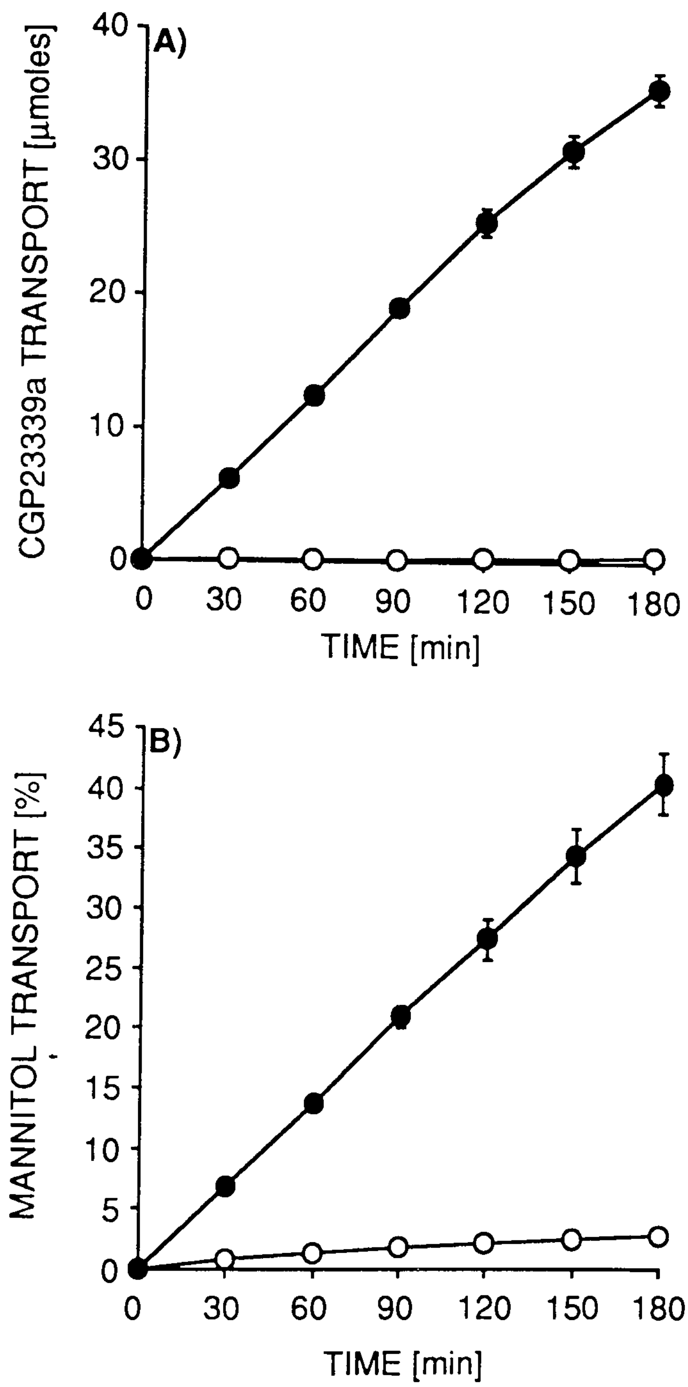

FIGURE 7.8 *Effect of Ap [^{14}C]CGP23339a on the permeability of the minimum calcium model.*

The kinetics of Ap-to-Bl [^{14}C]CGP23339a (**A**; 50 μM) and D-[^{3}H]mannitol (**B**) were determined in the presence (triangles) and absence (squares) of unlabelled CGP23339a (5 mM). Data are presented as mean values ± SD for three monolayers.

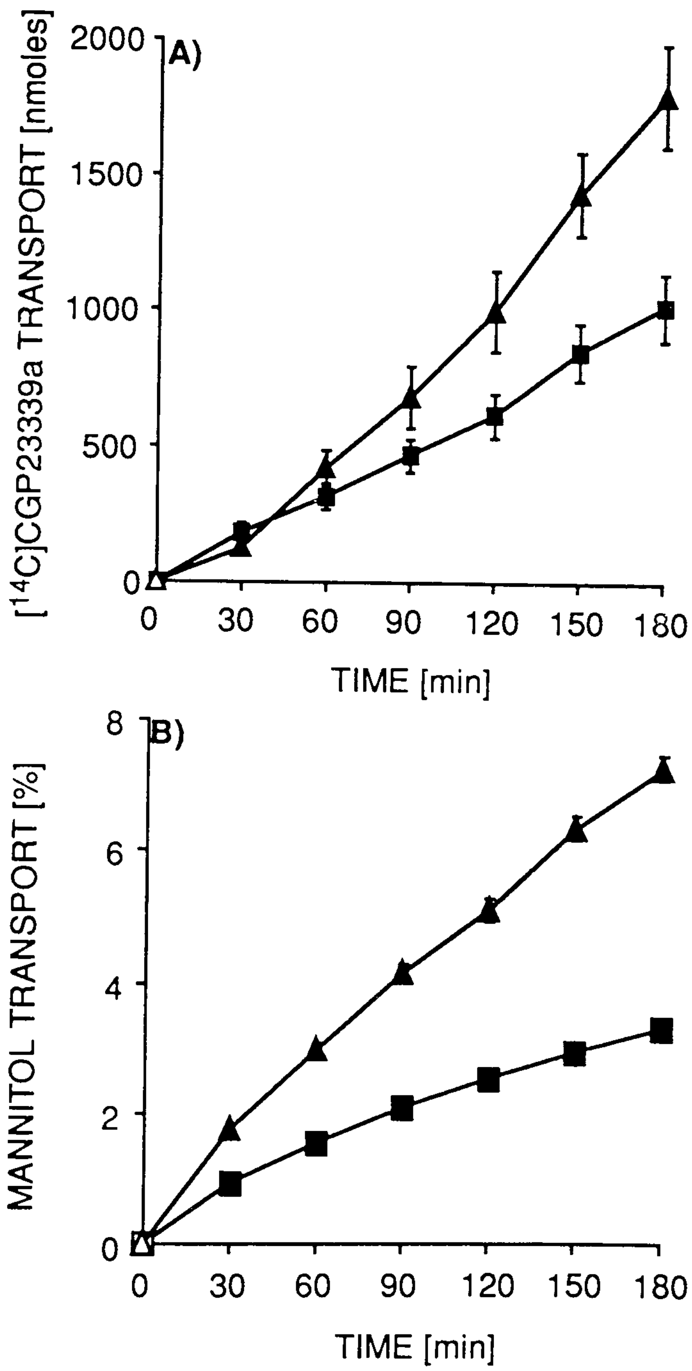

FIGURE 7.9 *Oral bioavailability predictions from the apparent permeability coefficients of CGP23339a transport across the conventional and minimum calcium Caco-2 monolayer models.*

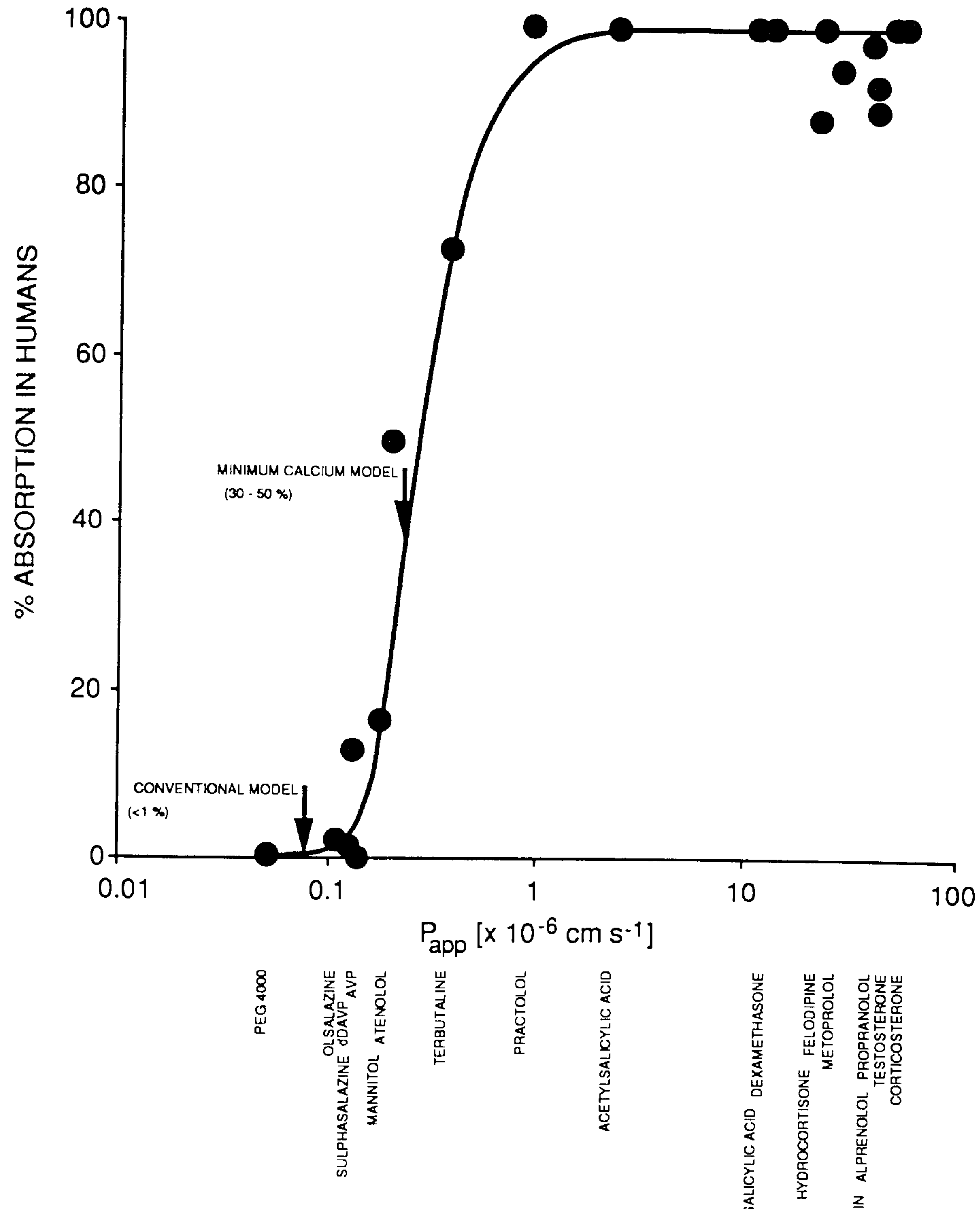

TABLE 7.1 *Comparative effect of calcium concentration and distribution on CGP23339a and D-mannitol transport across Caco-2 monolayers.*

Data are presented as mean values ± SD for three monolayers. * and ** Denote significant difference from control values at p<0.05 and p<0.001, respectively.

CONDITIONS Ap	CONDITIONS Bl	MANNITOL TRANSPORT [% h^{-1}] MEAN±SD	CGP23339a TRANSPORT [% h^{-1}] MEAN±SD	RATIO
+Ca	+Ca	0.910±0.047	0.186±0.048	4.892
-Ca	-Ca	13.533±0.847**	12.557±0.442**	1.078
-Ca	100μM Ca	1.108±0.033*	0.358±0.042*	3.095

TABLE 7.2 *Effect of Ap CGP23339a on the permeability of Caco-2 monolayers.*

Data are presented as mean values ± SD for three monolayers. * and ** Denote significant reductions from reference values at p<0.05 and p<0.001, respectively.

CONDITIONS Ap	CONDITIONS Bl	CGP23339a CONCENTRATION [μM]	TER [Ω cm^2] MEAN±SD
+Ca	+Ca	50	437.1±28.6
-Ca	-Ca	50	94.0±14.1**
+Ca	100μM Ca	50	417.8±12.3
-Ca	100μM Ca	50	415.2±15.1
+Ca	100μM Ca	5000	446.5±15.4
-Ca	100μM Ca	5000	327.4±13.6*

7.5 DISCUSSION

The GI epithelium comprises a single sheet of closely opposed cells which are joined at their lateral surfaces by inter-cellular junctional complexes. Drug molecules may traverse the GI epithelium by transcellular (across cell membranes) and/or paracellular (between cells) pathways which operate in parallel. Lipophilic permeants readily partition into lipid membranes and are absorbed transcellularly. However, many hydrophilic compounds will not partition readily into cell membranes and are excluded from this pathway. The alternative paracellular route presents a much lower surface area compared to the transcellular route and is gated by tight junctions. Nevertheless, the paracellular pathway is thought to be an important route for drug absorption from the GI tract.

The junctional complexes between cells are the mainstay of an intact epithelium. They have three components, the tight junction, intermediate junction and desmosomes. The tight junction is the most apically positioned component and penetration studies have shown that it is responsible for restricting diffusion between cells. The tight junction has a fundamental role in governing the transepithelial transport of permeants across an epithelial barrier. It contributes to the transepithelial permeability barrier by regulating the diffusional resistance to permeants through the paracellular pathway. It also has a crucial role in the organisation of the transcellular pathway since it is involved in the polarisation of the epithelial plasma membrane into distinct apical and basolateral domains. Moreover, the polarised distribution of nutrient-transporters is responsible for vectorial nutrient transport and ion channels are important for cellular and epithelial homeostasis.

The importance of calcium ions in the maintenance of epithelial tight junctions is well recognised [Gumbiner, 1987; Cereijido *et al.*, 1988]. Indeed, the integrity of Caco-2 monolayers is dependent upon extracellular calcium ions. The selective calcium chelator, ethylene glycol-*bis*-(ß-aminoethyl ether)-*N, N, N', N'*-tetra acetic acid (EGTA, 2.5 mM Ap and Bl), decreases the TER across Caco-2 monolayers by approximately 75% [Artursson and Magnusson, 1990]. Since TER predominantly reflects the resistivity across tight junctions rather than the cell membranes [Madara, 1983; Grassett *et al.*, 1984] this indicates that EGTA disrupts inter-cellular contacts. The present work shows that under uniform calcium-free conditions the permeability of Caco-2 monolayers towards D-[^{3}H]mannitol and [^{14}C]PEG$_{4000}$ is markedly increased and the post-transport TER is substantially decreased.

To investigate the influence of calcium and magnesium ions on the absorption of CGP23339a, its transport across an equivalent permeability barrier in the presence and total absence of these ions should be compared. However, this approach is not feasible because tight junctional integrity is reliant on extracellular calcium ions. In this study, a minimum calcium Caco-2 model was developed which displayed equivalent permeability properties to the conventional model but was maintained by a minimal calcium concentration with an optimal distribution.

Although Caco-2 monolayer integrity was disrupted under uniform calcium-free conditions, it was maintained after the unilateral removal of calcium ions from the Ap surface. This phenomenon has been confirmed in independent laboratories. Interestingly, TER is not maintained following the unilateral removal of calcium from their Bl surface [Dr Barry Hirst, University of Newcastle upon Tyne; personal communication]. This polar requirement for calcium ions is further corroborated by the greater sensitivity of Caco-2 monolayers towards basolaterally applied EDTA [Noach *et al.* 1992]. In these studies, the effectiveness of 2.5 mM EDTA in reducing the TER, and increasing the flux of permeability markers across Caco-2 monolayers was (Ap+Bl) > Bl > Ap.

The tight junction itself seems not to be directly dependent upon calcium ions. For instance, the treatment of a tight junction-enriched liver membrane preparation with a calcium chelator at 37°C failed to dissociate tight junctions [Stevenson and Goodenough, 1984]. However, other junctional components have been shown to be sensitive to extracellular calcium-depletion including the intermediate junction [Volberg *et al.*, 1986], the desmosomes [Watt *et al.*, 1984] and the adhesion molecule, uvomorulin [Gumbiner and Simons, 1987]. Therefore, although the integrity of epithelial tight junctions is known to be dependent on extracellular calcium ions, this dependence probably results indirectly *via* calcium effects on other structural elements of the junctional complex. In the Gumbiner model [Gumbiner, 1987], tight junction formation between two apolar cells is initiated by uvomorulin-mediated cell-to-cell adhesion. This cell-to-cell contact stimulates the formation of intermediate junctions between cells at their Ap poles. In turn, the intermediate junction provide the necessary adhesion contacts for tight junction assembly. In this model the opening of tight junctions by the removal of extracellular calcium results from a loss of calcium-dependent uvomorulin-mediated cell adhesion. This suggests that the loss of monolayer integrity upon calcium removal occurs *via* a cascade of events which are initiated at cell-to-cell contacts between the lateral membranes below the tight junctions. Since the apically positioned tight junction is the diffusion limiting component of the junctional complexes between cells, basolateral calcium ions have free access to the uvomorulin cell-adhesion molecules. Therefore, basolateral calcium alone would be expected to maintain Caco-2 monolayer integrity. In the presence of Ap calcium ions alone, the access of calcium ions to the uvomorulin cell-adhesion molecules is restricted by the tight junctions between cells. Consequently, the calcium requirement of the lateral cell-to-cell contacts would not be satisfied and would ultimately result in the loss of tight junction integrity. Therefore, as the calcium-dependent cell-to-cell contacts occur on the lateral surfaces of cells below the tight junctions this may explain the polarised requirement of integral Caco-2 monolayers for calcium ions. Therefore, the polarised requirement of Caco-2 cells for calcium ions is consistent with this Gumbiner model for the maintenance of tight junctions.

Calcium flux across Caco-2 monolayers cultured on polycarbonate permeable-supports has been characterised previously [Giuliano and Wood, 1991]. It is described by a saturable carrier-mediated component (K_m = 2.9±1.0 mM; V_{max} = 1.4±0.1 nmol min^{-1} (4.7 cm^2)$^{-1}$) superimposed onto non-saturable diffusional flux (K_d = 0.13±0.2 nmol min^{-1} (4.7 cm^2)$^{-1}$ mM^{-1}). Assuming the diffusional component to be non-vectorial, it is possible to extrapolate the levels of calcium expected to enter the Ap donor solution as a function of incubation time. For a 1260 μM Bl-to-Ap calcium gradient, the calcium concentration in the Ap donor solution would be 14.7 μM after 180 min. The calculation assumes that the carrier-mediated pathway does not re-cycle calcium back to the receiver-solution. This assumption is reasonable since the high affinity of CGP23339a for calcium means that it will sequestrate calcium away from the relatively low affinity carrier-mediated transport pathway. Clearly, with an initial concentration of 50 μM CGP23339a, a final calcium concentration of 14.7 μM may lead to an appreciable proportion (up to 29.4 %) of the permeant being chelated to calcium ions. Ap-to-Bl flux of magnesium ions would further increase the divalent metal cation concentrations in the Ap donor solution. The appearance of appreciable concentrations of calcium and magnesium ions in the Ap donor-solution would complicate interpretation of the transport data. In order to minimise the Bl-to-Ap flux, the minimum concentration of calcium required in the Bl receiver-solution to maintain monolayer integrity was titrated. A half-maximal decrease in Caco-2 monolayer permeability indices occurred between 15 and 20 μM. This is comparable to values of 50 μM and 100 μM reported for MDCK [Martinez-palomo *et al.*, 1980; Vega-Salas *et al.*, 1987] and LLC-PK_1 [Rabito *et al.*, 1986] monolayers, respectively. At 100 μM Bl calcium concentration all permeability indices were consistently indistinguishable from control levels and this concentration was used in the minimum calcium model. For a 100 μM Bl-to-Ap calcium gradient, the final calcium concentration in the donor solution after 180 min would be 1.2 μM. Therefore, in the minimum calcium model, the calcium concentration in the donor solution would remain much lower than that of CGP23339a. Consequently, in the minimum calcium model CGP23339a would remain overwhelmingly in the unchelated form and the interpretation of the transport data is simplified. This analysis of anticipated Bl-to-Ap calcium flux as a function of Bl calcium concentration highlights the importance of developing the minimum calcium model for these studies.

In the conventional Caco-2 transport model, the apparent permeability coefficient for CGP23339a of $7.90 \pm 0.68 \times 10^{-8}$ cm s^{-1} predicts an oral bioavailability of less than 1% in humans according to the correlation described by Artursson and Karlsson [1991] (Fig. 7.9). This agrees with its oral bioavailability of 0.3% in patients with breast cancer and bone metastases [Daley-Yates *et al.*, 1991]. Similarly, the estimated oral bioavailability (relative to the subcutaneous route) for CGP23339a administered to rats in their powdered food diet containing 0.4% calcium was 0.2% [Reitsma *et al.*, 1983]. Despite this low bioavailability in rats, the chronic oral administration of CGP23339a (1.5 to 2 years) resulted in a dose-dependent maintenance of metaphyseal bone. This indicates that in rats, a pharmacodynamic effect can be achieved following the oral administration of CGP23339a. However, such a low oral bioavailability would present potential problems with intra- and inter-patient variability in absorption resulting in unpredictable and highly variable plasma levels. Therefore, if an oral dosage form is to be feasible, a much higher oral bioavailability would be required. In the minimum calcium model, the apparent permeability coefficient of $2.11 \pm 0.25 \times 10^{-7}$ cm s^{-1} predicts a much greater oral bioavailability of between 30 and 50%. Moreover, this level of increased permeability was specific to CGP23339a. Whilst CGP23339a transport was increased 1.92-fold under minimum calcium conditions, D-mannitol flux was increased only 1.22-fold. Correspondingly, the ratio D-mannitol to CGP23339a flux in the conventional and minimum calcium models decreased from 4.892 to 3.095. These observations suggest that an interaction between calcium and/or magnesium ions and CGP23339a is a limiting factor in its transepithelial transport. There are a number of precedents for the absorption of drug molecules being limited by chelation with di- and trivalent metal cations in the lumen of the GI tract. For instance, the oral bioavailability of tetracycline [Neuvonen and Turakka, 1974] and quinolone [reviewed by Lomaestro and Bailie, 1991] antibiotics is reduced by co-administration with calcium, magnesium, aluminium and ferrous ions. Similarly, levadopa and methyldopa have been shown to complex with ferric ions and their absorption is reduced by the co-administration of ferrous gluconate or ferrous sulphate tablets [Campbell *et al.*, 1988; Campbell and Hasinoff, 1989]. Typically, absorption problems caused by chelation phenomena are circumvented by avoiding the co-administration of the drug and interacting ion(s). Therefore, preventing CGP23339a chelation with calcium and magnesium ions in the lumen of the GI tract may substantially improve its absorption and result in an acceptable oral bioavailability. This could possibly be achieved by simply avoiding co-administration with these ions or more likely by developing a formulation for CGP23339a which maintains a local environment of low calcium and magnesium ions in the GI lumen.

D-mannitol flux and TER measurements show that 5 mM CGP23339a non-specifically increases the permeability of the minimum calcium Caco-2 model. This raises a question about its safety after oral administration, particularly with chronic therapy. This concern may be especially pertinent for a formulation which maintains a low local calcium and/or magnesium concentration in order to facilitate absorption. The absorption enhancing effects of calcium-binding agents (*eg:* Na_2EDTA) is well-recognised. At concentrations of 1 to 7 % w/v, Na_2EDTA enhances the colonic absorption of cefoxitin [Nishihata *et al.*, 1985], and fosfomycin [Ishizawa *et al.*, 1987] in rats. Its mechanism of action was attributed to calcium complexation leading to increased permeability of the paracellular transport pathway. The effects of EDTA on intestinal drug absorption are non-specific and associated with mucosal damage [Nakanishi *et al.*, 1983]. CGP23339a has been shown to increase the rectal absorption of cefoxitin in rats [van Hoogdalem *et al.*, 1989]. Aqueous solutions of CGP23339a at concentrations of 0.5 to 6% w/v (13.6 to 162.6 mM) increased the absorption of cefoxitin from 14±12% to a maximum of 85±10% at 4% w/v (108.4 mM). In the Caco-2 system, an absorption-promoting effect was observed at concentrations of 5 mM which is lower than the minimal effective concentration in animal experiments. This was probably a result of the Caco-2 monolayers operating under minimum calcium conditions. The absorption promoting effect of CGP23339a *in vivo* was attributed to its ability to chelate calcium ions and increase the paracellular permeability. The prevention of a 5 mM CGP23339a induced decrease in TER across the minimum calcium model by using M4-medium (1260 μM calcium) as the donor solution supports that hypothesis.

Progress in understanding the influence of drug complexation with di- and trivalent metal cations has been restricted by the lack of a suitable *in vitro* experimental model. Indeed, the retardation of drug absorption by its chelation with metal cations in the GI lumen has typically been discovered by a reduction in its clinical efficacy upon their co-administration. Subsequently, these observations are usually investigated clinically in human subjects by pharmacokinetic monitoring after administration of the drug alone or with metal cations. However, human studies are limited to well-characterised drug molecules and for logistical reasons cannot be used routinely. Alternatively, the influence of metal cations on drug absorption and the influence of chelators on metal cation absorption can be studied *in vivo* using whole animal absorption models. However, in both the clinical and *in vivo* approaches, absorption occurs from a poorly defined ionic environment. For example, physiological pools of ions may interact with the drug compound and may complicate the interpretation of absorption data. An *in vitro* model would potentially provide numerous advantages over clinical and *in vivo* experimental models. Firstly, the ionic environment could be highly controlled and optimised to study the effects of chelation on absorption. Secondly, an *in vitro* model could be used to study new chemical entities so that potential absorption interactions could be identified prior to the development of a drug candidate. Surprisingly, however, there are no reports in the literature of *in vitro* models which are suitable for studying the interactions between drugs and metal cations on transepithelial transport.

The ionic environment of Caco-2 cells can be modified without causing detrimental effects on the monolayer permeability properties. Indeed, the comparable transport of marker compounds (D-mannitol and PEG_{4000}) and TER across the conventional (1260 μM calcium Ap and Bl) and minimum calcium (0 μM and 100μM calcium at Ap and Bl surfaces, respectively) Caco-2 models suggests they have equivalent permeabilities. These two models have been successfully employed to compare the epithelial transport in the presence and absence of calcium and magnesium ions. The greater rate of Ap-to-Bl pamidronate transport from a calcium- and magnesium-free donor solution suggests these ions impair its absorption. This work highlights the potential of the Caco-2 transport model as an *in vitro* screen for absorption interactions between drug molecules and metal cations.

7.6 CONCLUSION

Calcium and magnesium ions in the Ap donor-solution retard the Ap-to-Bl transport of pamidronate across Caco-2 monolayers.

CHAPTER EIGHT

EFFECT OF SELF-EMULSIFYING OLEIC ACID-TWEEN 80 FORMULATIONS ON CACO-2 MONOLAYERS

ABSTRACT

The effect of self-emulsifying oleic acid-Tween 80 formulations on Caco-2 monolayer integrity has been investigated. Functional Caco-2 monolayer integrity was monitored by D-mannitol flux and TER measurements. Their morphological integrity was assessed by laser-scanning confocal microscopy and transmission electron microscopy.

Oleic acid-Tween 80 (10:1) formulations produced a dose-dependent disruption of Caco-2 monolayer integrity. A 0.25% v/v formulation produced a rapid and complete loss of the functional and morphological properties. At 0.1% v/v, functional integrity was retained despite minor changes in monolayer morphology.

The effect of 0.1% v/v and 0.25% v/v formulations having different oleic acid-Tween 80 ratios was investigated. The rate of monolayer disruption was increased as the oleic acid content increased. Furthermore, low concentrations of oleic acid alone (4 mM, comparable to its final concentration in the formulations) caused total disruption of integrity. In contrast, Tween 80 alone was well tolerated.

These data suggest that oleic acid-Tween 80 formulations were highly disruptive towards Caco-2 monolayers. This disruption was related to the oleic acid content of the formulation.

8.1 BACKGROUND

The oral administration of drugs is the favoured route in terms of patient acceptability, convenience and compliance. However, some drugs have low oral bioavailabilities. This may occur for a variety of reasons including binding within the GI-tract, luminal degradation, poor penetration of the intestinal epithelium and/or extensive first-pass elimination (see Fig. 1.1). For many peptide-like drug candidates, penetration of the GI-epithelium is thought to be a major obstacle to achieving systemic availability. Consequently, strategies for improving the epithelial transport of peptides have received considerable attention. One approach is to design prodrugs of peptides which are efficiently transported and are converted to the active agent post absorption [Bundgaard, 1992]. Similarly, reducing the hydrogen-bonding potential of peptides can promote epithelial transport [Burton, *et al.*, 1992]. Alternatively, methods of selectively lowering the physical barrier properties of the GI epithelium to facilitate peptide absorption have been investigated [van Hoogdalem *et al.*, 1989]. The latter potentially offers a general, rather molecule-specific, approach to enhancing peptide absorption.

Recently, patents have been published describing lipid-based formulations which are claimed to enhance the intestinal absorption of peptide and protein pharmaceuticals [Cho, 1987; Cho and Flynn, 1989 a]. Indeed, insulin formulated in these lipid-based systems has been used to control hyperglycaemia in human diabetic patients [Cho and Flynn, 1989 b]. A notable feature of the patented formulations is their complexity. Recently, a simple self-emulsifying formulation of oleic acid and Tween 80 has been shown to increase the bioavailability of human calcitonin after intra-colonic delivery to rats [Lowe *et al.*, manuscript in preparation].

In the present study, the influence of oleic acid-Tween 80 formulations on Caco-2 monolayer integrity was monitored using a passive transport marker (D-[^{14}C]mannitol), TER and morphological assessment using laser-scanning confocal microscopy and transmission electron microscopy.

8.2 MATERIALS

D-[^{14}C]mannitol (49.3 Ci mmol^{-1}) and [^{3}H]oleic acid (10.0 Ci mmol^{-1}) were purchased from New England Nuclear (Dupont, Germany). Oleic acid and Tween 80 were obtained from BDH (Poole, UK). C_6NBD-ceramide and propidium iodide were supplied by Molecular Probes (USA) and Sigma Chemical Company (UK), respectively. Permafluor mountant for fluorescent microscopy was purchased from Biogenesis Ltd. (Bornemouth, UK).

M5-medium comprised Hanks' balanced salt solution (HBSS) containing 0.01% phenol red and 5 mM D-glucose and was buffered to pH7.2 with 14 mM HEPES.

8.3 METHODS

8.3.1 EMULSION PREPARATION

Self-emulsifying formulations were prepared from various molar ratios of oleic acid and Tween 80. The molar ratios of oleic acid to Tween 80 were 20:1, 10:1, 5:1, 3:1 and 1:1 assuming a molecular weight of 1309 for Tween 80. For experiments, a stock emulsion was prepared by vortexing a 10% w/v formulation in M5-medium for 1 min. The pH of the resultant emulsion was restored to pH7.2 using 4 M sodium hydroxide with vortexing after each addition of base. The emulsion was finally vortexed for 5 min to ensure complete dispersion. Lower emulsion concentrations (1.0, 0.75, 0.50, 0.25, 0.10 and 0.01% w/v) were prepared by dilution of the stock emulsion.

8.3.2 DETERMINATION OF OLEIC ACID CONCENTRATION

The limited aqueous solubility of oleic acid made it difficult to produce solutions of precisely known concentrations. Therefore, [^{3}H]Oleic acid was used to determine the concentration of oleic acid in M5-medium. Briefly, 40ml of M5-medium, pH7.2, was vortexed with 10 ml of oleic acid containing 0.4 μCi ml^{-1} of [^{3}H]oleic acid. The pH of this mixture was restored to pH7.2 by the addition of 4 M sodium hydroxide. It was centrifuged at 3000 x g (Denley DR401, UK) for 5 min in a 50 ml plastic centrifuge tubes (Costar, UK) to separate organic and aqueous phases. The plastic tube was pierced using a needle and a volume of each immiscible phase was collected into a syringe. The [^{3}H]-content was determined in a 100 μl aliquot of each phase. The oleic acid concentration in M5-medium was calculated from the ratio of [^{3}H]oleic acid in these two phases. Several tubes were simultaneously prepared in an identical manner but without the addition of [^{3}H]oleic acid. The M5-medium phase was collected from these tubes and diluted to the concentration required for transport studies.

8.3.3 ASSESSMENT OF MONOLAYER INTEGRITY

8.3.3.1 *D-MANNITOL TRANSPORT*

To assess the influence of oleic acid-Tween 80 emulsions on the functional barrier properties of Caco-2 monolayers, the effect on the transport of D-[^{14}C]mannitol and TER were investigated. For transport experiments, Caco-2 monolayers were washed with M5-medium (1 x 2 ml (Ap + Bl) x 15 min) before a donor emulsion containing

0.25 μCi ml^{-1} of D-[^{14}C]mannitol, was applied to the Ap surface. The culture-insert was immediately placed into a Bl receiver-solution. Monolayers were continuously agitated using an orbital-shaker (60 rpm) inside an incubator at 37°C to maintain dispersion of the emulsion. Culture-inserts were sequentially transferred into a fresh receiver-solution after 15, 30, 60, 90 and 120 min.

8.3.3.2 *TRANSEPITHELIAL ELECTRICAL RESISTANCE*

TER was measured after a 30 min equilibration in TER-medium at 37°C as described previously (see section 2.5) using a heated microscope-slide drying stage to maintain a constant temperature.

8.3.3.3 *MICROSCOPY*

For morphological assessment of monolayer integrity by laser-scanning confocal microscopy Caco-2 monolayers were dual-labelled with fluorescent stains for cell lipids (C_6NBD-ceramide; green) and cell nuclei (propidium iodide; red) as described in section 7.3.4. XY confocal images represent an optical section in a plane across the Caco-2 monolayer at a depth (Z) having the greatest nuclear signal. The XZ confocal images represent a transverse section of Caco-2 monolayers in a vertical plane (Y=255). For transmission electron microscopy monolayers were processed and viewed as described in section 2.6.1.

8.4 RESULTS

The maximum Ap concentration of oleic acid-Tween 80 (molar ratio = 10:1) formulation that could be tolerated by Caco-2 monolayers was titrated with respect to D-[^{14}C]mannitol transport and post-transport TER values. The Ap formulation concentrations (0 (control), 0.01, 0.25, 0.5, 0.75, 1 and 10 % v/v) can be divided into two groups, one set maintained monolayer integrity whilst the second caused rapid and complete monolayer destruction (Fig. 8.1 A and B). At Ap concentrations of 0.1% v/v and below, D-mannitol fluxes were low over the 120 min experiment. The mean D-mannitol fluxes for 0 (control), 0.01 and 0.1 % v/v Ap formulations were 0.25±0.02, 0.26±0.02 and 0.40±0.07 % h^{-1}, respectively. Although the mean transport rate from the 0.1% v/v formulation was greater than control values it was not significantly different and was less than 1.0% h^{-1} which is generally accepted to indicate Caco-2 monolayer integrity [Hu and Borchardt, 1990]. Since D-mannitol flux is controlled by the intact monolayer rather than the permeable-support (see Chapter Three) these observations suggest that the barrier function of Caco-2 monolayers is maintained up to 0.1% v/v formulation. These observations were confirmed by 30 min post-transport TER measurements (Fig. 8.2). Caco-2 monolayers treated for 120 min with 0 (control), 0.01 or 0.1% v/v formulation all presented substantial post-transport TER values (421.5±25.1, 443.7±26.3 and 362.7±10.2 Ω cm^2, respectively) which were not significantly different. Since TER predominantly reflects resistance to ion flux through the paracellular pathway [Madara, 1983; Grassett *et al.*, 1984] these data suggest that for up to 0.1% v/v the inter-cellular contacts are retained. In contrast, at 0.25% v/v and above D-mannitol transport was rapidly and dramatically increased above control fluxes. The mean D-mannitol flux over 120 min from Ap 0.25% v/v formulation was 36.0±0.21 % h^{-1} which represented a 90.2- and 141.4-fold increase over the 0.1% v.v formulation and control values, respectively. D-mannitol flux is controlled by the intact monolayer rather than the permeable-support, therefore, these observations suggest that the barrier-function of Caco-2 monolayers is destroyed by Ap formulation concentrations of 0.25% and above. This was confirmed by 30 min post-transport TER values. After a 120 min exposure to 0.25% v/v formulation the TER of Caco-2 monolayers was reduced to 56.5±11.7 Ω cm^2 which was significantly lower than the control values (421.5±25.1 Ω cm^2; $p<0.001$) and was consistent with a loss of monolayer integrity. At concentrations above 0.25% v/v, the terminal rate of D-mannitol fluxes are identical. However, the rate onset for loss of monolayer integrity was dependent on the concentration of Ap formulation. Indeed, there was a log dose-% response (100% defined as the 10% v/v formulation D-mannitol flux at 15 min) relationship between the Ap formulation concentration and D-mannitol flux after 15 min with a half-maximal effect occurring at an approximate concentration of 0.5% v/v Ap formulation (Fig. 8.3).

The above experiments showed that there was a narrow window between maintenance of monolayer integrity and monolayer destruction for various Ap concentrations of the oleic acid-Tween 80 (10:1) formulation. The influence of formulation composition on this window was investigated by varying the oleic acid to Tween 80 ratio between 20:1 and 1:1. Monolayer integrity was maintained for both 0.1 and 0.25% v/v of the oleic acid-Tween 80 1:1 formulation. For all other formulation compositions, the 0.25% v/v Ap concentration produced a greater rate of loss of monolayer integrity than the 0.1% v/v formulation with respect to D-[^{14}C]mannitol flux. For both Ap concentrations, the flux of these permeability markers increased with increasing oleic acid composition of the formulation (Fig. 8.4 A and B). These observations were confirmed by 30 min post-transport TER measurements (Fig. 8.5 A and B). The post-transport TER values for oleic acid-Tween 80 1:1 formulations at 0.1 and 0.25% v/v Ap concentrations were not significantly different to control values indicating that monolayer integrity was maintained. At higher oleic acid ratios, TER values were reduced. A 60 min exposure to 0.25% v/v Ap concentrations of the 3:1, 5:1, 10:1 and 20:1 formulations significantly reduced post-transport TER values (61.2±3.2, 76.8±4.4, 47.1±11.4 and 70.7±4.4 Ω cm^2, respectively; $p<0.01$) compared to control values (424.5±33.5 Ω cm^2). Meanwhile, a 120 min exposure to 0.1% v/v formulations produced a partial reduction in post-transport TER which was dependent on the formulation composition. Post-transport TER values for 3:1, 5:1, 10:1 and 20:1 formulations were 326.4±55.6, 263.8±35.3 ($p<0.05$), 216.7±51.7 ($p<0.05$) and 166.3±9.7 ($p<0.01$) Ω cm^2, respectively. A 120 min exposure to 0.1% v/v formulation with a molar ratio of oleic acid to Tween 80 of 20:1, 10:1 and 5:1 produced a significant reduction in post-transport TER compared to control values. These data suggest that as the proportion of oleic acid in the formulation increased the post-transport TER value decreased.

In addition to the self-emulsifying formulations, oleic acid (0 to 4 mM) or Tween 80 (0 to 82.5 mM) alone were applied to the Ap surface of Caco-2 monolayers. For oleic acid concentrations up to 1 mM Ap-to-Bl D-mannitol fluxes were less than 1.0% h^{-1} suggesting that monolayer integrity was maintained. However, at 4 mM oleic acid D-mannitol flux increased dramatically (Fig. 8.6 A). These data are consistent with the 30 min post-transport TER values which show that a substantial electrical resistance is maintained up to 1 mM (488.3±55.0 Ω cm^2) and thereafter is significantly reduced (0 mM (control) = 387.6±35.4 Ω cm^2 versus 4 mM = 114.6±28.4 Ω cm^2; $p<0.01$; Fig. 8.6 B). In contrast, Tween 80 alone was tolerated at much higher Ap concentrations. For Ap concentrations between 0 (0.26±0.04 % h^{-1}) and 8.25 mM (0.29±0.05 % h^{-1}) the Ap-to-Bl D-mannitol flux was less than 1% h^{-1} and not significantly different from control values (Fig. 8.7 A). At 41.25 and 82.5 mM Tween 80 Ap concentrations D-mannitol flux were 1.19±0.29 ($p<0.05$) and 3.85±0.50 ($p<0.01$) % h^{-1} and significantly greater than control levels. Interestingly, the 30 min post-transport TER values up to 41.5 mM Tween 80 (329±48.9 Ω cm^2) were comparable to control monolayers (0% v/v 305.0±4.7 Ω cm^2). At 82.5 mM, post-transport TER was significantly reduced (255.0±17.8; $p<0.05$; Fig. 8.6 B).

The control samples at 30 (Fig. 8.8 A) and 60 (Fig. 8.8 B) min had typical Caco-2 monolayer appearance after dual-staining with C_6NBD-ceramide and propidium iodide. That is, there was a uniform presence of cell nuclei and the inter-nuclear distance was small and was stained green suggesting it to be lipid-filled. There were no gaps between cells. The XZ section of Fig. 8.8 B at Y=255 (Fig. 8.8 C) showed that the monolayer was continuous and the lipids were closely associated with the cell nuclei. Similarly, transmission electron microscopy of control monolayers (Fig. 8.9) showed a typical appearance. Cells were closely opposed and had a well developed brush-border of microvilli, a well defined nucleus and intra-cellular glycogen stores.

The XY confocal images of Caco-2 monolayers after a 30 (Fig. 8.10 A) and 60 (Fig. 8.10 B) min exposure to 0.1% v/v oleic acid-Tween 80 (10:1) emulsion in M5-medium were not visually different from control samples. That is, there was a high density of cell nuclei and the inter-nuclear spaces were lipid-filled. There were no apparent gaps between cells. Interestingly, the 30 min sample (Fig. 8.10 A) exhibits droplets which were stained green suggesting they had a lipidic nature. Although their spherical shape suggests they probably represent the dispersed-phase of the formulation, the possibility that they may be blebs of cellular material cannot be ruled out. The XZ section at Y=255, confirmed that the Caco-2 monolayer was continuous with no gaps between cells. However, the green lipid staining at the Ap surface was less regular and less closely associated with the cell nuclei indicating some perturbation of the Ap surface membrane. This was confirmed by transmission electron microscopy (Fig. 8.11 A and B). Figure 8.11 A shows that after a 30 min exposure to 0.1% v/v formulation there was extensive denudation of microvilli and blebbing at the Ap surface. In addition, numerous vacuoles were present just below the Ap surface. Figure 8.11 B shows a region displaying more extensive blebbing. In both cases there was no evidence for separation of inter-cellular contacts.

The XY confocal images following exposure to 0.25% v/v formulation for 30 (Fig. 8.12 A) and 60 (Fig. 8.12 B) min are visually different from control samples. After 30 min, numerous cells were present on the permeable-support. However, the inter-nuclear distance was greater than in the control sample and regions of no staining between cells suggests inter-cellular contacts had been disrupted. After 60 min, there was considerable cell-loss from the permeable-support and the aggregates of remaining cells were highly fluorescent. The large voids between the loose-clusters of cells indicates a complete loss of monolayer integrity. This was confirmed by XZ sections at Y=255 which shows small groups of cells separated by large gaps (Fig. 8.12 C). The thin layer of green stain adjacent to the permeable-support region probably represents lipidic cell debris. Figures 8.13 A and B show the ultrastructural effects of 0.25% v/v formulation on Caco-2 monolayers after 15 and 60 min exposures, respectively. After a 15 min exposure, the Ap microvilli were very irregular, there was cell debris in the Ap region and there were numerous vacuoles beneath the brush-border. In addition, lateral intercellular gaps were apparent and were filled with droplets and cell debris. This probably represent an early stage in cell separation during the loss of monolayer integrity. After 60 min (Fig. 8.13 B), only cell debris was associated with the permeable-support.

FIGURE 8.1 *Effect of oleic acid-Tween 80 (10:1) formulation on D-mannitol transport.*

Caco-2 monolayers were washed (1 x 2 ml (Ap + Bl) x 15 min) with M5-medium before various concentrations of oleic acid-tween 80 formulation were applied to their Ap surface. **(A)** shows Ap-to-Bl D-mannitol transport for 0 (control), 0.25, 0.5, 0.75, 1 and 10% v/v Ap formulation concentrations. **(B)** represents an expanded scale for 0, 0.01 and 0.1% v/v concentrations. Data are presented as mean values ± SD for three monolayers.

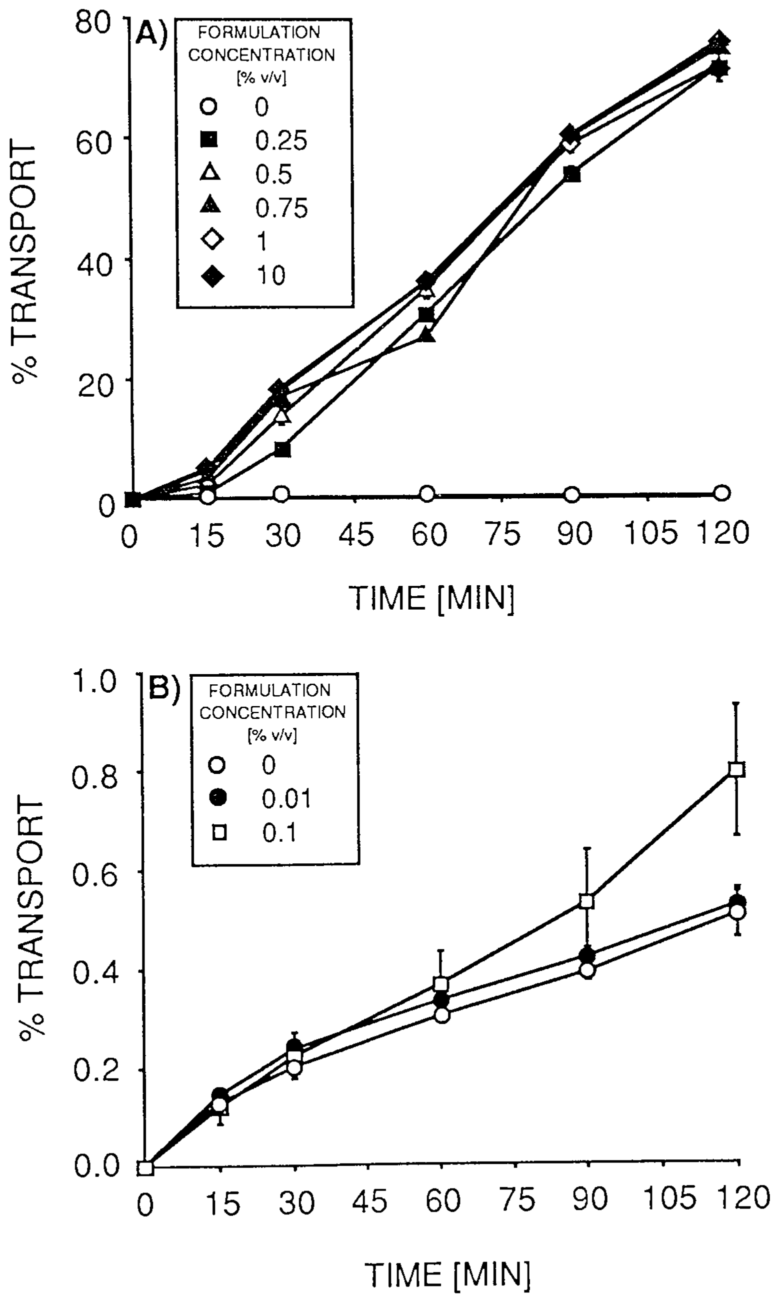

FIGURE 8.2 *Effect of oleic acid-Tween 80 (10:1) formulation on post-transport TER values.*

Caco-2 monolayers were washed (1 x 2 ml (Ap + Bl) x 15 min) with M5-medium then incubated with various concentrations of oleic acid-tween 80 (10:1) formulation. After 120 min the formulation was removed and replaced with TER-medium. TER was measured following a 30 min equilibration to 37°C. Data are presented as mean values ± SD for three monolayers. * Denotes a significant reduction from control values.

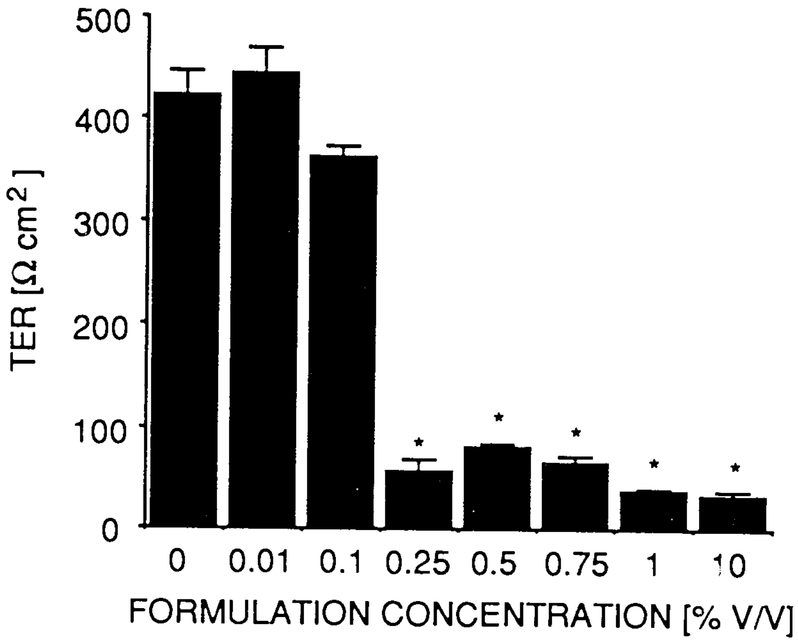

FIGURE 8.3 *A dose-response for the initial effect of oleic acid-Tween 80 (10:1) formulation on D-mannitol transport.*

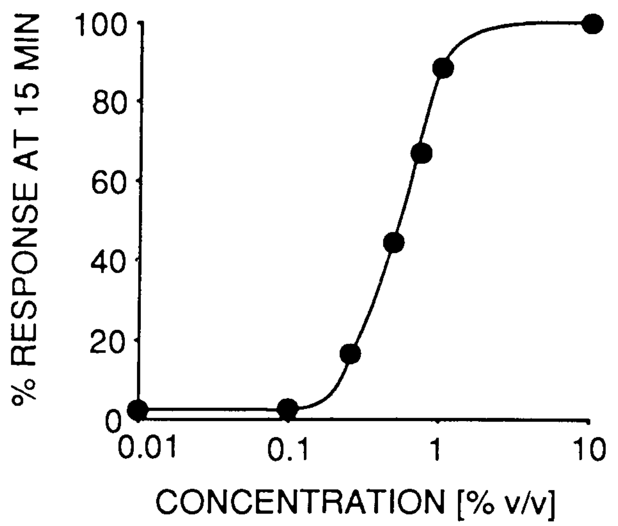

FIGURE 8.4 *The influence of emulsion composition on D-mannitol transport.* Caco-2 monolayers were washed (1 x 2 ml (Ap + Bl) x 15 min) with M5-medium before 0.25% v/v (**A**) or 0.1% v/v (**B**) formulation was applied to their Ap surface. The formulations were comprised 20:1, 10:1, 5:1, 3:1 and 1:1 molar ratios of oleic acid to Tween 80. Data are presented as mean ± SD for three monolayers.

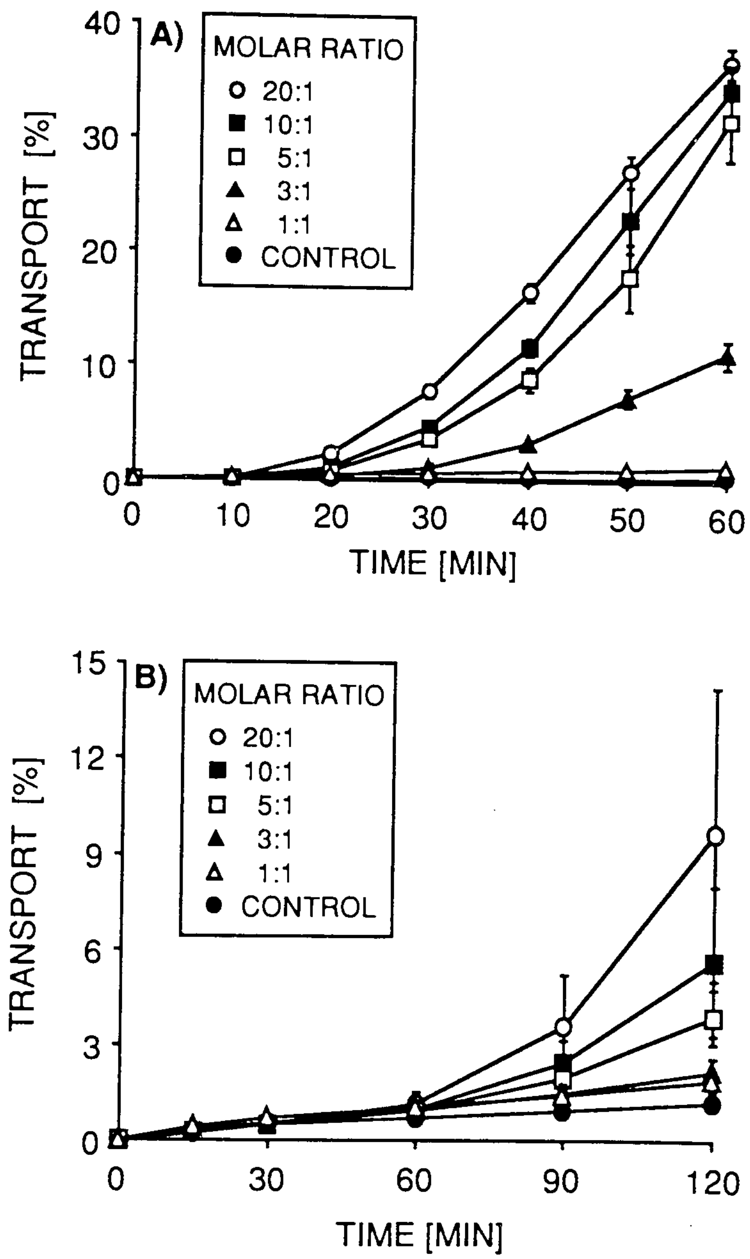

FIGURE 8.5 *The influence of emulsion composition on post-transport TER.* Caco-2 monolayers were washed (1 x 2 ml (Ap + Bl) x 15 min) with M5-medium then incubated with 20:1, 10:1, 5:1, 3:1 and 1:1 oleic acid-Tween 80 molar ratio formulations. Monolayers were exposed to 0.25% formulations for 60 min (**A**) or 0.1% v/v formulations for 120 min (**B**) before their 30 min post-transport TER was determined. *, ** and *** Denote significant reductions from control values at $p<0.05$, $p<0.01$ and $p<0.001$, respectively.

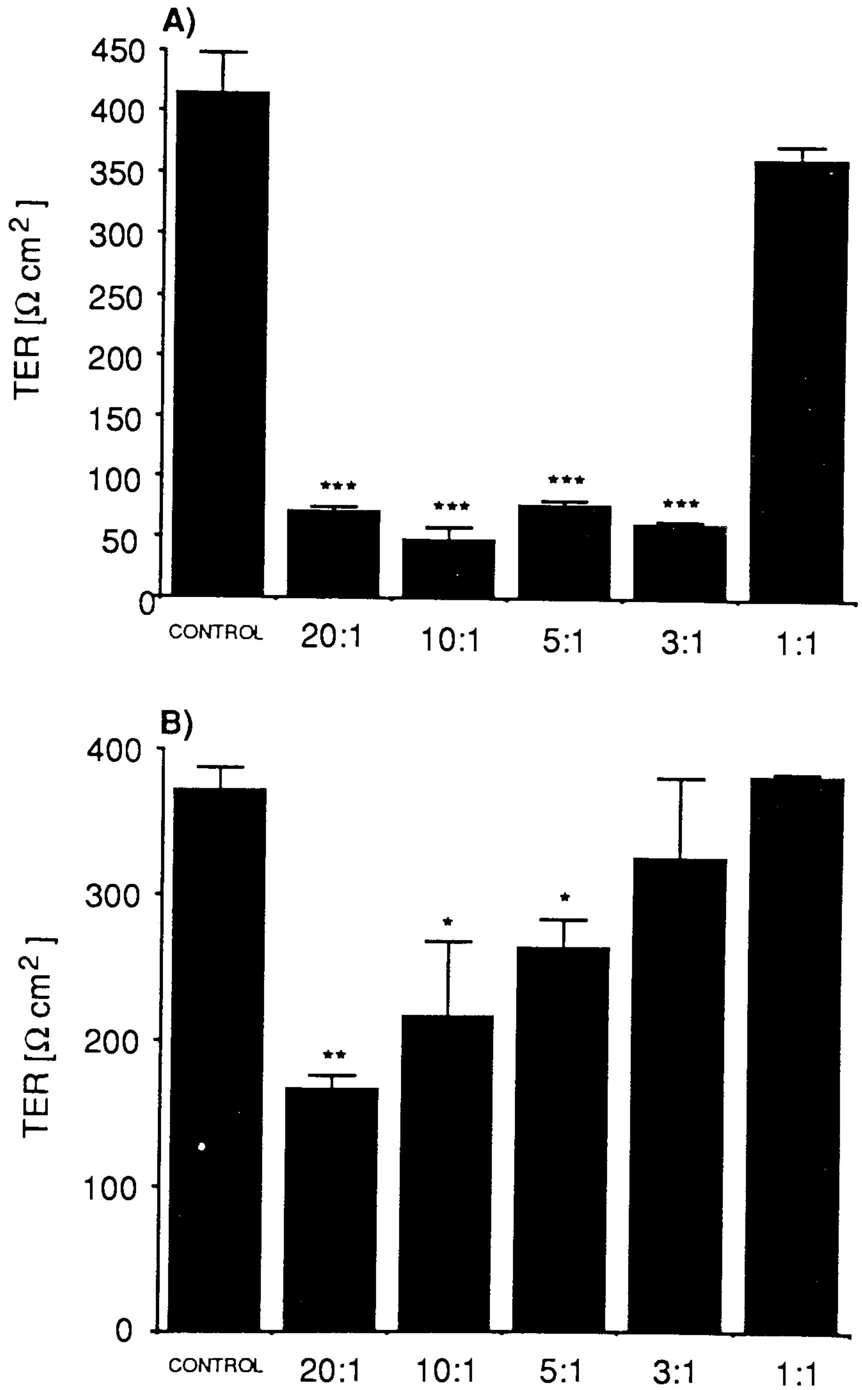

FIGURE 8.6 *The influence of oleic acid on Caco-2 monolayer integrity.*
Caco-2 monolayers were washed (1 x 2 ml (Ap + Bl) x 15 min) with M5-medium before the Ap-to-Bl transport of D-mannitol was determined from an Ap solution containing 0 (control), 0.001, 0.01, 0.1, 1 or 4 mM oleic acid (A). The 30 min post-transport TER was determined for each oleic acid concentration. * Denotes a significant reduction in post transport TER from control values at $p<0.05$. Data are expressed as mean values ±SD for three monolayers.

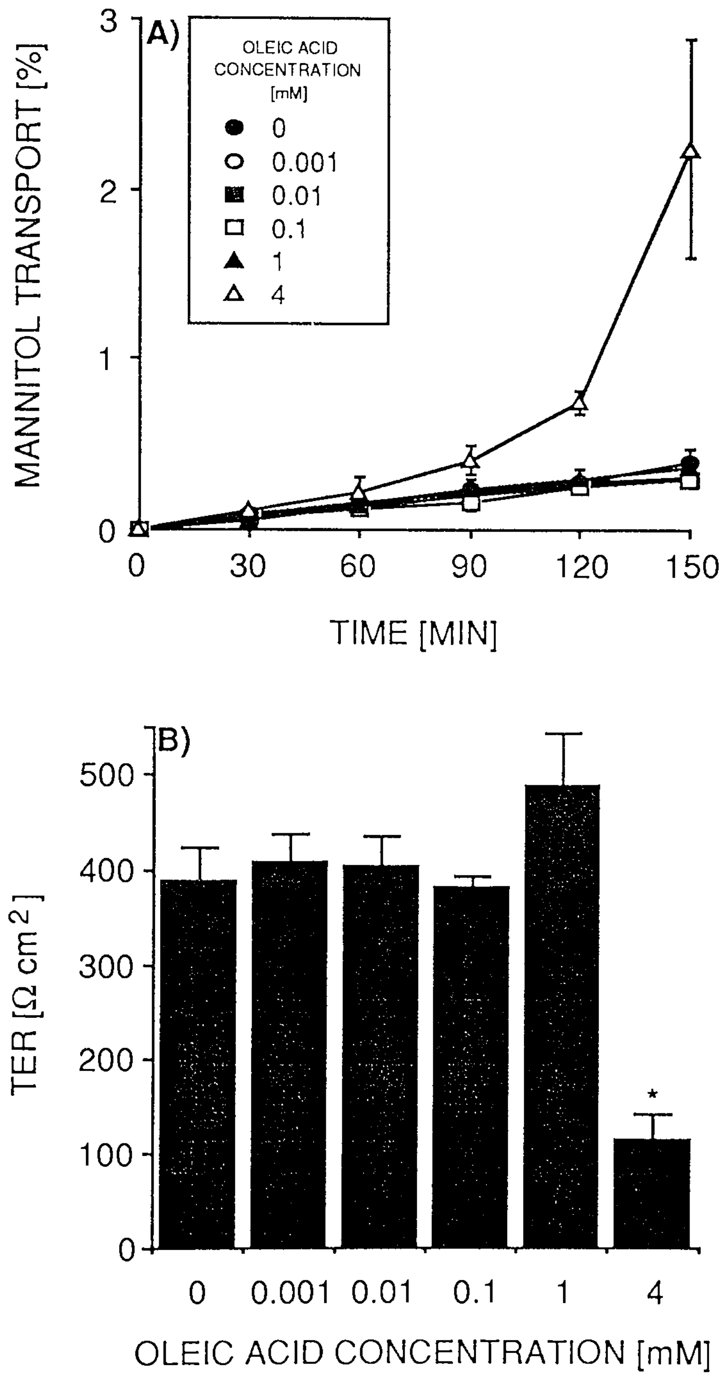

FIGURE 8.7 *The influence of Tween 80 on Caco-2 monolayer integrity.*
Caco-2 monolayers were washed (1 x 2 ml (Ap + Bl) x 15 min) with M5-medium before the Ap-to-Bl transport of D-mannitol was determined from an Ap solution containing 0 (control), 0.0825, 0.825, 8.25, 41.25 and 82.5 mM (**A**). The 30 min post-transport TER was determined for each Tween 80 concentration (**B**). Data are expressed as mean values ±SD for three monolayers.* and ** Denotes a significant difference from control values at $p<0.05$ and $p<0.001$, respectively.

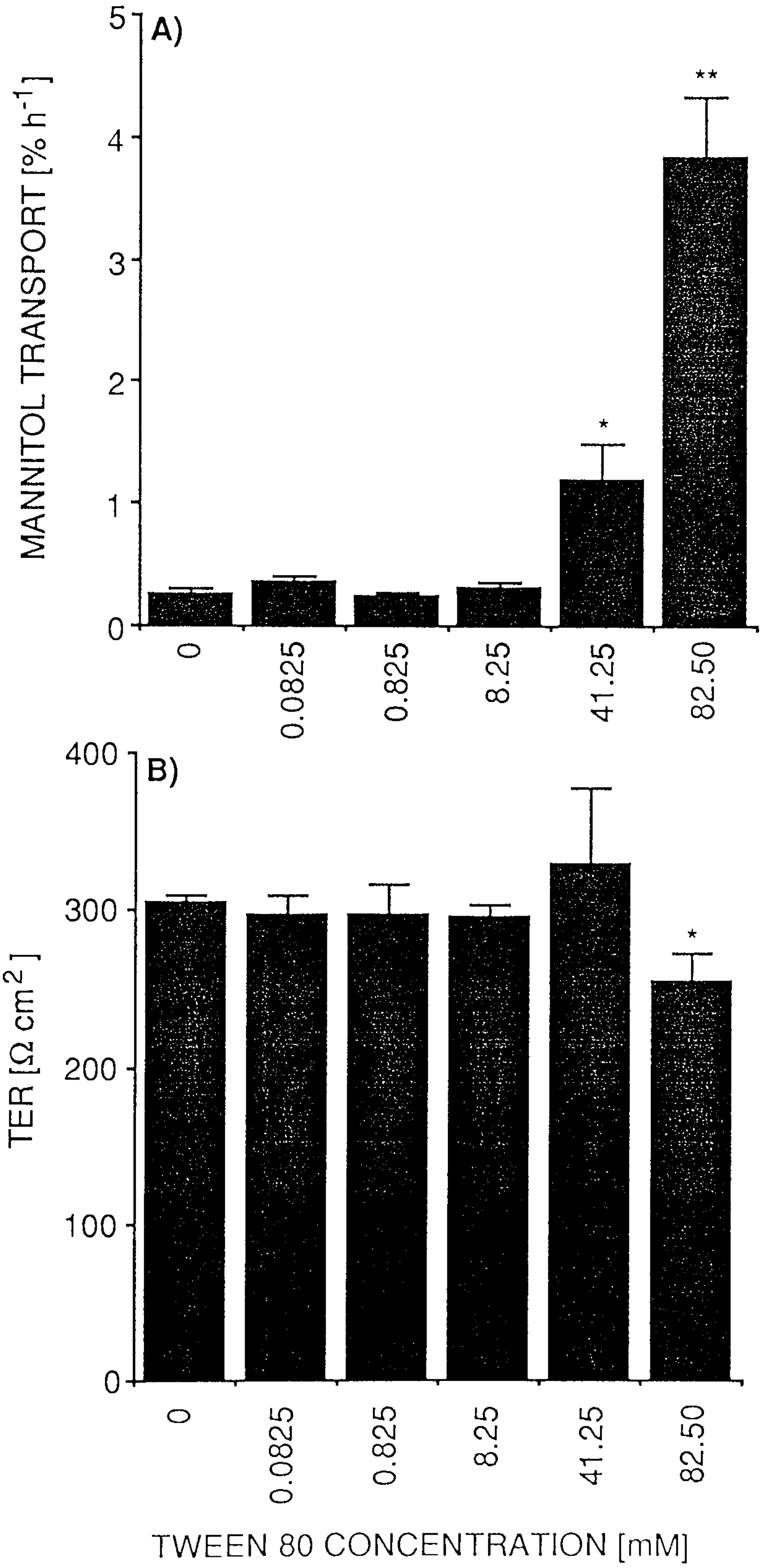

FIGURE 8.8 *Confocal laser-scanning micrographs of control Caco-2 monolayers.* Caco-2 monoloayers were washed (1 x 2 ml (Ap + Bl) x 15 min) with M5-medium before being incubated for 30 min (**A**) or 60 min (**B**,**C**) with M5-medium. The monolayers were fixed, then stained with C_6NBD-ceramide (green, lipids) and propidium iodide (nuclei, red). **A** and **B** represent XY images and **C** is an XZ image of **B** at Y=255. Scale bar = 25 μm.

A)

B)

C)

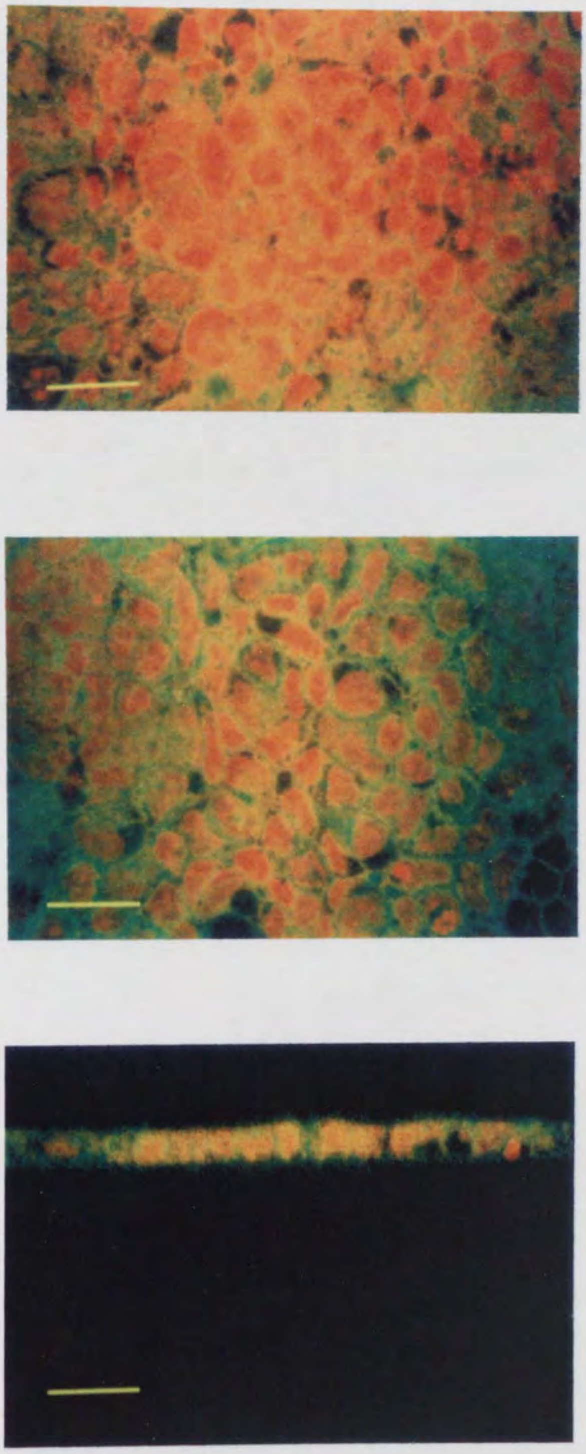

FIGURE 8.9 *Transmission electron micrograph of control Caco-2 monolayers.* Caco-2 monolayers were washed (1 x 2 ml (Ap + Bl) x 15 min) with M5-medium before being incubated for 30 min with M5-medium. MV = Microvilli, N = Nucleus and G = Glycogen. Magnification = x 8722, scale bar = 1.1 μm.

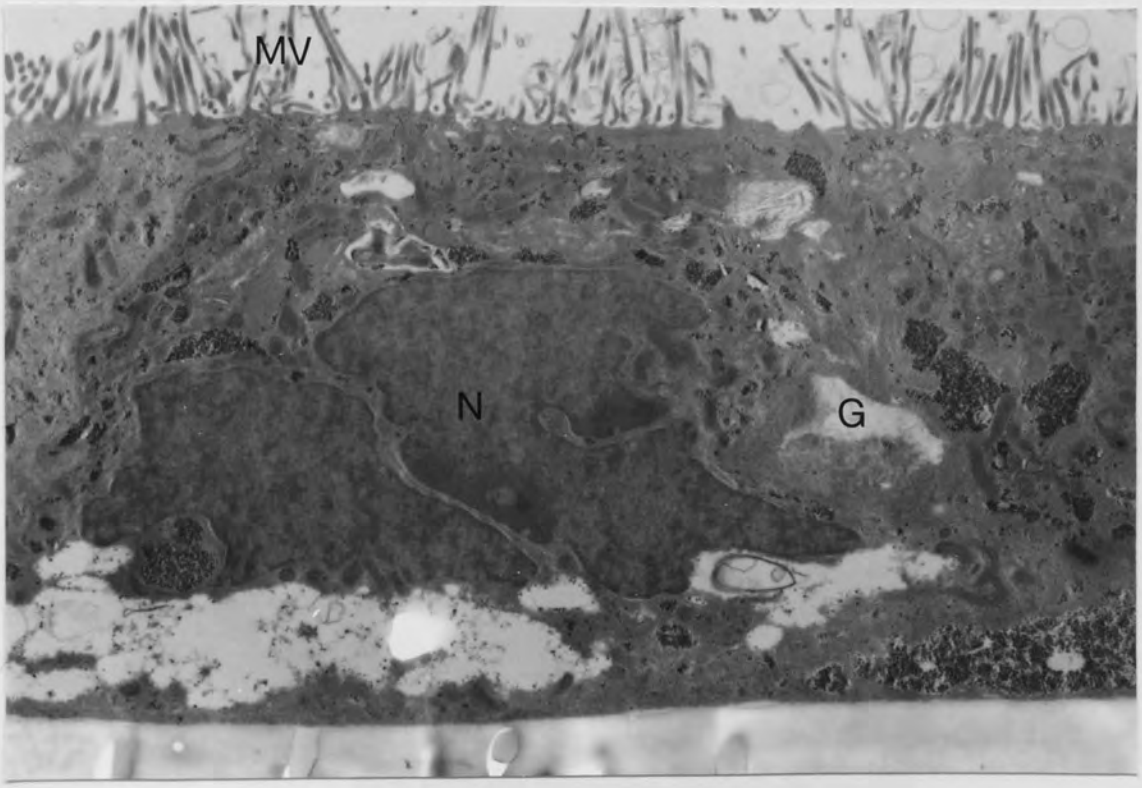

FIGURE 8.10 *Confocal laser-scanning micrographs of Caco-2 monolayers after exposure to 0.1% v/v oleic acid-Tween 80 (10:1) formulation.*

Caco-2 monoloayers were washed (1 x 2 ml (Ap + Bl) x 15 min) with M5-medium before being incubated for 30 min (**A**) or 60 min (**B**,**C**) with M5-medium containing 0.1% v/v oleic acid-Tween 80 (10:1) formulation. The monolayers were fixed, then stained with C_6NBD-ceramide (green, lipids) and propidium iodide (nuclei, red). **A** and **B** represent XY images and C is an XZ image of **B** at Y=255. Scale bar = 25 μm.

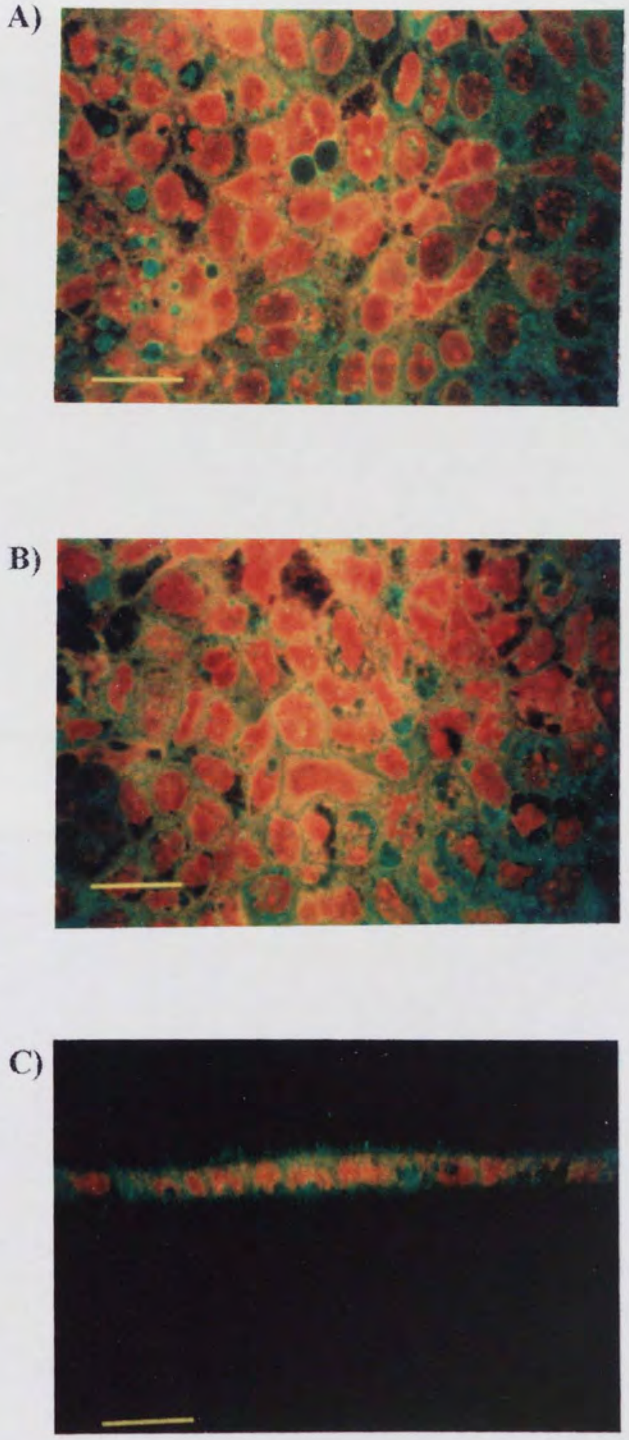

FIGURE 8.11 *Transmission electron micrographs of Caco-2 monolayers after exposure to 0.1% v/v oleic acid-Tween 80 (10:1) formulation.*

Caco-2 monolayers were washed (1 x 2 ml (Ap + Bl) x 15 min) with M5-medium before being incubated for 30 min with M5-medium containing 0.1% v/v oleic acid-Tween 80 (10:1) formulation. For **A** and **B** magnification = x 4933 and x 4967, respectively. Scale bar = 2 μm.

A)

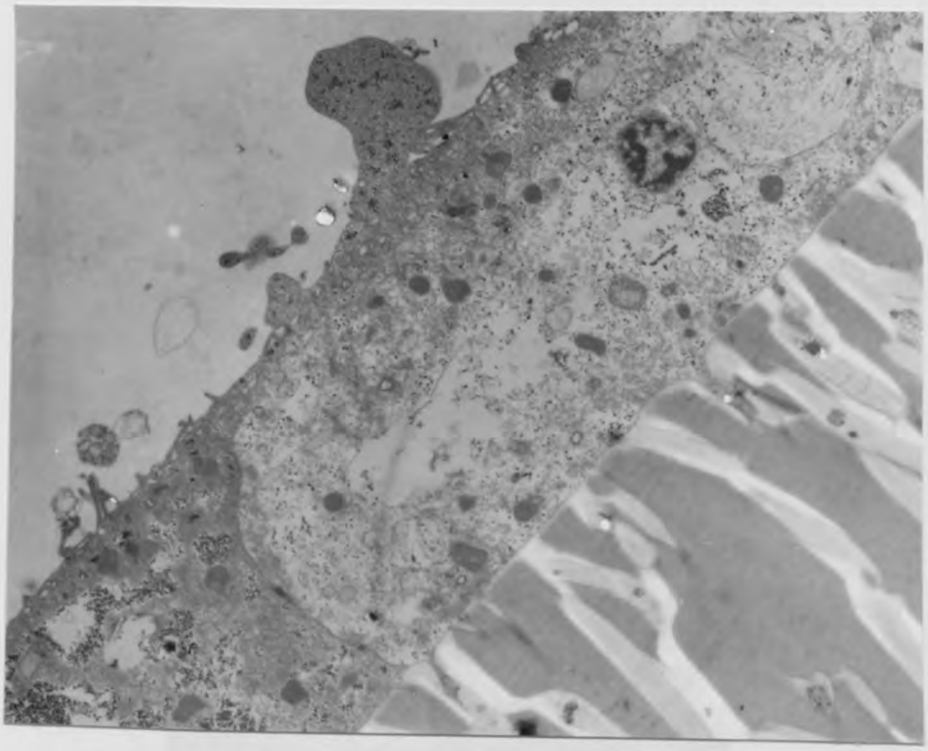

B)

FIGURE 8.12 *Confocal laser-scanning micrographs of Caco-2 monolayers after exposure to 0.25% v/v oleic acid-Tween 80 (10:1) formulation.*

Caco-2 monoloayers were washed (1 x 2 ml (Ap + Bl) x 15 min) with M5-medium before being incubated for 30 min (**A**) or 60 min (**B**,**C**) with M5-medium containing 0.25% v/v oleic acid-Tween 80 (10:1) formulation. The monolayers were fixed, then stained with C_6NBD-ceramide (green, lipids) and propidium iodide (nuclei, red). **A** and **B** represent XY images and C is an XZ image of **B** at Y=255. Scale bar = 25 μm.

A)

B)

C)

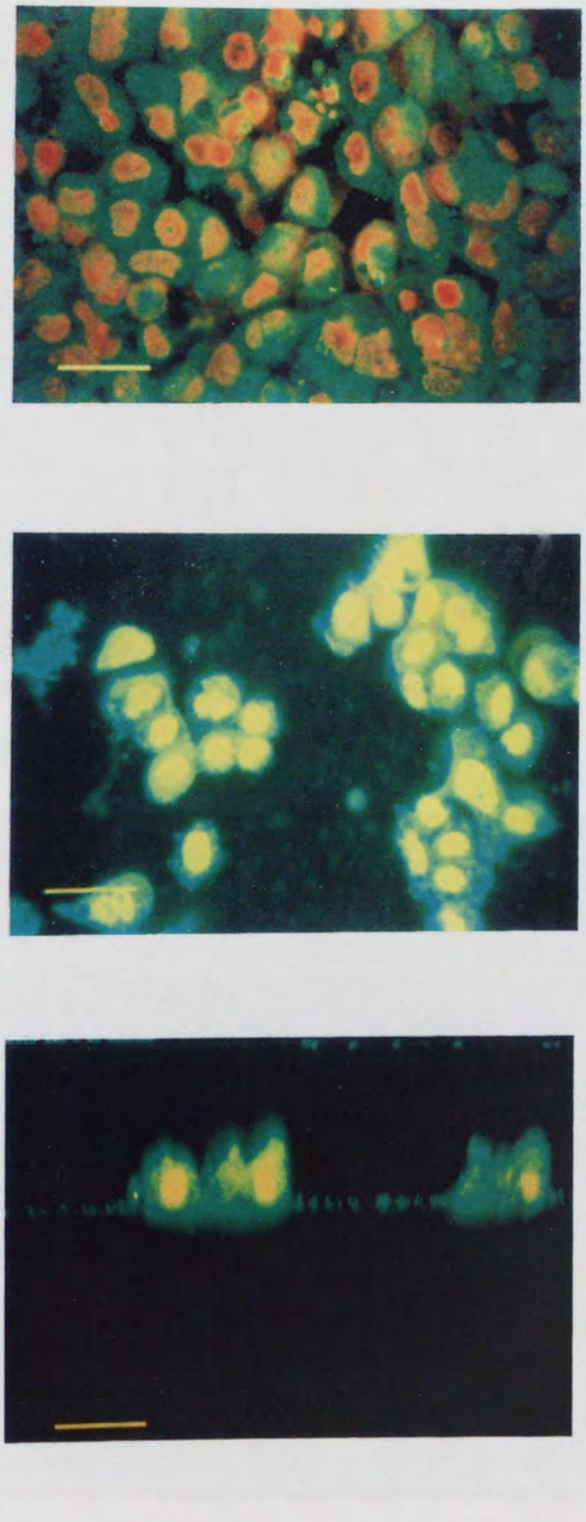

FIGURE 8.13 *Transmission electron micrographs of Caco-2 monolayers after exposure to 0.25% v/v oleic acid-Tween 80 (10:1) formulation.*

Caco-2 monolayers were washed (1 x 2 ml (Ap + Bl) x 15 min) with M5-medium before being incubated for 15 min (**A**) or 60 min (**B**) with M5-medium containing 0.25% v/v oleic acid-Tween 80 (10:1) formulation. For **A** and **B** magnification = x 4950 and x 8677 and scale bars = 2 μm and 1.1 μm, respectively.

A)

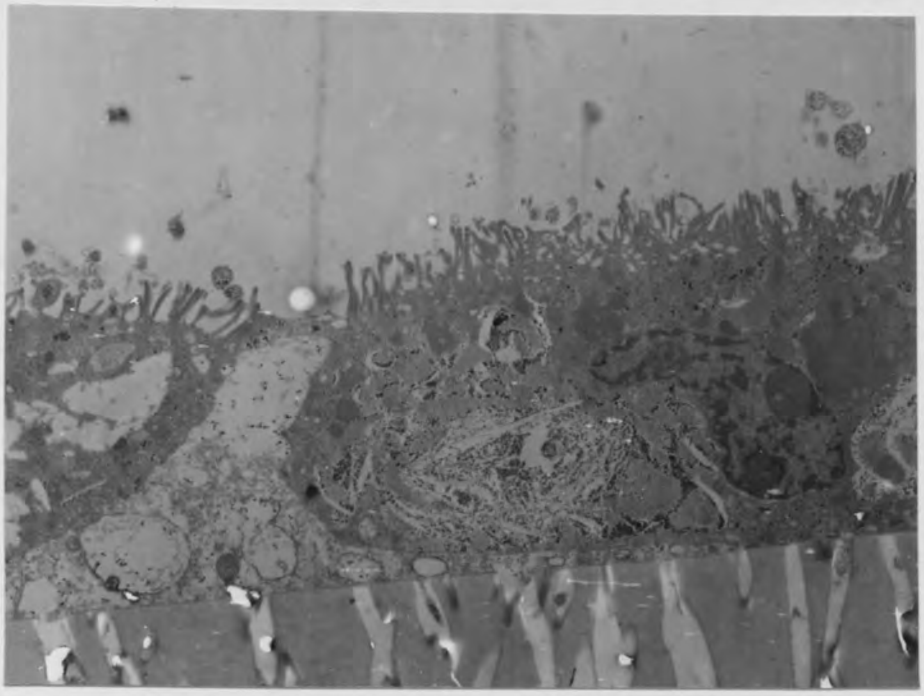

B)

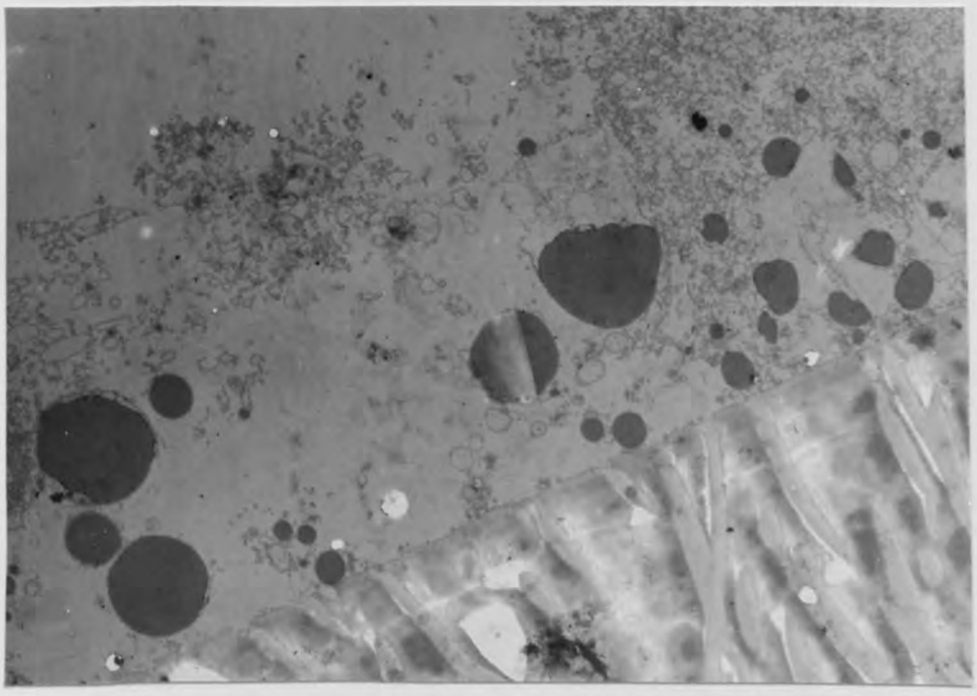

TABLE 8.1 *Oleic acid and Tween 80 concentrations at 0.1% v/v and 0.25% v/v as a function of formulation ratio.*

RATIO	OLEIC ACID CONCENTRATION [mM]		TWEEN 80 CONCENTRATION [mM]	
	0.25% v/v	0.1% v/v	0.25% v/v	0.1% v/v
20:1	6.46	2.58	0.32	0.13
10:1	5.49	2.19	0.55	0.22
5:1	4.23	1.69	0.85	0.34
3:1	3.26	1.30	1.09	0.43
1:1	1.55	0.62	1.55	0.62

8.5 DISCUSSION

The Caco-2 model has been proposed as a useful *in vitro* screen for agents which influence epithelial permeability [Schasteen *et al.*, 1992]. This model involves incubating Caco-2 monolayers with an Ap donor-solution containing fluorescent markers (Sulforhodamine (MWt = 625) and fluorescein isethionate-dextran (MWt = 10,000)) alone (control) or in the presence of a test substance. The release of cellular lactate dehydrogenase was measured simultaneously and used as an index of toxicity. Compounds which increased epithelial permeability usually exhibited cellular toxicity. For instance, the nonionic surfactant, polyoxyethylene-9-lauryl ether, was shown to increase the flux of transport markers, but this was correlated with high lactate dehydrogenase leakage. Exceptions to this rule were the smooth muscle relaxant aminophylline, the calmodulin antagonist calmidizolin (80 μM), the local anaesthetic pentobarbital, the enzyme phospholipase-A2 and the polymers of positively charged amino acids (arginine, lysine and ornithine).

In addition to being a screen for permeation enhancers, Caco-2 monolayers have been employed to investigate the absorption promoting mechanism(s) of bile acids and their derivatives (*eg:* sodium taurocholate, sodium taurodeoxycholate and sodium taurodihydrofusidate) [Anderberg *et al.*, 1992], starch microspheres [Bjork *et al.*, 1991], sodium caprate [Anderberg, 1991; Iso-Aho and Artursson, 1992] and surfactants (*eg*: sodium dodecyl sulphate, sodium dioctylsulphosuccinate, Polysorbate (Tween) 80, polyoxyl-40-hydrogenated caster oil) [Anderberg *et al.*, 1992].

The limited data describing the influence of absorption promoters on Caco-2 monolayers has concentrated on mono-component systems. In the present study, the effects of the self-emulsifying oleic acid-Tween 80 formulations on the functional and morphological integrity of Caco-2 monolayers was investigated. D-Mannitol flux and post-transport TER were used as indices of functional integrity, whilst laser-scanning confocal microscopy and transmission electron microscopy were used to assess morphological integrity. As D-mannitol flux increased post-transport TER decreased. In addition, the effect of formulations on monolayer appearance at the laser-scanning confocal microscope level were consistent with ultrastructural changes. Interestingly, formulation-induced changes in functional monolayer integrity correlated with their morphological effects. Therefore, the combined use of these techniques has permitted a detailed description of the influence of oleic acid-Tween 80 formulations on epithelial barrier function.

The effects of oleic acid-Tween 80 (10:1) formulations on Caco-2 monolayer integrity were dose-dependent and had a narrow window between toleration and gross disruptive effects. Up to Ap concentrations of 0.1% v/v formulation the functional integrity was maintained despite alterations in the morphology of Caco-2 cells. Meanwhile at Ap concentrations of 0.25% v/v and above there was a rapid and complete loss of functional and morphological integrity. The effects of the oleic acid-Tween 80 formulations about this narrow window were considered in more detail. Control Caco-2 monolayers displayed a typical appearance and permitted typically low D-mannitol fluxes. Meanwhile, after a 30 min exposure to 0.1% v/v formulation there was extensive denudation of microvilli and blebs were present at the Ap surface. However, there was no evidence for separation of inter-cellular contacts. Correspondingly, D-mannitol transport at 30 min was comparable to control values. Therefore, 0.1% v/v oleic acid-Tween 80 (10:1) formulation induces a partial loss of morphological integrity whilst functional integrity is retained. After a 15 min exposure to 0.25% v/v oleic acid-Tween 80 (10:1) there was a partial disruption of the Ap membrane and lateral inter-cellular gaps were beginning to develop. After 60 min exposure all recognisable cell structure was absent and only cell debris was associated with the permeable-support. Since D-mannitol transport across the Caco-2 cell-permeable-support composite is dependent on the presence of an intact monolayer (see Chapter Three) the above morphological sequence is consistent with the transport data. The initial partial disruption accounts for the lag-time prior to the very rapid transport upon complete loss of monolayer integrity.

To investigate which of the two emulsion components was principally responsible for the epithelial damage, Caco-2 monolayers were incubated with oleic acid (0 to 4 mM) or Tween 80 (0 to 82.5 mM). In addition, they were exposed to formulations having different ratios of oleic acid to Tween 80 (20:1 to 1:1). A 60 min exposure to Tween 80 alone at concentrations up to 8.25 mM failed to significantly increase D-mannitol flux and 82.5 mM was required to significantly decrease post-transport TER suggesting that the functional integrity of Caco-2 monolayers is maintained. Therefore, very high concentrations of Tween 80 were required to significantly influence the permeability properties of Caco-2 monolayers. This observation agrees with that of Anderberg *et al.* [1992] who showed that Tween 80 only exerts minor effects on D-mannitol flux, TER and lactate dehydrogenase release compared to anionic (*eg:* sodium dodecyl sulphate, sodium dioctylsulphosuccinate) surfactants and bile acids (*eg:* sodium taurocholate, sodium taurodeoxycholate, sodium taurodihydrofusidate) . In contrast, oleic acid was not well-tolerated by Caco-2 monolayers. At Ap concentrations greater than 1 mM, it induced increased D-mannitol flux and decreased post-transport TER. These observations suggested that oleic acid may be responsible for the formulation-induced damage to Caco-2 monolayers. This hypothesis is supported by the observation that Caco-2 monolayer permeability increased as the ratio of oleic acid to Tween 80 in formulations increased. Indeed, all formulations that caused a loss of monolayer integrity had a final oleic acid concentration between 2 and 6 mM (see Table 8.1) which is consistent with the threshold Ap concentration required to cause epithelial damage by oleic acid alone in solution. Meanwhile, the Tween 80 concentration in the monolayer-damaging formulations was considerably lower than that required for Tween 80 alone to induce damage.

It is acknowledged that oleic acid increases the intestinal absorption of some molecules. For instance, the co-administration of oleic acid with cinnarizine increases its oral bioavailability in dogs *in vivo* [Tokumura *et al.*, 1987]. In addition, oleic acid 'ufasomes' have been shown to transiently increase the absorption of carboxyfluorescin from the rat intestine using an *in situ* closed loop model [Murakami *et al.*, 1986]. The possibility that epithelial damage was the mechanism for enhancement was not investigated. However, data presented here suggests that oleic acid has the potential to induce epithelial damage and this cannot be discounted as its mechanism for absorption enhancement. Ufasomes only increased the absorption of carboxyfluorescin at final concentrations of 16 mM oleic acid and above. This is approximately one order of magnitude greater than the concentration that increases D-mannitol flux across Caco-2 monolayers. Interestingly, this agrees with the absorption promoting effects of sodium caprate (sodium decanoate) on Caco-2 monolayers which occurs at concentrations 10-fold lower than *in vivo*. The lower sensitivity towards enhancement by sodium caprate *in vivo* was attributed to the buffering capacity of luminal contents and the presence of a protective mucus layer [Anderberg, 1991].

Oleic acid-Tween 80 (10:1) formulations have been assessed *in vivo* for absorption promotion and toxicological effects [Lowe *et al.*, manuscript in preparation]. For these studies, 25 μl of formulation was injected directly into the lumen of a 1.5 cm ligated length of rat colon. Since the luminal volume of the colonic segment is of the order of 100 μl, the final formulation concentration was approximately 25% v/v. Under these conditions, the colonic absorption of immunoreactive human calcitonin and enzymatically intact HRP were promoted. After a 120 min exposure to the formulation the colonic segment was flushed with fixative and processed for histological examination. The colonic mucosa exposed to the formulation was indistinguishable from control tissues at the light microscopic level. Therefore, despite enhancing the absorption of these two marker compounds, the high luminal concentrations of oleic acid-Tween 80 (10:1) formulation were tolerated by the rat colon *in vivo*. In contrast, low apical concentrations (≥ 0.25% v/v) of this formulation caused gross disruption of Caco-2 monolayers. These data suggest that the *in vitro* Caco-2 model is at least 100-times more sensitive to this formulation than the rat colonic mucosa *in vivo*. There are several possible explanations for this greater sensitivity. Firstly, luminal contents may ameliorate the membrane damaging effects of the oleic acid-Tween 80 formulation. Secondly, the mucus layer may afford protection to the colonic epithelium *in vivo*. Since a mucus layer is absent in the conventional Caco-2 model this may render the monolayers susceptible to formulation-induced damage. In this respect the mucus-secreting Caco-2 and HT29GlucH co-culture model [Allen, 1992] may prove to be more relevant for studying formulation factors in influencing epithelial transport. Alternatively, the formulation may induce acute damage followed by re-epithelialisation. Kvietys *et al.* [1991] demonstrated exfoliation of the rat jejunal epithelium upon exposure to an emulsified mixture of oleic acid and bile salts. However, recovery was rapid and the epithelium was restored within 1 h. The process of epithelial restitution, which involves the migration of viable enterocytes to re-seal superficial mucosal lesions, was first observed in the gastric mucosa [Rutten and Ito, 1983; Silen and Susumu, 1985] but has subsequently been described in the small [Kvietys *et al.*, 1991] and large [Argenzio *et al.*, 1988 and 1991] intestine. Indeed, restitution is now recognised as a major repair mechanism following acute epithelial trauma. In light of the rapidity and efficiency of the repair mechanisms, tissue fixing 120 min after exposure to a formulation *in vivo*, may not reveal the true extent of formulation-induced epithelial damage. Therefore, the apparent greater susceptibility of Caco-2 monolayers to formulation induced damage may result from the absence or slower rate of recovery mechanisms *in vitro*.

Interestingly, T84 cell monolayers have been proposed as an *in vitro* model of restitution [Nusrat, *et al.*, 1992]. The restitutive potential of Caco-2 monolayers should be established before they can seriously considered as a relevant model for studying formulation effects on epithelial barriers.

8.6 CONCLUSION

Caco-2 monolayers represent a convenient model for investigating the effects of absorption enhancers on epithelial barrier function. They offer the advantages that experiments are performed in a well-defined environment and that the kinetics of monolayer integrity and toxicity can be monitored simultaneously [Schasteen *et al.*, 1992]. In addition, they are more easily processed for microscopic evaluation than whole tissue preparations. However, this work highlights some concerns about the relevance of the Caco-2 model to the *in vivo* situation. For instance, they were at least 100-times more sensitive to oleic acid-Tween 80 emulsions than the *in situ* rat colon. It is not clear whether this difference stems from a greater susceptibility of Caco-2 monolayers to this formulation or results from epithelial restitution mechanisms *in vivo*. These questions should be addressed in order to validate the assertion that Caco-2 monolayers represent a useful *in vitro* model for absorption enhancement.

CHAPTER NINE

SUMMARY

ABSTRACT
In this chapter the current issues in the application of Caco-2 monolayers as a relevant model of the human small intestinal epithelium are discussed.

Current knowledge of the mechanisms available for the absorption of drugs and nutrients from the gastrointestinal tract has been developed using a variety of models. These include luminal perfusions, isolated loops, everted sacs, intestinal rings, brush-border membrane vesicles and isolated enterocytes [Csakay, 1984; Osiescka *et al.*, 1985]. Each of these systems lacks the versatility and/or viability for detailed transport studies across the gastrointestinal epithelium. For these reasons, cell culture approaches to absorption studies have become increasingly popular. The development of primary intestinal cell culture has been limited by the poor retention of anatomical and biochemical features of cells found *in vivo* [Moyer, 1983]. Consequently, attention has focused on human colon adenocarcinoma cell lines, some of which display properties of differentiated enterocytes. Preliminary reports have proposed that Caco-2 monolayers represent a useful *in vitro* model of the human distal ileal epithelium [Hidalgo *et al.*, 1989; Wilson *et al.*, 1990]. The attention that Caco-2 monolayers have received in academic and industrial institutes is testimony to the requirement for a reliable model of the human gastrointestinal epithelium. This thesis has critically appraised the relevance of Caco-2 monolayers for absorption studies and together with recently published data has highlighted some of the limitations of the model. These limitations and their circumvention are discussed below.

A major concern of the usefulness of Caco-2 monolayers is their reproducibility between research groups. This probably reflects the heterogeneous nature of the cell line. Selection pressures resulting from different protocols used to maintain stock cultures can cause phenotypic shift from the parental population. Consequently, each research group undoubtedly develops its own sub-population of Caco-2 cells which have unique properties. This is compounded by the use of a range of apparatus and methods during the culture of Caco-2 cells for transport studies. The poor consistency in culture protocols between research groups makes extrapolation of transport data from one laboratory to another difficult. Indeed, it probably accounts for some of the conflicting observations presented in the literature. For instance, sodium-dependent L-phenylalanine transport has been reported by Hidalgo and Borchardt [1990 b] whereas its carrier-mediated transport has been shown to be sodium-independent by another research group [Personal communication, Ian Hassan]. If we are to achieve inter-laboratory reproducibility, standard techniques for the maintenance of stock cultures and for culturing cells for transport studies must be adopted.

In addition to the heterogeneity of the Caco-2 cell line, there are further limitations which one must consider when reviewing the literature. Presently, there is considerable interest in the potential application of Caco-2 monolayers as a screen for the ability of new chemical entities to diffuse passively across the GI epithelium. In these experiments, one studies the flux of a compounds across a cell-permeable support composite. As the support can influence the transport of a compound (see Chapter Three) it is important to select an appropriate culture-insert. The polycarbonate permeable-support displays uniformly low ligand binding and should therefore be adopted for all passive transport studies. Recently, numerous research groups have developed diffusion chambers which minimise the influence of the unstirred water layer on transport kinetics of a permeant across Caco-2 monolayers. Whilst the aim of this work is admirable, it detracts from the simplicity and rapidity of the Caco-2 monolayer model which are ideal properties for its use as a primary screen of the absorption potential for compounds. Furthermore, since a diverse array of diffusion chambers have been developed and the transport rates for compounds is device dependent, these may increase inter-laboratory inconsistencies. In a similar way to the problems with heterogeneity, the inconsistency in the methods used to study passive transport of compounds across Caco-2 monolayers is a major obstacle to meaningful extrapolation of data between laboratories. Standardisation of the apparatus and techniques used for transport studies are required. Caco-2 cells express a number of nutrient transporters (see Chapter One). However, the scarcity of data in human tissue makes assessing of the relevance of these data to the normal human intestine difficult. In this thesis the uptake and transport data have been compared and contrasted to the limited human data which are available. In the case of L-proline, its uptake mechanism into Caco-2 cells can at best only partially explain the intestinal absorption of imino acids (see Chapter Four). In contrast, acidic amino acid transport mechanism appears to be consistent with the known features of the human acidic amino acid transporter. However, since Caco-2 cells are neoplastic and are of colonic origin one must always question whether these transporters are equivalent to those expressed in the normal human enterocyte.

In conclusion, Caco-2 monolayers represent an important model for understanding absorption phenomena. However, as with all models they are only valuable when used with an appreciation of their limitations. Their role in the pharmaceutical industry as a primary screen for drug absorption and structure-absorption relationships is assured. In addition, I am sure they will be an important tool for developing hypotheses about the function and regulation of transporters which can then be tested as superior models become available.

REFERENCES

ABAZA, N.A., LEIGHTON, J. AND SCHULTZ, S.G. (1974). Effects of ouabain on the function and structure of a cell line (MDCK) derived from canine kidney, I: Light microscopic observations of monolayer growth. *In vitro*, **10**: 172-183.

ADDISON, J.M., BURSTON, D. and MATTHEWS, D.M. (1972). Evidence for active transport of the dipeptide glycylsarcosine by hamster jejunum in vitro. *Clinical Science*, **43**: 907-911.

AGAR, W.T., HIRD, F.J.R. and SIDHU, G.S. (1954). The uptake of the amino acids by the intestine. *Biochimica et Biophysica Acta*, **14**: 80-84.

ALLEN, J.D. (1992). Ph.D. Thesis, Brighton Polytechnic, UK.

ALLEN, R.H., SEETHARAM, B., ALLEN, N.C., PODELL, E. and ALPERS, D.H. (1978). Correction of cobalamin malabsorption in pancreatic insufficiency with a cobalamin analogue that binds with high affinity to R protein but not intrinsic factor. In vivo evidence that a failure to partially degrade R protein is responsible for cobalamin malabsorption in pancreatic insufficiency. *Journal of Clinical Investigation*, **61**: 1628-1634.

ALVAREZ-HERNANDEZ, X., NICHOLS, G.M. and GLASS, J. (1991). Caco-2 cell line: A system for studying intestinal iron transport across epithelial monolayers. *Biochimica et Biophysica Acta*, **1070**: 205-208.

ANDERBERG, E.K. (1991). Ph.D. Thesis, Uppsala University, Sweden.

ANDERBERG, E.K., NYSTROM, C. AND ARTURRSON, P. (1992). Epithelial transport of drugs in cell culture.VII: Effects of pharmaceutical surfactant excipients and bile acids on transepithelial permeability in monolayers of human intestinal epithelial (Caco-2) monolayers. *Journal of Pharmaceutical Sciences*, **81**: 879-887.

ANTONIN, K.H., SAANO, V., BIECK, P., HASTEWELL, J., FOX, R., LOWE, P. and MACKAY, M. (1992). Colonic absorption of human calcitonin in man. *Clinical Sciences*, **83**: 627-631.

ARGENZIO, R.A., HENRIKSON, C.K. and LIACOS, J.A. (1988). Restitution of barrier and transport function of porcine colon after acute mucosal injury. *American Journal of physiology*, **255**: G62-G71.

ARGENZIO, R.A. and MEUTEN, D.J. (1991). Short-chain fatty acids induce reversible injury of porcine colon. *Digestive Diseases and Sciences*, **36**: 1459-1468.

ARTURSSON P. (1990). Epithelial transport of drugs in cell culture.I: A model for studying the passive diffusion of drugs over intestinal absorptive (Caco-2) cells. *Journal of Pharmaceutical Sciences*, **79**: 476-482

ARTURSSON, P. and KARLSSON, J. (1991). Correlation between oral absorption in humans and apparent drug permeability coefficients in human intestinal epithelial (Caco-2) cell culture. *Biochemical and Biophysical Research Communications*, **175**: 880-885.

ARTURSSON, P. and MAGNUSSON, C. (1990). Epithelial transport of drugs in cell culture, II. Effect of extracellular calcium (Ca^{2+}) concentration on the paracellular transport of drugs of different lipophilicities across monolayers of intestinal epithelial (Caco-2) cells. *Journal of Pharmaceutical Sciences*, **79**: 595-600.

AUDUS, K.L., BARTEL, R.L., HIDALGO, I.J. and BORCHARDT, R.T. (1990). The use of cultured epithelial and endothelial cells for drug transport and metabolism studies. *Pharmaceutical Research*, **7**: 435-451.

AUDUS, K.L. AND BORCHARDT, R.T. (1986). Characteristics of the large neutral amino acid transport system of bovine brain microvessel endothelial cell monolayers. *Journal of Neurochemistry*, **47**: 484-488.

BARANCZYK-KUZMA, A., GARREN, J.A., HIDALGO, I. and BORCHARDT, R.T. (1991). Substrate specificity and some properties of phenol sulfotransferase from human intestinal Caco-2 cells. *Life Sciences*, **49**: 1197-1206.

BARNARD, J.A. and GHISHAN, F.K. (1987). Taurocholate transport by human ileal brush-border membrane vesicles. *Gastroenterology*, **93**: 925-933.

BARRY, P.H. and DIAMOND, J.M. (1984). Effect of unstirred layers on membrane phenomena. *Physiological Reviews*, **64**: 763-872.

BEAULIEU, J-F. and QUARONI, A. (1991). Clonal analysis of sucrase-isomaltase expression in the human colon adenocarcinoma Caco-2 cells. *Biochemical Journal*, **280**: 599-608.

BERTELOOT, A. (1984). Characteristics of glutamic acid transport by rabbit intestinal brush-border membrane vesicles: Effects of Na^+-, K^+- and H^+-gradients. *Biochimica et Biophysica Acta*, **775**: 129-140.

BERTELOOT, A. and MAENZ, D.D. (1990). Acidic amino acid transport in mammalian cells and tissues. *In:* Comparative aspects of sodium cotransport systems, Kinne, R.K.H. (Ed.), Comparative Physiology, Basel, Karger, pp130-185.

BEVERIDGE, T., GRATWHOL, A., MICHOT, F., NIEDERBERGER, W., UUESCH, E., NUSSBAUMER, K., SCHAUB. P. and SPECK, B. (1981). Cyclosporin A: pharmacokinetics after a single dose in man and serum levels after multiple dosing in recipients of allogenic bone marrow grafts. *Current Therapeutic Research*, **30**: 5-18.

BLAIS, A., BISSONNETT, P. and BERTELOOT, A. (1987). Common characteristics for Na^+-dependent sugar transport in Caco-2 cells and human foetal colon. *Journal of Membrane Biology*, **99**: 113-125.

BJORK, E., ISAKSSON, U., EDMAN, P. and ARTURSSON, P. (1992). Starch microspheres enhance insulin absorption across epithelial cells by affecting the integrity of tight junctions. *Journal of Controlled Release*, **21**: 206

BUNDGAARD, H. (1992). The utility of the prodrug approach to improve peptide absorption. *Journal of Controlled Release*, **21**: 63-72.

BURTON, P.S., CONRADI, R.A., HILGERS, A.R., HO, N.H.O. and MAGGIORA. L.L. (1992). The relationship between peptide structure and transport across epithelial cell monolayers. *Journal of Controlled Release*, **19**: 87-98.

BURTON, P.S., CONRADI, R.A., HILGERS, A.R. and HO, N.H.O. (1993). Evidence for a polarised efflux system for peptides in the apical membrane of Caco-2 cells. *Biochemical and Biophysical Research Communications*, **190**: 760-766.

CAMPBELL, N.R.C. and HASINOFF, B. (1989). Ferrous sulphate reduces levodopa bioavailability: Chelation as a possible mechanism. *Clinical Pharmacology and Therapeutics*, **45**: 220-225.

CAMPBELL, N.R.C., PADDOCK, V. and SUNDARAM, R.S. (1988). Alteration of methyldopa absorption, metabolism and blood pressure control caused by ferrous sulfate and ferrous gluconate. *Clinical Pharmacology and Therapeutics*, **43**: 381-386.

CANTRILL, J.A and ANDERSON, D.C. (1990). Treatment of Paget's disease of bone. *Clinical Endocrinology*, **32**: 507-518.

CARR, K.E. and TONER, P.G. (1984). Morphology of the intestinal mucosa. *In::*Pharmacology of intestinal permeation, I. Csaky, T.Z. (Ed.), Springer-Verlag, Berlin, Heidelberg, pp1-50.

CEFALU, W.T. and PARDRIDGE (1985). Resitrictive transport of a lipid soluble peptide (cyclosporine) through the blood brain barrier. *Journal of neurochemistry*, **45**: 1954-1956.

CEREIJIDO, M., ROBBINS, E.S., DOLAN, W.J., ROTUNNO, C.A. and SABATINI, D.D. (1978). Polarised monolayers formed by epithelial cells on permeable and translucent support. *Journal of cell Biology*, **77**: 853-880.

CEREIJIDO, M., GONZALEZ-MARISCAL, L. and CONTRERAS, R.G. (1988). Epithelial tight junctions. *American Reviews of Respiratory Diseases*, **138**: S17-S21.

CHANARIN, I., MUIR, M., HUGHES, A. and HOFFBRAND, A.V. (1970). Evidence of the intestinal origin of transcobalamin II during vitamin B_{12} absorption. *British Journal of Medicine*, **1**: 1454-1455.

CHANTRET, I., BARBAT, A., DUSSAULX, E., BRATTAIN, M.G., and ZWEIBAUM, A. (1988). Epithelial polarity, villin expression, and enterocytic differentiation of cultured human colon carcinoma cells: a su.vey of twenty cell lines. *Cancer Research*, **48**: 1936-1942

CHO, Y.W. (1987). Oral composition for administration of proteins especially insulin and comprises particles of emulsifying agent and surfactant with protein bound to surface and lipid coated. Patent WO87/05505

CHO,Y.W. and FLYNN, M.J. (1989 a). Orally or rectally administered formulations of biologically active material comprising a water-in-oil microemulsion. Patent WO90/03164.

CHO,Y.W. and FLYNN, M.J. (1989 b). Oral delivery of insulin. *Lancet ii*, 1518-1519.

CHOWHAN, Z.T. and AMARO, A.A. (1977). Everted rat intestinal sacs as an in vitro model for assessing absorptivity of new drugs. *Journal of Pharmaceutical Sciences*, **66** :1249-1253.

CHRISTENSEN, H. (1984). On the strategy of kinetic discrimination of amino acid transport systems. *Journal of Membrane Biology*, **84**: 97-103.

CHRISTENSEN, H. (1985). Organic ion transport during seven decades: The amino acids. *Biochimica et Biophysica Acta*, **779**: 255-269.

CHRISTENSEN, H.N., LAING, M. and ARCHER, E.G (1967). A distinct Na^+-requiring system for alanine, serine, cysteine and similar amino acids. *Journal of Biological Chemistry*, **242**: 5237-5246.

CHRISTENSEN, H. and MAKOWSKE, M. (1983). Recognition chemistry of anionic amino acids for hepatocyte transport and for neurotransmittory action compared. *Life Sciences*, **33**: 2255-2267.

COGBURN, J.N., DONOVAN, M.G. and SCHASTEEN, C.S. (1989). Correlation of Caco-2 transport with human oral bioavailability. *49th International congress of Pharmeceutical Sciences of FIP*, 62.

COGBURN, J.N., DONOVAN, M.G. and SCHASTEEN, C.S. (1991). A model of the human small intestinal absorptive cells, 1: Transport barrier. *Pharmaceutical Research*, **8**: 210-216.

COLEMAN, R.E. and RUBENS, R.D. (1987). 3-(amino-1,1-hydroxypropylidene) bisphosphonate (APD) for hypercalcaemia of breast cancer. *British Journal of Cancer*, **56**: 465-469.

CONRADI, R.A., HILGERS, A.R., HO, N.F.H. and BURTON, P.S. (1991). The influence of peptide structure on transport across Caco-2 cells. *Pharmaceutical Research*, **9**: 435-439.

CONRADI, R.A., HILGERS, A.R., HO, N.F.H. and BURTON, P.S. (1992). The influence of peptide structure on transport across Caco-2 cells, II. Peptide bond modification which results in improved permeability. *Pharmaceutical Research*, **8**: 1453-1460.

CORCELLI, A., PREZIOSO, G., PALMIERI, F. and STORELLI, C. (1982). Electroneutral Na^+/dicarboxylic amino acid cotransport in rat intestinal brush-border membrane vesicles. *Biochimica et Biophysica Acta*, **689**: 97-105.

CORCELLI, A. and STORELLI, C. (1983). The role of potassium and chloride ions on the Na^+/acidic amino acid cotransport system in rat intestinal brush-border membrane vesicles. *Biochimica et Biophysica Acta*, **732**: 24-31.

COYLE, J.T. (1987). Kainic acid: insights into excitatory mechanisms causing selective neuronal degradation. *Ciba Foundation Symposium*, **126**: 183-203.

CRANE, R.K. and WILSON, T.H. (1958). In vitro method for the study of the rate of intestinal absorption of sugars. *Journal of Applied Physiology*, **12**: 145-146.

CURTIS, D.R., PHILLIS, J.W. and WATKINS, J.C. (1959). Chemical excitation of spinal neurons. *Nature*, **183**: 61-613.

DALEY-YATES, P.T., DODWELL, D.J., PONGCHAIDCHA, M., COLEMAN, R.E. and HOWELL, A. (1991). The clearance and bioavailability of pamidronate in patients with breast cancer and bone metastases. *Calcified Tissue International*, **49**: 433-435.

DAMM, H.C. (1966). *In:* The Handbook of Biochemistry and Biophysics. Damm, H.C. (Ed.), The World Publishing Company, New York, pp39-57.

DANTZIG, A. and BERGIN, L. (1988 a). Cephalexin shares a transporter with dipeptides and p-aminohippuric acid in the human intestinal cell line, Caco-2. *FASEB Journal*, Abstract 2646.

DANTZIG, A. and BERGIN, L. (1988 b). Characterisation of cephalexin uptake in the human intestinal cell line, Caco-2. *FASEB Journal*, Abstract 6933.

DANTZIG, A. and BERGIN, L. (1990). Uptake of the cephalosporin, cephalexin, by a dipeptide transport carrier in the human intestinal cell line, Caco-2. *Biochimica et Biophysica Acta*, **1127**: 211-217.

DANTZIG, A., TABAS, L.B. and BERGIN, L. (1992). Cefaclor uptake by the proton-dependent dipeptide transport carrier of human intestinal Caco-2 cells and comparison to cephalexin uptake. *Biochimica et Biophysica Acta*, **1112**: 167-173.

D'ARCY, P.F. and McELNAY, J.C. (1987). Drug-antacid interactions: assessment of clinical importance. Drug Intelligence and Clinical Pharmacy, **21**: 607-617.

DARFEUILLE-MICHAUD, A., AUBEL, D., CHAUVIERE, G., RICH, C., BOURGES, M., SERVIN, A. and JOLY, B. (1990). Adhesion of Enterotoxigenic Escherichia coli to the human colon carcinoma cell line Caco-2 in culture. *Infection and Immunity*, **58**: 893-902.

DAWSON, J.R. AND SCHWENK, M. (1989). Isolated epithelial cells. *Progress in Pharmacology and Clinical Pharmacology*, **7**: 21-41.

DIX, C.J., HASSAN, I.F., OBRAY, H.Y., SHAH, R. and WILSON, G. (1990). The transport of Vitamin B_{12} through polarised monolayers of Caco-2 cells. *Gastroenterology*, **98**: 1272-1279.

DODWELL, D.J., HOWELL, A. and FORD, J. (1990). Reduction in calcium excretion in women with breast cancer and bone metastases using the oral bisphosphonate pamidronate. *British Journal of Cancer*, **61**: 123-125.

DOLUSIO, J.T., BILLUPS, N.F., DITTERT, L.W., SUGITA, E.T. and SWINTOSKY, J.V. (1969). Drug absorption, I: an in situ rat gut technique yielding realistic absorption rates. *Journal of Pharmaceutical Sciences*, **58**: 1196-1200.

DRAAIJER, M., KONINKX, J., HENDRICKS, H., KIK, M., VAN DIJK, J. and MOUWEN, J. (1989). Actin cytoskeletal lesions in differentiated human colon carcinoma Caco-2 cells after exposure to soybean agglutinin. *Biology of the Cell*, **65**: 29-35.

DREWE, J., BEGLINGER, C. and KISSEL, T. (1992 a). The absorption of cyclosporin in the human gastrointestinal tract. *British Journal of Clinical Pharmacology*, **33**: 39-43.

DREWE, J., MEIER, R., VONDERSCHER, J., KISS, D., POSANSKI, U., KISSEL, T. and GYR, K. (1992 b). Enhancement of the oral absorption of cyclosporin in man. *British Journal of Clinical Pharmacology*, **34**: 60-64.

DUCHIN, K.L., SINGHIVI, S.M., WILLARD, D.A., MIGDALOF, B.H. and McKINSTRY, D.N. (1982). Captopril kinetics. *Clinical Pharmacokinetics and Therapeutics,* **31**: 452-458.

EDMONDSON, J.W., LUMENG, L. and LI, T. (1979). Comparative studies of alanine and alpha-aminoisobutyric acid uptake by freshly isolated rat liver cells. *Journal of Biological Chemistry*, **254**: 1653-1658.

FAIGLE, J.W., KEBERLE, H. and DEGEN, P.H. (1981). Pharmakokinetik von Baclofen (Lioresal®). *In:* Therapie der Spastik, Baurer, H.J., Koella, W.P. and Struppler, A (Eds.), Verlag fur angewandte Wissenschaften, Munchen, pp137-147.

FARQUHAR, M.G. and PALADE, G.E. (1963). Junctional complexes in various epithelia. *Journal of Cell Biology,* **17**: 375-412.

FIELD, M., FROMM, D. and McCOLL, I. (1971). Rabbit ileum consisting of epithelium, lamina propria and muscularis mucoase. *American Journal of Physiology*, **220**: 1388-1396.

FINLAY, B.B. and FALKOW, S. (1990). Salmonella interactions with polarized human intestinal Caco-2 epithelial cells. *Journal of Infectious Diseases*, **162**: 1096-1106.

FLANAGAN, A.M. and CHAMBERS, T.J. (1988). Mechanism of inhibition of bone resorption by diphosphonates. *Bone*, **9**: 263.

FLEISCH, H. (1987). Bisphosphonates - history and experimental basis. *Bone*, **8** (Suppl. 1): 23-28.

FOGELMAN, I., SMITH, L., MAZESS, R., WILSON, M.A. and BEVAN, J.A. (1986). Absorption of oral diphosphonate in normal subjects. *Clinical Endocrinology*, **24**: 57-62.

FOGH, J., FOGH, J.M. and ORFEO, T. (1977). One hundred and twenty seven cultured human tumour cell lines producing tumours in nude mice. *Journal of the National Cancer Institute*, **59**: 221-226.

FOLEY, J., MORRISON, R., SINGHVI, S., MANNING, J. and WILLARD, D. (1988). Pharmacokinetics and pharmacodynamics of SQ29852, a new metabolically stable phosphorous containing angiotensin-converting enzyme (ACE) inhibitor. *Pharmacologist*, **30**: A156.

FRANCIS, M.D. and CENTNER, R.L. (1978). The development of diphosphonates as significant health care products. *Journal of Chemical Education*, **55**: 760-766.

FREY, F.J., HORBER, F.F., and FREY B.M. (1988). Trough levels and concentration time curves of cyclosporine in patients undergoing renal transplantation. *Clinical Pharmacology and Therapeutics*, **43**: 55-62.

FRIEDMAN, D.I. and AMIDON, G.L. (1989 a). Passive and carrier-mediated intestinal absorption components of two angiotensin converting enzyme (ACE) inhibitor prodrugs in rats: Enalapril and Fosinopril. *Pharmaceutical Research*, **6**: 1043-1047.

FRIEDMAN, D.I. and AMIDON, G.L. (1989 b). Intestinal absorption mechanism of dipeptide angiotensin converting enzyme inhibitors of the lysyl-proline type: Lisinopril and SQ29852. *Journal of Pharmaceutical Sciences*, **78**: 995-998.

GAILLARD, J-L., BERCHE, P., MOUNIER, J., RICHARD, S. and SANSONETTI, P. (1987). In vitro model of penetration and intracellular growth of *Listeria monocytogenes* in the human enterocyte-like cell line Caco-2. *Infection and Immunity*, **55**: 2822-2829.

GAZZOLA, D.C., DALL'ASTA, V., BUSSOLATI, O., MAKOWSKI, M. and CHRISTENSEN, H. (1981). A stereoselective anomally in dicarboxylic amino acid transport. *Journal of Biological Chemistry*, **256**: 6054-6059.

GIBSON, Q.H. AND WISEMAN, G. (1951). Selective absorption of stereoisomers of amino acids from loops of the small intestine of rat. *Biochemical Journal*, **48**: 426-429.

GIULIANO, A.R. and WOOD, R. J. (1991). Vitamin D-regulated calcium transport in Caco-2 cells: unique *in vitro* model. *American Journal of Physiology*, **260**: G207-G212.

GOCHOCO, C.H., SMITH, P.L. and HIDALGO, I. (1991 a). Characterisation of a cellular model for uptake and transepithelial transport of cephalexin (CPX). *Pharmaceutical Research*, **8** (Suppl.): PDD7358.

GOCHOCO, C.H., RYAN, F.M., MARKS, G.J., SMITH, P.L. and HIDALGO, I. (1991 b). Competition for uptake and transepithelial transport of cephalexin in Caco-2 cells and intestinal tissues: A comparative study. *Pharmaceutical Research*, **8** (Suppl.): PDD7360.

GOCHOCO, C.H., RYAN, F.M., MARKS, G.J., SMITH, P.L. and HIDALGO, I. (1991 c). Comparative aspects of Di-/Tripeptide transport in rabbit ileal mucosa and human intestinal (Caco-2) cells. *Pharmaceutical Research*, **8** (Suppl.): PDD7359.

GOON, D. and KLAASSEN, C.D. (1990). Dose-dependent intestinal glucuronidation and sulfation of acetaminophen in the rat in situ. *Journal of Pharmacology and Experimental Therapeutics*, **252**: 201-207.

GRASSET, E., PINTO, M., DASSAULX, E., ZWEIBAUM, A. and DESJEUX, J.F. (1984). Epithelial properties of a human colonic adenocarcinoma cell line Caco-2: Electrical parameters. *American Journal of Physiology*, **247**: C260-C267.

GREVEL, J., KUTZ, K., ABISCH, E. and NUEESCH, E. (1986). Evidence for zero order absorption of cyclosporin A. *British Journal of Clinical Pharmacology*, **22**: 220P-221P.

GUMBINER, B. (1987). Structure, biochemistry and assembly of epithelial tight junctions. *American Journal of Physiology*, **253**: C749-C758.

GUMBINER, B. and SIMONS, K. (1987). The role of uvomorulin in the formation of epithelial occluding junctions. *In:* Junctional complexes of Epithelial cells. Stoker, M. (Ed.), Ciba Foundation Symposium 125, Wiley, Chichester, pp168-186.

GUPTA, S.K., BAKRAN, A., JOHNSON, R.W.G. and ROWLAND, M. (1988). Erythromycin enhances the absorption of cyclosporin. *British Journal of Clinical Pharmacology*, **25**: 401-402.

HAASE, W., SCHAFER, A., MURER, H. and KINNE, R. (1978). Studies on the orientation of brush-border membrane vesicles. *Biochemical Journal*, **172**: 57-62.

HAGIHIRA, H., WILSON, T.H. and LIN, E.C.C. (1962). Intestinal transport of certain N-substituted amino acids. *American Journal of Physiology*, **203**: 637-640.

HAIGLER, E.D., HERSHMAN, J.M. and PITMAN, J.A. (1972). Response to orally administered synthetic thyrotrophin-releasing hormone in man. *Journal of Clinical Endocrinology and Metabolism*, **35**: 631-635.

HARIG, J.M., RAJENDRAN, V.M., BARRY, J.A. and RAMASWAMY, K. (1987). Transport characteristics of L-glutamate in human jejunal brush-border membrane vesicles. *Biochimica et Biophysica Acta*, **903**: 358-364.

HARRIS, D.S., SLOT, J.W., GEUZE, H.J. and JAMES, D.E. (1992). Polarized distribution of glucose transporter isoforms in Caco-2 cells. *Proceedings of National Academy of Sciences*, **89**: 7556-7560.

HASSAN, I.F. (1990). Ph.D. Thesis, Council for National Academic Awards, UK.

HASSAN, I.F., PARSONS, I.J. and MACKAY, M.W. (1991). Receptor-mediated transport of cobalamin in Caco-2 cells: Intracellular localisation of transcobalamin II. *In:* Pharmaceutical Applications of Cell and Tissue Culture to Drug Transport, Wilson, G., Davis, S.S. and Illum, L. (Eds.), Plenum Press, New York, pp107-120.

HASTEWELL, J.G. (1986). D.Phil. Thesis, University of York, UK.

HASTEWELL, J.G., LYNCH, S., WILLIAMSON, I., FOX, R. and MACKAY, M. (1992). Absorption of human calcitonin across the rat colon in vivo. *Clinical Sciences*, **82**: 589-594.

HAURI, H-P., STERCHI, E.E., BIENZ, D., FRANZEN, J.A.M. and MARXER, A. (1985). Expression and intracellular transport of microvillus membrane hydrolases in human intestinal epithelial cells. *Journal of Cell Biology*, **101**: 838-851.

HAYASHI, K., YAMAMOTO, S-I., OHE, K., MIYOSHI, A. and KAWASAKI, A. (1980). Na^+-Gradient-dependent transport of L-proline and analysis of its carrier system in the brush-border membrane vesicles of the guinea pig ileum. *Biochimica et Biophysica Acta*, **601**: 654-663.

HAYASHI, T. (1952). A physiological study of epileptic seizures following cortical stimulation in animals and its application to the human clinics. *Japanese Journal of Physiology*, **3**: 46-64.

HENDRICKS, H.G.C.J.M., KIK, M.J.L., KONINKX, J.F.J.G., VAN DEN INGH, T.S.G.A.M. (1991). Binding of kidney bean (*Phaseolus vulgaris*) isolectins to differentiated human colon carcinoma Caco-2 cells and their effect on cellular metabolism. *Gut*, **32**: 196-201.

HESSLING, J.J., MILLER, S.E. and LEVY, N.L. (1980). A direct comparison of procedures for the detection of mycoplasma in tissue culture. *Journal of Immunological Methods*, **38**: 315-324.

HEYMAN, M., CRAIN-DENOYELLE, A-M., NATH, S.K. and DESJEUX, J-F (1990). Quantification of protein transcytosis in the human colon carcinoma cell line Caco-2. *Journal of Cellular Physiology*, **143**: 391-395.

HIDALGO, I.J. and BORCHARDT, R.T. (1988). Amino acid transport in a novel model system of the intestinal epithelium (Caco-2 cell). *Pharmaceutical Research*, **5** (Suppl.): PD951.

HIDALGO, I.J. and BORCHARDT, R.T. (1990 a). Transport of a large neutral amino acid (phenylalanine) in a human intestinal epithelial cell line, Caco-2. *Biochimica et Biophysica Acta*, **1028**: 25-30.

HIDALGO, I.J. and BORCHARDT, R.T. (1990 b). Transport of bile acids in a human intestinal epithelial cell line, Caco-2. *Biochimica et Biophysica Acta*, **1035**: 97-103.

HIDALGO, I.J., HILLGREN, H.M., GRASS, G.M. and BORCHARDT, R.T. (1991). Characterisation of the unstirred water layer in Caco-2 cell monolayers using a novel diffusion apparatus. *Pharmaceutical Research*, **8**: 222-227.

HIDALGO, I.J., RAUB, T.J. and BORCHARDT, R.T. (1989). Characterisation of the human colon carcinoma cell line (Caco-2) as a model system for intestinal epithelial permeability. *Gastroenterology*, **96**: 736-749.

HILGERS, A.R., CONRADI, R.A. and BURTON, P.S. (1990). Caco-2 cell monolayers as a model for drug transport across the intestinal mucosa. *Pharmaceutical Research*, **7**: 902-910.

HO, N.F.H., DAY, J.S., BARSUHN, C.L., BURTON, P.S. and RAUB, T.J. (1990). Biophysical model approached to mechanistic transepithelial studies of peptides. *Journal of Controlled Release*, **11**: 3-24.

HOLBROOK, P. (1992). Ph.D. Thesis, Aston University, UK.

HOPFER, U. (1987). Membrane transport mechanisms for hexoses and amino acids in the small intestine. *In:* Physiology of the Gastrointestinal tract, II (Second Edition). Johnson, L.R. (Ed.), Raven Press, New York, pp1499-1526.

HOPFER, U., NELSON, K., PERROTTO, J. and ISSELBACHER, K.J. (1973). Glucose transport in isolated brush border membrane from rat intestine. *Journal of Biological Chemistry*, **248**: 25-32.

HU, M. and AMIDON, G.L. (1988). Passive and carrier-mediated intestinal absorption components of captopril. *Journal of Pharmaceutical Sciences*, **77**: 1007-1011.

HU, M. and BORCHARDT, R.T. (1990). Mechanism of L-alpha-methyldopa transport through a monolayer of polarised human intestinal epithelial cells (Caco-2). *Pharmaceutical Research*, **7**: 1313-1319.

HU, M. and BORCHARDT, R.T. (1992). Transport of a large neutral amino acid in a human intestinal epithelial cell line (Caco-2): Uptake and efflux of phenylalanine. *Biochimica et Biophysica Acta*, **1135**: 233-244.

HUMPHERY, M.J. (1986). The oral bioavailability of peptides and related drugs. *In;* Delivery systems for peptide drugs, Davis S.S., Illum, L. and Tomlinson, E. (Eds.), Plenum Press, New York, London, pp139-151.

INUI, K-I., YAMAMOTO, M. and SAITO, H. (1992). Transepithelial transport of oral cephalosporins by monolayers of intestinal epithelial cell line Caco-2: Specific transport systems in apical and basolateral membranes. *Journal of Pharmacology and Experimental Therapeutics*, **261**: 195-201.

ISHIZAWA, T., HAYASHI, M. and AWAZU, S. (1987). Enhancement of jejunal and colonic absorption of fosfomycin by promoters in the rat. *Journal of Pharmacy and Pharmacology*, **39**: 892-895.

ISO-AHO, T. and ARTURSSON, P. (1992). Studies on a medium chain fatty acid, decanoic acid, as absorption enhancer in Caco-2 cell monolayers. *Proceedings International Symposium on Controlled release and Bioactive Materials*, **19**: 293-294.

JOHNSTON, A., MARSDEN, J.T., HLA, K.K., HENRY, A. and HOLT, D.W. (1986). The effect of vehicle on the oral absorption of cyclosporin. *British Journal of Pharmacology*, **21**: 331-333.

KARLSSON, J. and ARTURSSON, P. (1991). A method for the determination of cellular permeability coefficients and aqueous boundary layer thickness in monolayers of intestinal epithelial cells (Caco-2) grown in permeable filter chambers. *International Journal of Pharmaceutics*, **71**: 55-64.

KARANEWSKY, D.S., BADIA, M.C., CUSHMAN, D.W., DEFORREST. J.M., DEJNEKA, T., LOOTS, M.J., PERRI, M.G., PETRILLO, E.W. and POWELL, J.R. (1988). (Phosphiyloxy)acyl amino acid inhibitors of angiotensin converting enzyme (ACE), 1. Discovery of (S)-1-[6-amino-2-[[hydroxy(4-phenylbutyl)phosphinyl]oxy]-L-proline, a novel orally active inhibitor of ACE. *Journal of Medicinal Chemistry*, **31**: 204-212.

KESSLER, M., ACUTO, O., STORELLI, C., MURER, H., MULLER, M. and SEMENZA, G. (1978). A modified procedure for the rapid preparation of efficiently transporting vesicles from small intestine brush border membranes. Their use in investigating some properties of D-glucose and choline transport systems. *Biochimica et Biophysica Acta*, **506**: 136-154.

KNUTTON, S., BALDWIN, T., WILLIAMS, P.H. and McNEISH (1989). Actin accumulation at sites of bacterial adhesion to tissue culture cells: basis of a new diagnostic test for enteropathogenic and enterohemorrhagic *Escherichia coli*. *Infection and Immunity*, **57**: 1290-1298.

KOLARS, J.C., STETSON, P.L., RUSH, B.D., RUWART, M.J., SCHMIEDLIN-REN, P., DUELL, E.A., VOORHEES, J.J. and WATKINS, P.B. (1992). Cyclosporine metabolism by P450III in rat enterocytes - Another determinant of oral bioavailability? *Transplantation*, **53**: 596-602.

KONINKX, J.F.J.G., HENDRIKS, H.J.M.A., VAN ROSSUM, J.M.A., VAN DEN INGH, T.S.G.A.M. and MOUWEN, J.M.V.M. (1992). Interaction of legume lectins with the cellular metabolism of differentiated Caco-2 cells. *Gastroenterology*, **102**: 1516-1523.

KUBO, S.H. and CODY, R.J. (1985). Clinical pharmacokinetics of the angiotensin converting enzyme inhibitors, a review. *Clinical Pharmacokinetics*, **10**: 377-391.

KVIETYS, P.R., SPECIAN, R.D., GRISHAM, M.B. and TSO, P. (1992). Jejunal mucosal injury and restitution: role of hydrolytic products of food digestion. *American Journal of Physiology*, **261**: G384-G391.

LEE, J-K., GORDON, P.R., STALL, G.M., GILCHREST, B.A. and KAPLAN, M.M. (1989). Phenolic and tyrosyl ring iodothyronine deiodination by the Caco-2 human colon carcinoma cell line. *Metabolism*, **38**: 1154-1161.

LEIGHTON, J., ESTES, L.W., MANSUKHANI, S. and BRADA, Z. (1970). A cell line derived from normal dog kidney (MDCK) exhibiting qualities of papillary adenocarcinoma and of renal tubular epithelium. *Cancer*, **26**: 1022-1028.

LERNER, J. and STEINKE, D.L. (1977). Intestinal absorption of glutamic acid in the chicken. *Comparative Biochemistry and Physiology*, **57A**: 11-16.

LEVINE, J.S., ALLEN, R.H., ALPERS, D.H. and SEETHARAM, B. (1984). Immunocytochemical localisation of intrinsic factor-cobalamin receptors in dog ileum: distribution of intracellular receptors during cell migration. *Journal of Cell Biology*, **98**: 1110-1117.

LEVINE, R.R., McNARY, W.F., KORNGUTH, P.J. and LEBLANC, R. (1970). Histological re-evaluation of everted gut technique for studying intestinal absorption. *European Journal of Pharmacology*, **9**: 211-221.

LIN, E.C.C., HAGIHIRA, H. and WILSON, T.H. (1962). Specificity of the transport system for neutral amino acids in the hamster intestine. *American Journal of Physiology*, **202**: 919-925.

LINDHOLM, A., HENRICSON, S., LIND, M. and DAHLQVIST, R. (1988). Intra-individual variability in the relative systemic availability of cyclosporin after oral dosing. *European Journal of Clinical Pharmacology*, **34**: 461-464.

LOMARSTRO, B.M. and BAILIE, G.R. (1991). Quinolone-cation interactions: a review. *Drug interactions an reactions update*, **25**: 1249-1258.

LORENZSONN, V. and OLSON, W.A. (1982). In vivo responses of rat intestinal epithelium to intraluminal dietary lectins. *Gastroenterology*, **82**: 838-848.

LUCKE, H., HAASE, W. and MURER, H. (1977). Amino acid transport in brush-border membrane vesicles isolated from human small intestine. *Biochemical Journal*, **168**: 529-532.

LUNDIN, S. MOSS, J. BUNDGAARD, H. and ARTURSSON, P. (1991). Absorption of thyrotrophin-releasing hormone (TRH) and a TRH prodrug in a human intestinal cell line (Caco-2). *International Journal of Pharmaceutics*, **76**: R1-R4.

MADARA, J. (1983). Increases in guinea pig small intestinal transepithelial resistance induced by osmotic loads are accompanied by rapid alterations in absorptive-cell tight-junction structure. *Journal of Cell Biology* , **97**: 125-136.

MADARA, J. and PAPPENHEIMER, J.R. (1987). Structural basis for physiological regulation of paracellular pathways in intestinal epithelia. *Journal of Membrane Biology*, **100**: 149-164.

MADARA, J.L. and TRIER, J.S. (1987). Functional morphology of the mucosa of the small intestine. *In:* Physiology of the gastrointestinal tract, Second Edition, Johnson, L.R. (Ed.), Raven Press, New York, pp1209-1249.

MAENZ, D.D., CHENU, C., BRETON, S. and BERTELOOT, A. (1992). pH-dependent heterogeneity of acidic amino acid transport in rabbit jejunal brush-border membrane vesicles. *Journal of Biological Chemistry*, **267**: 1510-1516.

MANGE, D., FAVENNEC, L., CHOCHILLON, C., GORENFLOT, A., MEILLET, D., KAPEL, N., RAICHVARG, D., SAVEL, J. and GOBERT, J.G. (1991). Role of cytoskeleton and surface lectins in *Giardia duodenalis* attachment to Caco-2 cells. *Parasitology Research*, **77**: 659-662.

MALO, C. (1991). Multiple pathways for amino acid transport in brush-border membrane vesicles from the human fetal small intestine. *Gastroenterology*, **100**: 1644-1652.

MARTINEZ-PALOMO, A., MEZA, I., BEATY, G. and CEREIJIDO, M. (1980). Experimental modulation of occluding junctions in a cultured transporting epithelium. *Journal of Cell Biology*, **87**: 736-745.

MATTHEWS, D.M. (1991). Absorption of peptides. *In:* Protein Absorption, Matthews, D.M. (Ed.), Wiley-Liss, New York, pp235-319.

MATTHEWS, D.M. and PAYNE, J.W. (1980). Transmembrane transport of small peptides. *Current Topics in Membranes and Transport*, **14**: 331-425.

MAZARIEGOS, M.R., TICE, L.W. and HAND, A.R. (1984). Alteration of tight junctional permeability in the rat parathyroid gland after isoproterenol stimulation. *Journal of Cell Biology*, **98**: 1865-1877.

MELDRUM, B. (1985). Possible therapeutic applications of antagonists of excitatory amino acid neurotransmitters. *Clinical Sciences*, **68**: 113-122.

MEHTA, M.U., VENKATARAMANAN, R., BURCKART, G.J., PTACHCINSKI, R.J., DELAMOS, B., STACHAK, S., VAN THIEL, D.H., IWATSUKI, D.H. and STARZL, T.E. (1988). Effects of bile on cyclosporin absorption in liver transplant patients. *British Journal of Clinical Pharmacology*, **25**: 579-584.

MOHRMANN, I., MOHRMANN, M., BIBER, J. and MURER, H. (1986). Sodium-dependent transport of P_i by an established intestinal epithelial cell line (Caco-2). *American Journal of Physiology*, **250**: G323-G330.

MOORE, L., KRAMER, P., FOLEY, J., TU, J., SWANSON, B. and DUCHIN, K. (1988). Ascending multiple-dose study of a new ACE inhibitor. *American Journal of Hypertension*, **3**: 36A.

MOYER, M.P. (1983). Culture of human gastrointestinal epithelial cells. *Proceedings of the Society for Experimental Biology and Medicine*, **174**: 11-15.

MOSS, J., BUUR, A. and BUNDGAARD, H. (1990). Prodrugs of peptides, 8. In vitro study of intestinal metabolism and penetration of thyrotrophin-releasing hormone (TRH) and its analogues. *International Journal of Pharmaceutics*, **66**: 183-191.

MUNCK, B.G. (1966). Amino acid transport by the small intestine of the rat. The existence and specificity of the transport of imino acids and its relation to the transport of glycine. *Biochimica et Biophysica Acta*, **120**: 97-103.

MUNCK, B.G. (1983). Comparative aspects of amino acid transport in guinea pig, rabbit and rat small intestine. *In:* Intestinal Transport, Gilles-Baillien, M. and Gilles, R. (Eds.), Sringer-Verlag, Berlin, Heidelberg, pp260-283.

MUNCK, B.G. (1985 a). Transport of neutral and cationic amino acids across the brush-border membrane of the rabbit ileum. *Journal of Membrane Biology*, **83**: 1-13.

MUNCK, B.G. (1985 b). Transport of imino acids and non-alpha-amino acids across the brush-border membrane of the rabbit ileum. *Journal of Membrane Biology*, **83**: 15-24.

MURAKAMI, M., YOSHIKAWA, H., TAKADA, K. and MURANISHI, S. (1986). Effect of oleic acid vesicles on intestinal absorption of carboxyfluoresin in rats. *Pharmaceutical Research*, **3**: 35-40.

MURER, H. and KINNE, R (1980). The use of isolated membrane vesicles to study epithelial transport processes. *Journal of Membrane Biology*, **55**: 81-95.

NAKANISHI, K., MASADA, M. and NADAI, T. (1983). Effect of pharmaceutical adjuvants on the rectal absorption of drugs, III. Effect of repeated administration and recovery of the permeability. *Chemical and Pharmaceutical Bulletins*, **31**: 4161-4166.

NEWEY, H. and SMYTH, D.H. (1964). The transfer system for neutral amino acids in the rat small intestine, *Journal of Physiology*, **170**: 328-343.

NEUTRA, M. and LOUVARD, D. (1989). Differentiation of Intestinal cells in vitro. *In;* Functional Epithelial Cells in Culture, Matlin, K.S. and Valentich, J.D. (Eds.), Alan R. Liss, Inc., New York, pp363-398.

NICKLIN, P.L. and IRWIN, W.J., (1991). Thyrotrophin-releasing hormone transport across monolayers of human intestinal absorptive (Caco-2) cells in vitro. *Journal of Pharmacy and Pharmacology*, **43** (Suppl.): 103P.

NICKLIN, P.L., IRWIN, W.J., HASSAN, I.F. and MACKAY, M. (1992 a). Proline uptake by monolayers of human intestinal absorptive (Caco-2) cells *in vitro*. *Biochimica et Biophysica Acta*, **1104**: 283-292.

NICKLIN, P.L., IRWIN, B., HASSAN, I., WILLIAMSON, I. and MACKAY, M. (1992 b). Permeable support type influences the transport of compounds across Caco-2 cells. *International Journal of Pharmaceutics*, **83**: 197-209.

NIMMERFALL, F. AND ROSENTHALER, J. (1980). Significance of the goblet cell mucin layer, the outermost luminal barrier to passage through the gut wall. *Biochemical and Biophysical Research Communications*, **94**: 960-966.

NISHIHATA, T., TOMIDA, H., FREDRICK, G., RYTTING, J.H. and HIGUCHI, T. (1985). Comparison of the effects of sodium salicylate, disodium ethylenediaminetetraacetic acid and polyoxyethylene-23-lauryl ether as adjuvants for the rectal absorption of cefoxitin. *Journal of Pharmacy and Pharmacology*, **37**: 159-163.

NIV, Y., BYRD, J.C., HO, S.B., DAHIYA, R. and KIM, Y.S. (1992). Mucin synthesis and secretion in relation to spontaneous differentiation of colon cancer cells in vitro. *International Journal of Cancer*, **50**: 147-152.

NOACH, A.B.J., ROOSEMALEM, M.C.M., KUROSAKI, Y., DE BOER, A.G. and BRIEMER, D.D. (1992). Effect of apical and/or basolateral application of EDTA on the permeability of hydrophilic compounds in a human intestinal epithelial cell line (Caco-2). *Journal of Controlled Release*, **21**: 206-207.

NUSRAT, A., DELP, C. and MADARA, J.L. (1992). Intestinal epithelial restitution. Characterization of a cell culture model and mapping of cytoskeletal elements in migrating cells. *Journal of Clinical Investigation*, **89**: 1501-1511.

O'HAGAN, D.T., PALIN, K.J. and DAVIS, S.S. (1987). Intestinal absorption of proteins and macromolecules and the immunological response. *Critical Reviews in Therapeutic Drug carrier Systems*, **4**: 197-220.

OKANO, T., INUI, K-I., MAEGAWA, H., TAKANO, M. and HORI, R. (1986 a). H^+-coupled uphill transport of aminocephalosporins via the dipeptide transport system in rabbit intestinal brush-border membranes. Journal of Biological Chemistry, 261: 14130-14134.

OKANO, T., INUI, K-I., TAKANO, M. and HORI, R. (1986 b). H^+-Gradient-dependent transport of aminocephalosporins in rat intestinal brush-border membrane vesicles. *Biochemical Pharmacology*, **35**: 1781-1786.

OSIESCKA, I., PORTER, P.A., BORCHARDT, R.T., FIX, J.A. and GARDNER, C.R. (1985). *In vitro* drug absorption models. Brush border membrane vesicles, isolated mucosal cells and everted intestinal rings: Characterisation and salicylate accumulation. *Pharmaceutical Research*, **2**: 284-293.

OWEN, R.L. and JONES, A.L. (1974). Epithelial cell specialisation with human Peyer's patches: an ultrastructural study of intestinal lymphoid follicles. *Gastroenterology*, **66**: 189-203.

OXENDER, D.L. and CHRISTENSEN, H.N. (1963). Distinct mediating systems for the transport of neutral amino acids by the Ehrlich cell. *Journal of Biological Chemistry*, **238:** 3686-3699.

PAPAPOULOS, S.E., LANDMAN, J.O., BIJVOET, O.L.M., LOWIK, C.W.G.M., VALKEMA, R., PAUWELLS, E.K.J. and VERMEIJ, P. (1992). The use of bisphosphonates in the treatment of osteoporosis. *Bone*, **13**: S41-S49.

PAPPENHEIMER, J.R. and REISS, K.Z. (1987). Contribution of solvent drag through intercellular junctions to absorption of nutrients by the small intestine of the rat. *Journal of Membrane Biology*, **100**: 123-136.

PETERS. T. and VANTRAPPEN, G. (1975). The Paneth cell: A source of intestinal lysozyme. *Gut*, **16**: 553-558.

PINTO, M., ROBINE-LEON, S., APPAY, M.D., KEDINGER, M., TRIADOU, N., DUSSAULX, E., LACROIX, B., SIMON ASSMAN, P., HAFFEN, K., FOGH, J. and ZWEIBAUM, A. (1983). Enterocyte-like differentiation and polarization of the human colon carcinoma cell line Caco-2 in culture. *Biology of the Cell*, **47**: 323-330.

PINTO DA SILVA, P. and KACHAR, B. (1982). On tight junction structure. *Cell*, **28**: 441-450.

POELMA, F.G.J. and TUKKER, J.J. (1987). Evaluation of a chronically isolated internal loop in the rat for the study of drug absorption kinetics. *Journal of Pharmaceutical Sciences*, **76**: 433-436.

POLACHE, A., PLA-DELFINA, J.M. and MERINO, M. (1991). Partially competitive inhibition of intestinal baclofen absorption by beta-alanine, a non-essential dietary amino acid. *Biopharmaceutics and Drug Disposition*, **12**: 647-660.

POTTEN, C.S. and MORRIS, R.J. (1988). Epithelial stem cells in vivo. *Journal of Cell Science*, **10**: 45-62.

PTACHCINSKI, R., VENKATARAMANAN, R., ROSENTHAL, J.T., BURCKART, G.T., TAYLOR, R.J. and HAKALA, T.R. (1985). The effect of food on cyclosporin absorption. *Transplantation*, **40**: 174-176.

PTACHCINSKI, R., VENKATARAMANAN, R. and BURCKART, G.T. (1986). Clinical pharmacokinetics of cyclosporin. *Clinical Pharmacokinetics*, **11**: 107-132.

QUICK, T.C. and ONG, D.E. (1990). Vitamin A metabolism in the human intestinal Caco-2 cell line. *Biochemistry*, **29**, 11116-11123.

RABITO, C.A. (1986). Occluding junctions in a renal cell line (LLK-PK_1) with characteristics of proximal tubular cells. *American Journal of Physiology*, 250, F734-F743.

RABITO, C.A. and KARISH, M.V. (1983). Polarized amino acid transport by an epithelial cell line of renal origin (LLC-PK_1). *Journal of Biological Chemistry*, **258**: 2543-2547.

RABITO, C.A., TCHAO, R., VALENTICH, J. and LEIGHTON, J. (1978). Distribution and characteristics of the occluding junctions in a monolayer of a cell line (MDCK) derived from canine kidney. *Journal of Membrane Biology*, **43**: 351-365.

RAJENDRAN, V.M., ANSARI, S.A., HARIG, J.M., ADAMS M.B., KHAN, A.H. and RAMASWAMY, K. (1985). Transport of glycyl-L-proline by human intestinal brush border membrane vesicles. *Gastroenterology*, **89**:1298-1304.

RAJENDRAN, V.M., HARIG, J.M. and RAMASWAMY, K. (1987 a). Characteristics of glycyl-L-proline transport in intestinal brush-border membrane vesicles. *American Journal of Physiology*, 252, G281-G286.

RAJENDRAN, V.M., HARIG, J.M., ADAMS M.B. and RAMASWAMY, K. (1987 b). Transport of acidic amino acids by human jejunal brush-border membrane vesicles. *American Journal of Physiology*, **252**: G33-G39.

RAMANUJAM, K.S., SEETHARAM, S., RAMASWAMY, M. and SEETHARAM, B. (1991). Expression of cobalamin transport proteins and cobalamin transcytosis by colon adenocarcinoma cells. American Journal of Physiology, 260: G416-G422.

RAMASWAMY, K. and RADHAKRISHNAN, A.N. (1963). Studies on intestinal transaminases with special reference to human intestinal glutamic-aspartic transaminase. *Indian Journal of Biochemistry*, **1**, 1-6.

RAMASWAMY, K. and RADHAKRISHNAN, A.N. (1970). Labelling patterns using ^{14}C-labelled glutamic acid, aspartic acid and alanine in the transport studies with everted sacs of rat intestine. *Indian Journal of Biochemistry*, **7**, 50-54.

RANADRIVE, S.A., CHEN, A.X. and SERAJUDDIN, A.T.M. (1992). Relative lipophilicities and structural-pharmacological considerations of various angiotensin-converting enzyme (ACE) inhibitors. *Pharmaceutical Research*, **9**: 1480-1486.

RAYMOND, M.J., MARTINOT-PEIBNOUX, M. and ERLINGER, S. (1985). Dome formation in the human colon carcinoma cell line Caco 2 in culture. Influence of ouabain and permeable supports. *Biology of the Cell*, **4**: 89-92.

REITSMA, P.H., BIJVOET, O.L.M., POTOKAR, M., VAN DER WEE-PALS, L.J.A. and VAN-WIJK-VAN LENNEP, M.M.L. (1983). Apposition and resorption of bone during oral treatment with (3-Amino-1-hydroxypropylidene)-1,1-bisphosphonate (APD). *Calcified Tissue International*, **35**: 357-361.

RILEY, S.A., WARHURST, G., CROWE, P.T. and TURNBERG, L. (1991). Active hexose transport across cultured human Caco-2 cells: characterisation and influence of culture conditions. *Biochimica et Biophysica Acta*, **1066**: 175-182.

RINDLER, M.J. and TRABER, M.G. (1988). A specific sorting signal is not required for the polarized secretion of newly synthesised proteins from cultured intestinal epithelial cells. *Journal of Cell Biology*, **107**: 471-479.

ROBINSON M.B. and COYLE, J.T. (1987). Glutamate and related acidic excitatory neurotransmitters: from basic science to clinical application. *FASEB Journal*, **1**: 446-455.

RODNING, C.B., WILSON, I.D. and ERLANDSEN, S.L. (1976). Immunoglobulins within human small intestinal Paneth cells. *Lancet*, **1**: 984-986.

RUTTEN, M.J. and ITO, S. (1983). Morphology and electrophysiology guinea pig gastric mucosal repair in vitro. *American Journal of Physiology*, **244**: G171-G182.

SCALERA, V., STORELLI, C., STORELLI-JOSS, C., HAASE, W. and MURER, H. (1980). A simple and fast method for the isolation of lateral and basal membranes from rat small intestinal epithelial cells. *Biochemical Journal*, **186**: 177-181.

SCHASTEEN, C.S., DONOVAN, M.G. and COGBURN, J.N. (1992). A novel *in vitro* screen to discover agents which increase the absorption of molecules across the intestinal epithelium. *Journal of Controlled Release*, **21**: 49-62.

SHAH, P.K., HIDALGO, I.J. and BORCHARDT, R.T. (1990). A simple diffusion device to study transport across cells cultured in microporous membranes. *International Journal of Pharmaceutics*, **63**: 281-283.

SILEN, W. and SUSUMU, I. (1985). Mechanisms for rapid re-epithelialization of the gastric mucosal surface. *Annual Review of Physiology*, **47**: 217-229.

SINGHVI, S.M., McKINSTRY, D.N., SHAW, J.M., WILLARD, D.A. and MIGDALOF, B.H. (1982). The effect of food on the bioavailability of captopril in healthy subjects. *Journal of Clinical Pharmacology*, **22**: 135-140.

SLOVITER, R.S. (1986). On the role of seizure activity and endogenous excitatory amino acids in mediating seizure-associated hippocampal damage. *In:* Excitatory amino acids and epilepsy, Schwarcz, R. and Ben-Ari, Y. (Eds.), Plenum, New York, pp659-671.

SMITH, T.K., GIBSON, C.L., HOWLIN, B.J. and PRATT, J.M. (1991). Active transport of amino acids by gamma-glutamyl transpeptidase through Caco-2 cell monolayers. *Biochemical and Biophysical Research Communications*, **178**: 1028-1035.

SOUBA, W.W., PAN, M. and STEVENS, B.R. (1992). Kinetics of the sodium-dependent glutamine transporter in human intestinal cell confluent monolayers. *Biochemical and Biophysical Research Communications*, **188**: 746-753.

SPENCER, R.P. and BRODY, K.R. (1964). Intestinal transport of cyclic and non-cyclic amino acids. *Biochimica et Biophysica Acta*, **88**: 400-406.

STEVENS, B.R., ROSS, H.J. and WRIGHT, E.M. (1982). Multiple transport pathways for neutral amino acids in rabbit jejunal brush border vesicles. *Journal of Membrane Biology*, **66**: 213-225.

STEVENS, B.R., KAUNITZ, J.D. and WRIGHT , E.M. (1984). Intestinal transport of amino acids and sugars: Advances using membrane vesicles. *Annual Review in Physiology,* **46**: 417-433.

STEVENSON, B.R. and GOODENOUGH, D.A. (1984). Zonulae occludenates in junctional complex-enriched fractions from mouse liver: preliminary morphological and biochemical characterisation. *Journal of cell Biology*, **98**: 1209-1221.

STEWART, B.H., DANDO, S.A.and MORRISON, R.A. (1990). In vitro uptake of SQ29852 by everted rat intestinal rings. *Pharmaceutical Research*, **7** (Suppl.): PDD 7179.

STRATFORD, R., BERGIN, L., GIMPLE, M., KIHFELD, M., VAN PELT, S. and DANTZIG, A. (1988). Effect of basement membrane on properties of a human intestinal cell line (Caco-2). *Pharmaceutical Research*, **5** (Suppl.): PD951.

SUGAWARA, M., ISEKI, K., MIYAZAKI, K., SHIROTO, H., KONDO, Y. and UCHINO, J-I. (1991) Transport characteristics of ceftibuten, cefixime and cephalexin across human jejunal brush-border membrane. *Journal of Pharmacy and Pharmacology*, **43**: 882-884.

TAKAYAMA, A., OKAZAKI, Y., FUKUDA, K-I., TAKANO, M., INUI, K-I and HORI, R. (1991). Transport of cyclosporine A in kidney epithelial cell line (LLC-PK_1). *Journal of Pharmacology and Experimental Therapeutics*, **257**: 200-257.

TEIJEMA, H.L., VAN GELDERAN, H.H., GIESBERTS, M.A.H. and LAURENT DE ANGULO, M.S. (1974). Dicarboxylic aminoaciduria: An in born error of glutamate and aspartate transport with metabolic implications, in combination with hyperprolinemia. *Metabolism*, **23**: 115-123.

THWAITES, D.T., SIMMONS, N.L. and HIRST, B.H. (1992). Intestinal absorption of thyrotrophin-releasing hormone (TRH): studies with membrane vesicles and epithelial cell monolayers. *Proceedings of the United Kingdom association of Pharmaceutical Scientists*, **1**: 20.

TOKUMURA, T., TSUSHIMA, Y., TATSUISHI, K., KAYANO, M., MACHIDA, Y. and NAGI, T. (1987). Enhancement of the oral bioavailability of cinnarizine in oleic acid in beagle dogs. *Journal of Pharmaceutical Sciences*, **76**: 286-288.

TOMON, M., TENENHOUSE, H.S. and JONES, G. (1990). Expression of 25-Hydroxyvitamin D3-24-Hydrolase activity in Caco-2 cells. An in vitro model of intestinal vitamin D catabolism. *Endocrinology*, **126**: 2868-2875.

TRABER, M.G., KAYDEN, H.J. and RINDLER, M.J. (1987). Polarized secretion of newly synthesised lipoproteins by the Caco-2 human intestinal cell line. *Journal of lipid Research*, **28**: 1350-1362.

TRIER, J.S. (1980). Organ culture of the mucosa of human small intestine. *Methods in Cell Biology*, **21**: 365-384.

USSING, H.H. and ZERAHN, K. (1951). Active transport of sodium as the source of electric current in the short-circuited isolated frog skin. *Acta Physiologica Scandinavica,* **23**: 110-127.

VAN BREE, J.M.B.B., AUDUS, K.L. and BORCHARDT, R.T. (1988). Carrier-mediated transport of baclofen across monolayers of bovine brain brain endothelial cells in primary culture. *Pharmaceutical Research*, **5**: 369-371.

VAN HOOGDALEM, E.J., WACKWITZ, A.T.E., DE BOER, A.G. and BREIMER, D.D. (1989). 3-Amino-1-hydroxypropylidene-1,1-diphosphonate (APD): a novel enhancer of rectal cefoxitin absorption in rats. *Journal of Pharmacy and Pharmacology*, **41**: 339-341.

VEGA-SALAS, D.E., SALAS, P.J.I. and RODRIGUEZ-BOULAN, E. (1987). Modulation of the expression of an apical membrane protein of Madin-Darby Canine Kidney epithelial cells: cell-cell interactions control the appearance of a novel intracellular storage compartment. *Journal of cell Biology*, **104**: 1249-1259.

VINCENT, M.L., RUSSELL, R.M. and SASAU, V. (1985). Folic acid uptake characteristics of a human colon carcinoma cell line, Caco-2. *Human Nutrition. Clinical Nutrition*, **39C**: 355-360.

VOLBERG, T., GEIGER, B., KARTENBECK, J. and FRANK, W.W. (1986). Changes in membrane microfilament interaction in intercellular adherens junctions upon removal of extracellular Ca^{2+} ions. *Journal of Cell Biology*, **103**: 1832-1842.

WADHWA, N.K., SCHROEDER, T.J., O'FLAHERTY, E., PEACE, A.J., MYRE, S.A. and FIRST, M.R. (1987). The effect of oral metoclopramide on the absorption of cyclosporine, *Transplant Proceedings*, **19**: 1730-1733.

WATKINS, J.C. and EVANS, R.H. (1981). Excitatory amino acid transmitters. *Annual Review of Pharmacology and Toxicology*, **21**: 165-204.

WATT, F.M., MATTEY, D.L. and GARROD, D.R. (1984). Calcium-induced reorganisation of desmosomal components in cultured keratinocytes. *Journal of cell Biology*, **99**: 2211-2215.

WEARLEY, L.L. (1991). Recent progress in protein and peptide delivery by non-invasive routes. *Critical Reviews in Therapeutic Drug Carrier Systems*, **8**: 331-394.

WELLNER, D. and MEISTER, A. (1981). A survey of inborn errors of amino acid metabolism and transport in man. *Annual Reviews in Biochemistry*, **50**: 911-968.

WILSON, G., HASSAN, I.F., DIX, C.J., WILLIAMSON, I., SHAH, R., MACKAY, M. and ARTURSSON, P. (1990). Transport and permeability properties of human Caco-2 cells: An *in-vitro* model of the intestinal epithelial cell barrier. *Journal of Controlled Release*, **11**: 25-40.

WILSON, Q.H. and WISEMAN, G. (1954). The use of sacs of everted small intestine for the study of the transference of substances from the mucosal to the serosal surface. Journal of Physiology, 123:116.

WINGROVE, T.G. and KIMMICH, G.A. (1987). High affinity L-aspartate transport in chick small intestine. *American Journal of Physiology*, **252**: C105-C114.

WISEMAN, G. (1953). Absorption of amino acids using an in vitro technique. *Journal of Physiology*, **120**: 63-72.

WOODCOCK, S., WILLIAMSON, I., HASSAN, I. AND MACKAY, M. (1991). Isolation and characterisation of clones from the Caco-2 cell line displaying increased taurocholic acid transport. *Journal of Cell Science*, **98**: 323-331.

YAKATAN, G.J., POYNER, W.J., TALBERT, R.L., FLOYD, B.F., SLOUGH, C.L., AMPULSKI, R.S. and BENEDICT, J.J. (1982). Clodronate kinetics and bioavailability. *Clinical Pharmacology and Therapeutics*, **313**: 402-410.

YOKOHAMA, S., YAMASHITA, K., TOGUCHI, H., TAKEUCHI, J. and KITAMORI, N. (1984 a). Absorption of thyrotrophin-releasing hormone after oral administration of TRH tartrate monohydrate in rat, dog and human. *Journal of Pharmacobiodynamics*, **7**: 101-111.

YOKOHAMA, S., YOSHIOKA, T., YAMASHITA, K. and KITAMORI, N. (1984 b). Intestinal absorption mechanisms of thyrotrophin-releasing hormone. *Journal of Pharmacobiodynamics*, **7**: 445-451.

YOSHIOKA, M., ERICKSON, R.H., MATSUMOTO, H., GUM, E. and KIM, Y.S. (1991). Expression of dipeptidyl aminopeptidase IV during enterocytic differentiation of human colon cancer (Caco-2) cells. *International Journal of Cancer*, **47**: 916-921.

APPENDIX ONE

ABBREVIATIONS

ACE	Angiotensin-converting enzyme
AM	Assay-medium
AMPA	DL-Alpha-amino-3-hydroxy-5-lethylisoxazole-4-propionate
Ap	Apical
Ap-to-Bl	Apical-to-basolateral
BBMV	Brush-border membrane vesicles
Bl	Basolateral
BLMV	Basolateral membrane vesicles
BSA	Bovine serum albumin
°C	Degrees Celsius
C_6NBD	7-Nitro-2,1,3-benzoxadiazol-4-yl
Cbl	Cobalamin (vitamin B_{12})
Ci	Curie
cm	Centimetre
CO_2	Carbon dioxide
CPM	Counts per minute
CsA	Cyclosporin A
d	Day
D	Distribution coefficient
kDa	Kilodalton
DMEM	Dulbecco's modification of Eagle's medium
DNA	Deoxyribose nucleic acid
DPM	Decays per minute
E_a	Activation energy
EDTA	Ethylenediaminetetraacetic acid
EGTA	Ethylene glycol-bis-(ß-aminoethyl ether)-N, N, N', N'-tetraacetic acid
ELISA	Enzyme linked immunosorbent assay
FBS	Foetal Bovine serum
FITC	Fluorescein isothiocyanate
GI	Gastrointestinal
h	Hour
HBSS	Hanks' balanced salt solution
HEPES	N-[2-hydroxyethyl]piperazine-N'-[2-ethanesulphonic acid]
HRP	Horseradish peroxidase
IF	Intrinsic factor
K_d	Diffusional rate constant
K_i	Inhibition constant
kJ	Kilojoule

K_m	Michaelis constant
LNAA	Large neutral amino acid
m	Metre
M	Molar
MeAIB	Alpha-(methylamino) isobutyric acid
mg	Milligram
mm	Millimetre
mM	Millimolar
min	Minute
mol	mole
MWt	Molecular weight
N_3+2-DG	Sodium azide + 2-deoxyglucose
NEAA	Non-essential amino acids
ng	Nanogram
nM	Nanomolar
NMDA	N-methyl-D-aspartate
NT	Not tested
O_2	Oxygen
P_{app}	Apparent permeability coefficient
PBS	Phosphate buffered saline
PEG	Polyethylene glycol
pmol	Picomole
PS	Penicillin / streptomycin
R	Universal gas constant
RIA	Radioimmunoassay
RNA	Ribose nucleic acid
rpm	Revolutions per minute
SD	Standard deviation
SDil	Standard diluent
T	Temperature [Kelvin]
TCA	Trichloroacetic acid
TCII	Transcobalamin II
TER	Transepithelial electrical resistance
TRH	Thyrotrophin-releasing hormone
TX100	Triton X100
UWL	Unstirred water layer
V^{cm}	Carrier-mediated velocity
V^{d}	Diffusional velocity

V_{max}	Maximal velocity
V^{sd}	Sodium-dependent velocity
V^{si}	Sodium-independent velocity
V^{t}	Total velocity
%	Percent
μl	Microlitre
μm	Micrometre
μM	Micromolar
Ω	Ohm